1333

DATE LABEL

Call No5.4	• • •	Date	19.411.55

J. & K. UNIVERSITY LIBRARY

This book should be returned on or before the last stamped above. An overdue charges of 6 nP. will be levied for each day. The book is kept beyond that day.



Vol.			Сору		
Acce	ssion l	No.		DC 44.	
70000400000					

Class No.	Book No.
Vol.	Сору
Accession No.	

DESIGN OF CRYSTAL VIBRATING SYSTEMS FOR PROJECTORS AND OTHER APPLICATIONS

BY
WILLIAM J. FRY
JOHN M. TAYLOR
BERTHA W. HENVIS



NAVAL RESEARCH LABORATORY

A. H. VAN KEUREN, REAR ADMIRAL, U.S.N.

DIRECTOR

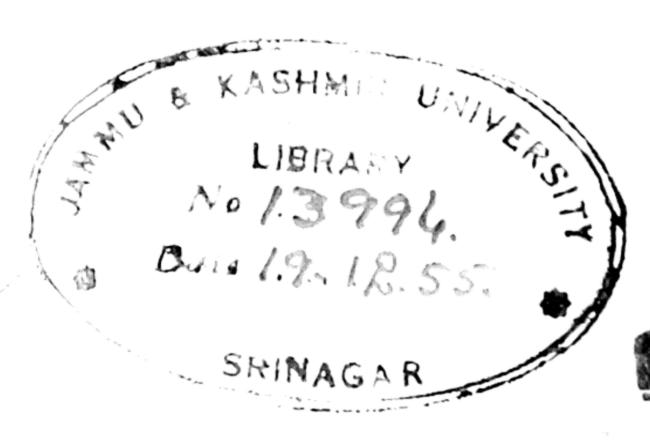
SOUND DIVISION • H. C. HAYES, SUPT.

DOVER PUBLICATIONS, INC.
NEW YORK

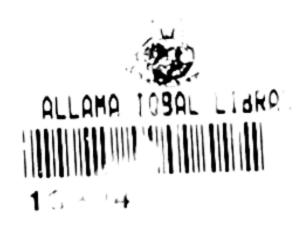
The first edition of this book was printed by the Government Printing Office in 1945. This Second, Revised Edition has been published with the helpful cooperation of the Office of Technical Services of the Department of Commerce and the United States Navy Office of Research and Inventions, Naval Research Laboratory. Grateful acknowledgement is also made to Mr. Groff Conklin, Mr. M. E. Jansson and Mr. William J. Fry for their assistance.

All secrecy restrictions on the contents of this document (PB 22410) have been lifted. In quoting or citing the report, please give the proper credit to the authors and the sponsoring agency. The Publication Board assumes no responsibility for the completeness and accuracy of the reports or for any opinions expressed. Products and processes described may be the subject of U. S. Patents, and the usual patent search is recommended before making practical applications.





COPYRIGHT 1948 BY DOVER PUBLICATIONS, INC.





PREFACE

This investigation is an outgrowth of numerous requests to calculate the characteristics of particular crystal vibrating systems, each of which required a separate analysis and laborious computation. As the number and complexity of the problems increased, the value of a thorough analysis covering all such situations became obvious. Accordingly, a general analysis of a large class of crystal vibrating systems was made and a set of design curves constructed on the basis of this analysis.

The validity of the calculations was established by experimental check of the predictions based on the curves. It is believed that the time and effort spent was well justified since the extremely slow procedure of building and testing numerous experimental models has been eliminated.

The analysis and curves as presented here cover a good portion of the systems and materials likely to be used. It is hoped that this has been achieved without any sacrifice of compactness and convenience in use.

This project was undertaken under the authorization of the Sonar Design Section of the Bureau of Ships, in connection with development of crystal materials and their application to Naval equipment.

ol	Copy _		
ccession N	0.		
		3 4 1	
	and companies of the control of the		
grande, company			

CONTENTS

1 CALCULATION OF γ. 2 RESONANT FREQUENCY. 3 ACOUSTIC IMPEDANCE OF BACKING MATERIAL COMBINATIONS. 4 RESONANT FREQUENCIES OF SYSTEMS WITH MULTIPLE-MATERIAL BACKING. 5 ELECTRICAL INPUT IMPEDANCE AND TRANSMITTING RESPONSE. 6 SENSITIVITY AND ACOUSTIC INPUT IMPEDANCE. 7 EFFICIENCY AND STRESS. 8 ACOUSTIC INPUT IMPEDANCE OF PARTICULAR BACKING MATERIAL SYSTEMS. PART II—THEORY 1 FUNDAMENTAL EQUATIONS. 2 ELECTRICAL INPUT IMPEDANCE.
2 RESONANT FREQUENCY. 3 ACOUSTIC IMPEDANCE OF BACKING MATERIAL COMBINATIONS. 4 RESONANT FREQUENCIES OF SYSTEMS WITH MULTIPLE-MATERIAL BACKING. 5 ELECTRICAL INPUT IMPEDANCE AND TRANSMITTING RESPONSE. 6 SENSITIVITY AND ACOUSTIC INPUT IMPEDANCE. 7 EFFICIENCY AND STRESS. 8 ACOUSTIC INPUT IMPEDANCE OF PARTICULAR BACKING MATERIAL SYSTEMS. PART II—THEORY 1 FUNDAMENTAL EQUATIONS
ACOUSTIC IMPEDANCE OF BACKING MATERIAL COMBINATIONS RESONANT FREQUENCIES OF SYSTEMS WITH MULTIPLE-MATERIAL BACKING. ELECTRICAL INPUT IMPEDANCE AND TRANSMITTING RESPONSE. SENSITIVITY AND ACOUSTIC INPUT IMPEDANCE. FEFICIENCY AND STRESS. ACOUSTIC INPUT IMPEDANCE OF PARTICULAR BACKING MATERIAL SYSTEMS. PART II—THEORY 1 FUNDAMENTAL EQUATIONS.
TIONS 4 RESONANT FREQUENCIES OF SYSTEMS WITH MULTIPLE-MATE RIAL BACKING. 5 ELECTRICAL INPUT IMPEDANCE AND TRANSMITTING RESPONSE. 6 SENSITIVITY AND ACOUSTIC INPUT IMPEDANCE. 7 EFFICIENCY AND STRESS. 8 ACOUSTIC INPUT IMPEDANCE OF PARTICULAR BACKING MATERIAL SYSTEMS. PART II—THEORY 1 FUNDAMENTAL EQUATIONS
4 RESONANT FREQUENCIES OF SYSTEMS WITH MULTIPLE-MATE RIAL BACKING. 5 ELECTRICAL INPUT IMPEDANCE AND TRANSMITTING RESPONSE. 6 SENSITIVITY AND ACOUSTIC INPUT IMPEDANCE. 7 EFFICIENCY AND STRESS. 8 ACOUSTIC INPUT IMPEDANCE OF PARTICULAR BACKING MATERIAL SYSTEMS. PART II—THEORY 1 FUNDAMENTAL EQUATIONS
RIAL BACKING. 5 ELECTRICAL INPUT IMPEDANCE AND TRANSMITTING RESPONSE. 6 SENSITIVITY AND ACOUSTIC INPUT IMPEDANCE. 7 EFFICIENCY AND STRESS. 8 ACOUSTIC INPUT IMPEDANCE OF PARTICULAR BACKING MATERIAL SYSTEMS. PART II—THEORY 1 FUNDAMENTAL EQUATIONS
5 ELECTRICAL INPUT IMPEDANCE AND TRANSMITTING RESPONSE. 6 SENSITIVITY AND ACOUSTIC INPUT IMPEDANCE. 7 EFFICIENCY AND STRESS. 8 ACOUSTIC INPUT IMPEDANCE OF PARTICULAR BACKING MATERIAL SYSTEMS. 1 FUNDAMENTAL EQUATIONS.
SPONSE. 6 SENSITIVITY AND ACOUSTIC INPUT IMPEDANCE. 7 EFFICIENCY AND STRESS. 8 ACOUSTIC INPUT IMPEDANCE OF PARTICULAR BACKING MATERIAL SYSTEMS. PART II—THEORY 1 FUNDAMENTAL EQUATIONS.
6 SENSITIVITY AND ACOUSTIC INPUT IMPEDANCE. 7 EFFICIENCY AND STRESS. 8 ACOUSTIC INPUT IMPEDANCE OF PARTICULAR BACKING MATERIAL SYSTEMS. 1 FUNDAMENTAL EQUATIONS.
7 EFFICIENCY AND STRESS
8 ACOUSTIC INPUT IMPEDANCE OF PARTICULAR BACKING MATERIAL SYSTEMS
TERIAL SYSTEMS
1 FUNDAMENTAL EQUATIONS
1 FUNDAMENTAL EQUATIONS
1 FUNDAMENTAL EQUATIONS
2 ELECTRICAL INPUT IMPEDANCE
3 ACOUSTIC INPUT IMPEDANCE
4 RESONANT FREQUENCY
5 SENSITIVITY
6 STRESS
APPENDICES

Vol	Сору	
Accession No.		
	1 11 11 11 11 11 11 11 11 11 11 11 11 1	

INTRODUCTION

This publication presents a detailed study of crystal vibrating systems and design procedures essential to the design of projectors. These procedures involve a general set of curves based on fundamental piezoelectric relations. Use of the curves reduces the computation required to a simple and straightforward method, which is adequate to cover any system composed of a piezoelectric material, vibrating in either thickness or longitudinal mode, in combination with any backing system and driving any medium. The performance of other piezoelectric devices such as wave filters, blast gages, and accelerometers can also be treated by following the procedures presented for projectors.

Part I contains the design curves and detailed explanations of their use. Particular systems using ADP and X-cut Rochelle salt crystals are discussed as an additional guide to the use of the curves, and to illustrate important changes in the performance of the system brought about by changes in the design or the operating conditions. Specific topics covered by the design procedure include resonant frequency, electrical input impedance, transmitting response, receiving sensitivity, and efficiency. Part I is subdivided into eight sections. Section 1 is concerned with the quantity γ , which is used throughout the remainder of Part I as a parameter. The subsequent sections

treat the specific topics mentioned above.

Part II contains the mathematical analysis and the derivations of the expressions used in constructing the curves of Part I. Detailed study of Part II is not necessary for intelligent use of the first Part.

Appendices A and B contain units, definitions, symbols. conventions, and tables and graphs of physical constants.

Vol	Book No. 2 Copy	
Accession No.		

SECTION 1 CALCULATION OF \(\gamma \)

The quantity γ is used throughout the design curves as a variable. An inspection of the equations derived in Part II will show that most quantities to be calculated are periodic functions of γ , where $\gamma = \frac{\omega L}{V}$ and

 $\omega = 360^{\circ} \text{ F or } 360^{\circ} \text{ N } (10)^3$,

N=frequency in kilocycles,

L=Length in centimeters of that part of the system under consideration, and V=velocity of sound in cm/sec in the part of the system under considera-

tion.

Because of the periodic nature of the functions, we are able to cover an infinite range of N, L, and V by a plot of the functions for one period $(0^{\circ} \le \gamma \le 360^{\circ})$.

The curves, therefore, cover only the range $0^{\circ} \le \gamma \le 360^{\circ}$, and the calculated γ must be reduced, if it exceeds 360° , to a positive angle between 0° and 360° by subtraction of the appropriate multiple of 360° .

Although it appears from the definition of γ that a simple slide rule calculation will suffice, the accuracy will be poor when several multiples of 360° must be subtracted. The curves given in this section are designed to eliminate this difficulty. They may be used to obtain values of γ for a large range of the variables L, V, and N.

From the first set of curves given here (consisting of one family, page 5), we find the quantity $L' \propto L/V$. L is plotted along the horizontal axis, V is the parameter from curve to curve, and L' is plotted along the vertical axis. Note that the L scale can be multiplied or divided by any quantity if the L' scale is multiplied or divided by the same quantity. Three such scales have been provided.

The second set of curves (consisting of three families, pages 6, 7, and 8) gives the required γ as a function of L' and the frequency N. Here γ , in degrees, is plotted along the vertical axis, N, in kilocycles, along the horizontal axis, and L' is the parameter from curve to curve.

Points to be noted in the use of the second set are:

1. Interpolation is exactly linear.

2. The value of L' obtained from the first set determines which of the three families of the second set is to be used:

if $L' \le 0.1$, use Family 1, page 6; if $0.1 \le L' \le 10$, use Family 2, page 7; if L' > 10, use Family 3, page 8.

- 3. For Family 1 (page 6) of the second set, N is plotted along the horizontal axis for values from 0 to 100 kc. γ is plotted in degrees along the vertical axis in two scales, and two corresponding scales of L' are tabulated along the right as indicated by the arrows at the top.
- 4. For Family 2, page 7, N is again plotted along the horizontal axis for values from 0 to 100 kc, and γ in degrees is plotted along the vertical axis. The group of dotted curves on this graph gives γ for $0.1 \le L' \le 1.0$. Values of L' from the dotted lines are tabulated on the right just inside the graph. The remaining curves apply to the case $1.0 \le L' \le 10$: Notice that the curve for L'=2 has two cycles over a range of N from 0 to 100 kc. Similarly, the one for L'=3has three cycles, and so on to L'=10 with ten cycles. The interpolation between two integral values of L' can be carried out as shown in the following example: To find γ for L'=5.7 and N=36. First, choose the closest integral values of L' which bound the given value of L'. For L'=5.7, the bounding values will be 5 and 6. Then starting from the frequency axis $(\gamma = 0)$, move toward increasing values of γ along the ordinate for the given value of frequency (N=36) and read the value of γ (290°) at the first intersection of this ordinate with the curve for the smaller integral value of L' (5, in this case). This value of γ will always be less than 360°. Next, continue toward increasing values of γ ($\gamma > 290^{\circ}$) along the same ordinate (N=36) and read the value of γ (417°) at the first intersection of this ordinate with the curve for the larger value of L' (6). The desired value of γ is then given by linear interpolation $\gamma = 290^{\circ} + 0.7(417^{\circ} - 1000)$ 290°) = 379°]. If the resulting value of γ exceeds 360°, it must be reduced by subtract-

ing 360° (379°-360°=19°). Values obtained from these curves will never exceed 720° and may always be reduced to the required angle by subtracting 360° when the γ obtained lies in the range 360° $<\gamma \le 720$ °.

5. For Family 3 (page 8) N is plotted along the horizontal axis in tenscales. The range of the parameter L' is from 10 to 100. Interpolation is the same as for Family 2.

To summarize the procedure:

- 1. Knowing L (length in cm) and V (velocity in cm/sec), we read L' from Set 1, page 5.
- 2. With this value of L' we choose the proper Family 1, 2, or 3, of Set 2, pages 6, 7, 8, and from L' and the given N (frequency in kc) we obtain the value of γ (in degrees) corresponding to the given value of L, L, and L.

Table 1 on page 3 gives the longitudinal bar and bulk velocities in various solids. The velocity of sound in some liquids is also given in the table.

The effective velocity of sound, V, to be used in these calculations is a rather complex function of the exciting frequency and the shape and dimensions of the vibrating element. Very few three dimensional elastic solid prob-

lems have been studied in detail, but the following comments may be used as a guide in obtaining an approximate value of the effective velocity in the elements of most of the vibrating systems considered in this report.

- 1. For cylindrical elements of approximately circular or square cross section, with free sides, the effective velocity varies with the ratio of diameter to wavelength as illustrated by Fig. 1a, page 4.
- 2. For rectangular elements with free sides (for example, crystals) whose thickness is less than the width, the effective velocity for the element vibrating in extension (not thickness) varies with the ratio of width to wavelength as illustrated by Fig. 1b, page 4.
- 3. Constraints on the sides of the cylindrical elements have the effect of increasing the ratio of diameter to wavelength. Similarly, the effective ratio of width-to-wavelength for rectangular elements is increased by constraining the sides.
- 4. The velocity for a zero diameter-to-wavelength ratio is the long bar velocity and the velocity for an infinite diameter-to-wavelength ratio is the bulk (plate) velocity.

TABLE 1 VELOCITIES

Material	Longitudinal bar veloc- ity (cm/sec) × 10 ⁻⁵	Bulk (plate) velocity (cm/sec.) ×10 ⁻⁵
Aluminum	5.25	6.4
Brass	3.42	4.25
Copper	3.58	4.6
Lead	1.25	2.4
Nickel	4.76	5.6
Steel	5.05	6.1
Glass	4.5-5.5	4.9-5.8
Magnesium	4.9	
ADP (NH ₄ H ₂ PO ₄) 45° Z-cut	3.28	4.92
Rochelle Salt 45° Y-cut	2.47	
Rochelle Salt 45° X-cut	See graph page 4	
Quartz X-cut	5.44	5.72
Tourmaline Z-cut		7.54

Material	Velocity cm/sec ×10 ⁻⁵
Water (fresh) Water (sea) Alcohol Mercury Pentane	1.44
Air	0.331

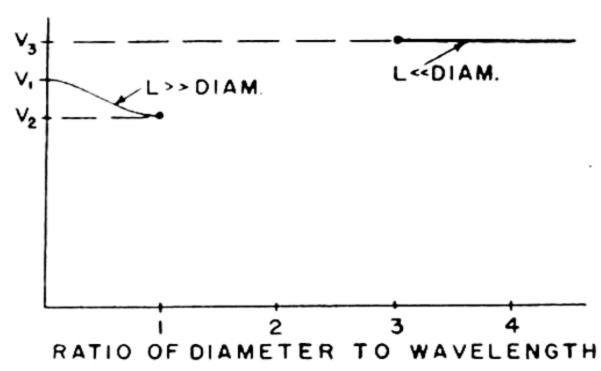


Figure 1a.—Approximate variation of the effective velocity in a cylindrical element of a vibrating system as a function of the ratio of diameter to wavelength. V_3 is the bulk velocity and V_4 is the long bar velocity. For most of the metal backing materials the ratio V_2/V_1 is about 0.65.

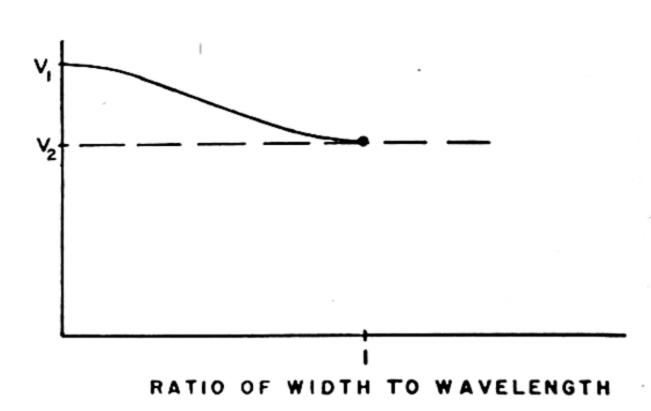
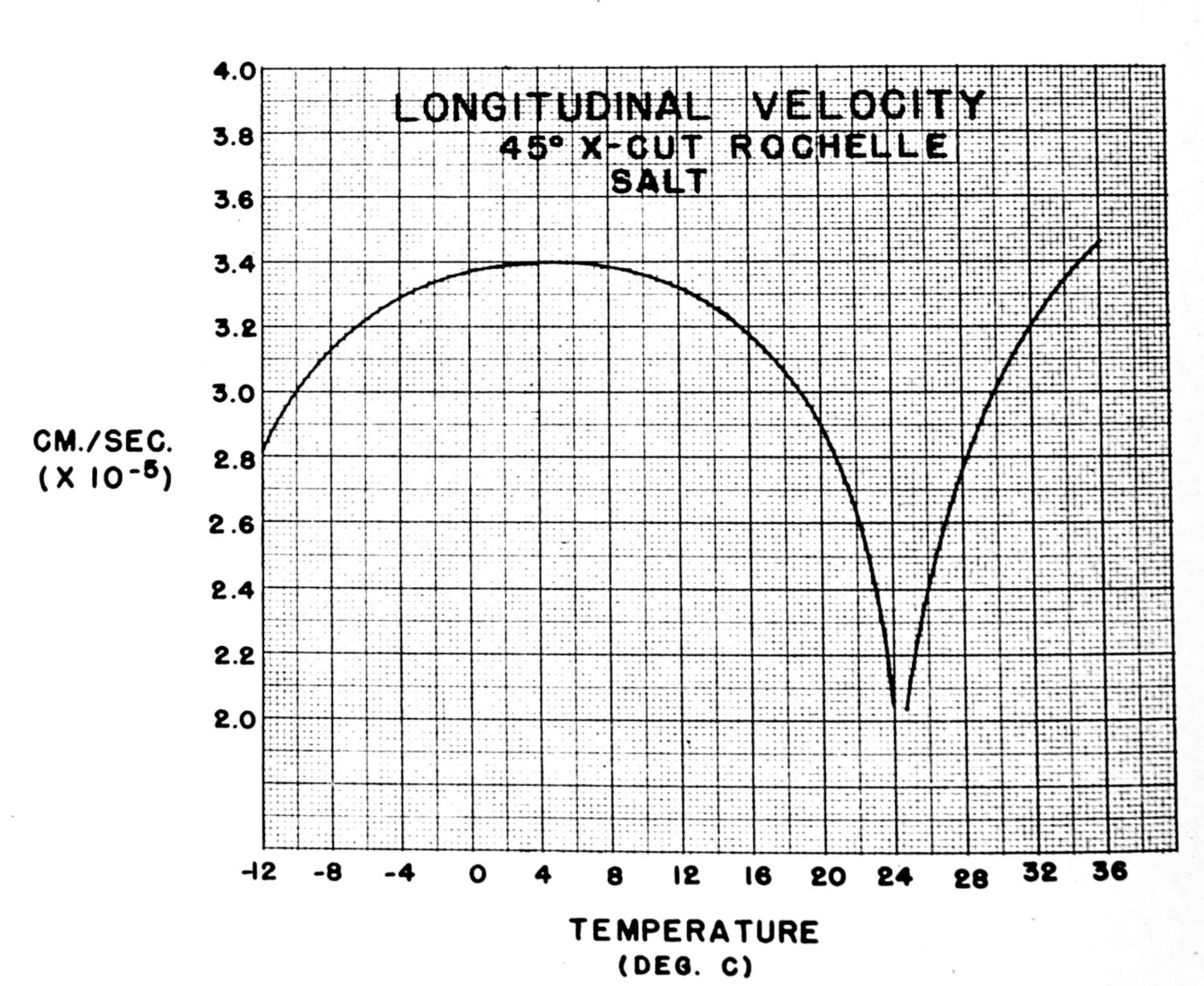
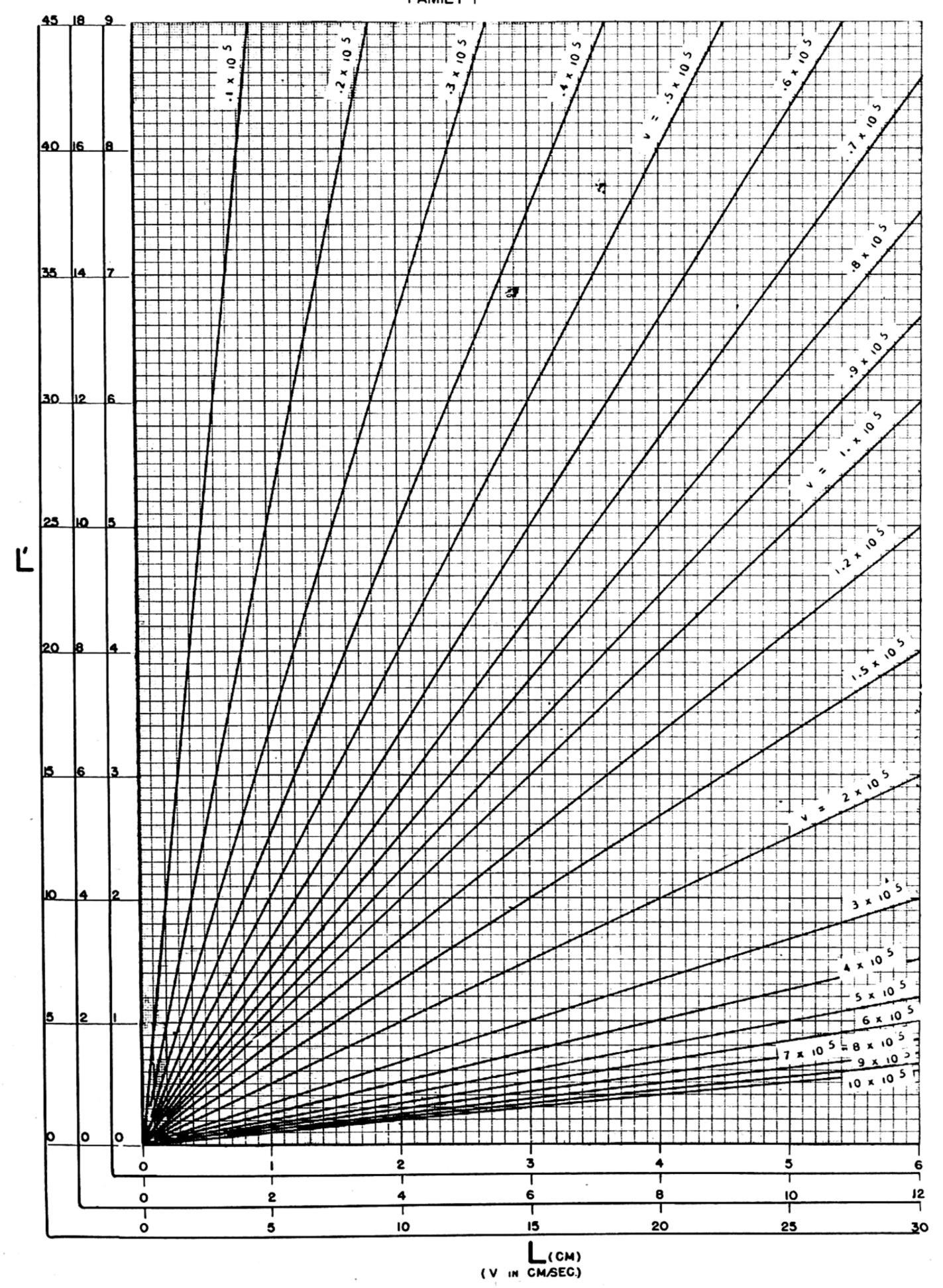
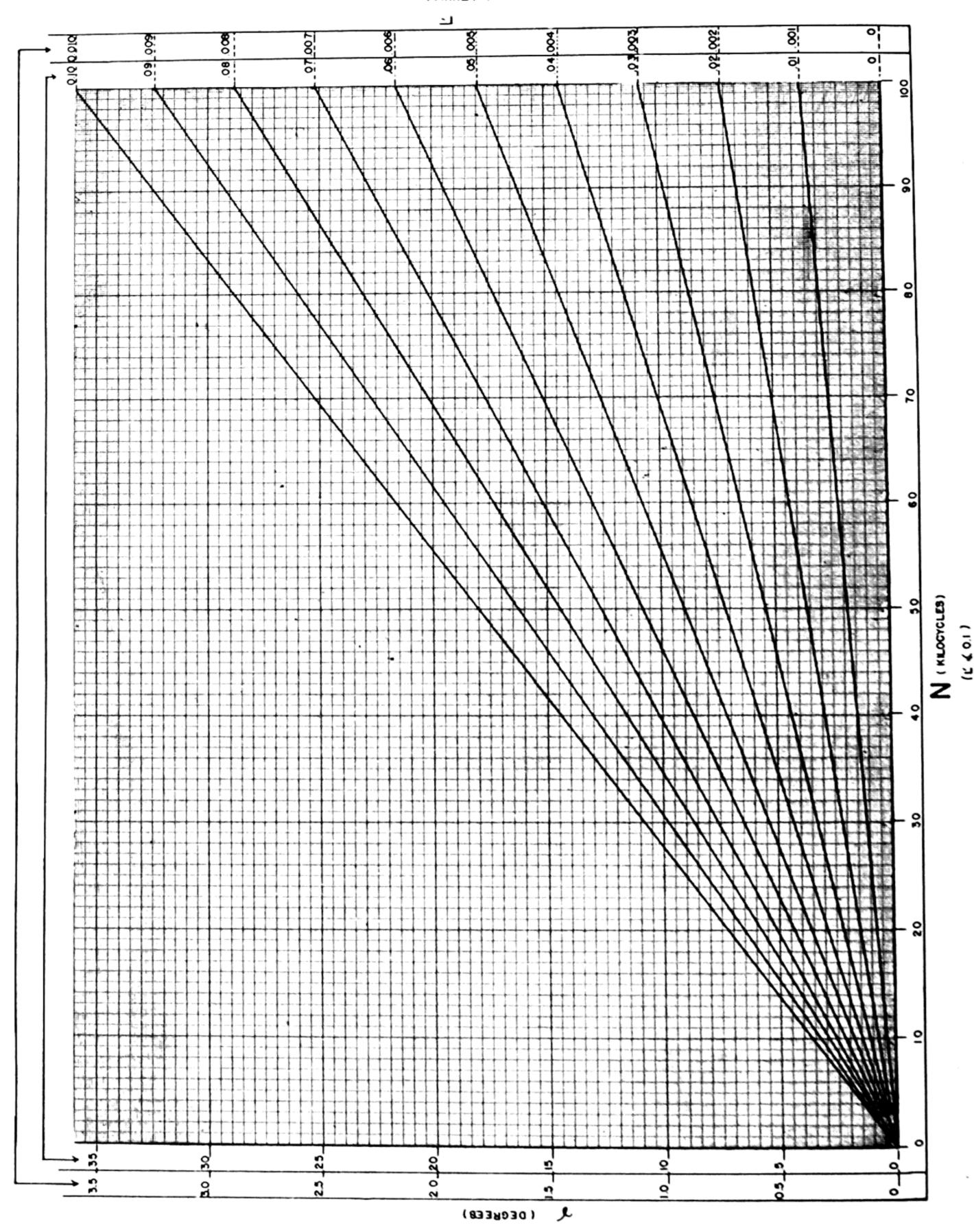


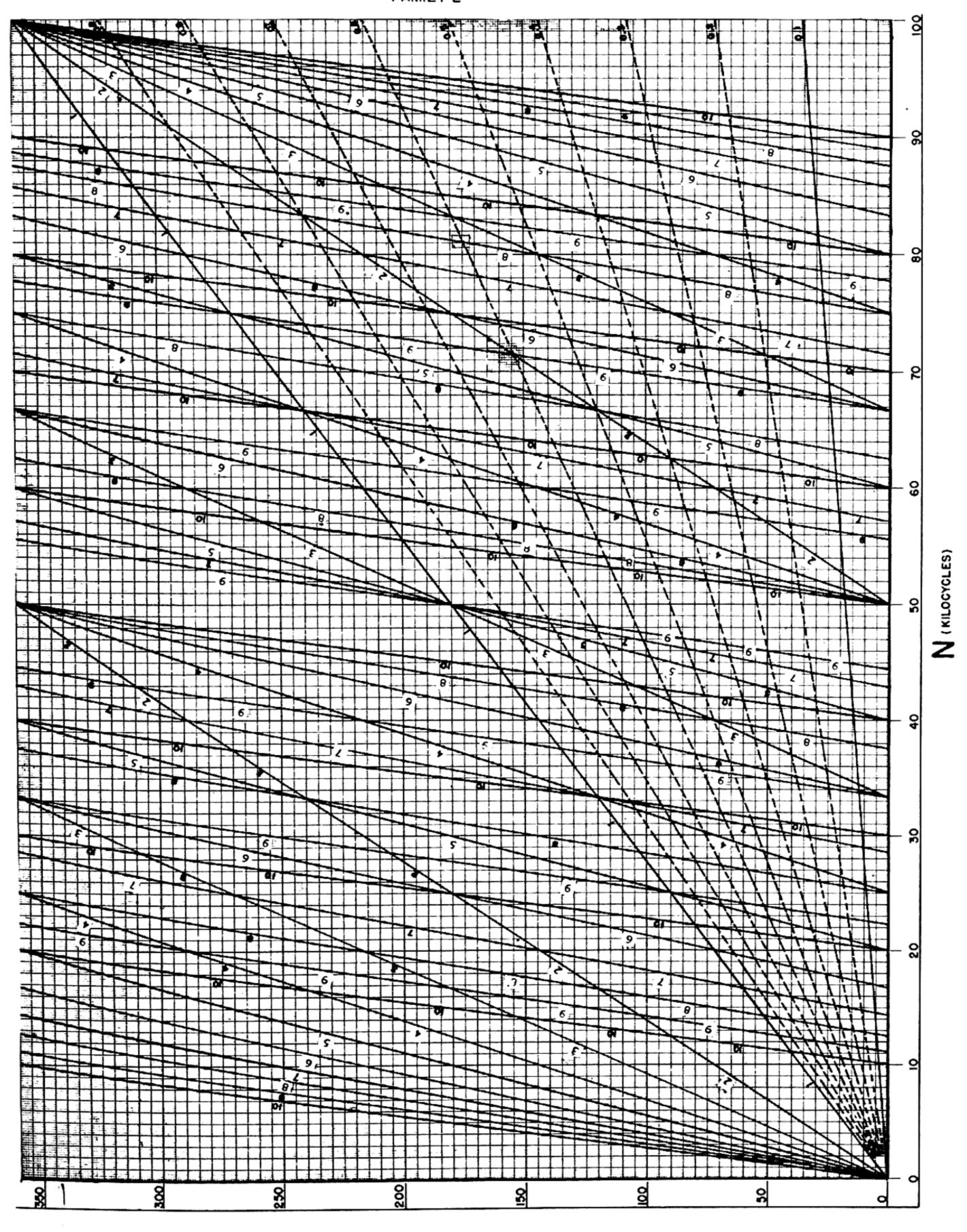
Figure 1b.—Approximate variation of the effective velocity in an element of rectangular cross section with thickness less than the width, as a function of the ratio of width to wavelength. V_1 is the long bar velocity. Crystals are usually of such size that this curve is applicable. The ratio V_2/V_1 can be taken equal to 0.8 for most of the cuts of crystals used.



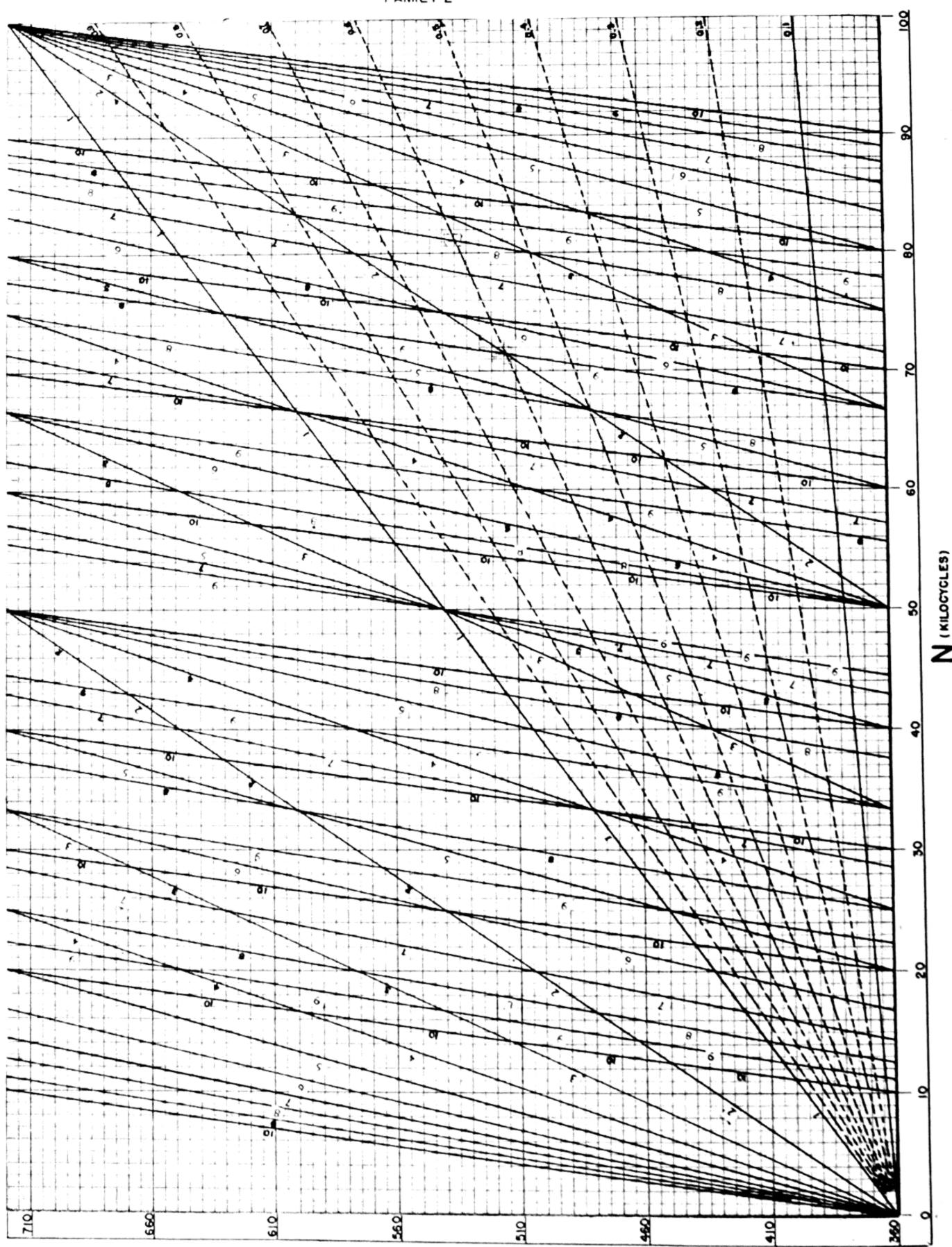
SET | FAMILY |



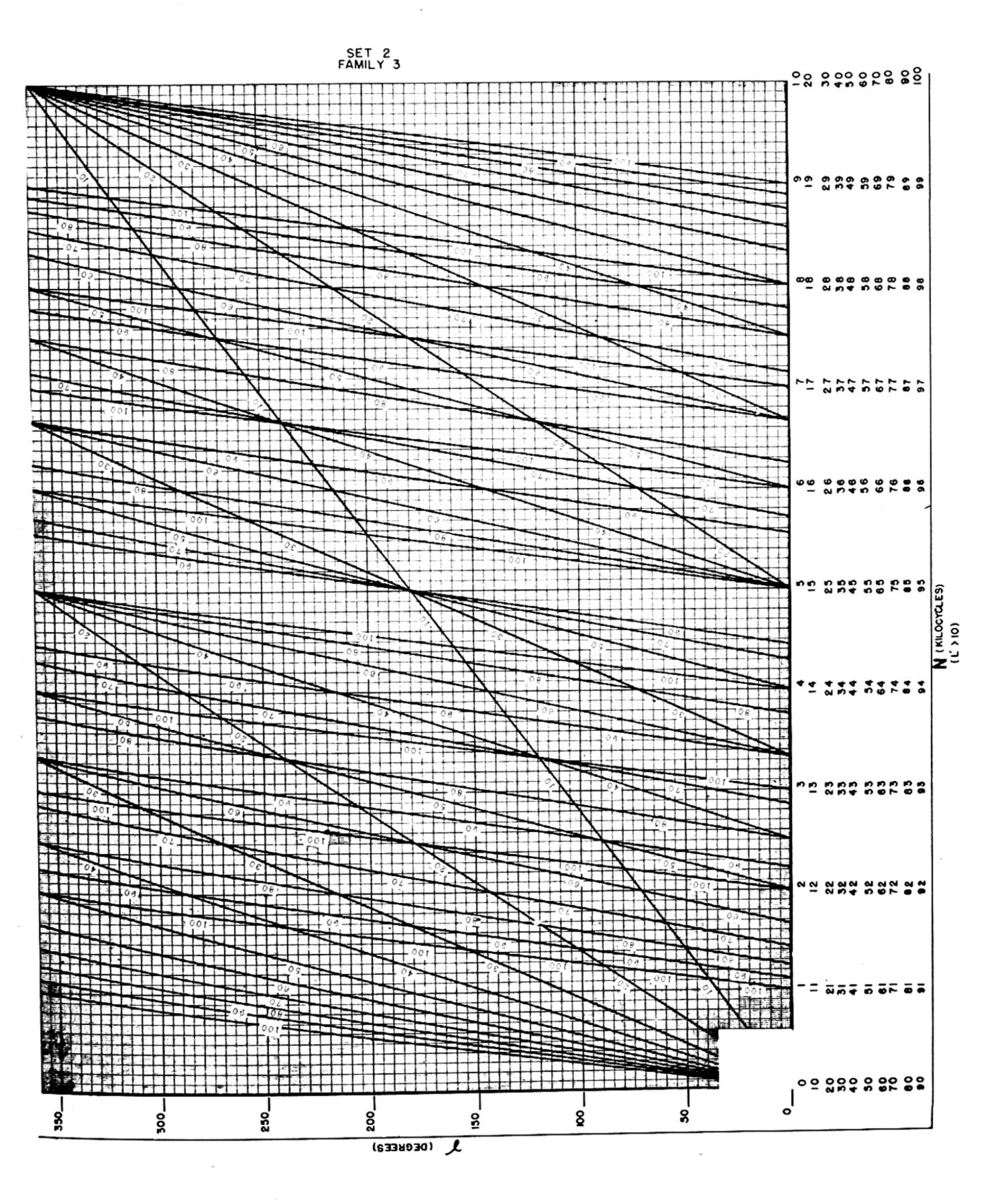


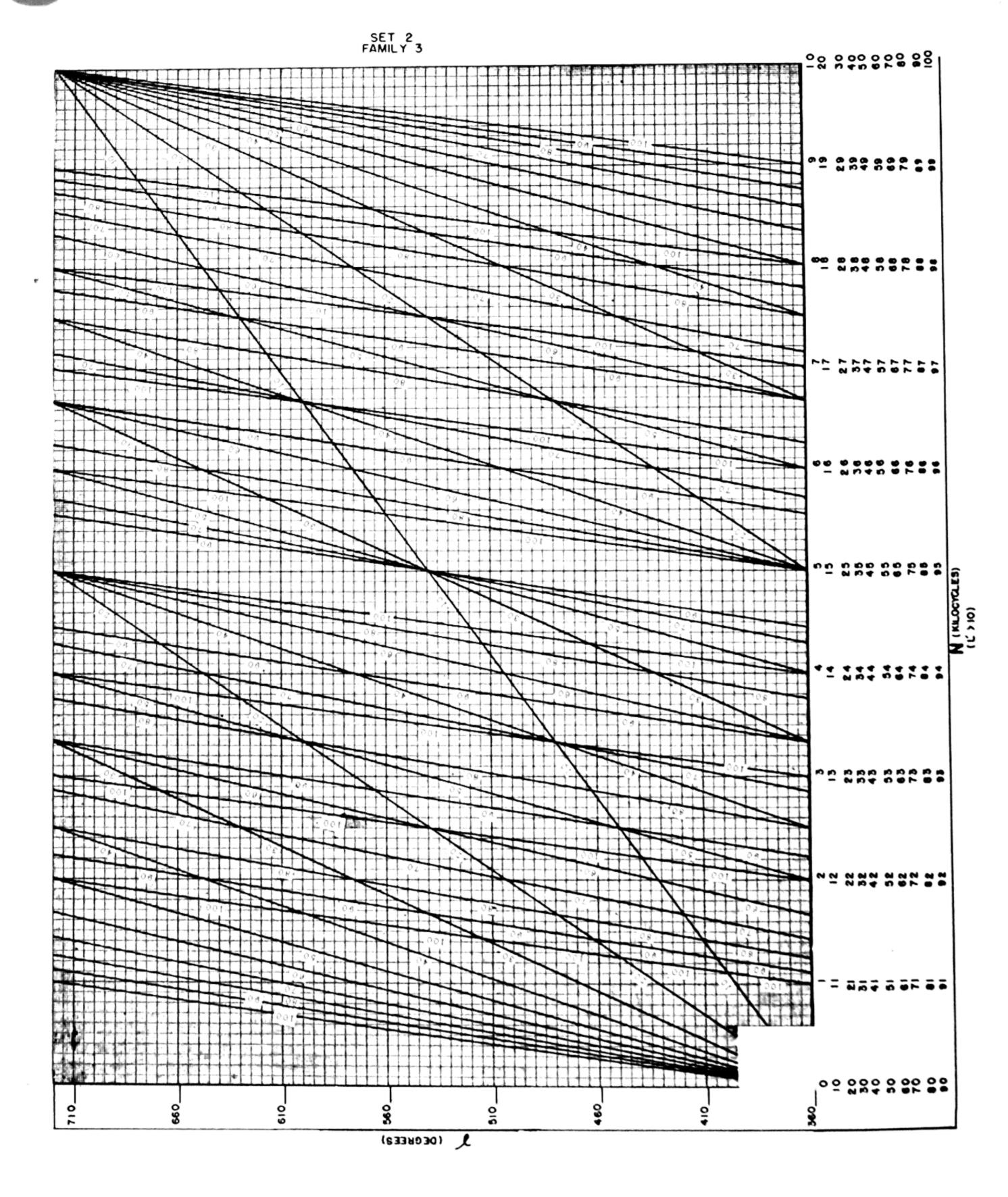


Д (DEGBEE3)



& (DEGREES)





SECTION 2 RESONANT FREQUENCY

In radiating systems (for example, many underwater projectors) where first consideration must be given to an efficient transfer of energy, it is desirable to operate in the neighborhood of a resonance. In other systems a flat response characteristic is desired and the system must be operated off resonance. In any case, the position of the resonances determines the frequency bands over which the system may be operated for a specific application. This is more fully discussed in Section 4.

The resonant frequencies may always be determined from a suitable reactance curve. When, however, a reactance curve is not needed, the curves of this section may be used to obtain values of the resonant frequencies directly. They apply to undamped systems composed of a crystal with a single backing material on either or both ends.

The curves given here are divided into several sets. The first two sets are plotted particularly for first and second resonances of ADP crystals (NH₄H₂PO₄) but also give a good approximation for Y-cut Rochelle salt. The last set is for determining all resonances of any crystal in combination with any backing material.

The first set of curves (page 12), consisting of one family, shows the variation of the first resonant frequency (in kilocycles) of a free ADP crystal as a function of the length of the crystal and its length-to-width ratio. The length of the crystal is plotted along the horizontal axis on a reciprocal scale for lengths of crystal from 1 cm to infinity. The frequency (in kc) of the first resonance is plotted along the vertical axis on a linear scale; the parameter from curve to curve is the length-to-width ratio.

The higher resonant frequencies of a free crystal with infirite length-to-width ratio are odd integral multiples of the fundamental. This condition is effectively reached for L/l_w ~3.0.

Each page of the second set* (pages 13 to 17) applies to a particular length of ADP crystal and covers both the situation in which plate

velocity in the backing material is used, and that in which longitudinal velocity in backing material is used. The abbreviations designate different backing materials as follows: AL, aluminum; ST, steel; BR, brass, and LE, lead. The subscripts 1 and 2 designate first and second resonant frequency respectively. Length and type of backing material for obtaining a given first and second resonant frequency may be obtained easily from these curves.

Interpolation between the longitudinal and plate cases is possible. See page 2, Section 1, for a discussion of the influence of the ratio of diameter to wave length on the effective velocity.

A comparison of the curves for first and second resonant frequencies shows that the ratio of frequencies of second to first resonance can be varied through rather wide limits.

Note that lead is much more effective in lowering resonant frequency than any of the other three metals, and that aluminum is as effective as steel in obtaining low resonant frequencies for backing lengths greater than 1.5 or 2 cm.

The plateaus occurring in the curves show that in certain regions the resonant frequency is insensitive to changes in the length of backing material. This property is very useful in designing systems in which both the first and second resonant frequencies are specified.

The third set of curves (page 18) consists of one family which can be used to obtain the resonant frequencies in the general case where a crystal has a single backing material on one end or on both ends. This set of curves is based on the following condition for resonance, which is derived in Part II, Section 4:

$$\gamma_c + \alpha_1 + \alpha_2 = n(180^{\circ})$$
 (1).

where n takes on integral values. Setting n equal to one provides the condition for the first resonance; n=2 the condition for the second resonance, etc. The subscripts 1 and 2 on α refer to material on ends 1 and 2 of the crystal.

^{*}These curves are plotted for the system free (not radiating). In many systems, immersion in water causes only a negligible shift in the resonant frequency. If it is suspected that an appreciable shift will be introduced by immersion, an impedance curve should be plotted. See Section 5.

By convention, end 1 will be the left end when the crystal-metal system lies along the X-axis. γ_c (the subscript c denotes crystal) is defined in Section 1 and may be evaluated from the curves given there.

 α (in degrees) is plotted along the vertical axis as a function of γ (in degrees). The parameter from curve to curve is the ratio of impedances $\frac{\rho_i V_i}{\rho_e V_e} \left(\frac{A_i}{A_e}\right) (i=1,2)$, where $\rho_i V_i$ is the characteristic impedance of the material on the ith end of the crystal, $\rho_{\epsilon}V_{\epsilon}$ is the characteristic impedance of the crystal, and A_{ℓ}/A_{ϵ} is the ratio of areas. A table of characteristic impedances is given on page 11 of this section.

A system using a given crystal material with a given backing material on only one end (let us say end 1) may be designed to have a specified first resonance by the following procedure (extension to nth resonance will be discussed later):

1. Choose a convenient length of crystal.

2. Evaluate γ_e (Section 1) for the particular crystal material at the desired resonant frequency.

3. From Eq. (1) calculate α_1 . (Since there is no backing on end 2, $\alpha_2 = 0$, and we have $\alpha_1 = 180^{\circ} - \gamma_{e}$

4. Calculate the parameter $\frac{\rho_i V_i}{\rho_c V_c} \left(\frac{A_i}{A_c}\right)$. ratio indicates which curve of the family

should be used.

5. The appropriate γ (the γ_1 for the backing material) is read from the intersection of the line for α_1 and the correct curve of the parameter.

6. Find the required length (cm) of backing

material from

$$L = \gamma_1 \frac{V}{360N(10)^3}$$
 cm

where V=velocity of sound in cm/sec in the material on end 1 (See page 3 for table of velocities)

N=desired resonant frequency in kc.

If the crystal is to have backing material on both ends, the length of one of the backing materials as well as a length of crystal must be chosen arbitrarily. Suppose the length of material on end 2 is chosen. After γ_2 has been obtained from Section 1 and the ratio $\frac{\rho_2 V_2}{\rho_c V_c} \left(\frac{A_2}{A_c}\right)$ evaluated, α_2 is read from the curves of Set 5

page 18. α_1 is then given by Eq. (1) as $\alpha_1 = 180^{\circ} - (\gamma_c + \alpha_2)$. The length of material for end 1 is determined as in steps 5 and 6 above.

In the event that α calculated from Eq. (1) is negative, the value of γ_c and/or the other α (if not zero) must be made smaller by choosing a shorter length of crystal and/or backing material.

The graph may be extended to cover the case of the nth resonant frequency, by adding $(n-1)(180^{\circ})$ to both the horizontal and vertical scales of the family and applying the condition

$$\gamma_c + \alpha_1 + \alpha_2 = n(180^\circ).$$

The graph has scales for obtaining both first and second resonant frequencies. Inner scales should be used for first resonance and outer scales for second resonance.

Several interesting effects are illustrated by the curves of this set. The rapid rise of the

curves for small γ and large ratios $\frac{\rho_i V_i}{\rho_c V_c} \left(\frac{A_i}{A_c}\right)$

indicates a rapid lowering of resonant frequency for small thicknesses of backing materials which have a characteristic impedance larger than the characteristic impedance of the crystal. The level portion near the center of the graph for the same materials is a region where the resonant frequency is relatively insensitive to changes in length of the backing material. There is another sensitive region for those materials as γ approaches 180°.

For materials of small ratios $\frac{\rho_i V_i}{\rho_c V_c} \left(\frac{A_i}{A_c}\right)$ the

sensitive region is in the center, and the insensitive region is near the ends.

An important factor limiting the operation of vibrating systems about a resonant frequency is the usable frequency band (usable band width). For example, the usable band width about the second resonant frequency varies from zero to a band as wide as that associated with the first resonance. If the designer wishes to operate the system in the region of the second resonance, he should make certain that the band is sufficiently wide for effective operation.

As the length of backing material decreases, the band width about the second resonance approaches zero, so that for a free crystal this particular resonance has disappeared entirely, and the next resonance above the first appears at a frequency three times that of the first resonance.

See Section 4 for a fuller discussion of band widths.

Obviously, the third set of curves in this section may also be used to obtain the resonant frequency of a system of given dimensions. For this purpose, a curve of resonant frequency

versus length of one of the elements must be plotted. Points for such a curve are obtained as follows:

- 1. Assume an arbitrary value for the resonant frequency.
- 2. Choose the length of some convenient element of the system as a variable and solve for this length as previously described.
- 3. Vary the assumed resonant frequency and calculate another length.

Two or three points obtained in this manner are usually sufficient to locate the resonant frequency of the given system.

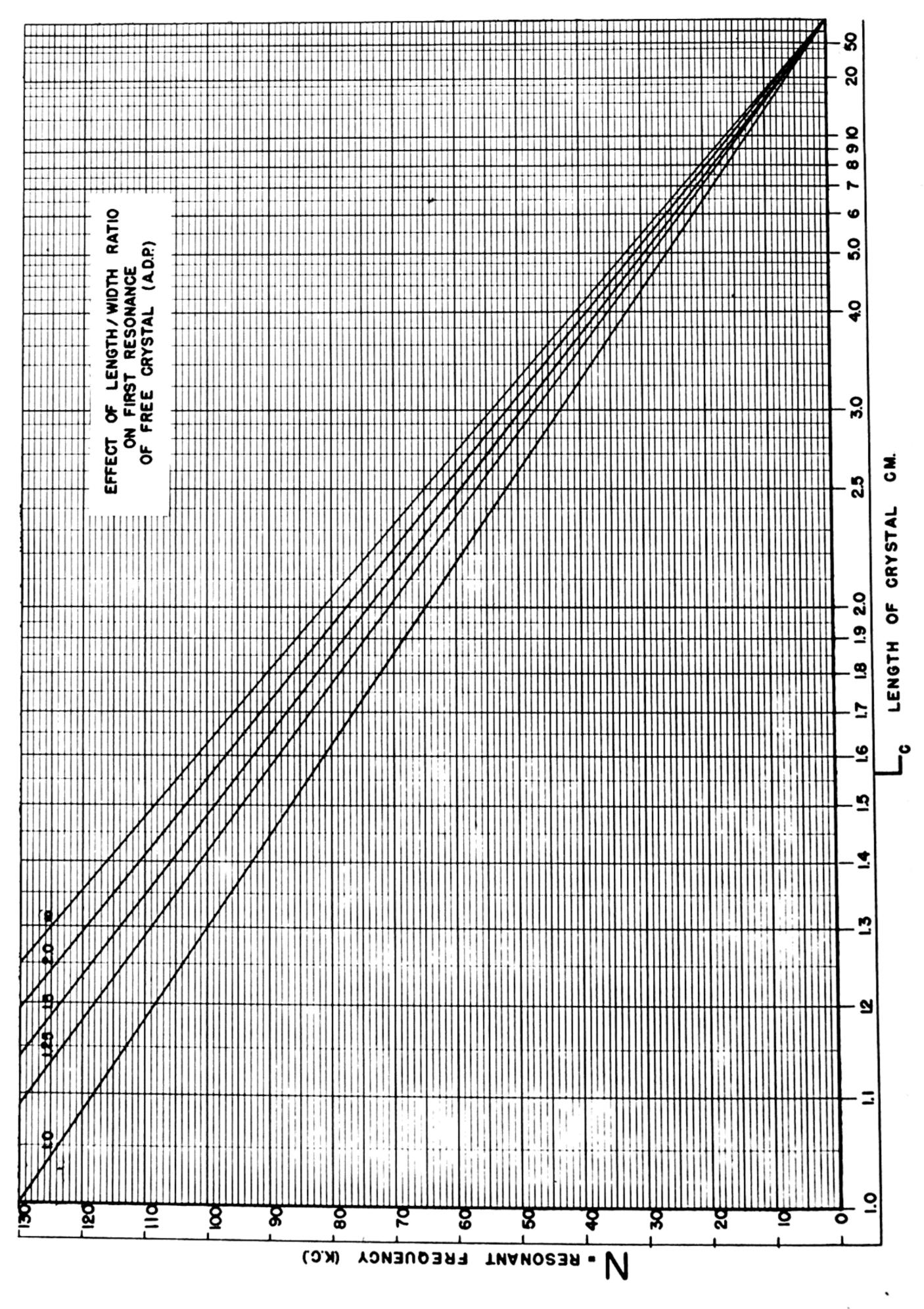
TABLE 2 CHARACTERTISTIC IMPEDANCE (ρV)

SOLIDS AND LIQUIDS

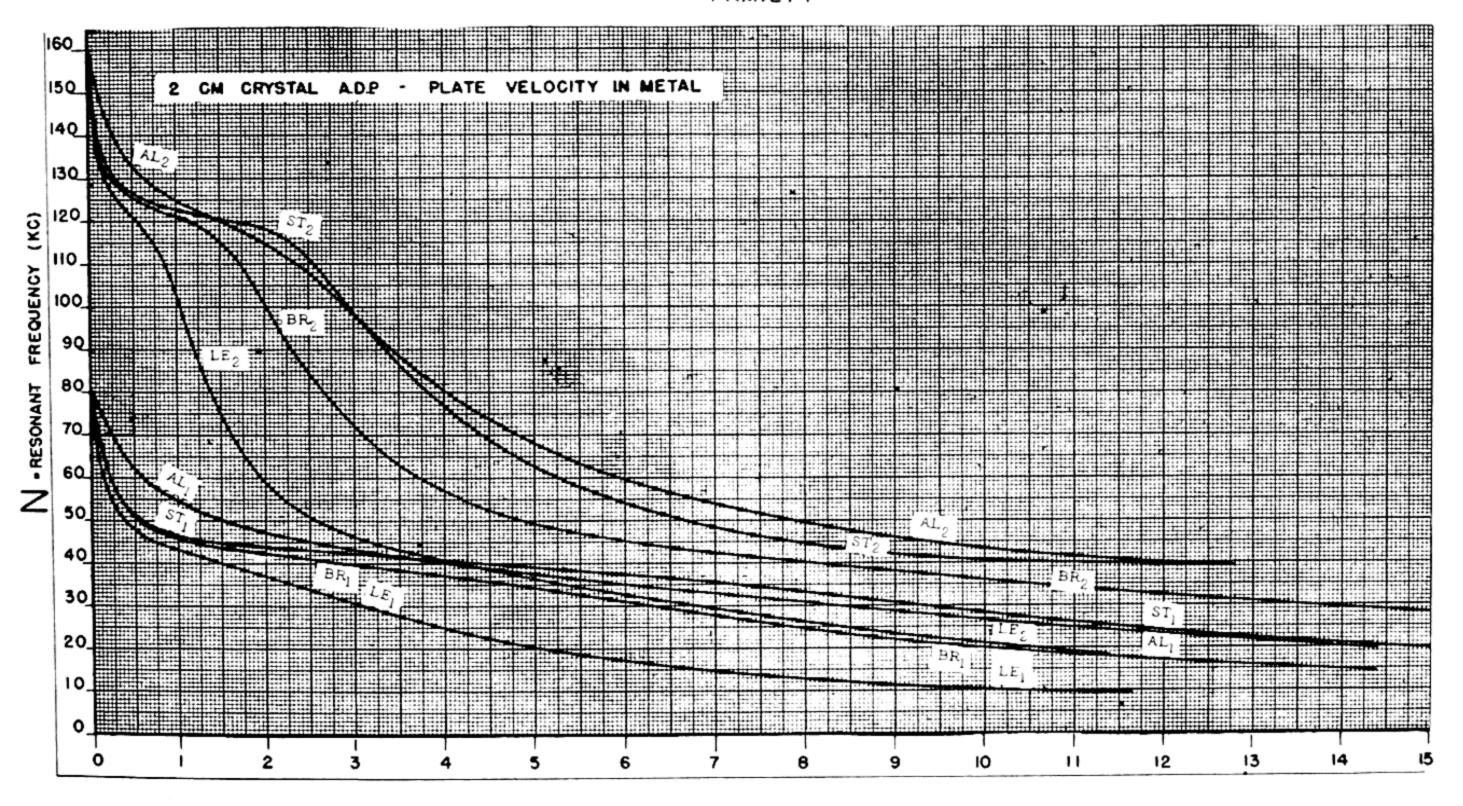
Material	Density p	Characteristic impedance ρV (bar velocity)	Characteristic impedance ρV (plate velocity)
	g/cm^3	$g/(cm^2sec.)$	$g/(cm^2sec.)$
Aluminum	2.65	$1.39(10)^6$	$1.70(10)^6$
Brass	8. 5	2. 90	3.61
Copper	8. 93	3. 20	4.11
Lead	11.4	1.42	2.73
Nickel	8.9	4. 23	4. 98
Steel	7.8	3. 93	4. 76
Glass	2.5-5.9	1. 12-3. 2	1. 2-3. 4
Magnesium	1.74	0.85	
Water (fresh)	1. 00	1. 43(10)5	
Water (sea)	1.00	1. 55	
Alcohol	0.79	1. 14	
Pentane	0.70	0. 53	
Mercury	13. 6	19. 8	
Air	$1.29(10)^{-3}$	43	

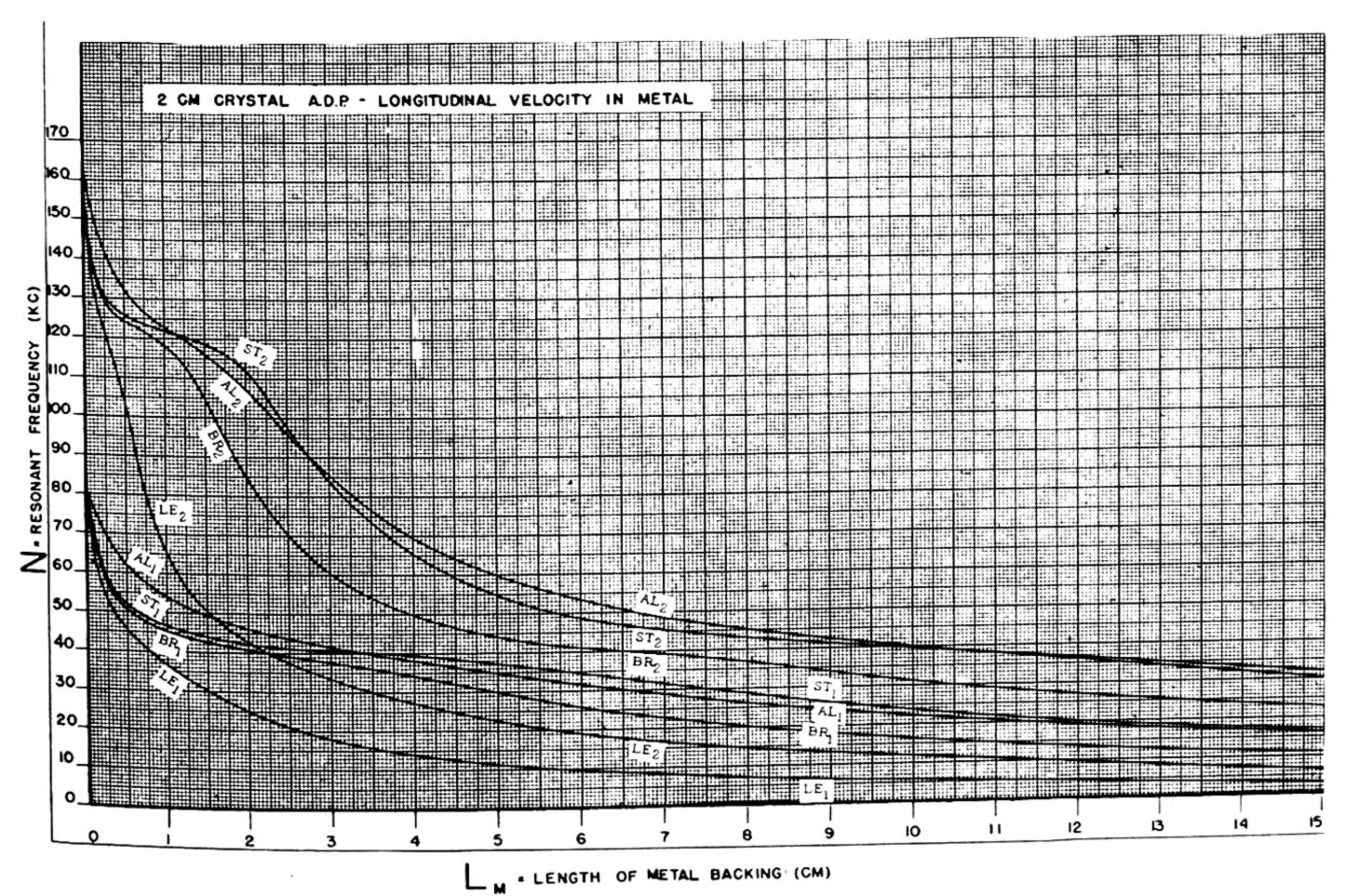
CRYSTALS

Plated crystal	Density p	Characteristic impedance ρV (bar velocity)
45° Z-cut ADP 45° Y-cut Rochelle 45° X-cut Rochelle X-cut Quartz Z-cut Tourmaline	g/cm ³ 1. 80 1. 77 1. 77 2. 65 2. 98-3. 2	g/(cm ² sec.) 5. 90(10) ⁵ 4. 37 Use graph page 4 14. 4

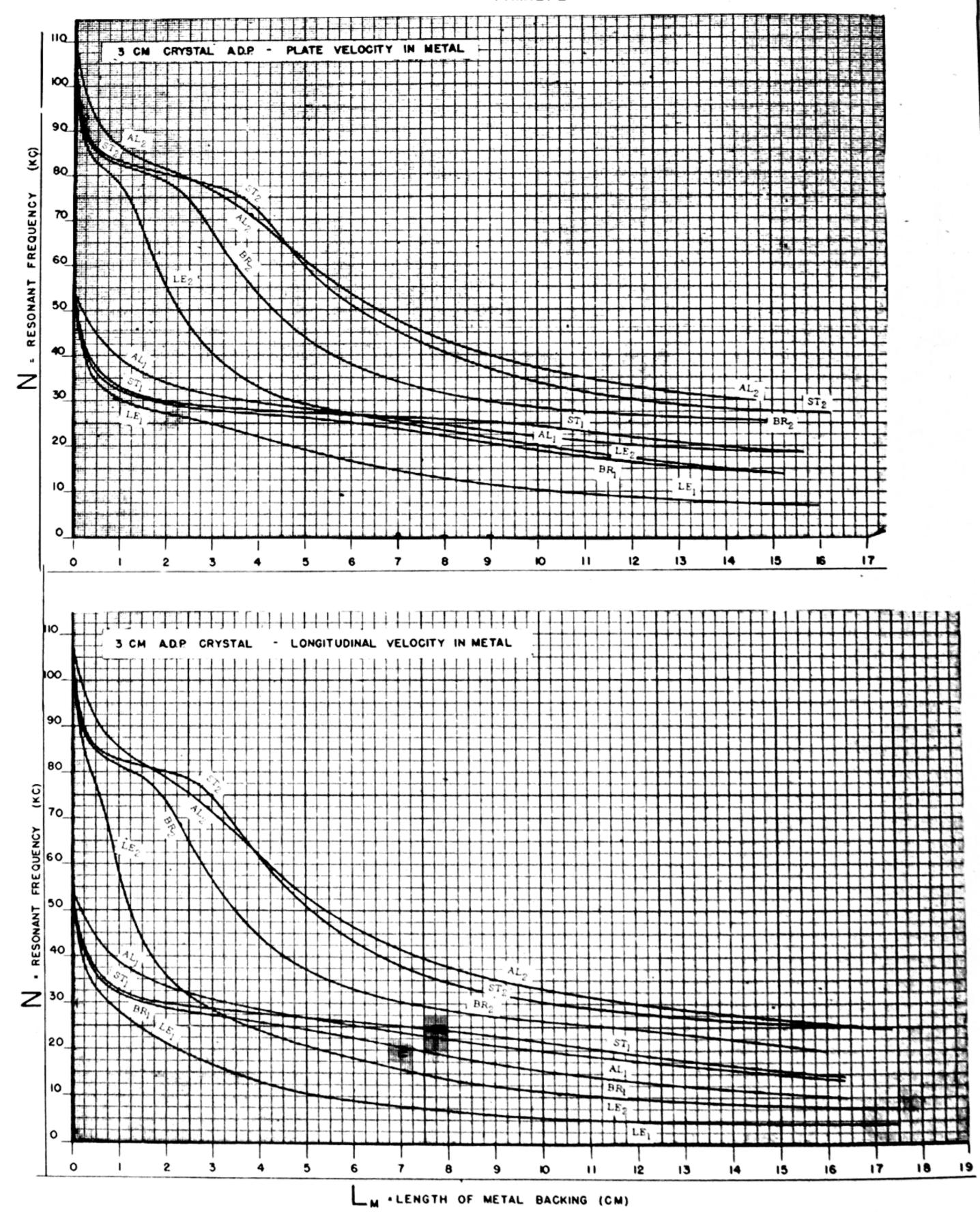


SET 4 FAMILY

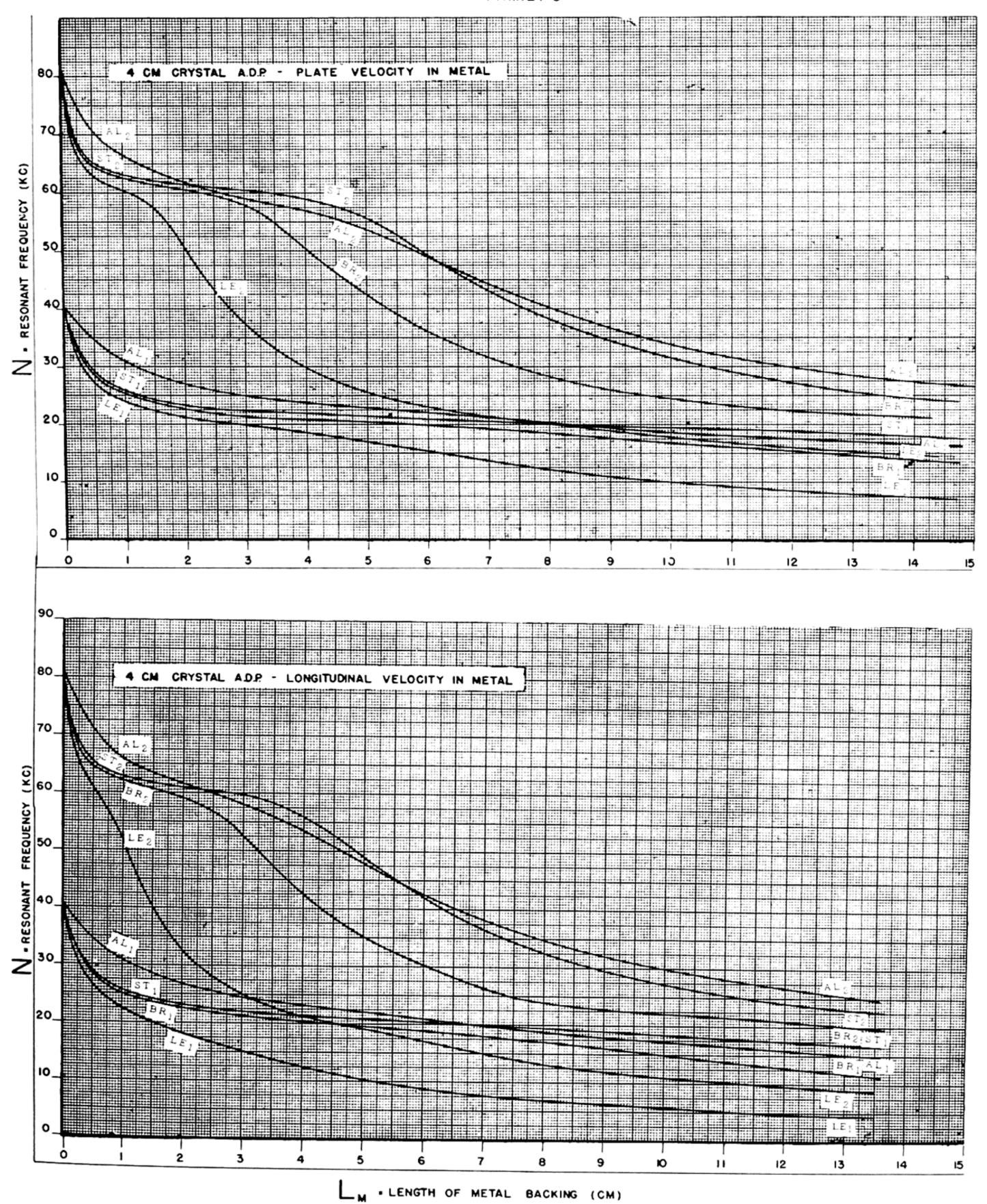




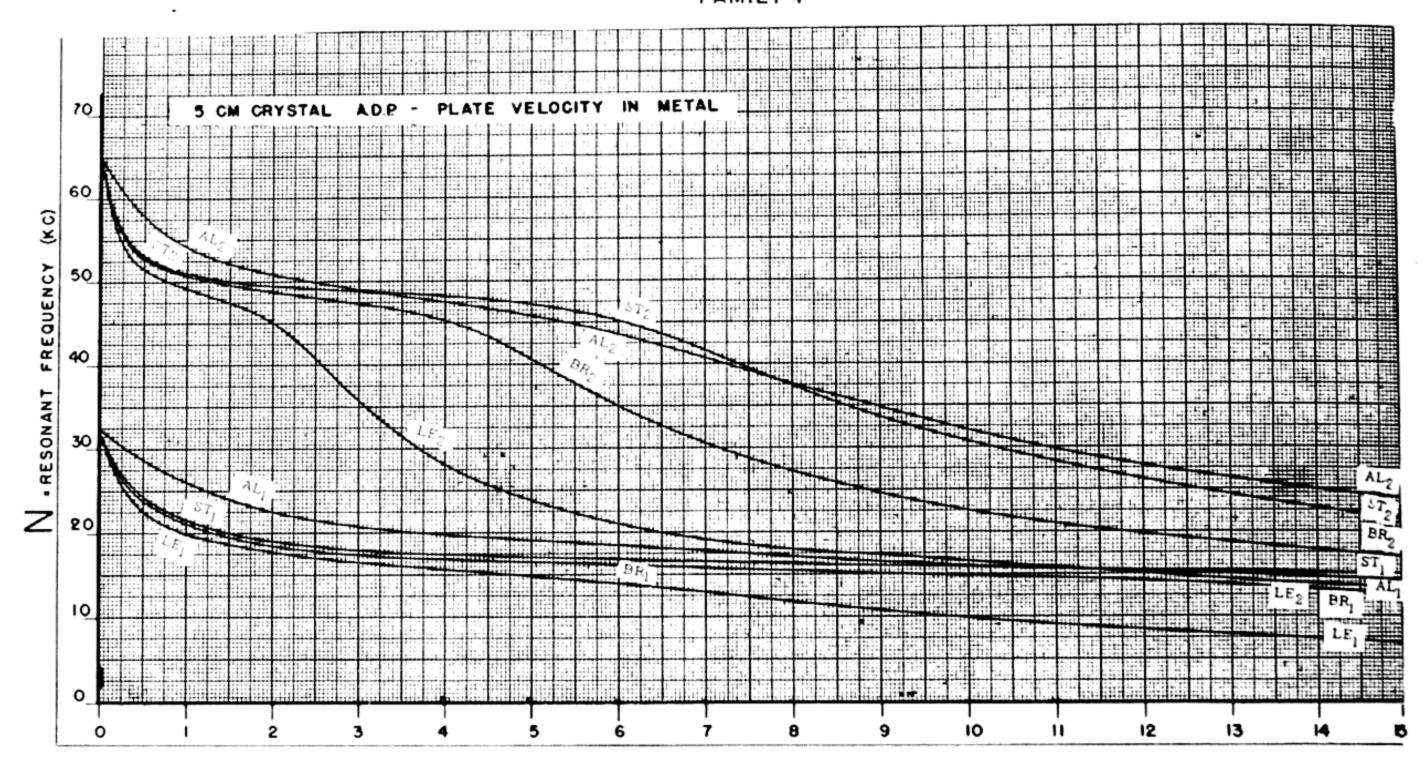


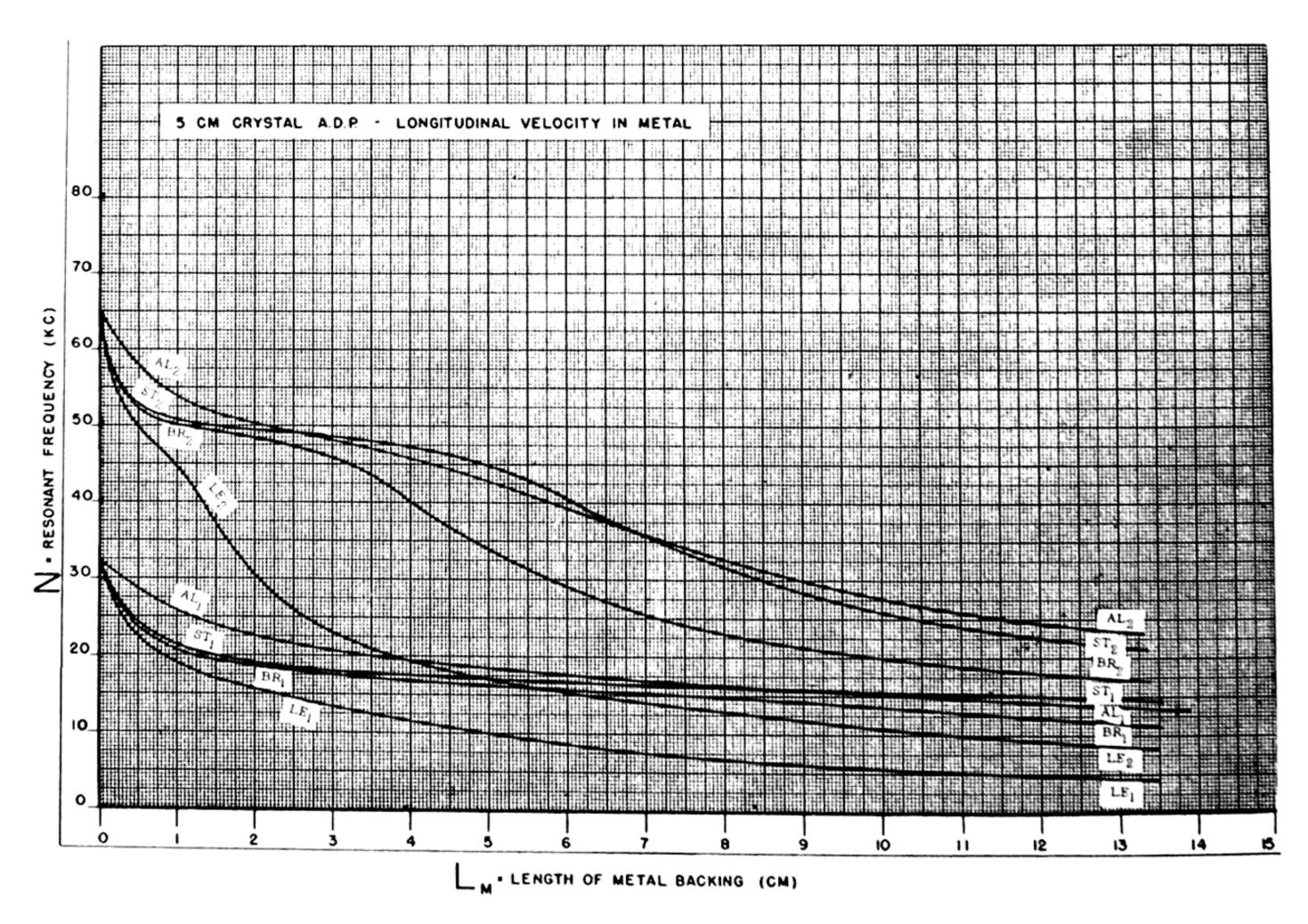


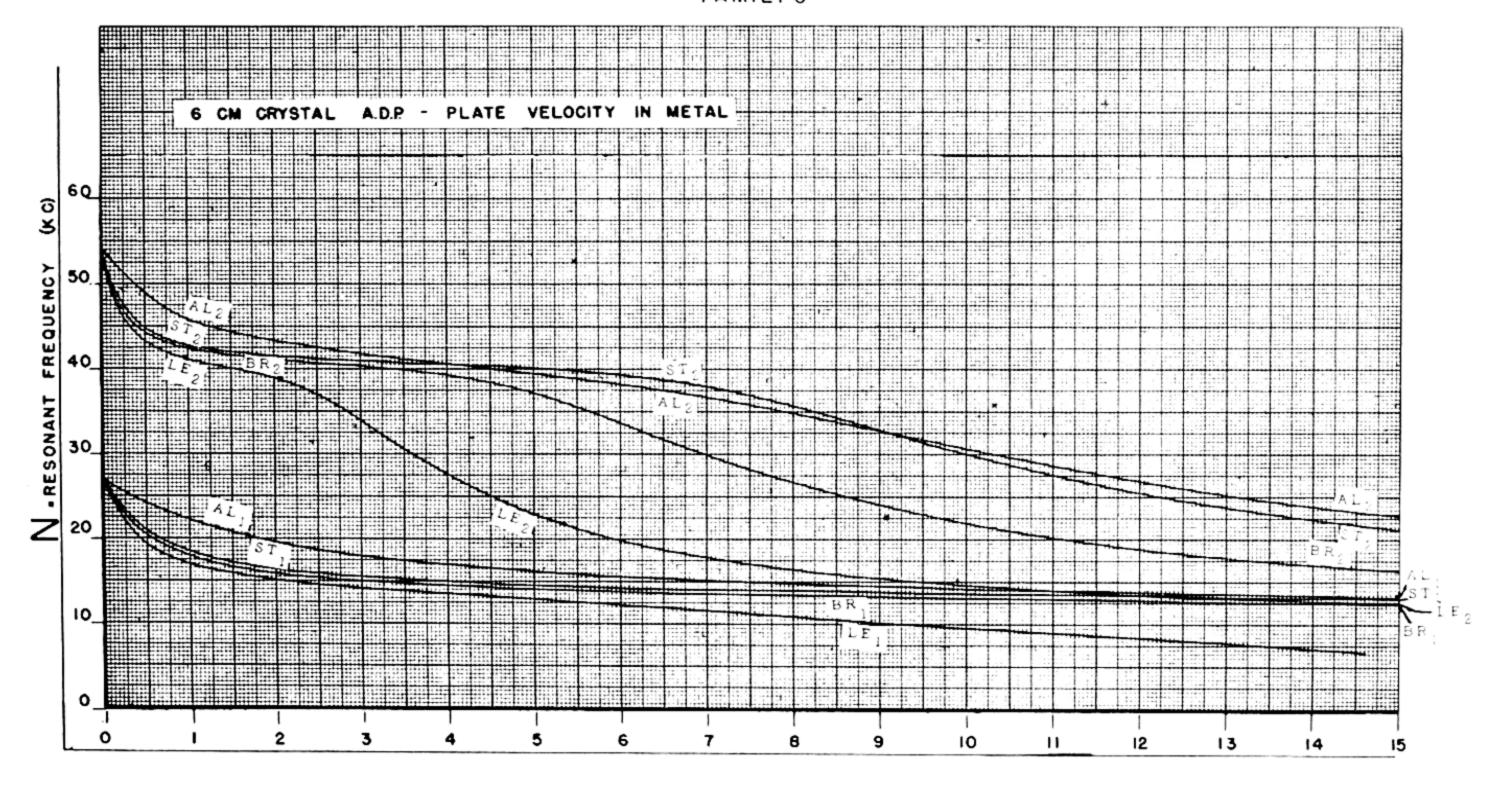
SET4 FAMILY 3

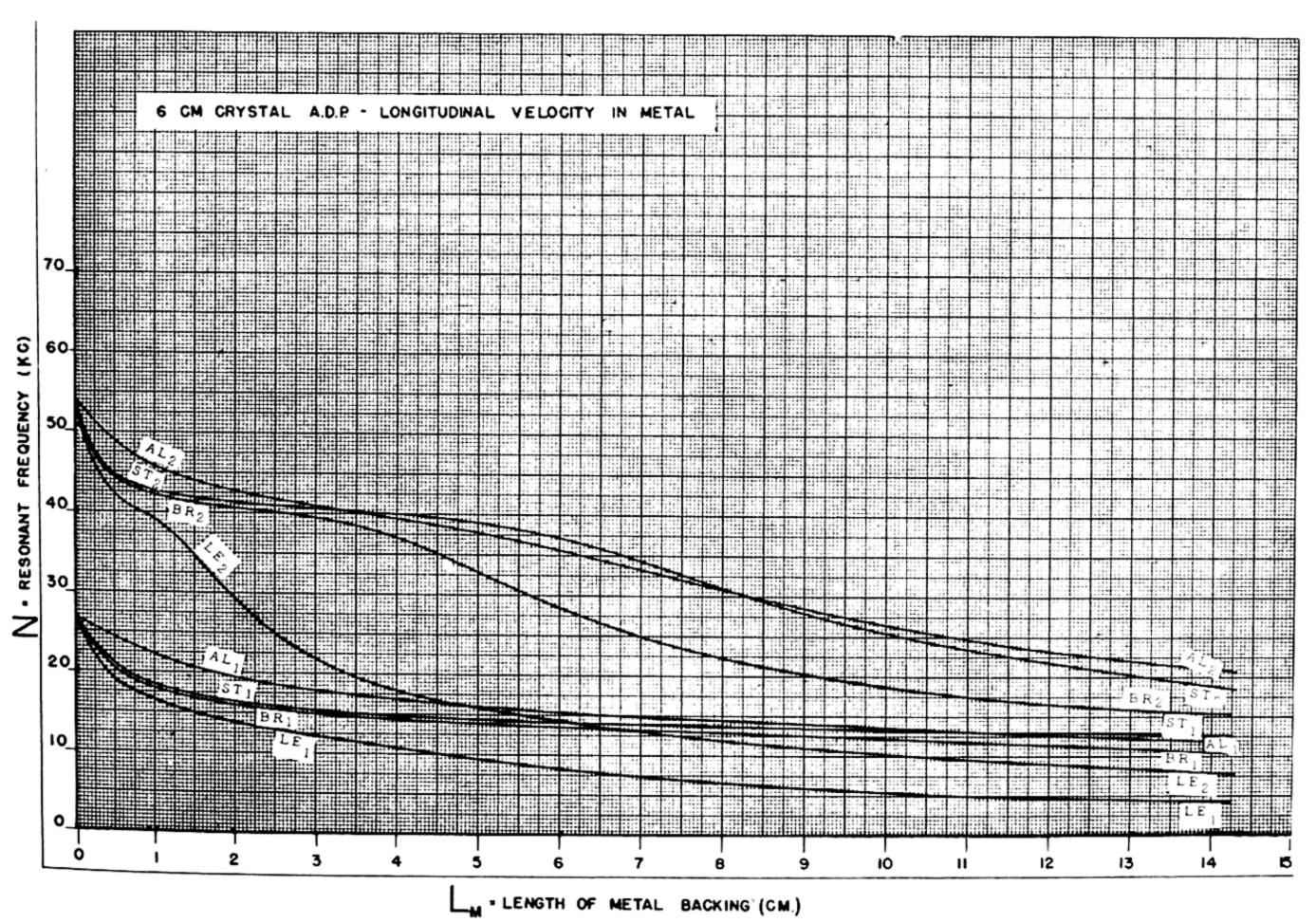


SET 4

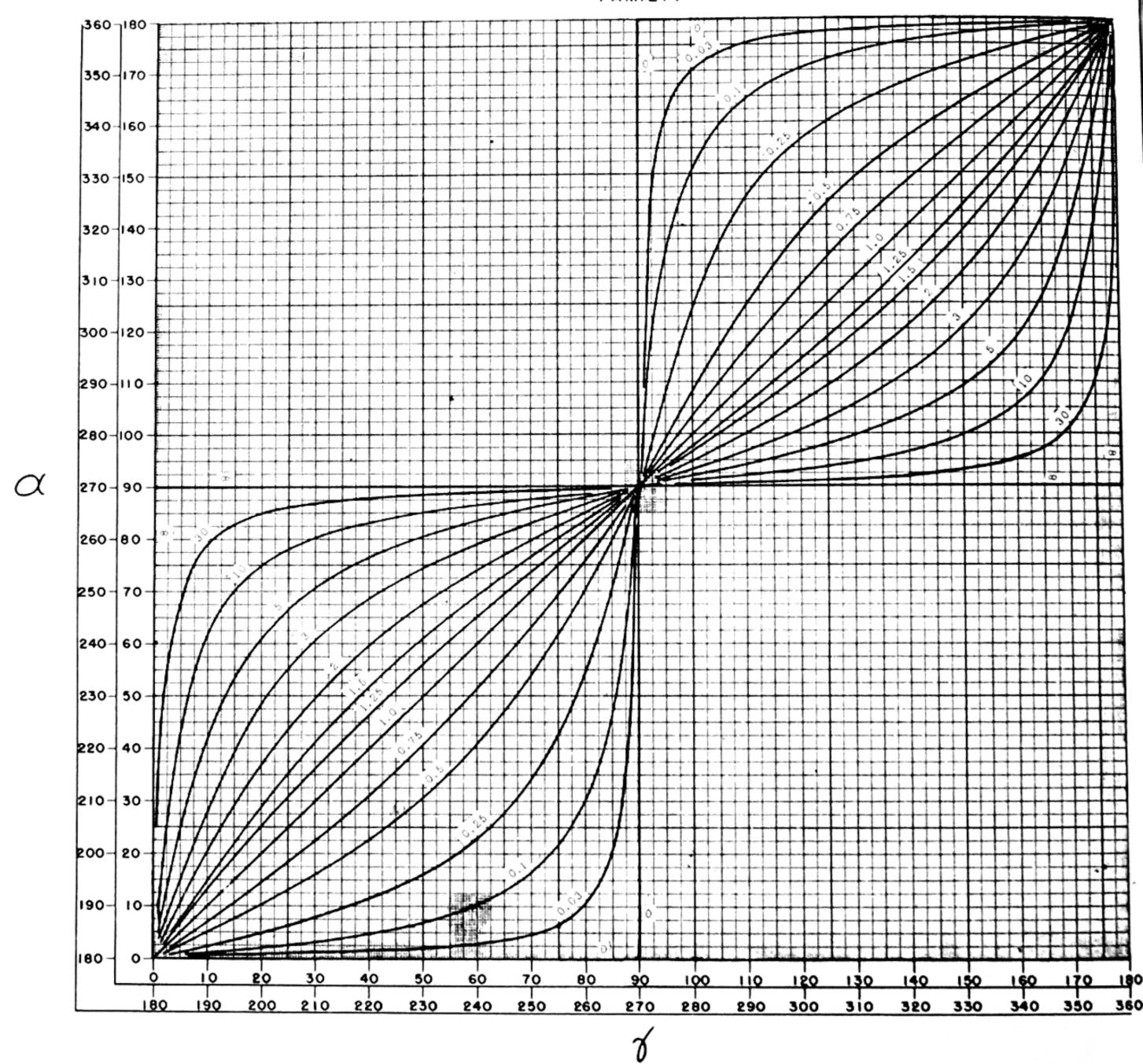












SECTION 3

ACOUSTIC IMPEDANCE OF BACKING MATERIAL COMBINATIONS

In any crystal system the resonant frequency, electrical input impedance, and response are determined to a great extent by the mechanical systems to which the crystal is coupled. Both the type of material and the geometrical configuration of the coupled system must be considered.

One-dimensional mechanical systems are conveniently characterized by the acoustic impedance, defined by $Z=P/\xi$, where P is the force per unit area (stress) and ξ is the particle velocity.*

The curves of this section, which are divided into two sets, permit the evaluation of the acoustic impedance of single or multiple-material backing systems. The first set (consisting of two families, pages 23 and 24) is for use with single-material backing systems terminated in a pressure release material, such as air or cork, and the second set (consisting of one family, page 25) is for use in evaluating the impedance of multiple systems and of single systems not terminated in zero impedance. Obviously, this second set could also be used for all single-material systems.

A table of the necessary physical constants is given in Appendix B.

The first set of curves, pages 23 and 24, shows the variation of the quantity $G_{1c}U_1$ plotted on a logarithmic scale along the vertical axis as a function of γ_m in degrees (obtained from Section 1). γ_m is the γ of the backing material. $G_{1c}=$

$$\frac{\rho_n V_n}{\rho_e V_e} \left(\frac{A_n}{A_e}\right)$$
 is the parameter from curve to curve.

The quantity $(G_{1c}U_1)$ is the acoustic impedance of the backing material at the crystal interface

multiplied by
$$\left(\frac{A_n}{A_c}\right)\frac{1}{\rho_c V_c}$$
 where A_n/A_c is the

ratio of the area of backing material driven by the crystal to the area of the crystal, and $\rho_c V_c$ is the characteristic impedance of the crystal (See Table 2, page 11, for values). If the ratio A_n/A_c deviates very far from unity, an estimate

should be made of the effective area driven by the crystal. This will not coincide with the geometric area. In general, elements of widely different areas should be joined not directly but by inserting a smoothly tapered section between them.

Four different scales are given for γ_m , and $G_{1c}U_1$ has four corresponding scales:

For $0^{\circ} \le \gamma_m \le 90^{\circ}$, read the values for $G_{1c}U_1$ as positive;

90° $\leq \gamma_m \leq 180$ °, read the values for $G_{1c}U_1$ as negative;

180° $\leq \gamma_m \leq 270$ °, read the values for $G_{1c}U_1$ as positive;

 $270^{\circ} \le \gamma_m \le 360^{\circ}$, read the values for $G_{1c}U_1$ as negative.

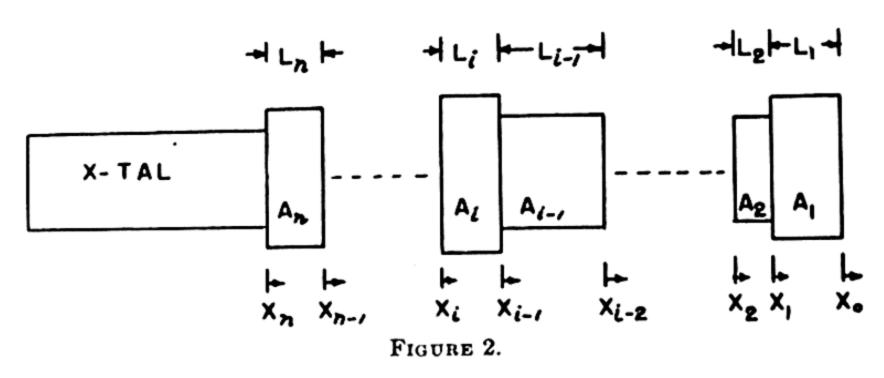
To obtain values of $G_{1c}U_1$ for values of G_{1c} not shown on the curves, the given values of G_{1c} can be divided or multiplied by any number if the vertical scale, $G_{1c}U_1$, is also divided or multiplied by the same number. The horizontal scale (γ_m) remains unchanged.

The second set of curves shows the variation of the quantity $X_i/\rho_i V_i$ plotted along the vertical axis as a function of γ_i , plotted in degrees along the horizontal axis. The parameter from curve to curve is the quantity $\frac{X_{i-1}}{\rho_i V_i} \left(\frac{A_{i-1}}{A_i} \right).$ γ_i is plotted in two scales, $0^{\circ} \le \gamma_i \le 180^{\circ}$, and $180^{\circ} \le \gamma_i \le 360^{\circ}$. When using the vertical scale, it should be noted that for values of $X_i/\rho_i V_i \leq -0.1$ and $X_i/\rho_i V_i \geq +0.1$ a logarithmic scale is used, and for $-0.1 \le X_i/\rho_i V_i \le +0.1$ a linear scale is used. This method enables one to plot the entire range of values of $X_i/\rho_i V_i$ on one sheet. The scale for the linear part of the curve was chosen to make the slope continuous.

A repetitive procedure is followed in using this set. Note that the zero boundary is the first boundary on the right. This places the nth boundary to the left of the nth material. The diagram (Fig. 2) illustrates the convention.

 X_o is the input reactance per unit area into the medium on the right of the first backing material. $X_o=0$ if the medium is a pressure-release material. X_i is the acoustic input

^{*}See P. M. Morse—Vibration and Sound, Chapter VI, McGraw-Hill Book Co.



impedance into the ith material at the ith interface. In general, if the total reactance at the zero boundary is X_{o_T} and the effective area of the medium driven by the material at this boundary is A_{o_T} , then $X_o = X_{o_T}/A_{o_T}$. Using the constants of the system and the calculated X_o , the parameter, $\frac{X_o}{\rho_i V} \left(\frac{A_o}{A_i}\right)$, is evaluated for the first material (i=1), and the curves of this set are used to find the value of X_1/ρ_1V_1 . The required γ is obtained from Section 1. Multiplying X_1/ρ_1V_1 by $\frac{\rho_1V_1}{\rho_2V_2}\left(\frac{A_1}{A_2}\right)$ gives the value of the parameter $\frac{X_1}{\rho_2 V_2} \left(\frac{A_1}{A_2}\right)$ to be used in calculating X_2/ρ_2V_2 , which is then multiplied by $\frac{\rho_2 V_2}{\rho_2 V_2} \left(\frac{A_2}{A_2}\right)$ to obtain the next parameter, etc. The process is repeated as often as necessary to obtain $X_n/\rho_n V_n$. Multiplying $X_n/\rho_n V_n$ by $j\rho_n V_n$ gives the reactance per unit area.

In projector design it is convenient to use the quantity $G_{1e}U_1$, which is the load per unit area of the crystal divided by the characteristic impedance of the crystal, and is given in terms of $X_n/\rho_n V_n$ by the following relation:

$$G_{1c}U_{1} = \left(\frac{\rho_{n}V_{n}}{\rho_{c}V_{c}}\right)\left(\frac{A_{n}}{A_{c}}\right)\left(\frac{X_{n}}{\rho_{n}V_{n}}\right)$$

where $\rho_n V_n$ is the characteristic impedance of the medium next to the cyrstal, A_n is the area of the medium (per crystal) next to the crystal, $\rho_c V_c$ is the characteristic impedance of the crystal, A_c is the area of the crystal, and $X_n/\rho_n V_n$ is the quantity obtained from the curve. Notice that if the areas of the backing materials are all equal, all ratios $A_{1-1}/A_1=1$ with the possible exception of A_0/A_1 .

The following form of table (Fig. 3) has been found convenient in recording values obtained from these curves.

Input impedances have been calculated for the three systems given below to illustrate the use of the curves. See Table 3 for a sample table of calculations, and page 22 for a comparison of the impedances. Additional illustrations are furnished by the curves of particular systems in Section 8. The following systems are free on one end.

Example 1: Calculate the input impedance per unit area into the steel end of a steel-aluminum combination as illustrated in Fig. 4-a. The effective velocity here is the longitudinal bar velocity.

The calculations are given in Table 3 on page 21, and the quantity X_2/ρ_2V_2 (the input im-

N	٧,	۵ ₂	8 _N	x .	<u>X</u> 6,7,	<u>X</u>	g _e u _i
FREQ. K.C.	Lı	Lg	LN	,			X A.

FIGURE 3.—Table illustrating arrangement of work.

pedance of the system divided by the characteristic impedance of steel) is plotted on page 22 as a function of frequency.

Example 2: Calculate the input impedance per unit area into the aluminum end of the same combination as Example 1 (see Fig. 4-b). The quantity plotted on page 22 is $X_2/\rho_2 V_2$ where $\rho_2 V_2$ is the characteristic impedance of aluminum.

Example 3: Calculate the input impedance per unit area into the aluminum end of the aluminum-lead system illustrated in Fig. 4c. Longitudinal bar velocity is again the effective velocity. The quantity $X_2/\rho_2 V_2$ is plotted on page 22.

Notice that the input impedance in this system is the same from either end because the characteristic impedances of lead and aluminum are practically equal when the longitudinal bar velocities are used.

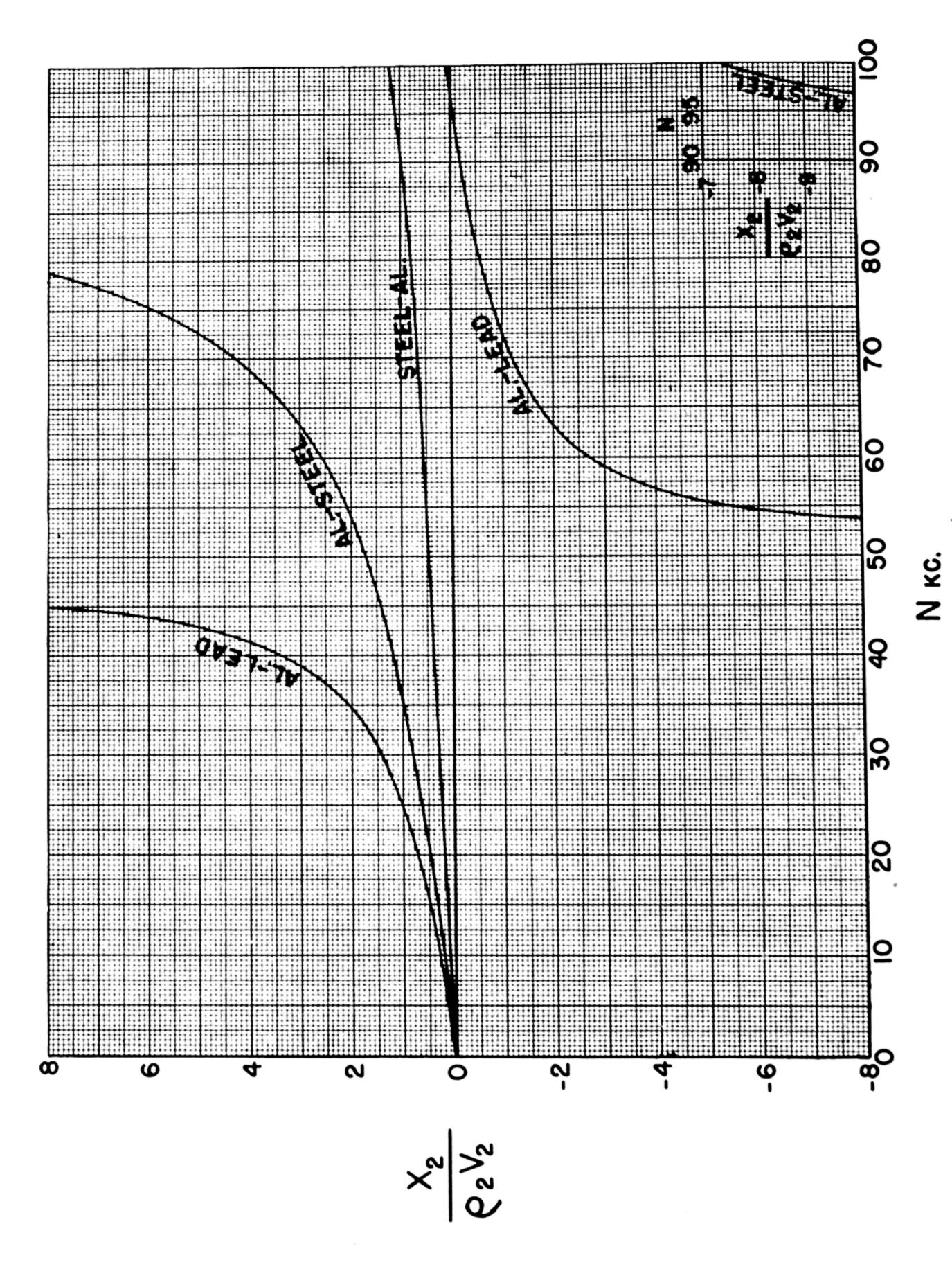
	STEEL	ALUM.
	O.5 CM.	0.5 CM.
•		(a)
í	ALUM.	STEEL
-	0.5 CM.	0.5 CM.
,		(<i>b</i>)
	•	
	ALUM.	LEAD
	0.5 CM.	0.5 CM.
		(C)

FIGURE 4.

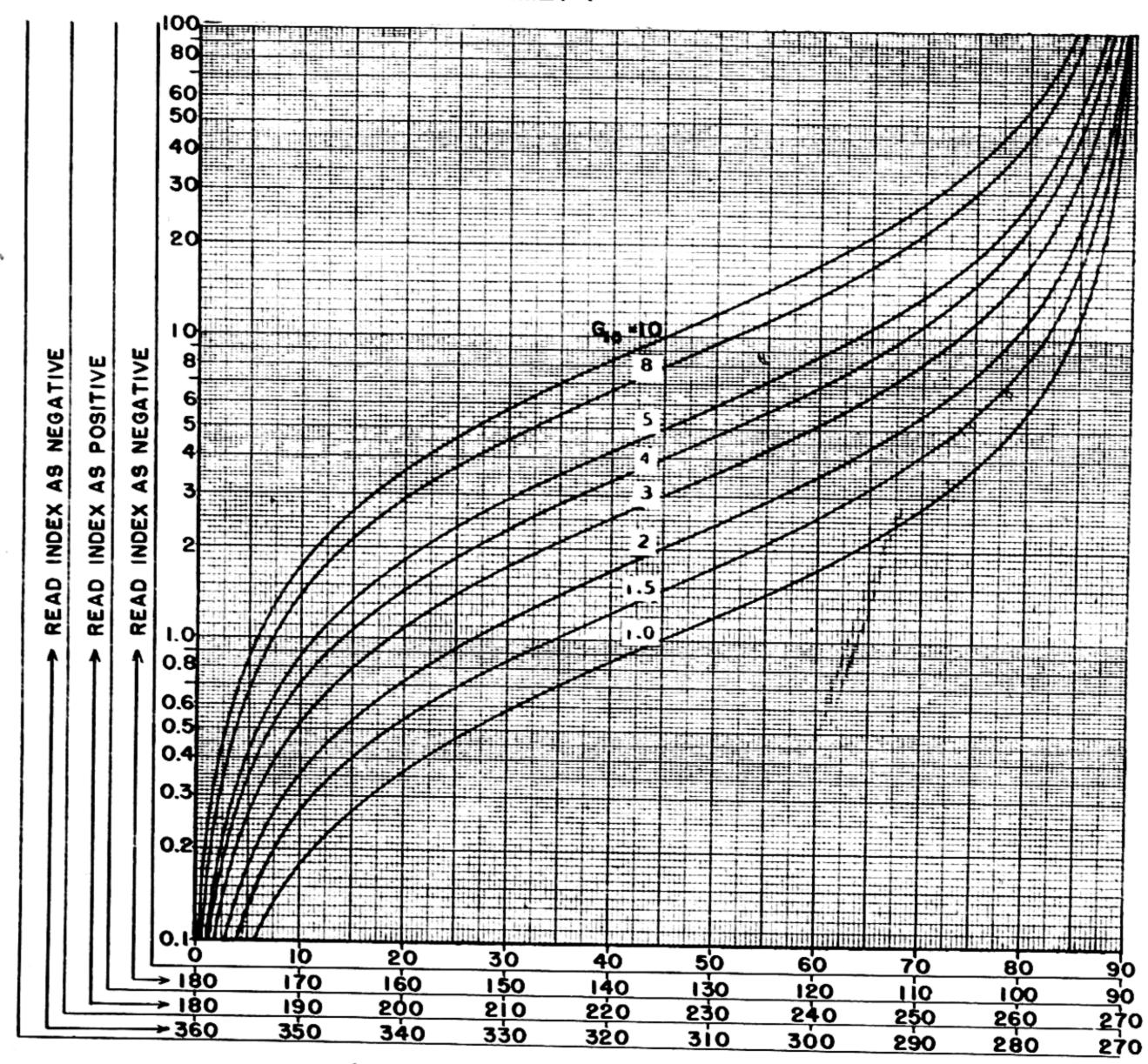
TABLE 3

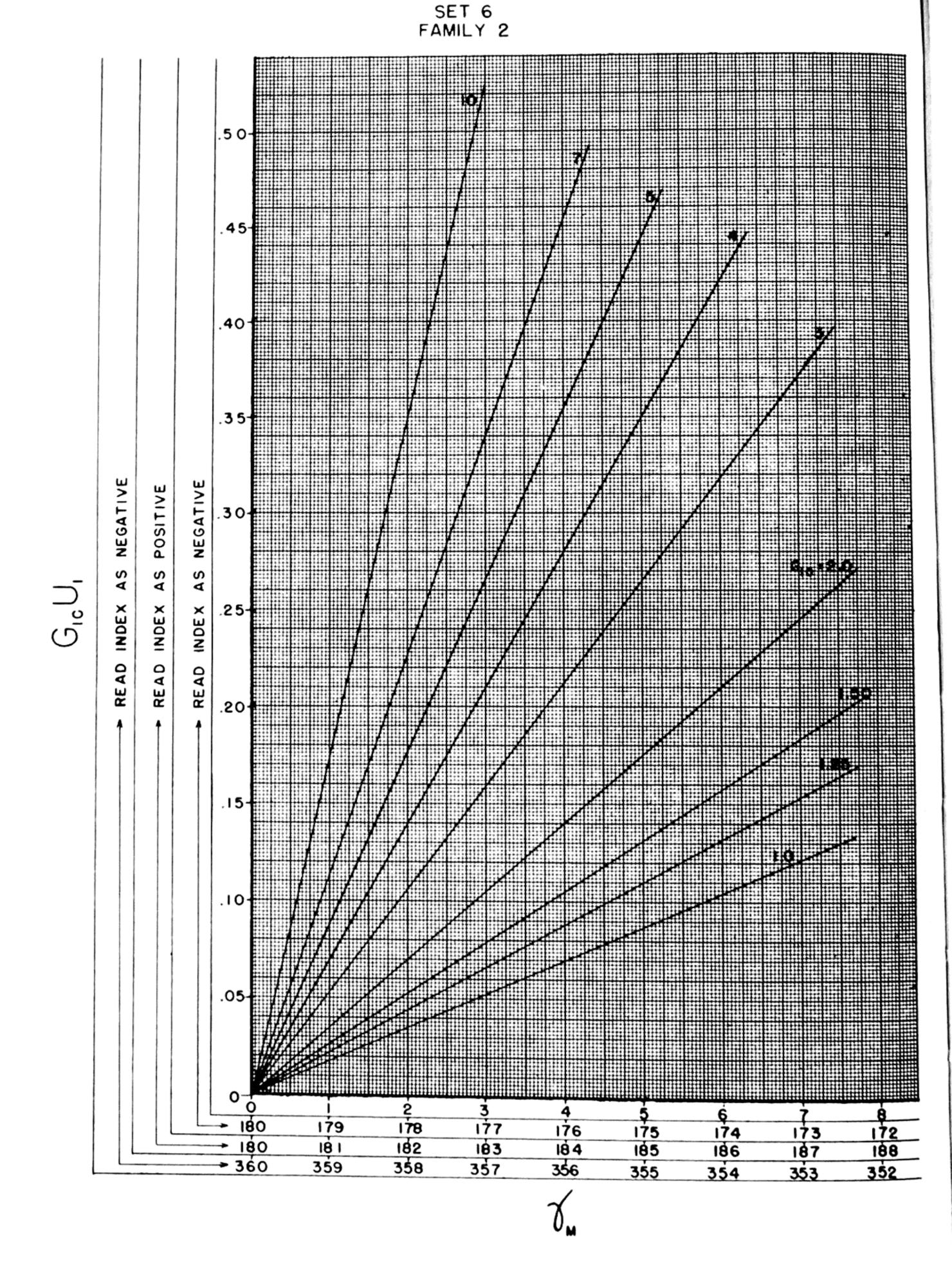
 $L_1 = 0.5 \text{ cm.}; L_1' = 0.096$ $L_2 = 0.5 \text{ cm.}; L_2' = 0.100$ $\rho_1 V_1/\rho_2 V_2 = 0.354; A_1/A_2 = 1.0$

N freq. Kc.	γι	γ2	X_{0}	$\frac{X_1}{\rho_1 V_1}$	$\frac{X_1}{\rho_2 V_2} \left(\frac{A_1}{A_2}\right)$	$\frac{X_2}{\rho_2 V_2}$	$G_{1\epsilon}U_{1} = \frac{X_{2}}{\rho_{\epsilon}V_{\epsilon}} \left(\frac{A_{2}}{A_{\epsilon}}\right)$
10	3. 4	.4.0	0	0. 06	0. 02	0. 10	0. 73
15	5. 1	5. 5	0	. 09	. 03	. 13	. 95
20	6. 9	7. 0	0	. 12	. 04	. 17	1. 24
25	8. 6	9. 0	0	. 145	. 05	. 22	1. 60
30	10.4	11.0	0	. 18	. 06	. 26	1. 89
35	12. 1	12. 5	. 0	. 215	. 08	. 30	2. 18
40	13.8	14. 0	0	. 25	. 09	37	2. 69
45	15. 5	16. 0	0 ,	. 285	. 10	. 41	2. 98
50	17. 2	18.0	0	. 315	. 11	. 46	3. 35
55	19.0	20.0	0	. 35	. 12	. 53	3. 86
60	20.7	21. 5	0	. 38	. 13	. 56	4. 08
65	22.4	23. 5	0	. 41	. 14	. 61	4. 44
70	24. 1	25. 0	0	. 44	. 15	. 66	4. 80
75	25. 9	27. 0	0	. 49	. 17	. 75	5. 46
80	27.6	29. 0	0	. 52	. 18	. 81	5. 90
85	29. 4	30. 5	0	. 56	. 20	. 88	6. 41
90	31.0	32. 0	0	. 60	. 21	. 96	7. 00
95	32. 8	34. 0	0	. 65	. 23	1. 07	7. 79
100	34. 5	36. 0	0	. 69	. 24	1. 20	8. 74

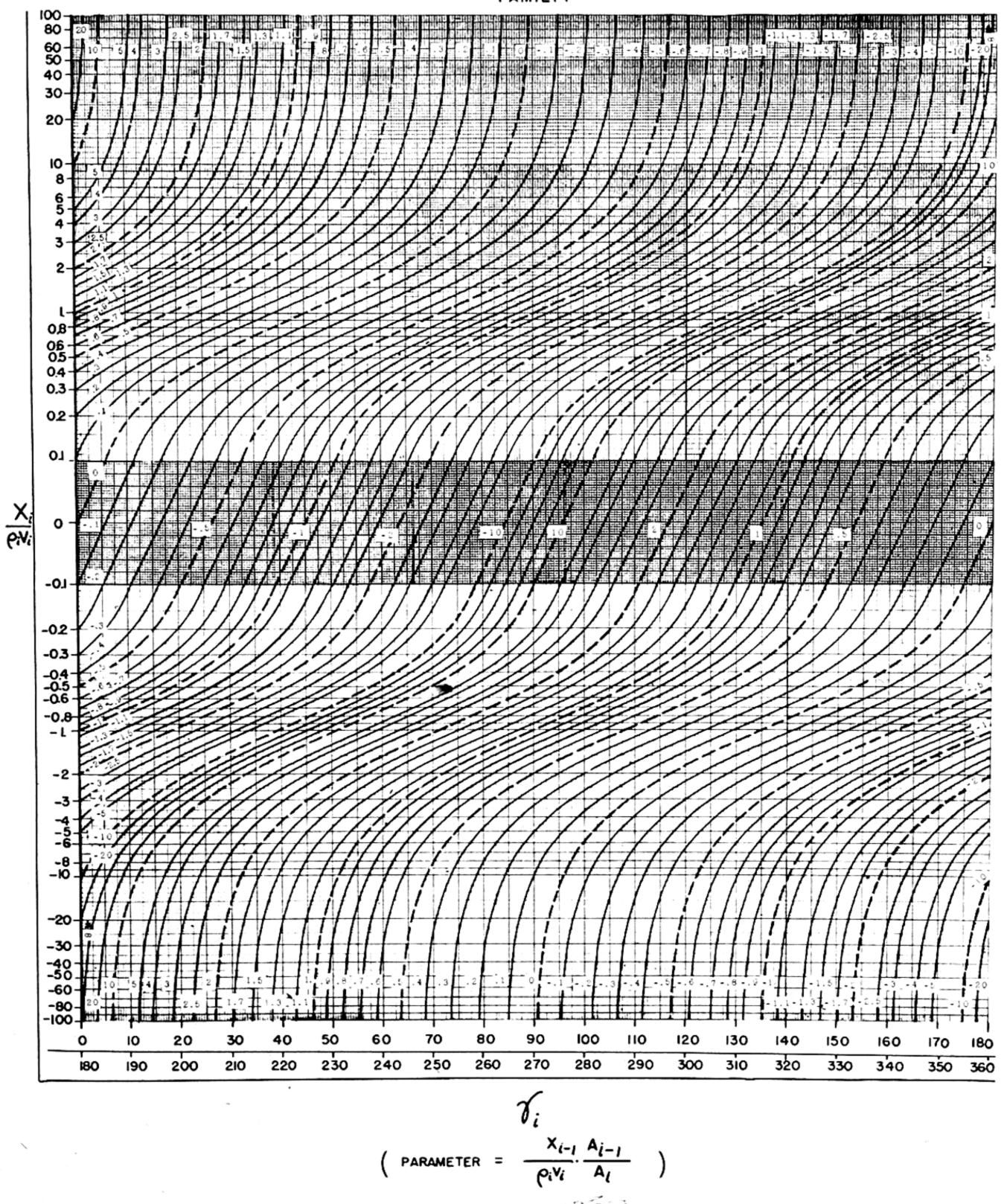


SET 6 FAMILY I









THE JAMMU & KASHMIR UNIVERSITY LIBRARY.

DATE LOANED

Vol	
Accession No.	

SECTION 4

RESONANT FREQUENCIES OF SYSTEMS WITH MULTIPLE-MATERIAL BACKING

In Section 2 curves are given for obtaining the resonant frequencies of a system in which the crystal is coupled to a single backing material. However, in designing a system to have several given resonant frequencies and given band widths about these frequencies, a combination of several backing materials is often desirable. This section enables the designer to evaluate the electrical resonant frequencies of these multiple systems and to obtain, at the same time, values for the approximate band widths of the transmitting response and receiving sensitivity.

Curves of the resonant frequency of the system as a function of the elastic constant of one of the components of the system may also be plotted. Such curves are useful in determining elastic constants dynamically when the material to be measured cannot be fastened directly to the crystal. They also enable one to choose a configuration for which the resonant frequencies of the system are sensitive to changes in the elastic constant of the material under measurement.

To find the resonant frequencies of undamped systems with multiple backing, the curves of this section (consisting of a single family, page 32) must be used with those on acoustic impedance (Sets 6, 7) given in Section 3.

A damping medium usually has a negligible effect on the resonant frequency, but if it is necessary to consider the shift caused by damping, the methods of Section 5 are applicable.

The motional reactance X_0/Z_0 (see Part II, Section 2 for theory) is plotted on page 32 as a function of γ_c (obtained from Section 1). The quantity G_{2c} (tabulated in the upper left corner) is determined by the medium into which the system is radiating. When the radiation is zero, $G_{2c}=0$. The parameter from curve to curve is the quantity $G_{1c}U_1$, defined in the preceding section. Curves for evaluating this quantity are given in Section 3.

Notice that the curves are labeled only for positive values of the parameter $G_{1c}U_1$. With these positive values the inner scales along the

axes should be used; that is, the scales in which γ_{ϵ} increases from left to right and X_0/Z_0 increases from the bottom of the page to the top. For negative values of $G_{1\epsilon}U_1$ the two outer scales for γ_{ϵ} and X_0/Z_0 are used.

The positions of the vertical asymptotes of the X_0/Z_0 curves are indicated on the horizontal axis by dotted lines and appropriate labels.

Figure 5 shows a convenient arrangement for the work.

N kc.	γο	$G_{1\epsilon}U_{1}$	X_0/Z_0

FIGURE 5.

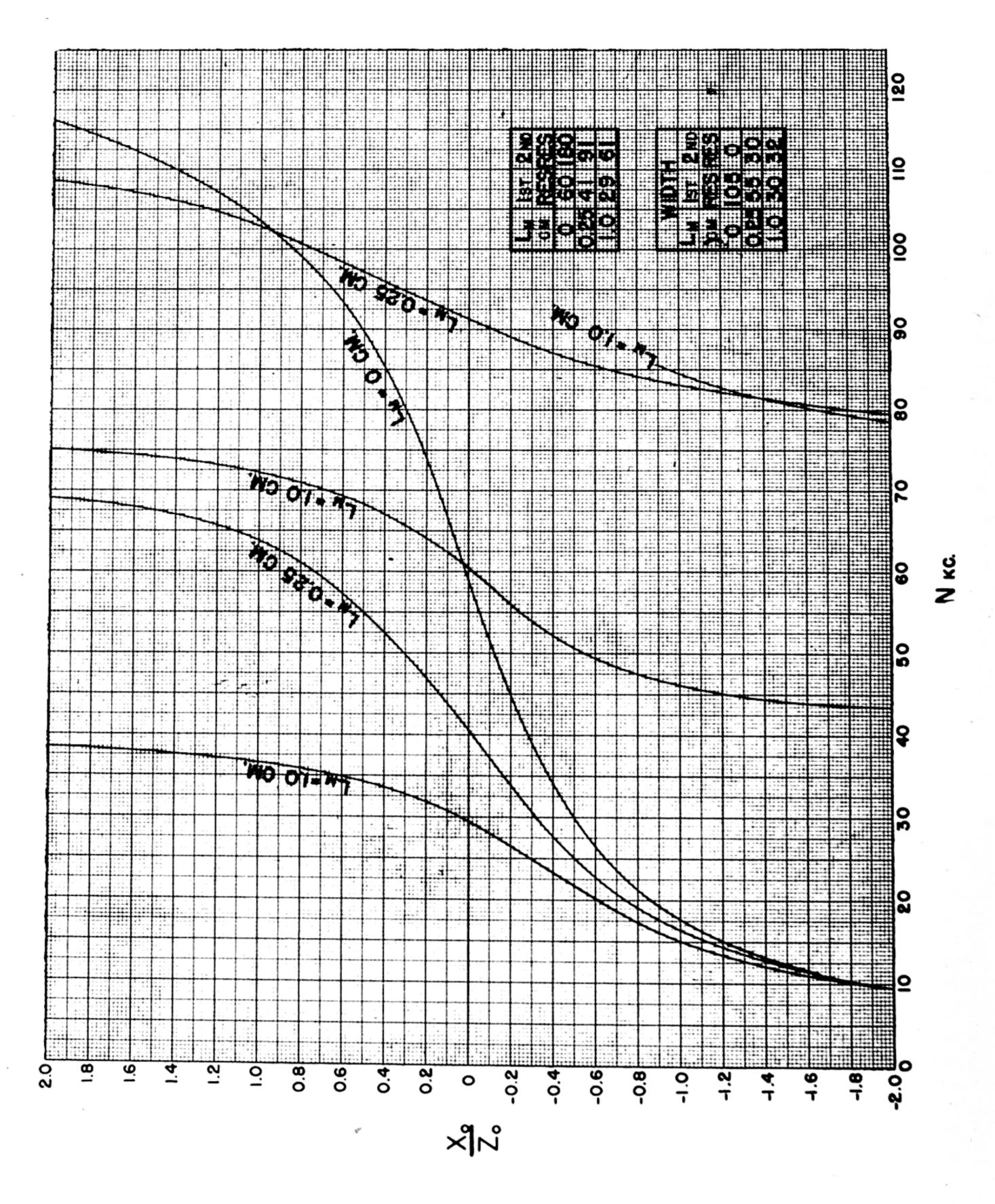
The family of curves given in this section is used to obtain a single curve of X_0/Z_0 vs. N for the particular system under consideration. The positions of the zeros of this X_0/Z_0 curve give the resonant frequencies of the system. The asymptotes of this curve locate the approximate positions of the minima in the transmitting response and in the receiving sensitivity. Since each resonant frequency is enclosed between two such minima, it is clear that the spacings of the minima determine, to a great extent, the usable band width about each resonant frequency.

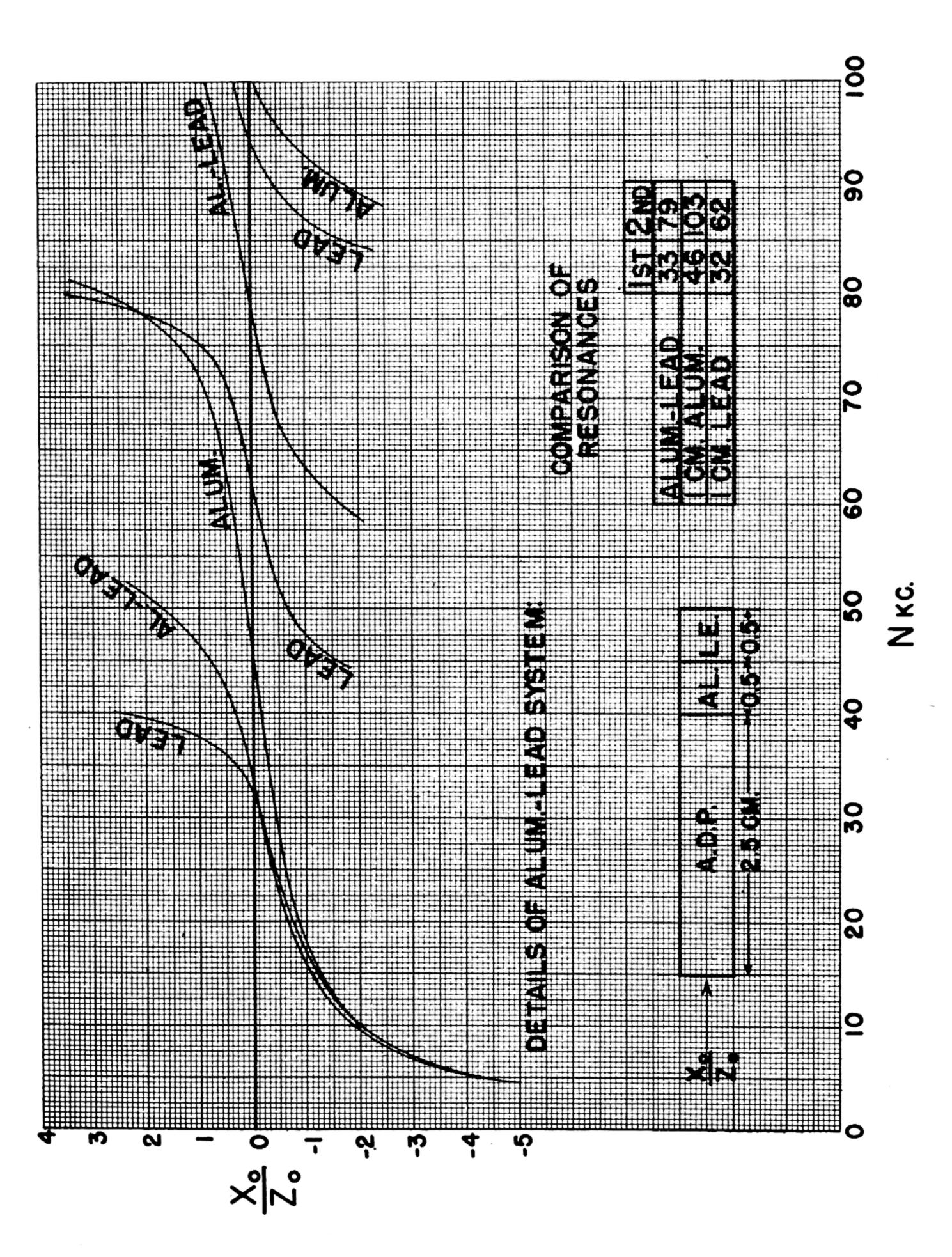
For the effect of radiation on resonant frequency and for more complete information on band widths Section 5 should be consulted.

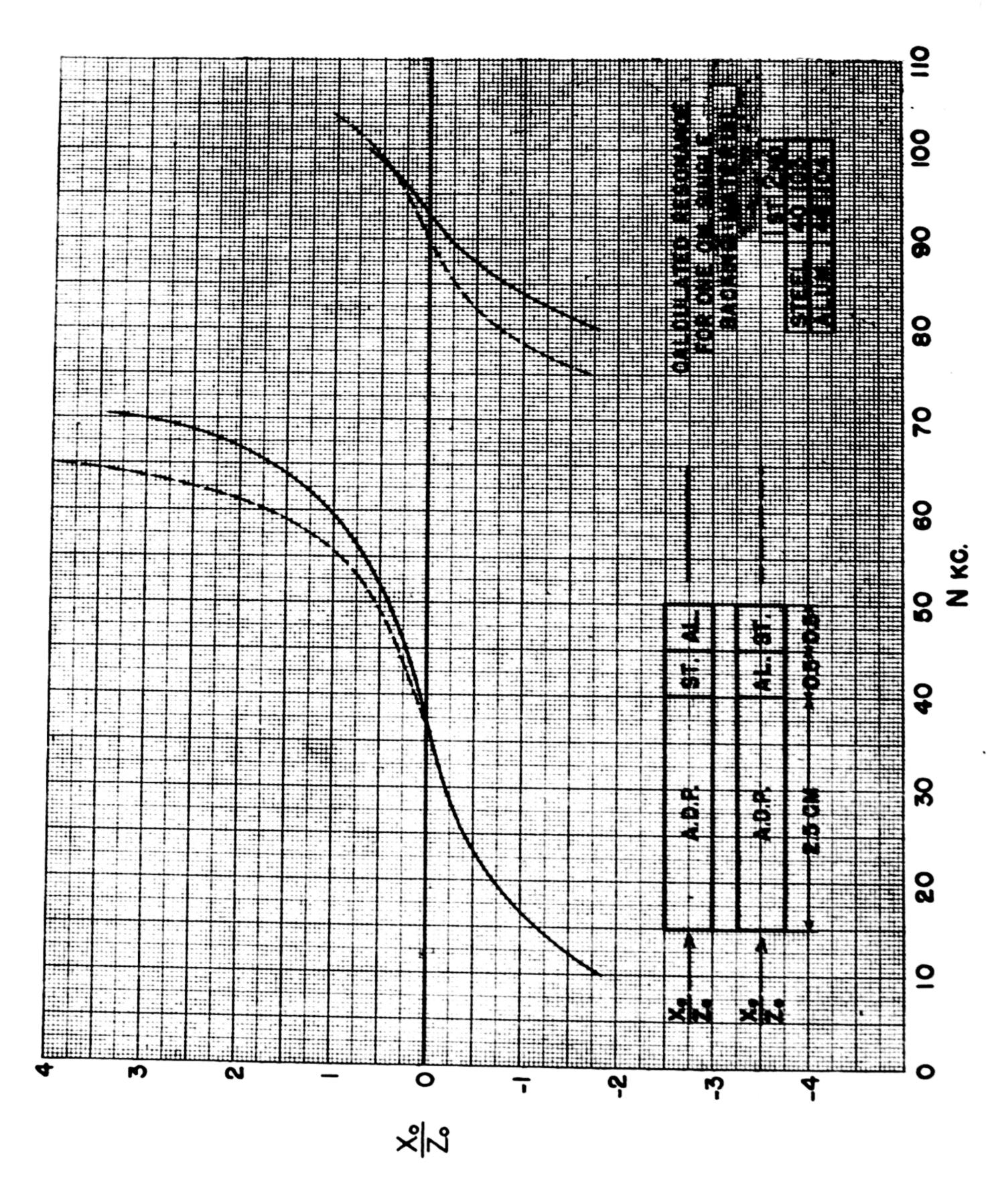
The curves on pages 28, 29, and 30 show the motional reactance for several particular systems. Relative band widths can be obtained by considering the spacings between the minima.

The curves on page 28 illustrate the change in reactance with length of backing material for a single backing material (lead).

The curves on page 29 compare the effect of a double backing material (aluminum and lead) with the effect of an equal length of either of the materials separately, when the velocities for the two materials are identical although the







separate densities and velocities differ. Note that in this example there is a shift of the second resonance but no shift of the first resonance.

The curves on page 30 compare the resonant frequencies of a double backing material system composed of steel and aluminum when the crystal is attached to the steel, with the resonant

frequencies of the system when the crystal is attached to the aluminum. Calculations for these curves are found in table 4. The calculated first and second resonant frequencies for a single backing material of the same overall dimensions are tabulated on page 30 for comparison.

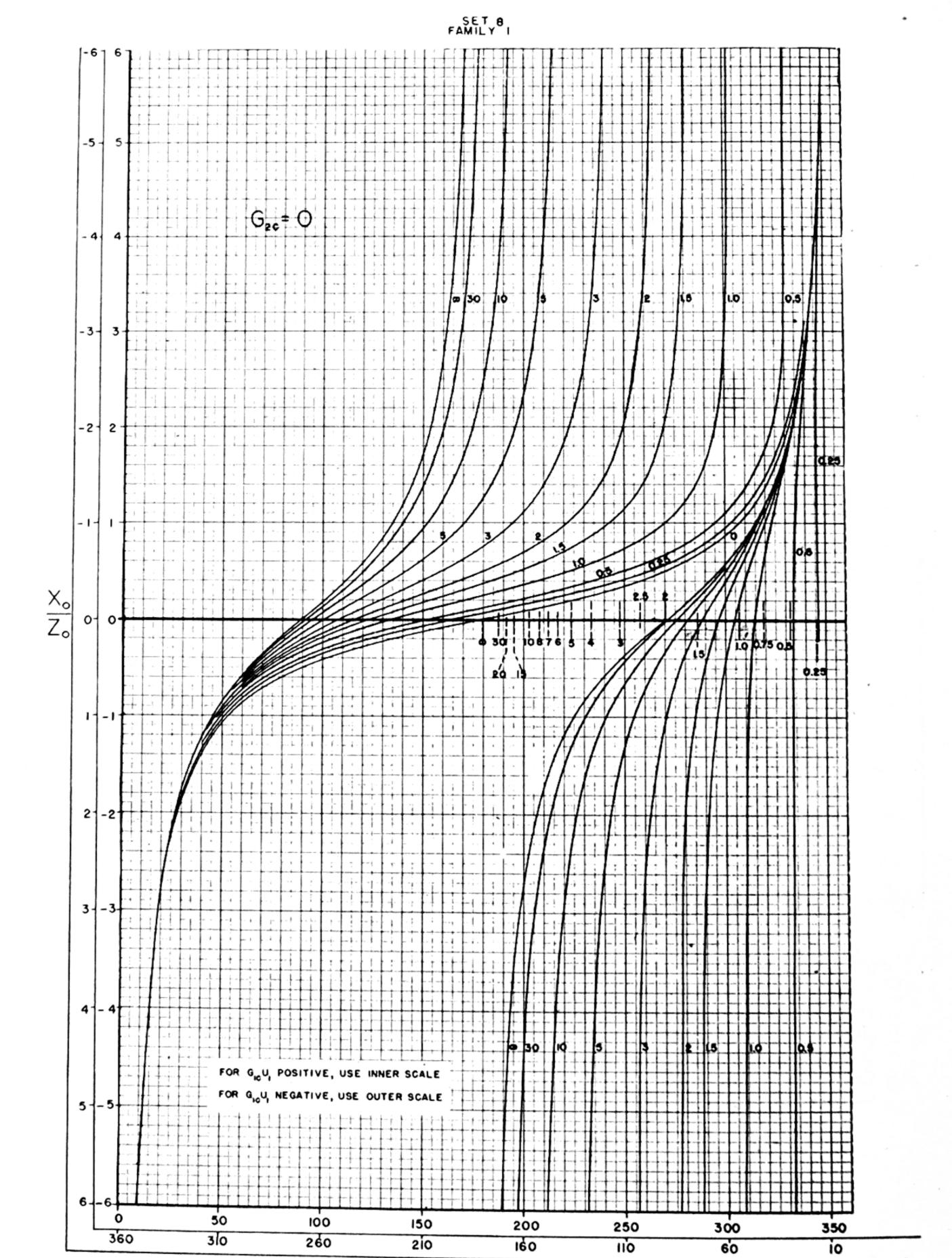
TABLE 4

ADP	$L=2.5~\mathrm{cm}$
Aluminum	$L=0.5\mathrm{cm}$
Steel	$L=0.5~\mathrm{cm}$

			_
N kc	γ _e deg	$G_{1c}U_{1}$	X_0/Z_0
10	30	0. 67	-1.84
15	45	0. 87	-1.10
20	60	1. 23	-0.71
25	75	1. 59	-0.46
30	90	2.11	-0.24
35	105	2.49	-0.08
40	120	3, 29	-0.15
45	135	3. 60	0. 32
50	150	4.37	0, 56
55	165	5. 14	0. 90
60	180	6. 68	1. 7
65	195	8.48	4. 0
70	210	10. 5	
75	225	15.4	-1.7
80	240	21, 1	-0.75
85	255		
90	270		
95	285		
100	300	-19.0	-0.58

ADP	L=2.5 cm
Steel	$L{=}0.5~\mathrm{cm}$
Aluminum	$L=0.5~\mathrm{cm}$

N ke	γ, deg	$G_{1e}U_{1}$	X_0/Z_0
10	30 45 60 75 90 105 120 135 150 165 180 195 210 225 240	0. 73 . 95 1. 24 1. 60 1. 89 2. 18 2. 69 2. 98 3. 35 3. 86 4. 08 4. 44 4. 80 5. 46 5. 90	-1. 84 -1. 10 -0. 70 -0. 46 -0. 25 -0. 08 -0. 09 0. 26 0. 44 0. 72 1. 0 1. 69 3. 1 -1. 8
85 90	255 270	6. 41 7. 00	$-0.8 \\ -0.2$
95 100	285 300	7. 79 8. 74	0. 16 0. 62
	,		



 χ_{c}

SECTION 5

ELECTRICAL INPUT IMPEDANCE TRANSMITTING RESPONSE

For any crystal system the electrical input impedance characteristics (motional and total) can be used directly to obtain values of such quantities as resonant frequencies, sharpness of tesonance, usable band widths, and transmitring response. In addition, a knowledge of the electrical input impedance characteristics is necessary for the design of a suitable driver and coupling circuits.

The curves of this section yield both motional input impedance and total input impedance. The range is sufficient to cover all values of both the density and the elastic constants of the crystals, the backing materials, and the driven medium.

It is convenient first to describe the curves roughly, and then to indicate directions for their use by a single example. Following this, effects resulting from varying certain quantities are discussed and illustrated by examples.

The curves of this section are divided into five main sets, pages 63 to 101. The first three sets are concerned with the quantities R_0/Z_0 and X_0/Z_0 (see Part II, Section 2 for theory). Electrical resistance and reactance (motional) in ohms are obtained by multiplying R_0/Z_0 and X_0/Z_0 by Z_0/φ^2 :

$$Z_{i}=R_{i}+jX_{i}=\frac{Z_{0}}{\varphi^{2}}\left(\frac{R_{0}}{Z_{0}}+\frac{jX_{0}}{Z_{0}}\right)$$

where

 Z_i = the motional impedance per crystal; that is, the contribution of the mechanical motion of the crystal to the electrical impedance.

 $Z_0 = \rho_e V_e A_e$, the characteristic impedance of the crystal multiplied by the area of the crystal,

 $\varphi = (d/s)l_w$

 l_{w} =width of the crystal, and

(d/s) = a constant for any specific cut of a particular crystal (d is the piezoelectric constant and s is the elastic constant).

The first set of curves (consisting of twelve families, pages 63 to 74) shows the variation of R_0/Z_0 plotted on a linear scale along the vertical axis as a function of γ_c , in degrees (obtained

from Section 1) plotted along the horizontal axis. The parameter from curve to curve is $G_{ic}U_1$, the impedance load of the backing material per unit area of crystal divided by the characteristic impedance of the crystal. The values of $G_{1c}U_1$ are obtained from Section 3 on the acoustic impedance of backing material combinations. The range of $G_{1c}U_1$ on the curves is from 0 to ∞ . When $G_{1c}U_1$ is positive, use the γ_c scale which varies from 0° to 360° from left to right; when $G_{1c}U_1$ is negative, consider the signs of the labels negative and use the γ_c scale which varies from 0° to 360° from right to left.

The parameter from family to family is G_{2c} ,

defined by
$$G_{2c} = \frac{\rho_w V_w}{\rho_c V_c}$$
; i. e., the ratio of the

characteristic impedance of the driven medium to the characteristic impedance of the crystal. A family of curves is given for each of twelve values of G_{2c} from 0.1 to 10. It is suggested that instead of trying to interpolate between families the designer choose a family on each side of the given value of G_{2c} , draw two characteristic curves of R_0/Z_0 , and interpolate between these. A table of characteristic impedance values is given on page 11, Section 2.

The example to be used as an illustration is as follows: 1,000 ADP crystals are mounted on high Q lead alloy backing units. The dimensions of the composite units are such that the longitudinal velocity is realized. Crystals are 2.5 cm long, 1.0 cm wide and 0.5 cm thick. The lead backing is 0.25 cm thick. The medium driven is water. The units are coupled to the driver through a cable which has a capacity of 2.00(10)⁻⁸ farads and a Q of 50. We now calculate the input impedance and transmitting response.

The value of G_{2c} for the example is 0.26. For accurate results, we should plot curves of R_0/Z_0 vs. frequency (N) for values of $G_{2c}=0.2$ and $G_{2c}=0.3$ and interpolate for the intermediate value $G_{2c}=0.26$. This method is often simpler than direct interpolation between

families of R_0/Z_0 vs. γ_c curves. Since our example was chosen only to illustrate the essential steps in obtaining the characteristic curves, we will use the family for $G_{2c}=0.3$ and ignore the interpolation. This curve (R_0/Z_0) vs. N is plotted on page 38, and the work is arranged as in Table 5, page 41.

Each curve for R_0/Z_0 has a peak somewhere in the range $180^{\circ} \le \gamma_{e} \le 360^{\circ}$ (for positive $G_{1e}U_{1}$), which at times makes interpolation in this region difficult. The second set of curves (page 75 to 86) is a plot of R_0/Z_0 on a log scale for γ_c between 180° and 360° for positive $G_{1\epsilon}U_1$, (or between 0° and 180° for negative G_1, U_1). The log scale permits the entire peak to be plotted, thus aiding interpolation. There are twelve families, one corresponding to each family of the first set. The parameters and the methods of using the curves are exactly similar to those of the first set. Even with this set, accurate interpolation near the peak is not always possible but since the peaks occur in the "antiresonant" region (or region of low transmitting response), the positions are of more interest than the actual heights.

The third set of curves (pages 87 to 99), consisting of thirteen families, shows the variation of X_0/Z_0 plotted along the vertical as a function of γ_c (obtained from Section 1) plotted along the horizontal. $G_{1c}U_1$ is the parameter from curve to curve and G_{2c} is the parameter from family to family. It should be noted that in this set the inner scales of γ_c and X_0/Z_0 are used with positive values of $G_{1c}U_1$, and the outer scales are used with negative values of $G_{1c}U_1$. Certain sections of several of the families have been enlarged on the lower right hand side of the same sheet.

In our illustrative example we again use the sheet for $G_{2\epsilon}=0.3$. For this particular example, the X_0/Z_0 vs. N curve for the projector radiating is almost identical with the X_0/Z_0 curve for the free projector (i. e., in a vacuum, $G_{2\epsilon}=0$). X_0/Z_0 vs. N is plotted on page 38, and the work is arranged as in Table 5, page 41.

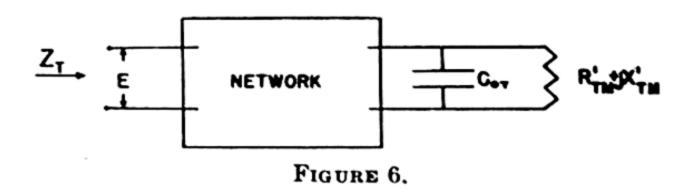
To obtain the components of the motional impedance in electrical ohms, multiply the quantities R_0/Z_0 and X_0/Z_0 by Z_0/φ^2 . Using MKS units (coulombs/meter²) for d/s (see Table 8 on page 59), and expressing l_w in meters, then

 φ , equal to $(d/s)l_w$ will be in MKS units of coulombs/meter. For this example $\varphi=0.49$ - $(10)^{-2}$. To convert $Z_0=\rho_c V_c l_c l_w$ from the cgs system to the MKS system, multiply the value of Z_0 in grams/sec by $(10)^{-3}$. For the example,

$$Z_0 = (10)^{-3} 5.9(10)^{5}(1)(0.5)$$

= $2.9(10)^{2}$ kg/sec,
and $Z_0/\varphi^2 = \frac{2.9(10^{2})}{0.25(10)^{-4}} = 1.1(10)^{7}$ ohms

After the motional impedance per crystal has been expressed in units of electrical ohms, the motional impedance of the crystal combination is obtained and is then combined with the impedance of the purely electrical elements (C_{0T}) , coupling network to obtain the total electrical input impedance (Z_T) of the system. The equations have been set up in such a way that the impedance components due to motion (R_{TM}, X_{TM}) are coupled to the electrical system as illustrated in Fig. 6 (see Part II, Section 2, for theory).



 C_{0T} represents the longitudinally clamped capacity of the crystal combination. A table of dielectric constants for several cuts of various longitudinally clamped crystals is given on page 59 of this section. The capacity can be

calculated by using the formula $C_0 = \frac{KA}{4\pi l_i}$, where

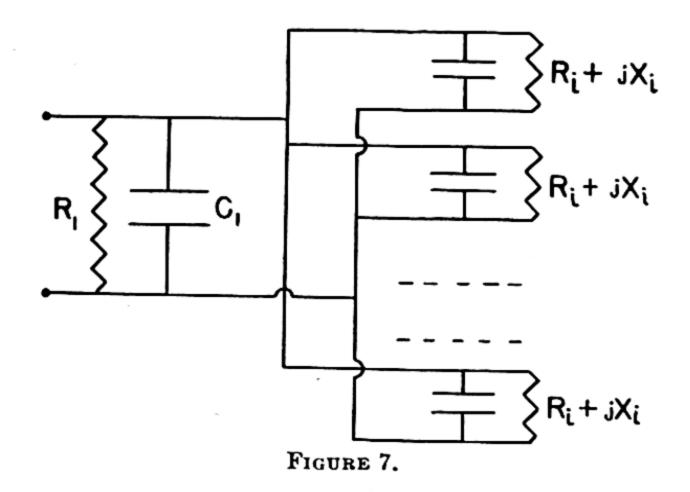
K=dielectric constant

A=area of crystal

 l_i = distance between the electroded faces

If K is used as the ratio of the dielectric constant of the crystal to the dielectric constant of air, and l_i is expressed in cm, the capacity C_0 will be in units of cm. C_0 can be converted to farads by multiplying by $1.1(10)^{-13}$ or to micromicrofarads by multiplying by 1.1. For the particular example under discussion:

$$C_0 = \frac{14.0(2.5)(1.0)}{4\pi(0.5)} = 5.57$$
 cm
or $6.13(10)^{-12}$ farads.



Consider the example illustrated by Fig. 7. It consists of a number of exactly similar crystal systems in parallel coupled to a driver through a cable of paralled electrical components C_1 and R_1 . A resistance would in general be in parallel with C_0 because of the finite conductivity of the crystal and dielectric loss in the glue, but in many cases it can be neglected. In evaluating the electrical input impedance of a system such as that in Fig. 7, it is convenient to change the impedances to admittances, add the parallel admittances, and then change back to impedance.

To facilitate this evaluation, two sets of curves are given in this section on pages 100 and 101. The first set (consisting of one family, page 100) is an impedance-admittance transformation chart, i. e., the transformation G-jB=1/(R+jX). The plot is on log-log paper so that it may cover a wide range of values of the ratio of one component to the other (from 0.001 to 1000). On this chart, the variables R and Xare plotted along the horizontal and vertical scales respectively, and the curves of constant G and constant B form the sets of intersecting curves. The curves of constant G meet the horizontal axis at right angles and the curves of constant B meet the vertical axis at right angles. The chart gives only the positive value of the components, but the proper sign can be determined by noting that in changing from impedance to admittance, or vice versa, the sign of the imaginary component in the result is the opposite of that in the given quantity. The range of values of R and X shown explicitly on the scale of the chart is 0.10 to 100 and the range of G and B is 0.0000125 to 4.0. However, P and X scales can be multiplied by any power of ten if the G and B scales are divided by the same power of ten.

The second set of curves for use in combining impedances is given on page 101. These are graphs of the admittance of condensers of various sizes as a function of frequency.

Table 6 (page 42) shows the arrangement of the work for the illustrative example. The graph on page 39 is a plot of the series components of the input impedance.

The transmitting response of the crystal system may be calculated from the components of the input impedance. One convenient definition for transmitting response is the acoustic power output at a specified point of the system per unit current input. This quantity can be determined by first obtaining the current through the motional resistance R_{TM} for unit current into the system and then applying the power formula $P=i^2R_{TM}$. For a particular system such as Fig. 7, where the R_i+jX_i are in parallel with the other electrical elements of the network (i. e., the voltage Eapplied to the system is also the voltage across the impedances R_i+jX_i), the expression for power output per unit current input takes the following form:

$$P = R_{TM} \frac{G_{TM}^2 + B_{TM}^2}{G_T^2 + B_T^2}.$$
 But
$$R_{TM} = \frac{G_{TM}}{G_{TM}^2 + B_{TM}^2};$$
 so
$$P = \frac{G_{TM}}{G_T^2 + B_T^2}.$$

The quantities $G_{TM}+jB_{TM}$, G_{T} , and B_{T} have already been obtained in the evaluation of the input impedance so that the transmitting response, P, follows immediately. For our example the arrangement of the work is illustrated by Table 7, page 43, and the transmitting response appears on page 40. Note that the transmitting response has been plotted in decibels above 1 watt. A db. chart appears on page 62 of this section.

If the transmitting response is to be expressed as pressure amplitude on the axis at a specified distance, this can be obtained from the beam pattern and the transmitting response expressed in total power output. We use the beam pattern to obtain the ratio (D) of total power radiated (f Ids) to that which would be radiated if the intensity were everywhere equal to the intensity along the axis of the main beam $(f I_A ds = 4\pi r^2 I_A)$, i. e.,

$$D = \frac{\int I ds}{4\pi r^2 I_A}.$$
 (1)

D might be called the directivity ratio.

We can calculate I_A from expression (1) since the transmitting response expressed in total power output gives the value of the quantity $\int Ids$, and the beam pattern provides the directivity ratio, D.

$$I_A = \frac{\int Ids}{4\pi r^2 D}$$

The root-mean-square pressure on the axis of the main beam is then given by the formula $P = \sqrt{I_A \rho V}$. See page 49 for a graph of the transmitting response plotted as pressure amplitude.

The transmitting response as obtained in this section will be lowered somewhat because of losses in the glue joint and the method of mounting. For example, if the efficiency is 50%, 3 db. should be subtracted from the transmitting response characteristic. See page 127, Section 7 for a more complete discussion.

Since we have described the various curves and illustrated their use with a simple example, it is now possible to point out some of the principal features to be expected in the characteristic curves of a few systems. All of the illustrative curves given have been plotted using the graphs of this and the preceding sections.

The graph on page 44 illustrates the change in input electrical impedance caused by a change in the Q of the coupling cable ($Q=R\omega C$ for parallel components as used here). In this illustration, the resistance curve has been shifted upward by an amount which increases toward the low frequency end of the spectrum and approaches infinity at zero frequency. As the value of Q decreases, the frequencies at which the minima occur in the resistance curve shift toward the higher values. To increase

transmitting response at low frequency it is necessary, therefore, either to raise the Q of the cable or to use a crystal of higher electromechanical coupling.

The graph on page 45 illustrates the change in the series input impedance components when a series inductance of finite Q is added to the system. In this case the value of the inductance was chosen to tune out the capacity at the resonant frequency. The Q was arbitrarily chosen as 50. The magnitude of the resistive component is shifted to larger values when the inductance is added to the system. This shift increases linearly with frequency if Q is held constant.

In the example just discussed, the value of Q was held fixed as the frequency changed; however, no essential complications are introduced by letting Q vary.

It should be noted that for a large number of systems the resonant frequencies (as determined by the zeros of the function X_0/Z_0) occur in a flat region of the R_0/Z_0 curve. See, for example, the graph on page 38 of this section. Here the first resonant frequency occurs at 40 kc where the R_0/Z_0 characteristic is very flat. The second resonant frequency is at 90 kc where the R_0/Z_0 characteristic is fairly flat. The region of high reactance occurs in the same part of the frequency spectrum as the region of peak resistance. When such conditions hold, the resistive component of the total impedance has the characteristic form of the curve on page 39, i. e., smooth single peaks in the resonant regions. The transmitting response characteristic has single peaks at the resonant frequencies; see the graph on page 40 for example.

Such conditions do not always exist. It is possible to design systems so that a peak of the R_0/Z_0 curve is near a zero of the X_0/Z_0 curve. The X_0/Z_0 characteristic of these systems sometimes shows secondary peaks and troughs. To illustrate, consider the following system: 170 ADP crystals in parallel are mounted on lead alloy units of such cross section as to obtain the longitudinal velocity in the lead. The crystals are 1% long, % wide, and % thick. The lead backing units are 1% thick.

The characteristic curves for this system appear on pages 46 to 49.

Consider first the X_0/Z_0 curve given on page 47; a secondary peak occurs at 76 kc and a secondary trough occurs at 20 kc. It is immediately clear that the peak at 76 kc will cause a secondary resonance to appear around 80 kc if the resistive component does not completely override the reactance throughout this region. The transmitting response characteristic, page 49, shows a secondary resonance at 78 kc comparable to the primary resonance at 66 kc. In the region 15 to 22 kc it is impossible to distinguish between primary and secondary resonances. The curves on pages 46 and 47 show. that the minima at 19 kc and 78 kc in the X_0/Z_0 curve occur near a maximum in the R_0/Z_0 curve and the zeros at 29, 47, and 66 kc occur in regions of comparative flatness of the R_0/Z_0 curve.

When the motional impedance components are combined with the purely electrical impedances the curves given on page 48 result. Secondary maxima appear at 20 kc and 76 kc in the resistive component. These maxima are a result of the particular type of motional characteristics discussed above.

The curves just discussed were very successful in explaining the characteristics of an experimental projector constructed at this laboratory. The relations between the resonances both primary and secondary, and the relative heights of the peaks on the transmitting response characteristic checked closely.

To illustrate the change in the impedance and transmitting response due to a change in the electromechanical coupling coefficient, the characteristic curves for a projector using X-cut Rochelle salt crystals at 5° C are given on pages 50, 51, 52, and 55. These can be compared with the curves on pages 38, 39, and 40

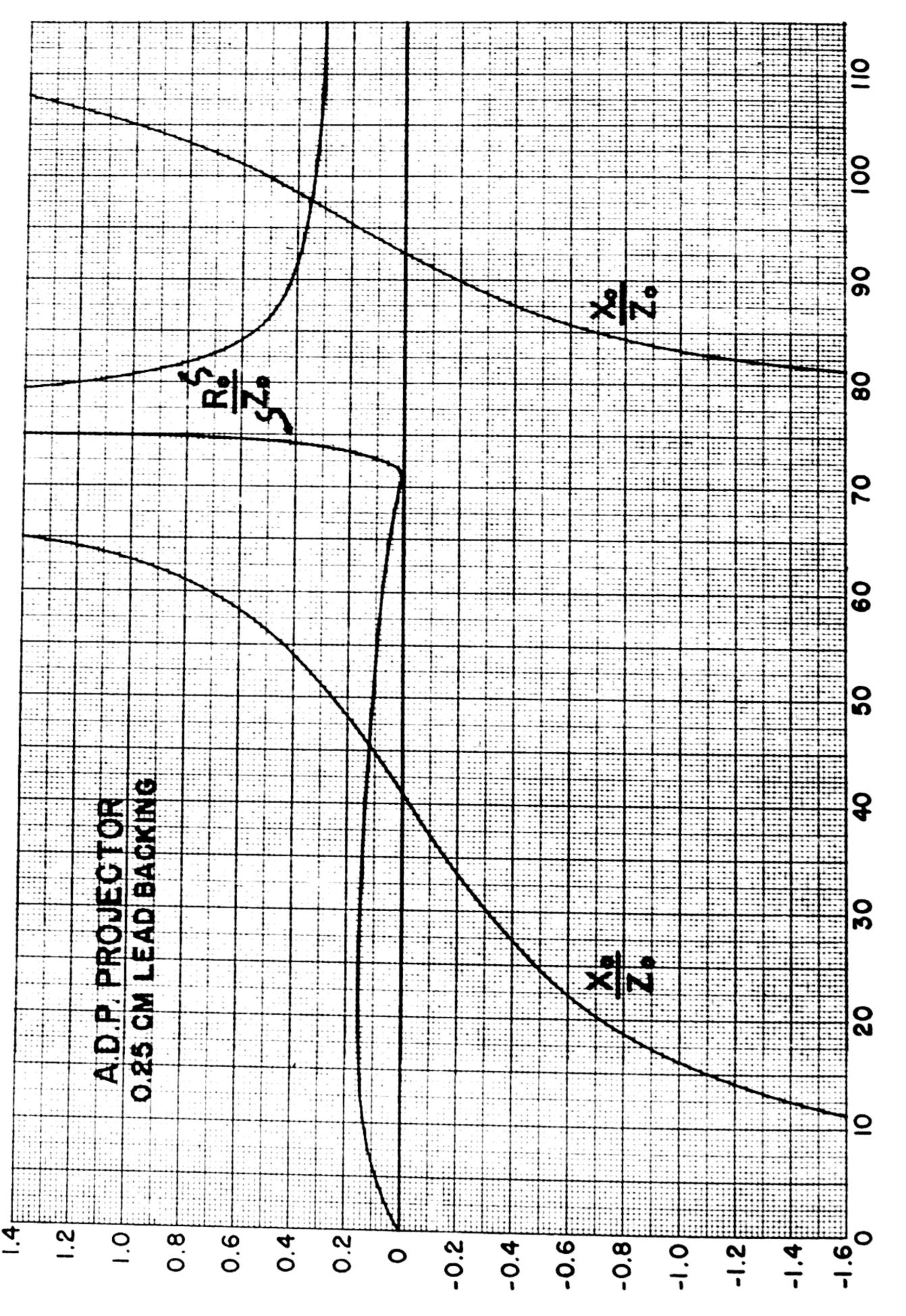
of this section. The electromechanical coupling coefficient for the X-cut Rochelle salt is greater than the coupling coefficient for ADP.

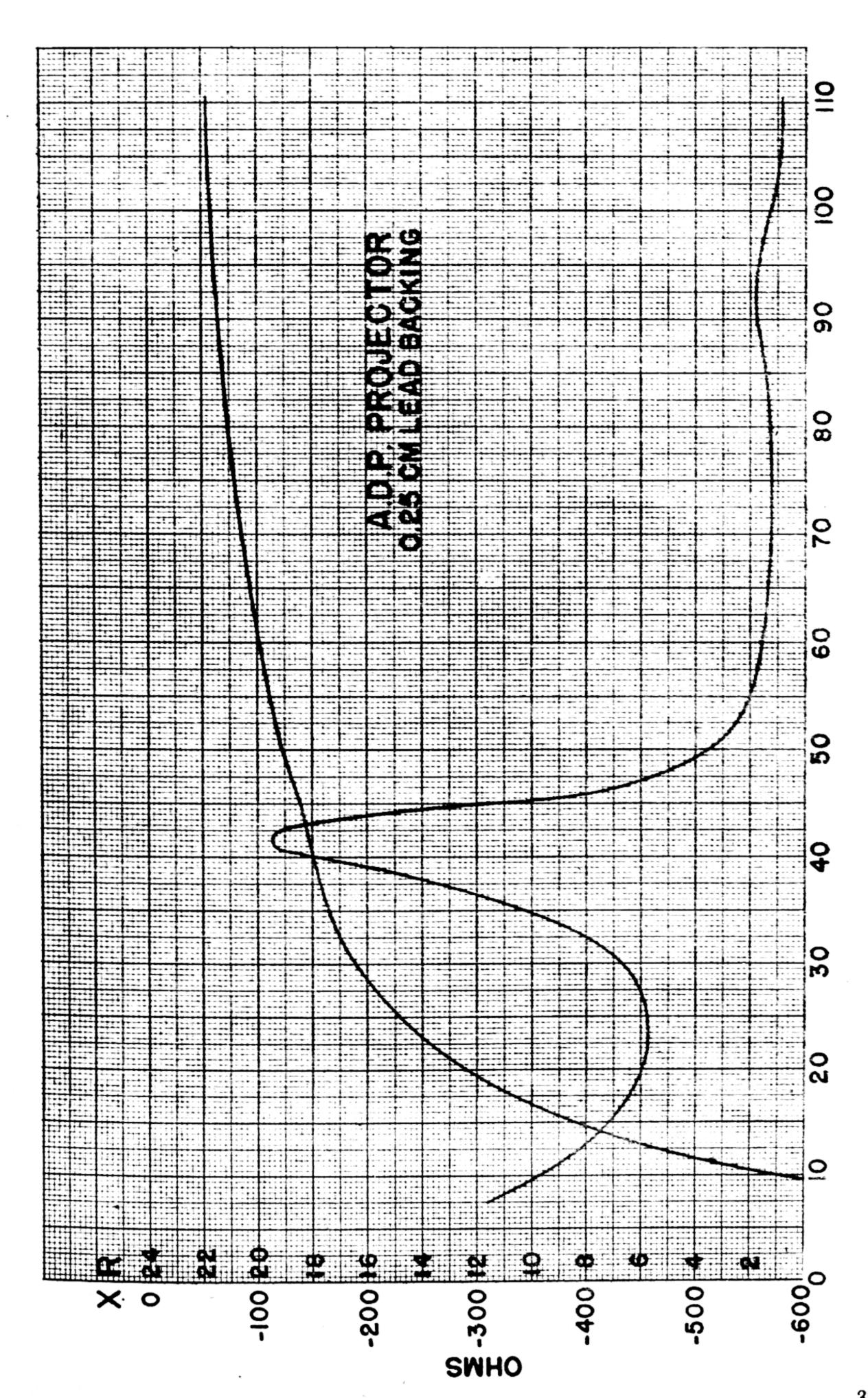
A set of curves on pages 50 to 57 show how the characteristics of an X-cut Rochelle salt projector vary with temperature. Curves of motional impedance, total impedance, and transmitting response are given for three different temperatures: 5°, 20°, and 24° C. The Curie point is approximately 24° C, consequently the characteristics vary greatly with temperature in this region. Under ordinary measuring conditions the temperatures of various regions of the projector are seldom equal and the beam pattern may change because of temperature differentials in the crystal assembly.

Notice that the resonant frequencies as obtained from the zeros of the motional reactance curves, X_0/Z_0 , do not correspond to the peaks on the total impedance. This lack of correspondence is due to the high electromechanical coupling of X-cut Rochelle salt.

In design it is often assumed that the elements making up a projector are exactly similar and that the mounting is precisely symmetrical. As a result, sharp maxima and minima sometimes appear in the calculated characteristics. In most projectors, however, slight variations in the mounting will cause the sharp peaks to be rounded off and the sharp troughs to be partially filled.

The many possibilities in design which are suggested by a study of the curves of this section would supply topics for an interesting series of supplements to this report.





TRANSMITTING RESPONSE

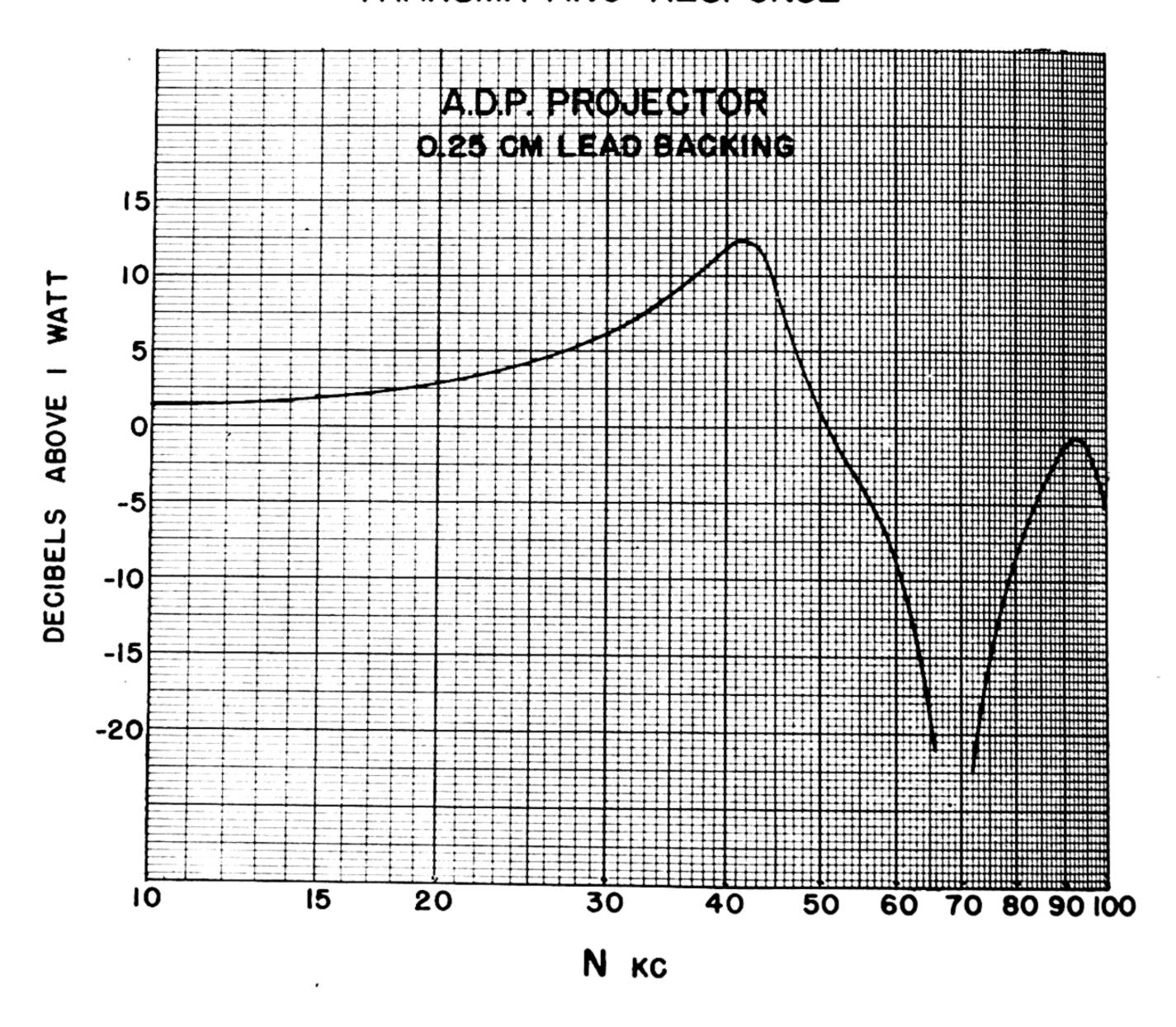


TABLE 5

1000 ADP crystals, 2.5 cm long, backed by 0.25 cm lead
(Long bar velocities)

				4-1
<i>N</i> kc	$G_{1e}U_{1}$	γ.	R_{o}/Z_{0}	X ₀ /Z ₀
10	0. 34	30	0. 14	-1.8
15	. 52	45	. 14	-1.1
20	. 69	60	. 15	-0.70
25	. 83	75	. 14	— . 50
30	1. 05	90	. 13	- . 30
35	1. 25	105	. 13	— . 15
40	1. 55	120	. 13	 04
45	1. 80	135	. 12	. 10
50	2. 10	150	. 11	. 30
55	2. 40	165	. 10	. 50
60	2.75	180	. 075	. 70
65	3.2	195	. 04	1.4
70	3. 6	210	. 01	2. 4
10	0.0	210	. 01	
75	4. 2	225	1. 5	5. 0
80	5. 1	240	1. 2	-2.2
85	6. 1	255	0. 55	-0.70
90	7. 5	270	. 42	—. 20
95	10. 0	285	. 36	. 20
100	14. 0	300	. 32	. 50
100	1	315	. 32	1. 0
105	24.0	330	. 305	1.8
110	65. 0	345	. 303	3.7
115	-65.0	343	. 50	",
		1		1

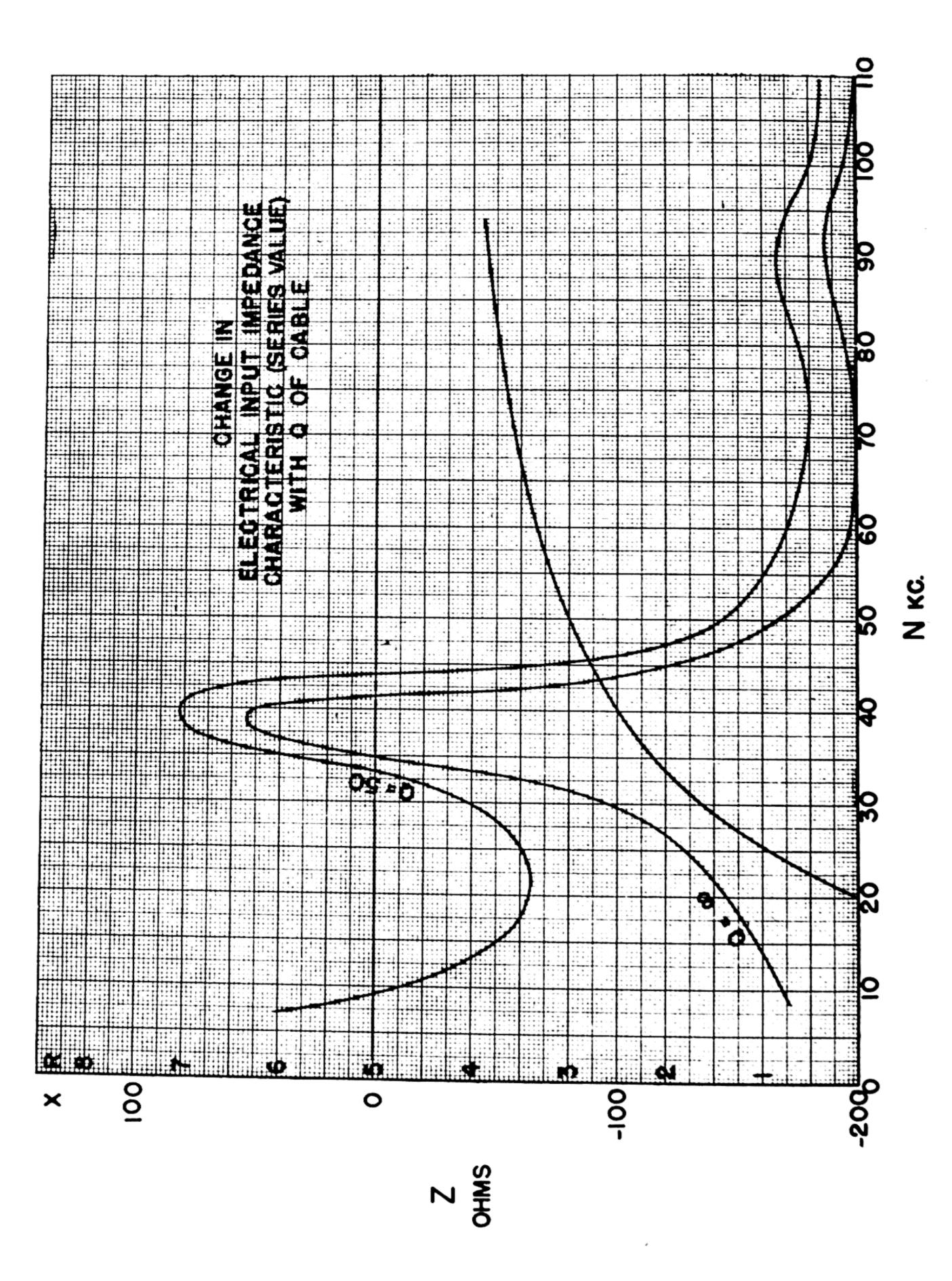
 $Z_0/\varphi^2 = 1.1(10)^7$ ohms $C_0 = 6.13(10)^{-12}$ farads

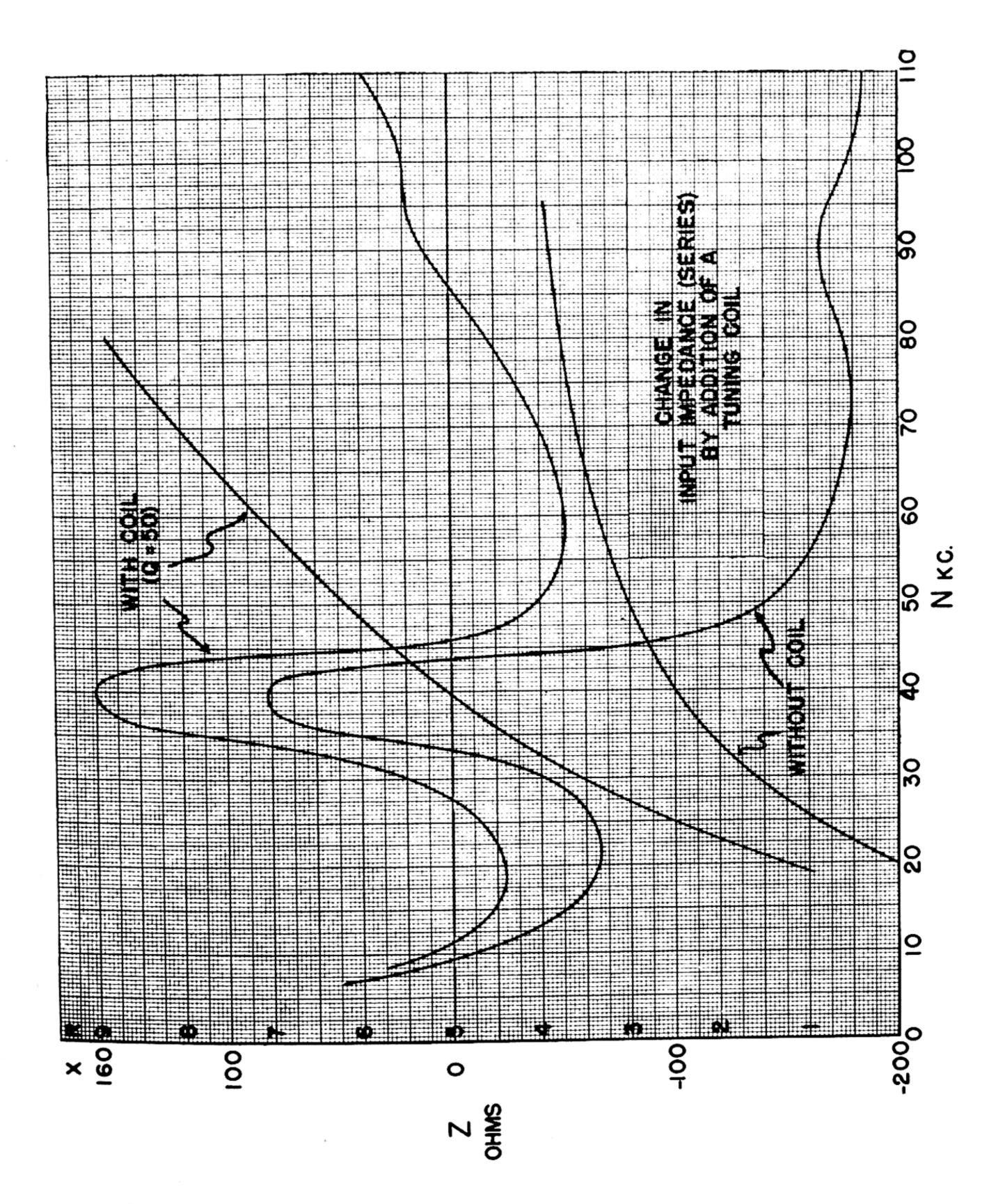
Cable admittance $= (0.025+j1.27) (10)^{-4} N$ mhos Admittance of longitudinally clamped capacity of crystals $= j0.385 (10)^{-4} N$ mhos Total admittance (cable capacity and clamped capacity of crystals) $= (0.025+j1.67) (10)^{-4} N$ mhos $= (0.025+j1.67) (10)^{-4} N$ mhos

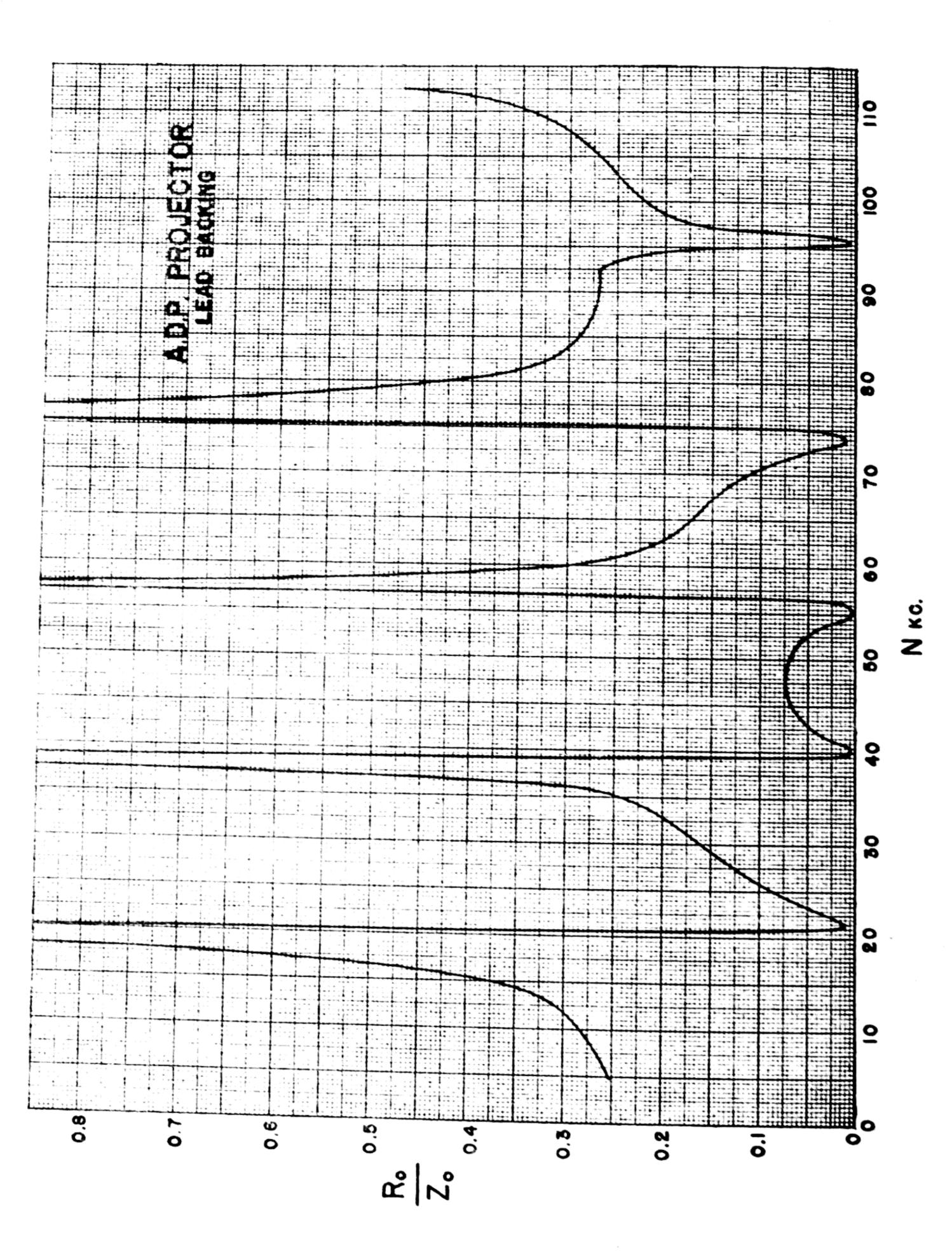
1	1	1																				
Total impedance	$X_{T}(10)^{-3}$	186 0-	8 88		231	190		152	140	123	111	101	092	085	080	074	070	990 .—	063	061	—. 057	— . 055
Total in	$R_{\tau}(10)^{-3}$	0.0098		. 0064	. 0058	. 0065		. 0173	. 011	. 0033	. 0020		. 0014	. 0012	. 0012	001		00	. 0017	. 0012	6000 .	6000 .
Total ad- mittance	$B_T(10)^3$	1. 72	. 5		4.34	5. 25		6.50	7.13	8. 13	9.02		16.8	11.7	12. 5		14.2	15.1	15.8	16.5	17.4	18.0
Total	$G_T(10)^3$	0.029		. 077	. 11	. 18	. 39	. 74	. 56	. 22	. 17	. 16	. 16	. 17	. 19	. 22	. 27		. 43	. 33	. 28	. 28
Admittance of cable and lamped capacity of crystals	$B_{TC}(10)^3$	1.67		3.34	4. 17	5.00	5.8		7.5	8. 4	9.5		10.9	11.7	12. 5	13.4	14.2	15.0	15.9	16.7	17.5	18.4
Admitta cable clamped ity of cry	$G_{TC}(10)^3$	0.025	. 037	. 050	. 062	. 075	. 087	. 10	. 11	. 12	. 14	. 15	. 16	. 17	. 19	. 20	. 21	. 22	. 24	. 25	. 26	. 27
otal motional admittance	$B_{TM}(10)^3$	0.0502	. 0813	. 124	. 169	. 255	. 346	196	373	267	175	- . 128	0649	— . 0379	0167	. 0318	. 0803	. 0840	107	129	0829	0491
Total	$G_{TM}(10)^3$	0.0039	. 0103	. 0266	. 0472	. 110	. 300	. 638	. 447	0860 .	. 0350	. 0137	. 00185	. 00015	. 0050	. 0174	. 0631	. 176	. 193	. 0825	. 0257	. 0083
onal admit- (per crystal)	$B_i(10)^{6}$	0.0502	. 0813	. 124	. 169	. 255	. 346	196	373	267	175	-, 128	0649	— . 0379	0167	. 0318	. 0803	. 0840	107	129	— . 0829	—. 0491
Motional tance (per	G,(10)*	0. 0039	. 0103	. 0266	. 0472	. 110	. 300	. 638	. 447	0860 .	. 0350	. 0137	. 00185	. 00015	. 0050	. 0174	. 0631	. 176	. 193	. 0825	. 0257	. 0083
Motional imped- ance (per crystal)	X,(10)-6				-5.5	-3.3	-1.65	-	1.1			7.7		26. 4	55.0	-24.2	7.7	-2.2	2.2	5.5	11.0	19.8
Motion ance (pe	R,(10)-6	1.54	1.54		1. 54	1.43			I. 32		1. 10	. 825	. 44	Ξ.	16.5	13.2	6.05	4.62	3.96	3. 52	3.41	3.35
N kc		10	15	20	79	30	35	40	45	50	25	09	65	70	75	80	85	06	85	100	105	110-

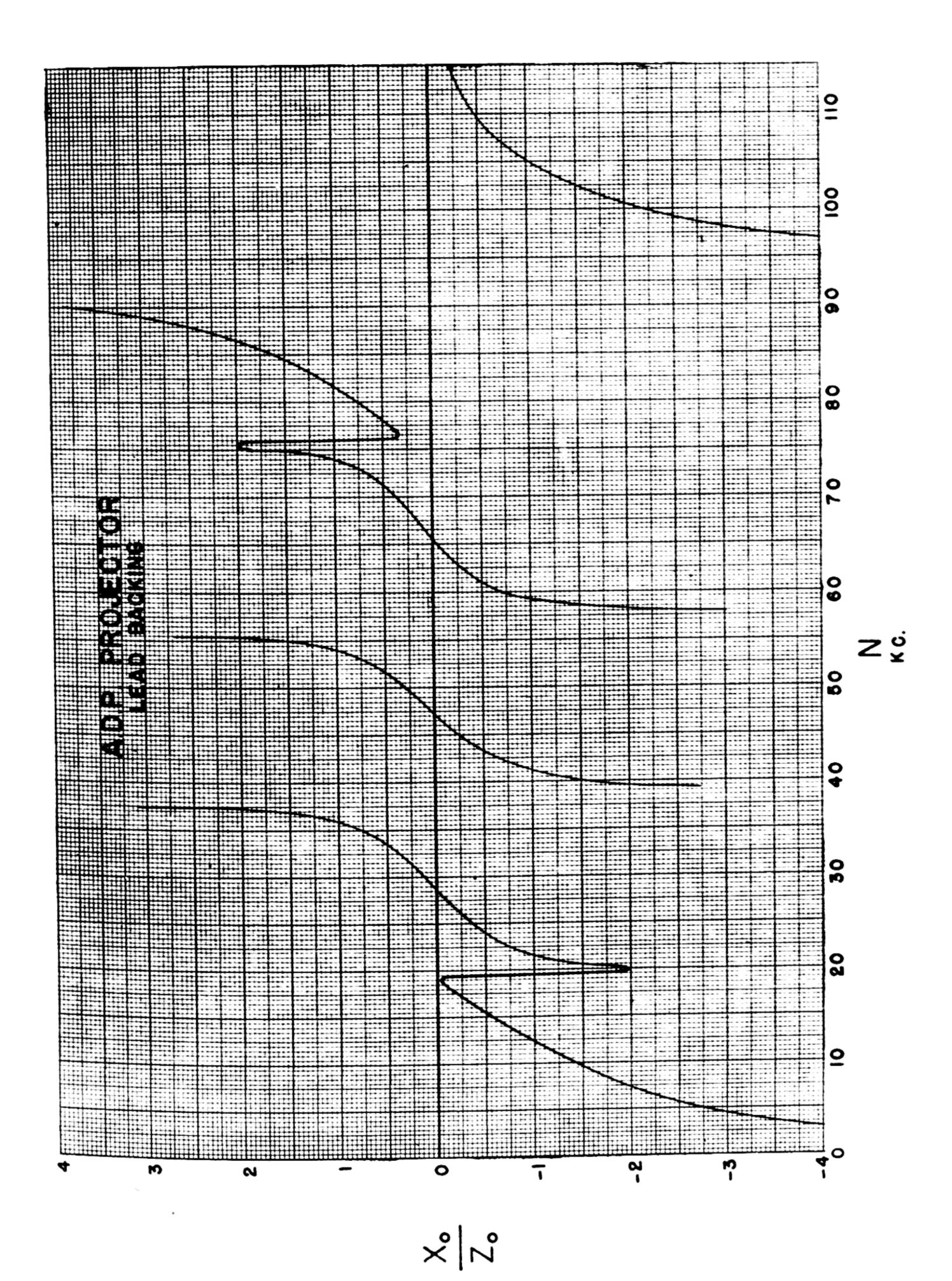
TABLE 7

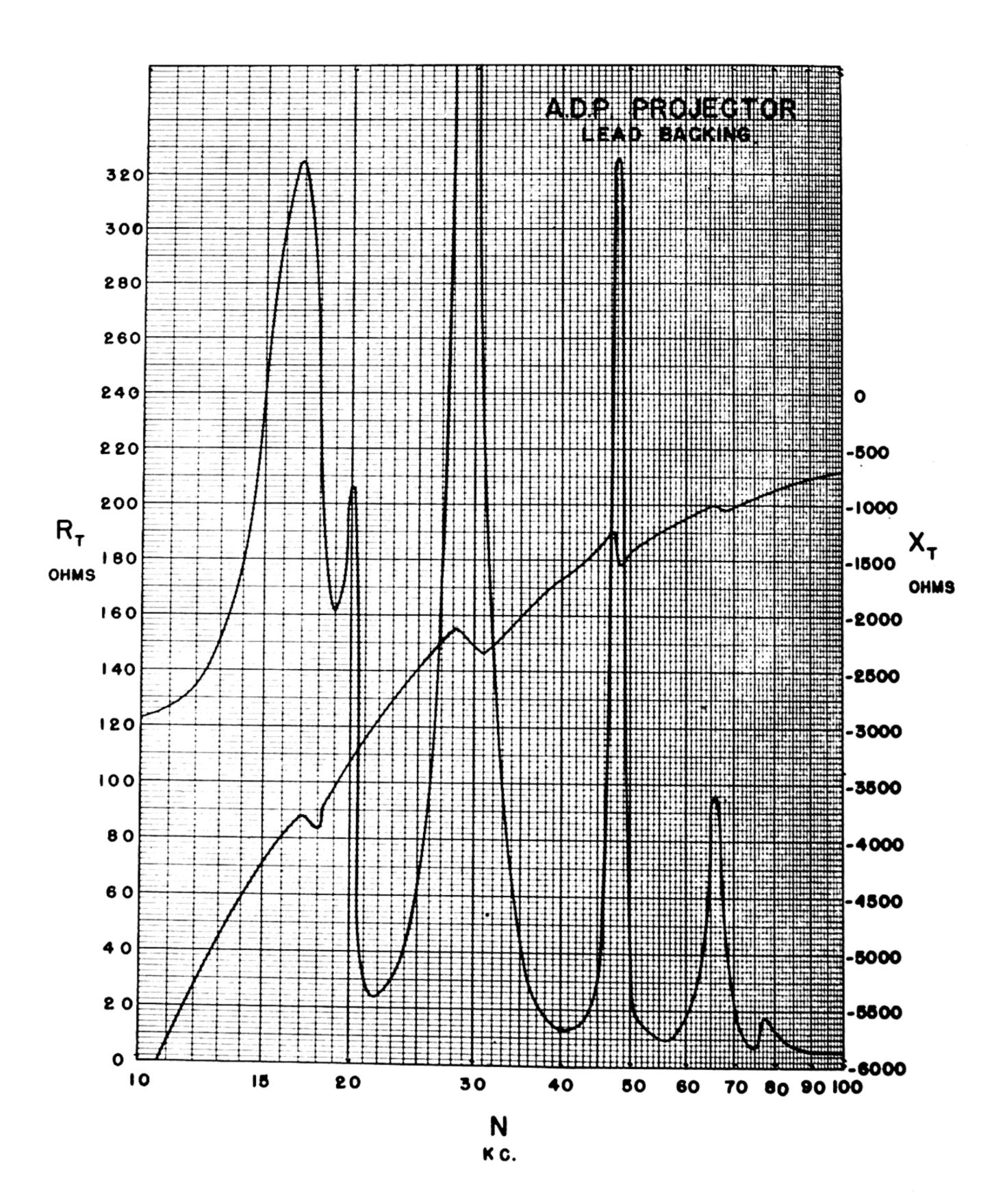
N kc	$G_{TM}(10)^3$	$(G_{\tau}^2 + B_{\tau}^2)$ $(10)^6$	Power output (watts) $\frac{G_{TM}}{(G_T^2 + B_T^2)}$	Power output db above 1 watt
10	0. 0039	2. 96	1. 31	1. 2
15	. 0103	6. 66	1. 54	1. 9
20	. 0266	12. 0	2. 22	3. 5
25	. 0472	18. 8	2. 51	4. 0
30	. 110	27. 6	3. 98	6. 0
35	. 300	38. 0	7. 89	9. 0
40	. 638	42. 8	14. 9	11. 7
45	. 447	51. 0	8. 76	9. 4
50	. 0980	66. 1	1. 48	1.7 -3.6 -8.5 -18.2 -39.5
55	. 0350	81. 4	. 43	
60	. 0137	97. 4	. 141	
65	. 0018	117	. 015	
70	. 00015	137	. 0011	
75	. 0050	156	. 032	-14.9 -10.1 -5.0 -1.1 -1.1
80	. 0174	180	. 097	
85	. 0631	202	. 312	
90	. 176	228	. 772	
95	. 193	250	. 772	
100	. 0825	272	. 303	-5.2
105	. 0257	303	. 085	-10.7
110	. 0083	324	. 026	-15.9

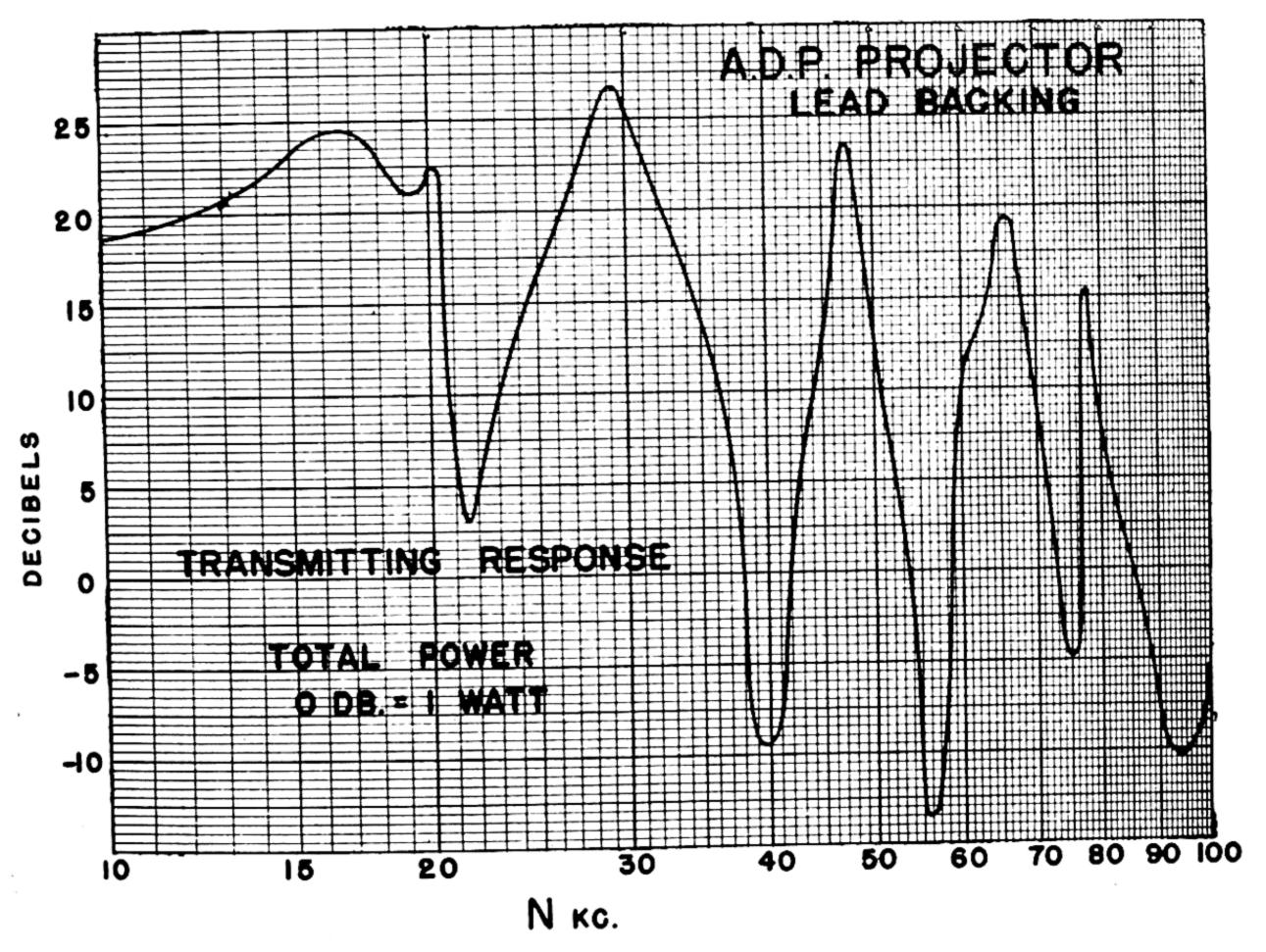


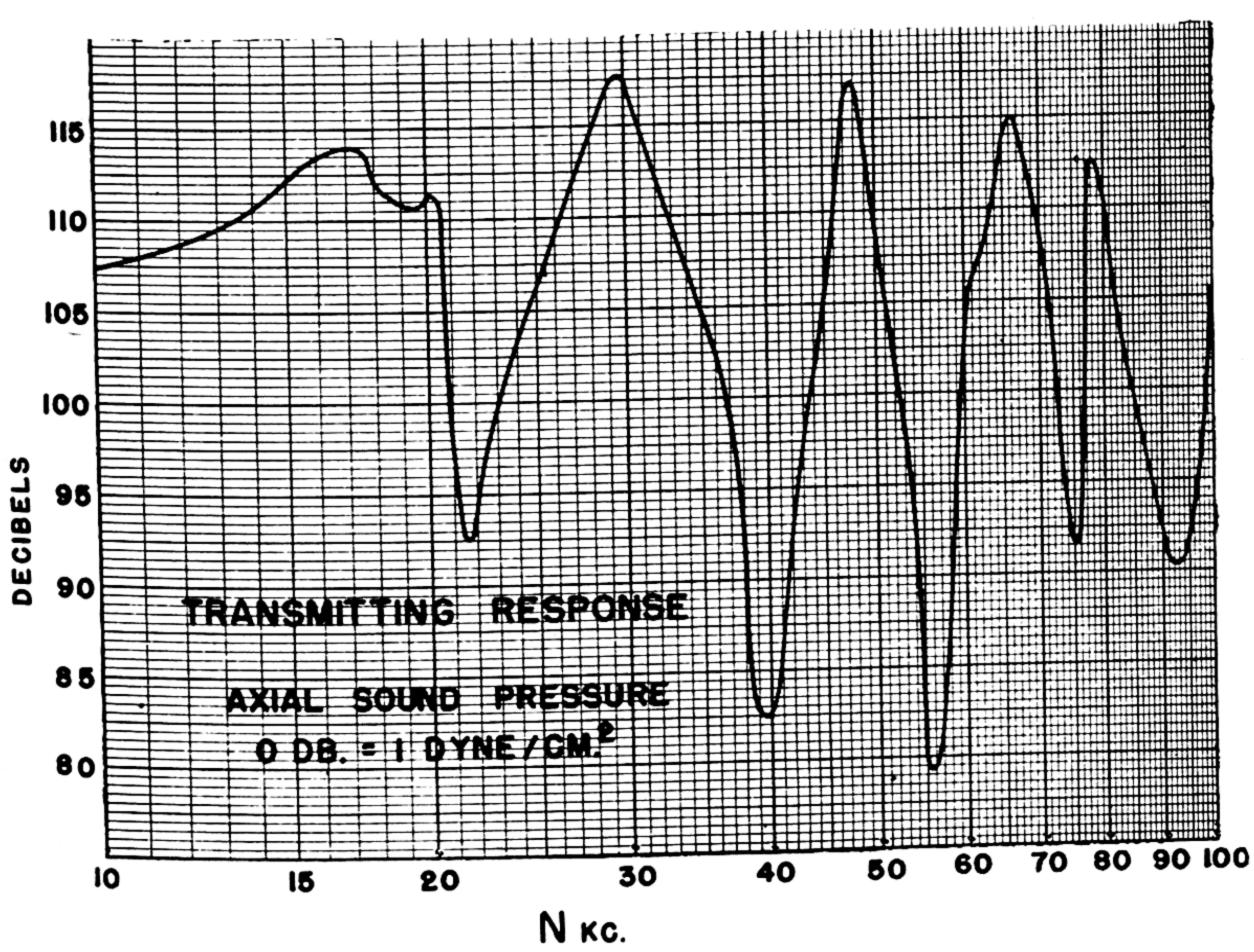


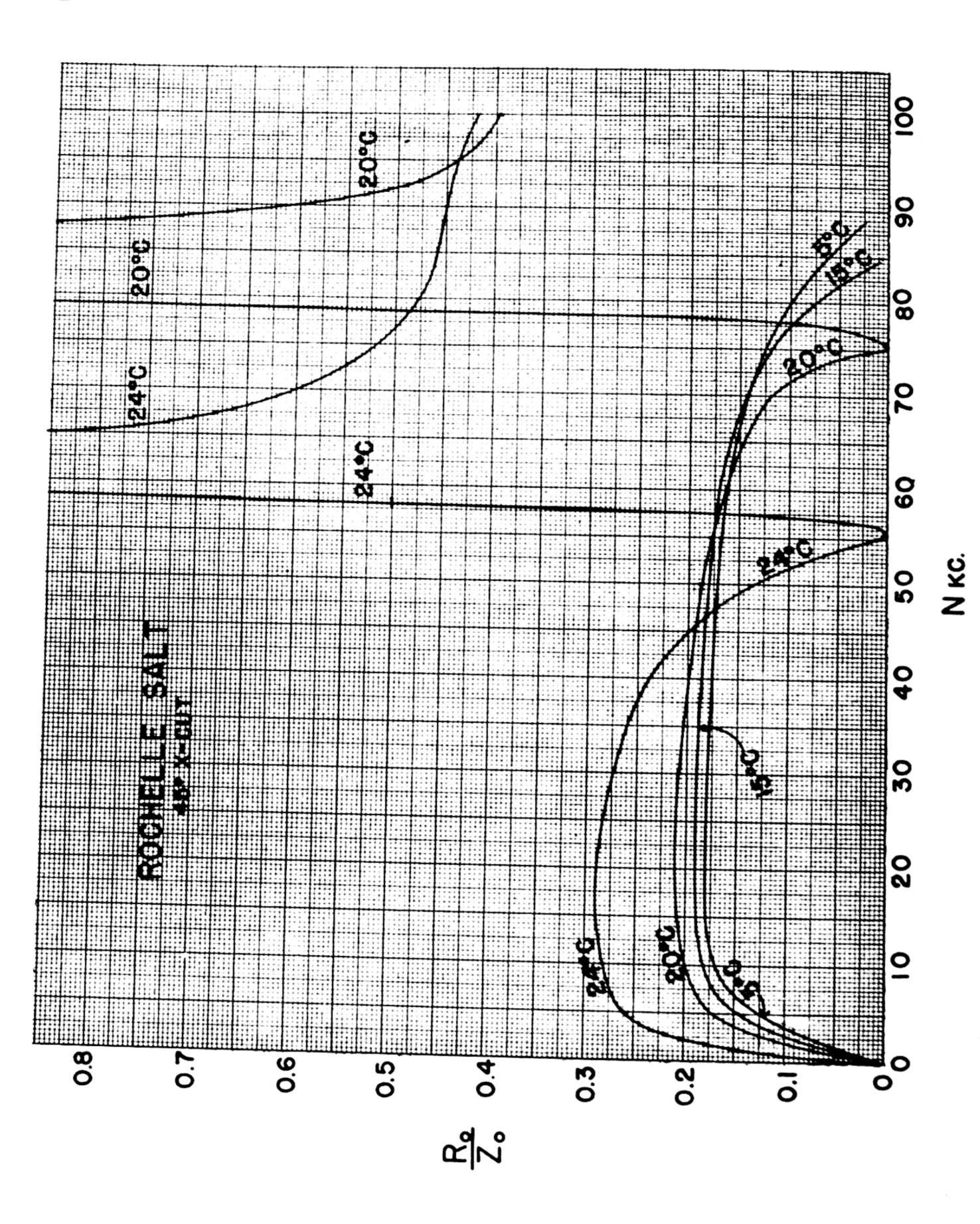


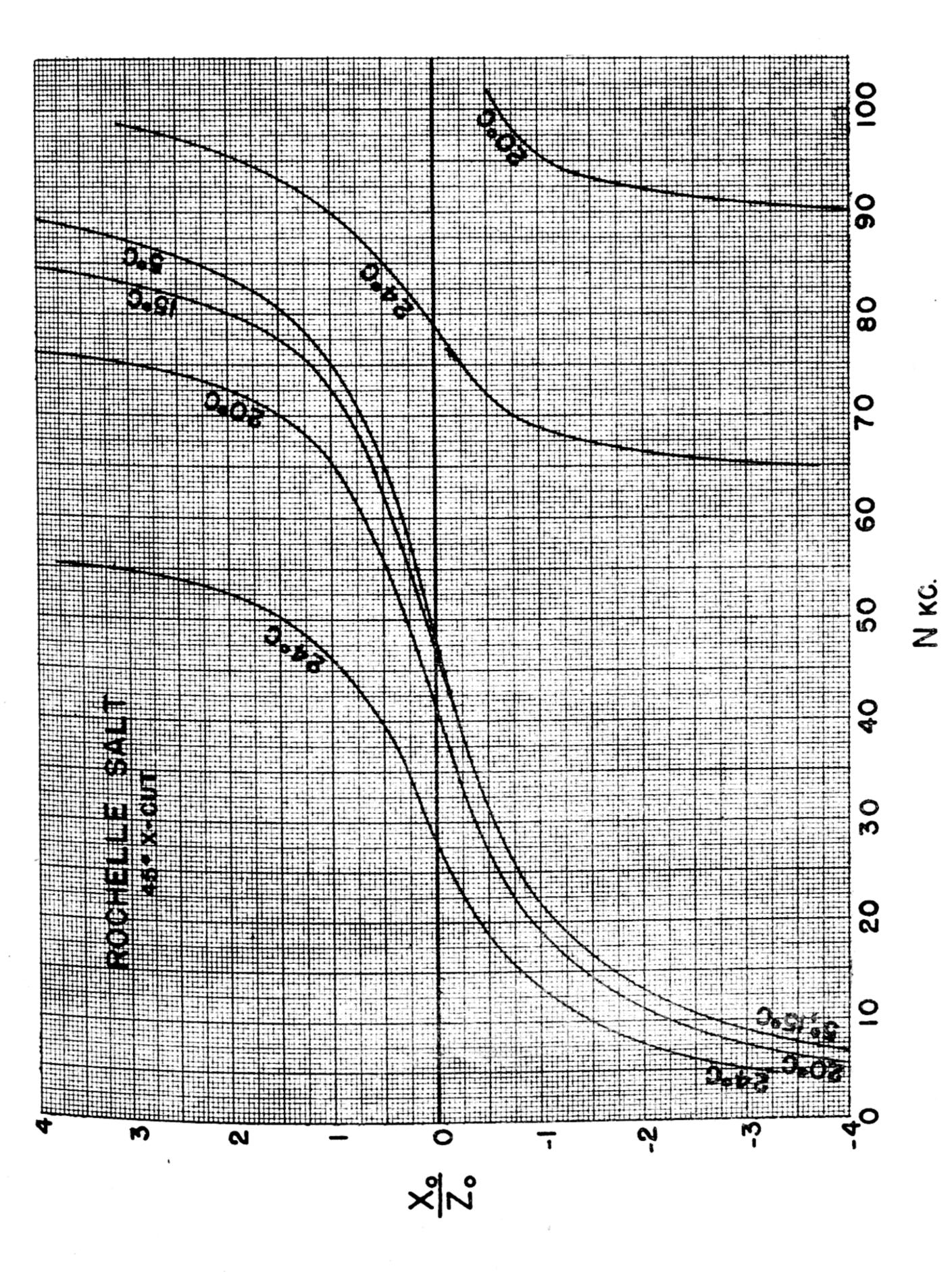


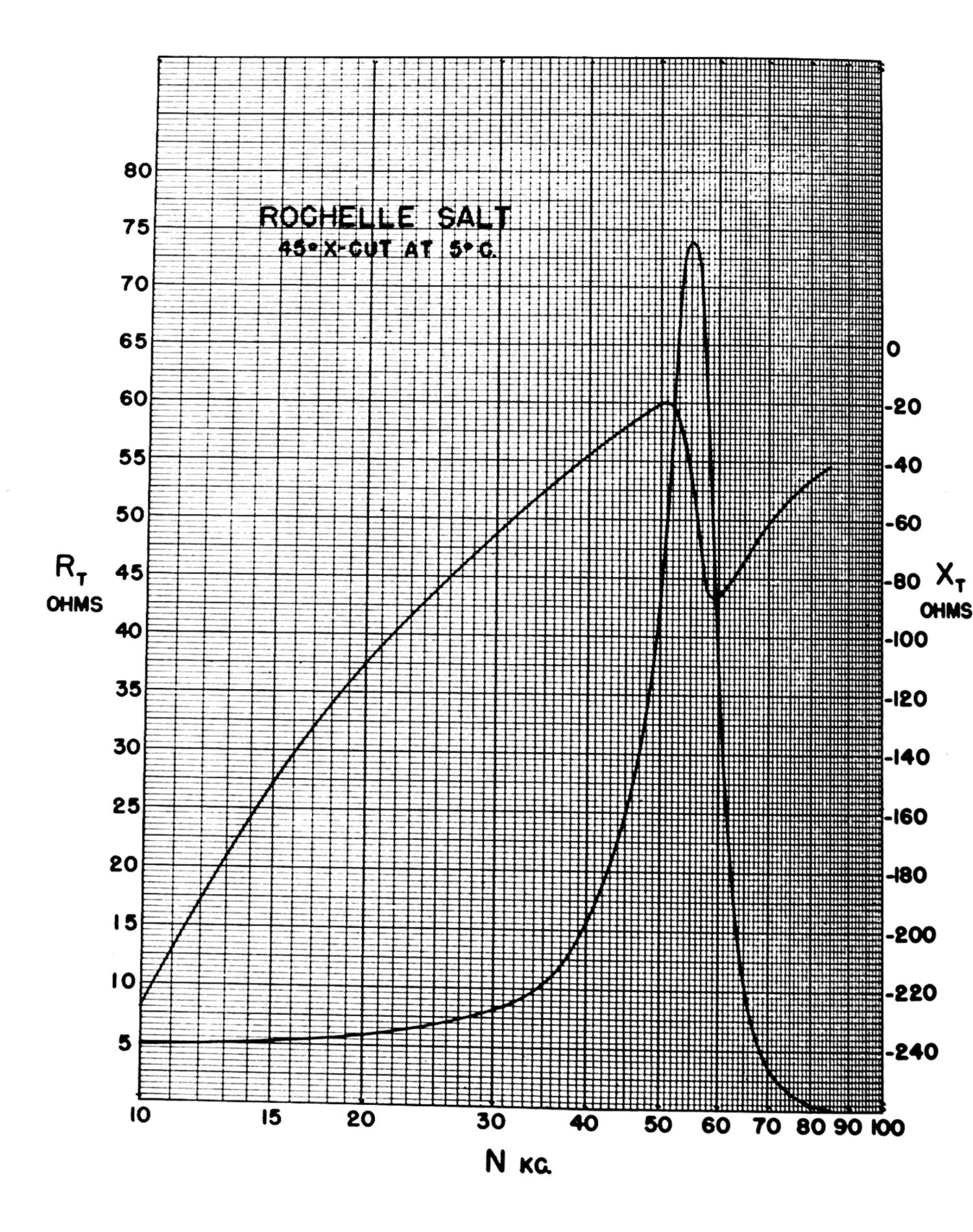


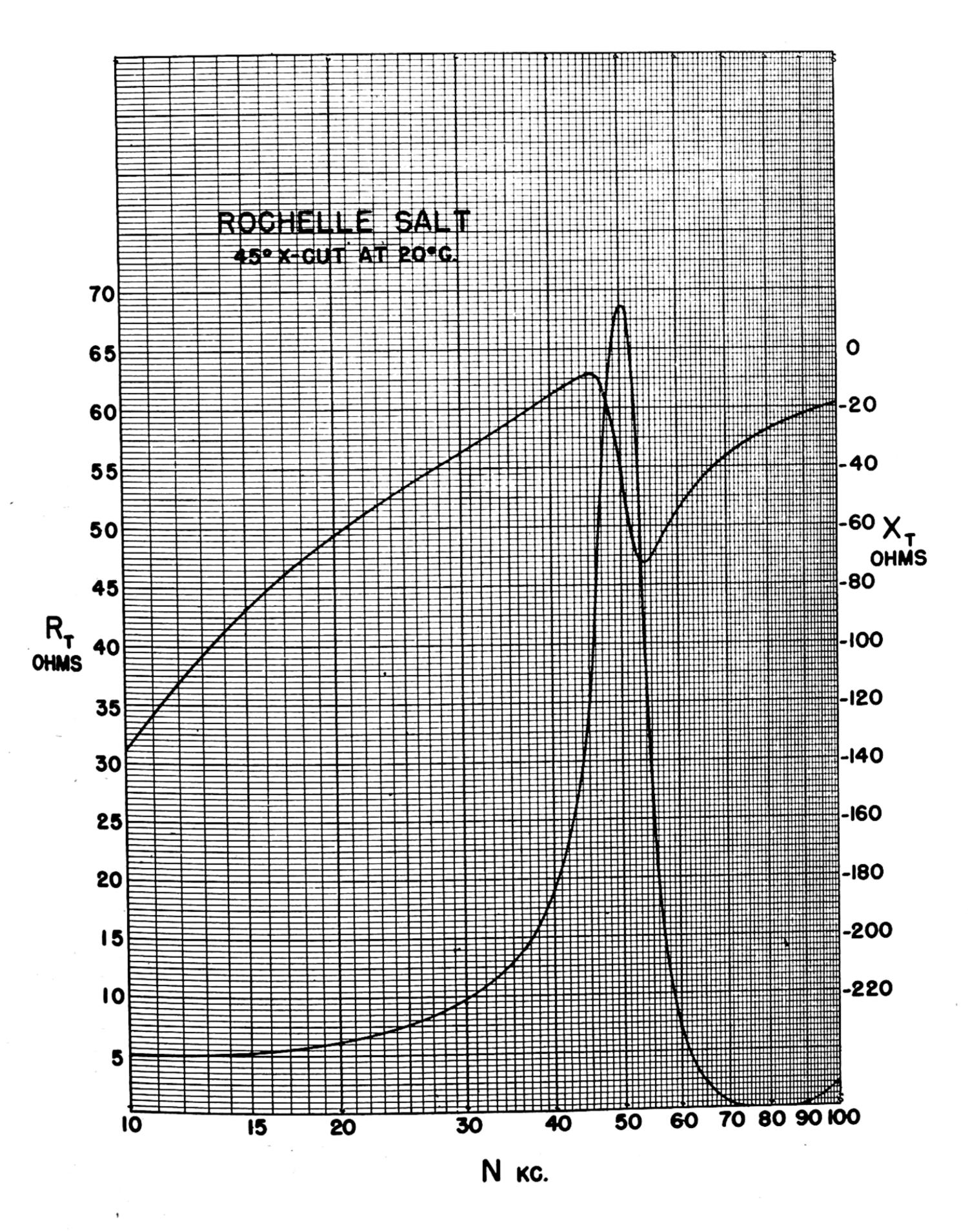


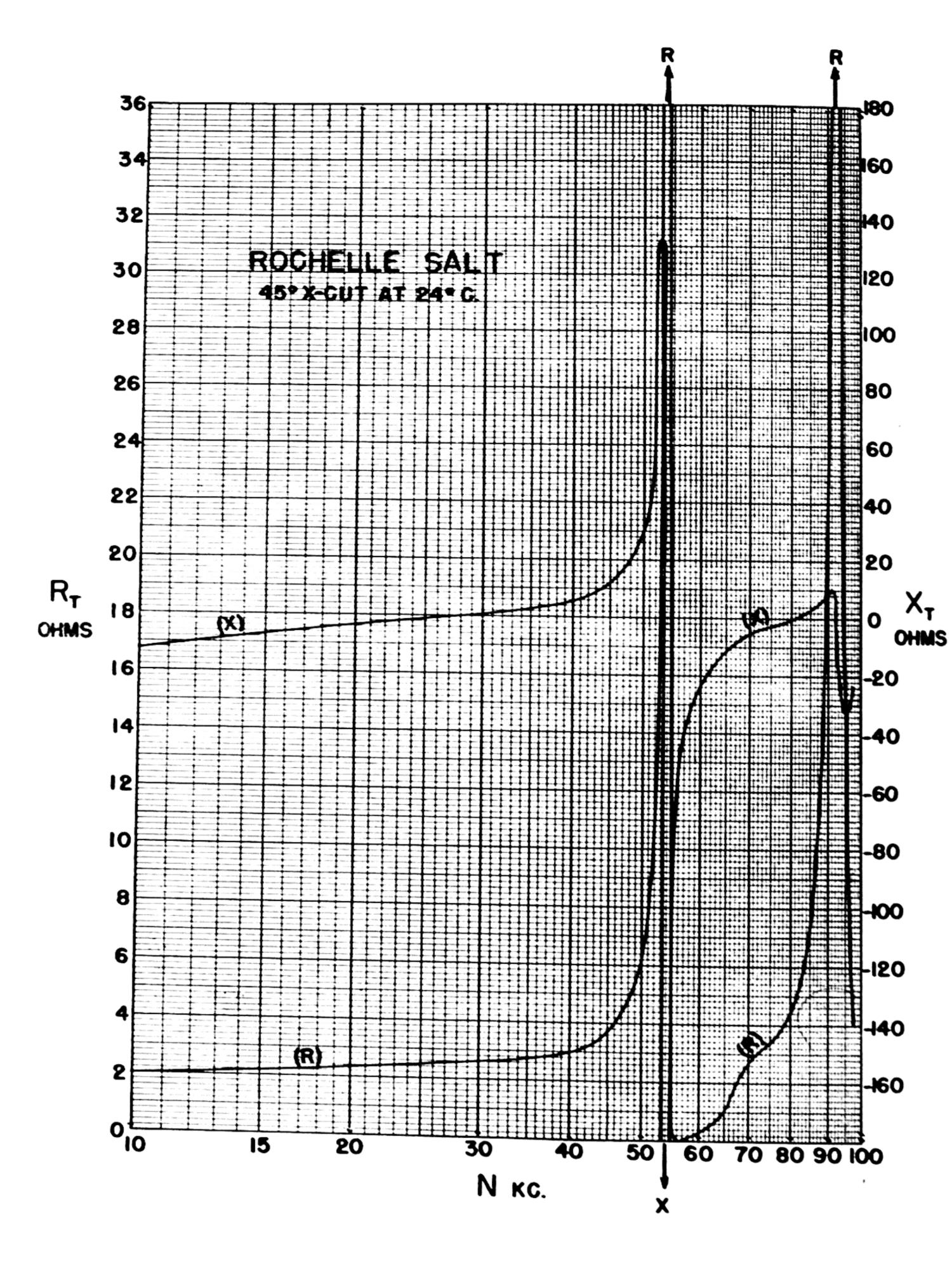


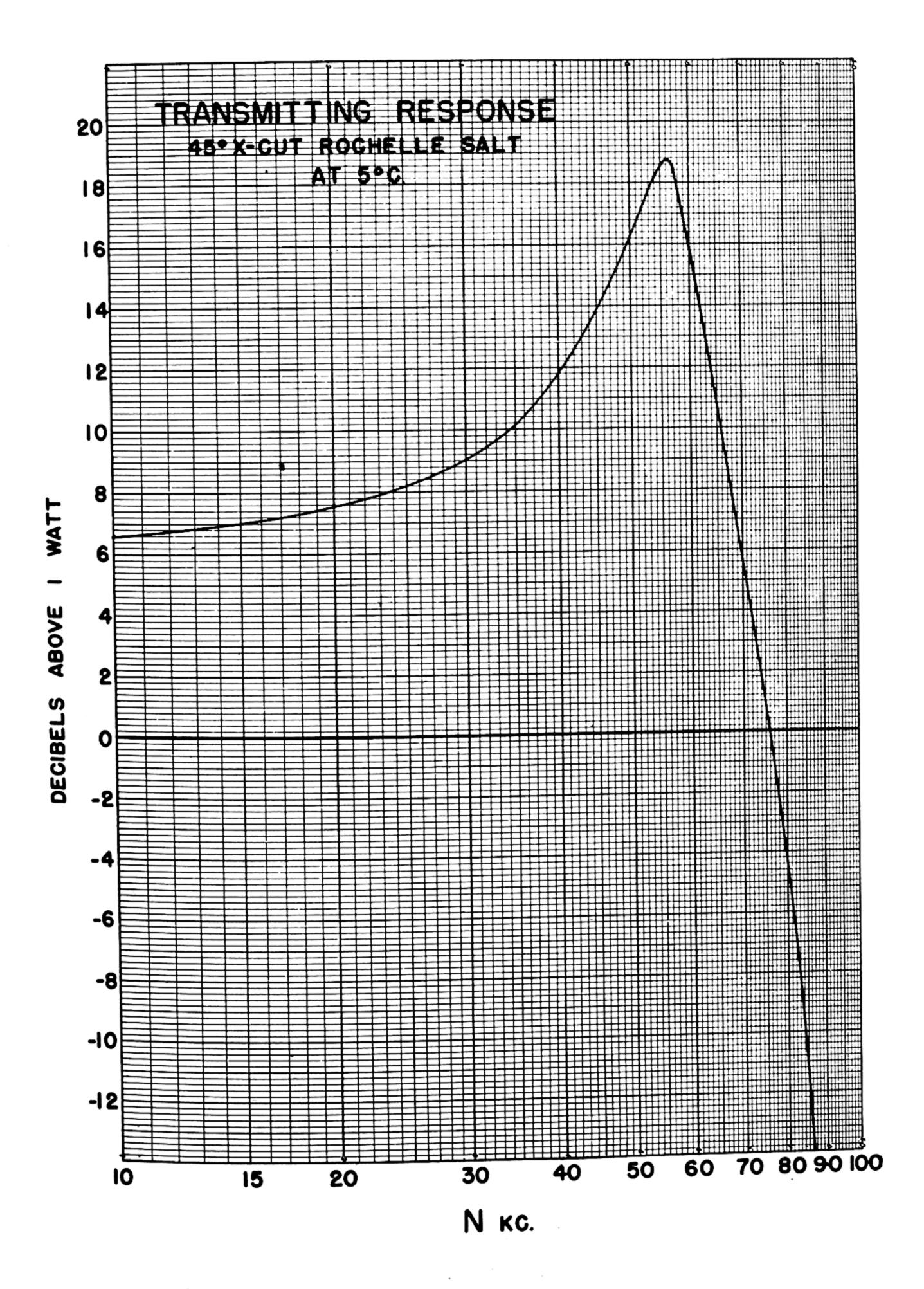


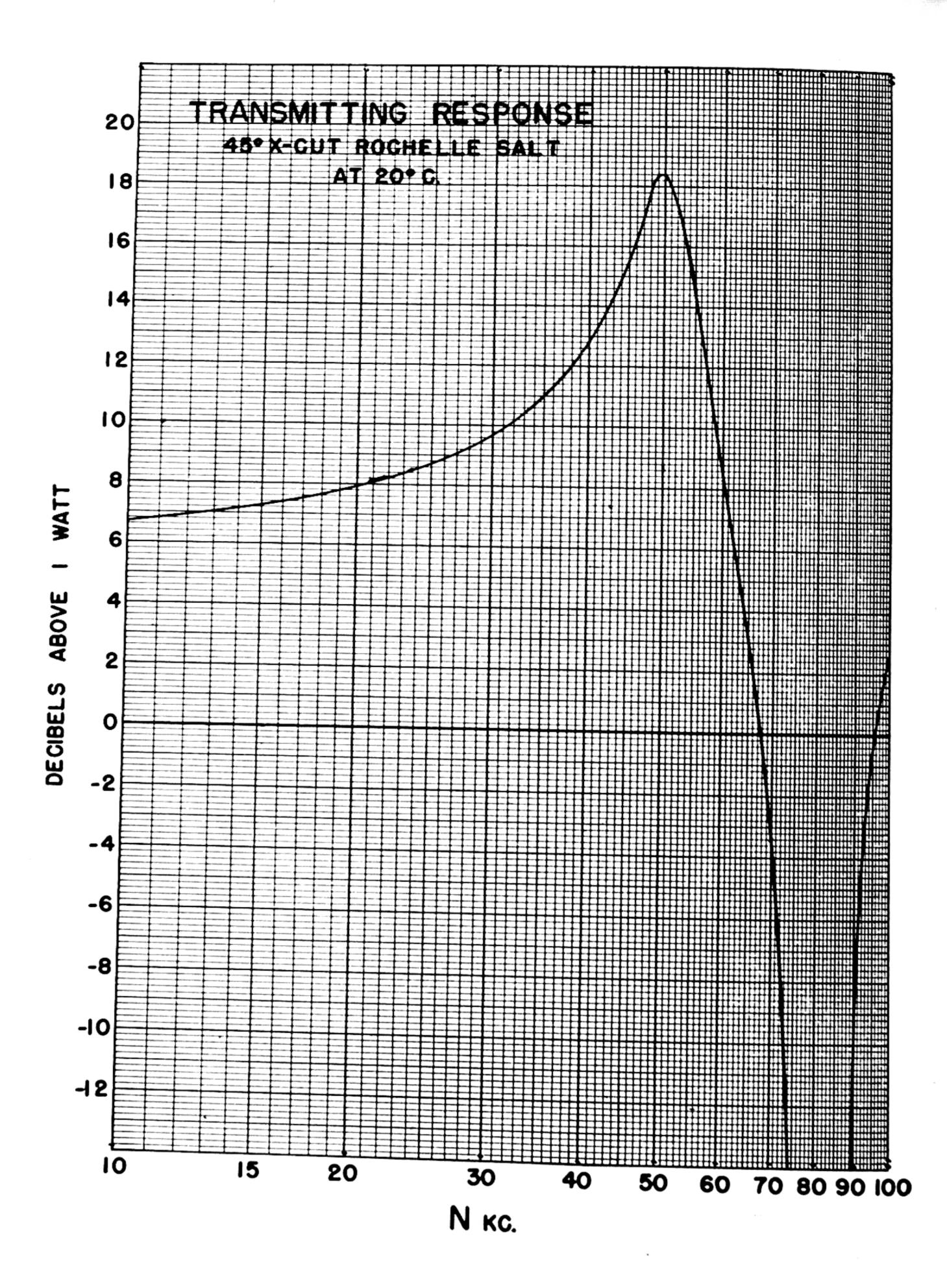


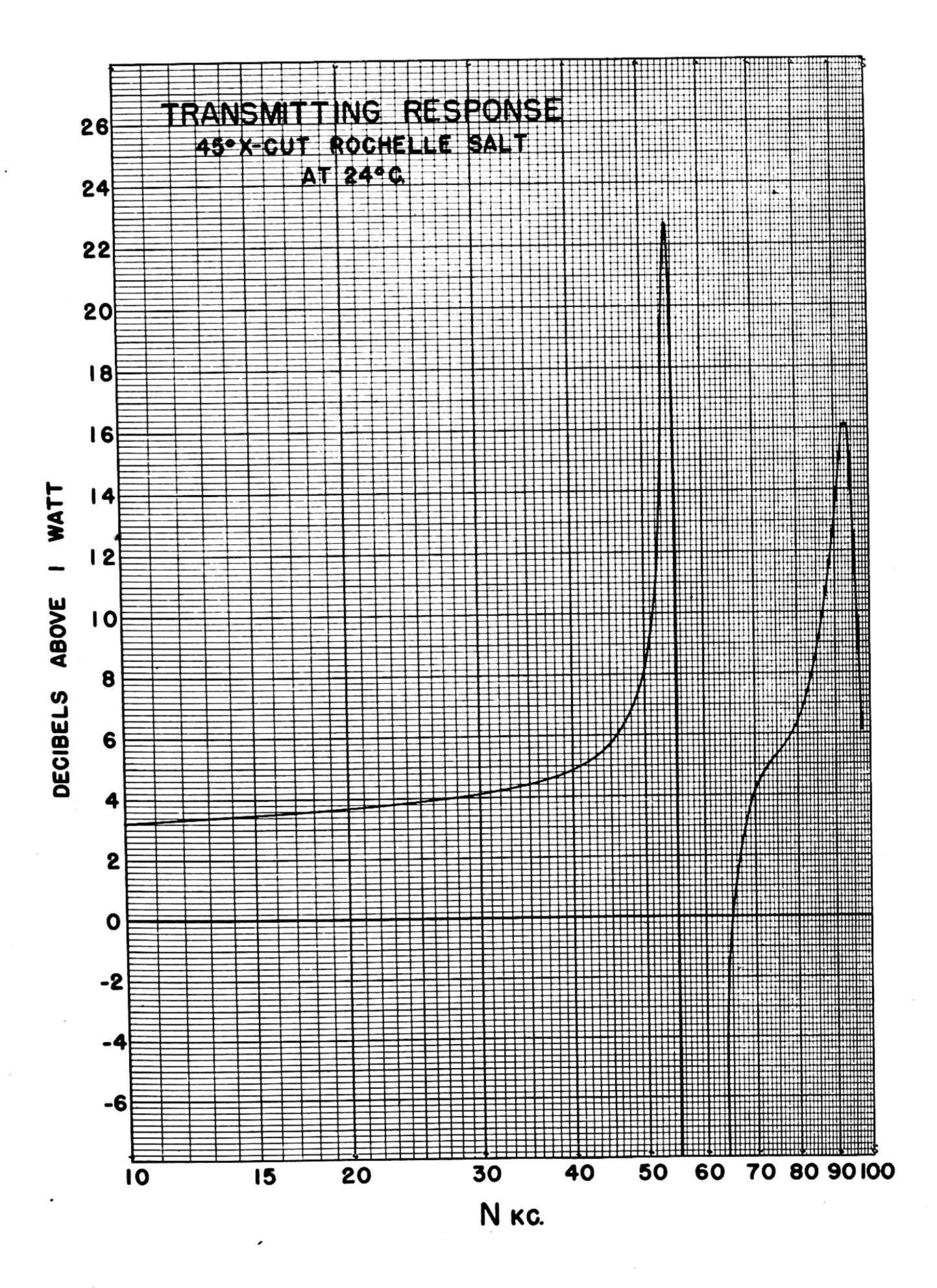












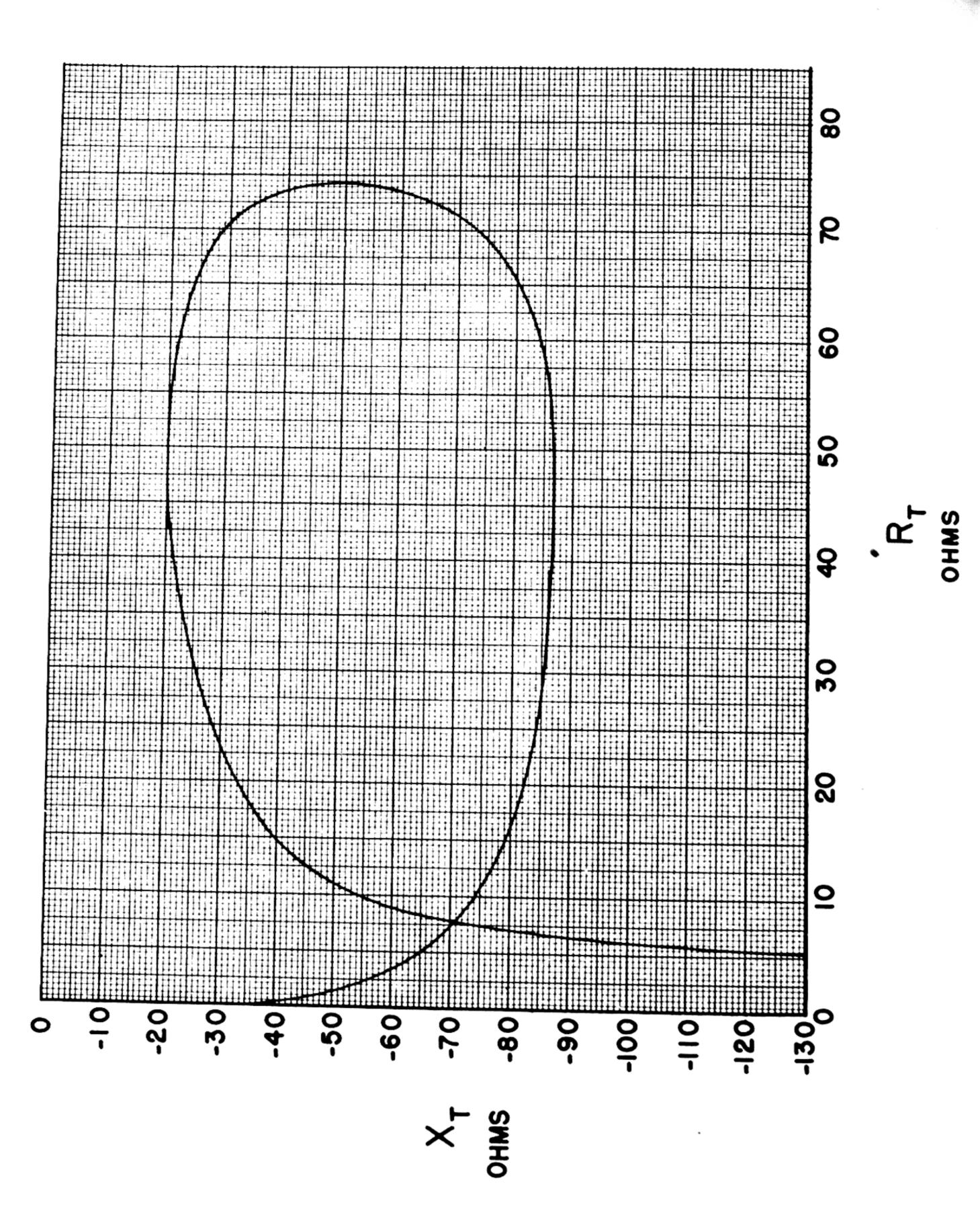
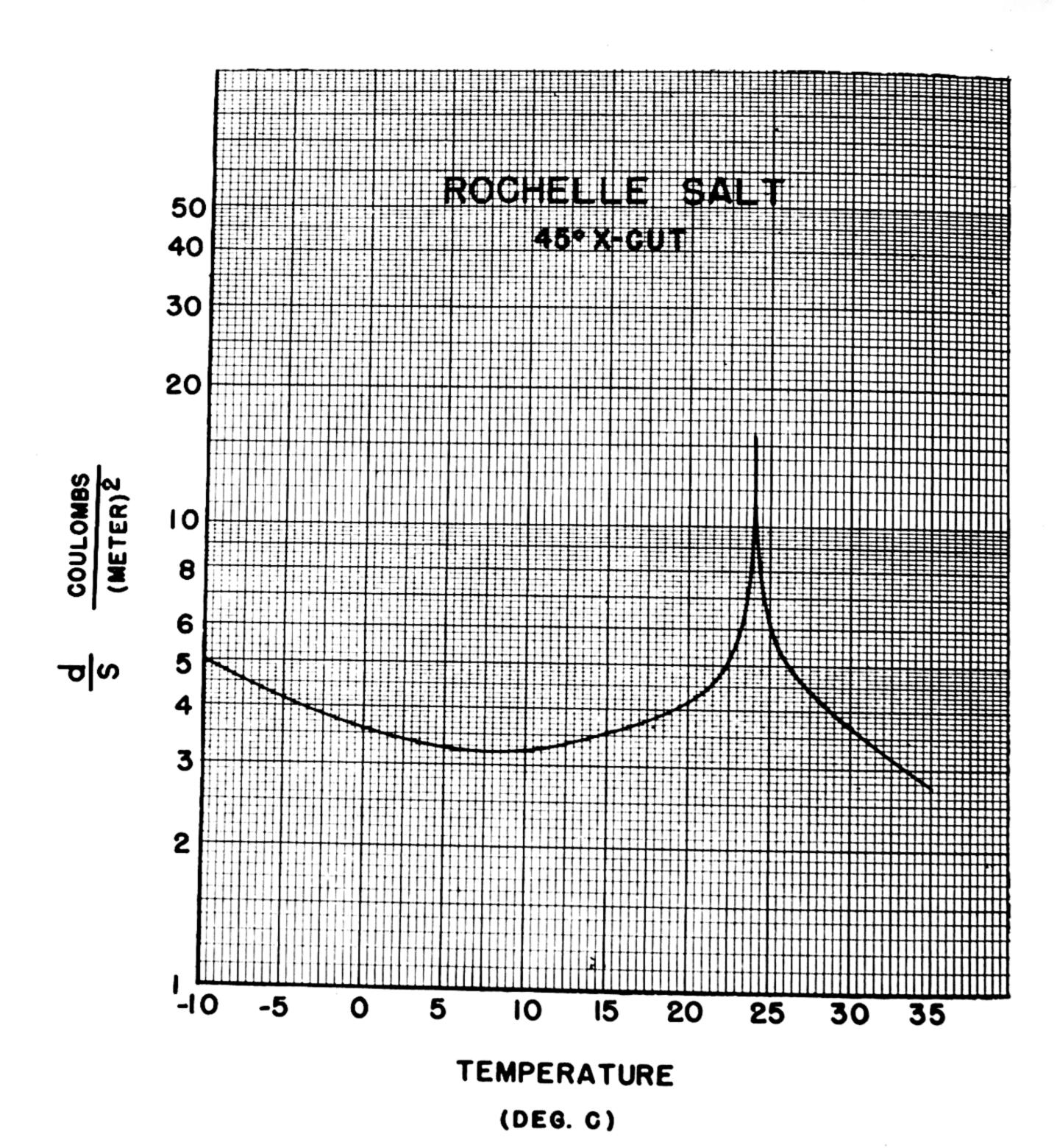


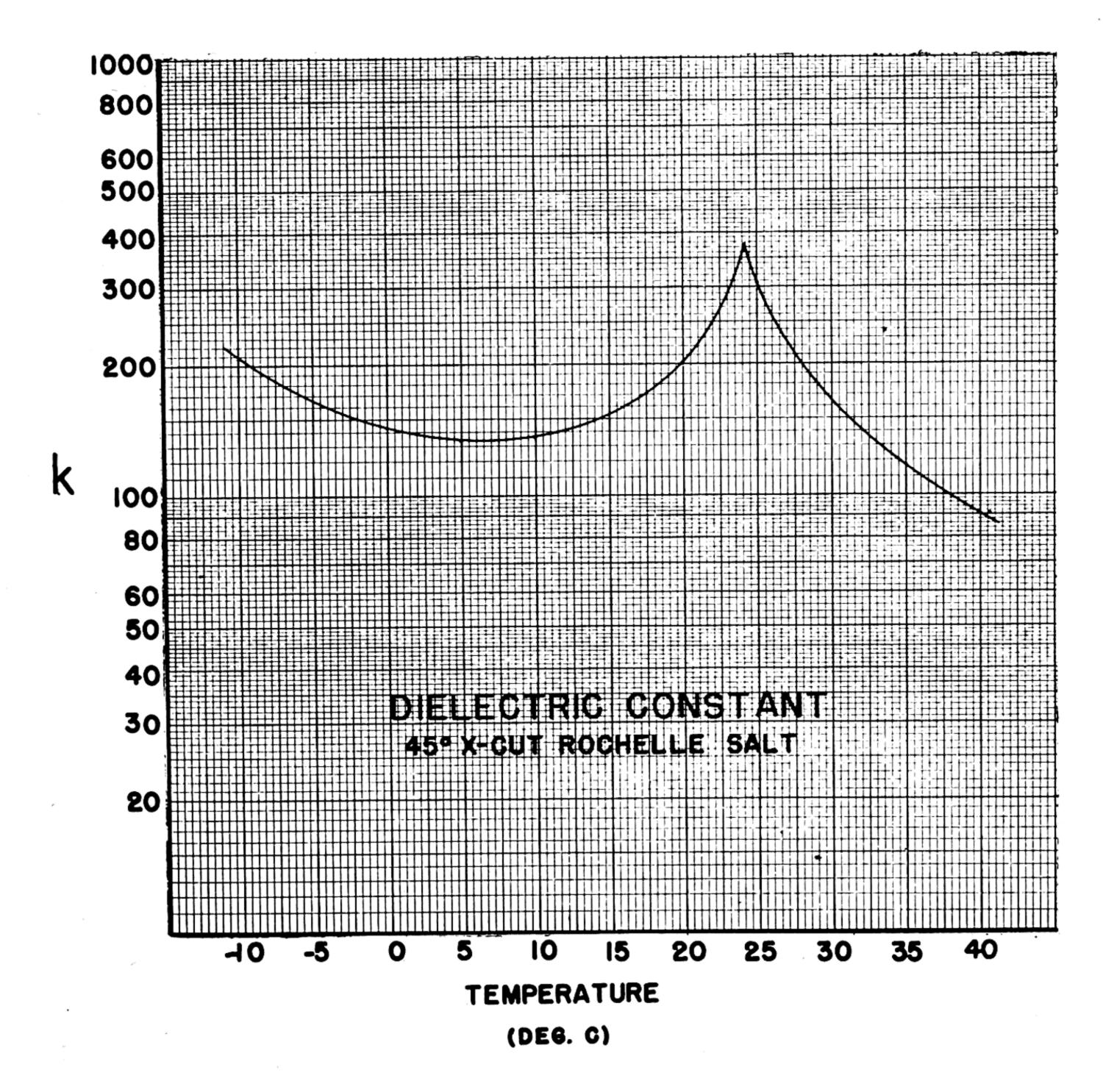
TABLE 8

Crystal	Piezoelectric interaction constant d/s	Piezoelectric interaction constant d/s
ADP (NH ₄ H ₂ PO ₄) 45° Z-	esu. of charge sq. cm. 1.48(10) ⁵	coulombs sq. meter 0.493
Rochelle salt 45° Y-cut bar.	0.92(10)5	0.307
Rochelle salt 45° X-cut bar. Quartz X-cut bar. Tourmaline Z-cut plate	See graph page 60. 0.528(10) ⁵ 1(10) ⁵	See graph page 60. 0.176 0.333

TABLE 9

Crystal	Dielectric Constant, K K (air) = 1
ADP (NH ₄ H ₂ PO ₄) 45° Z-cut.	14. 0
Rochelle salt 45° Y-cut.	10. 0
Rochelle salt 45° X-cut.	See graph, page 61.
Quartz X-cut	4. 5
Tourmaline Z-cut.	5 - 6

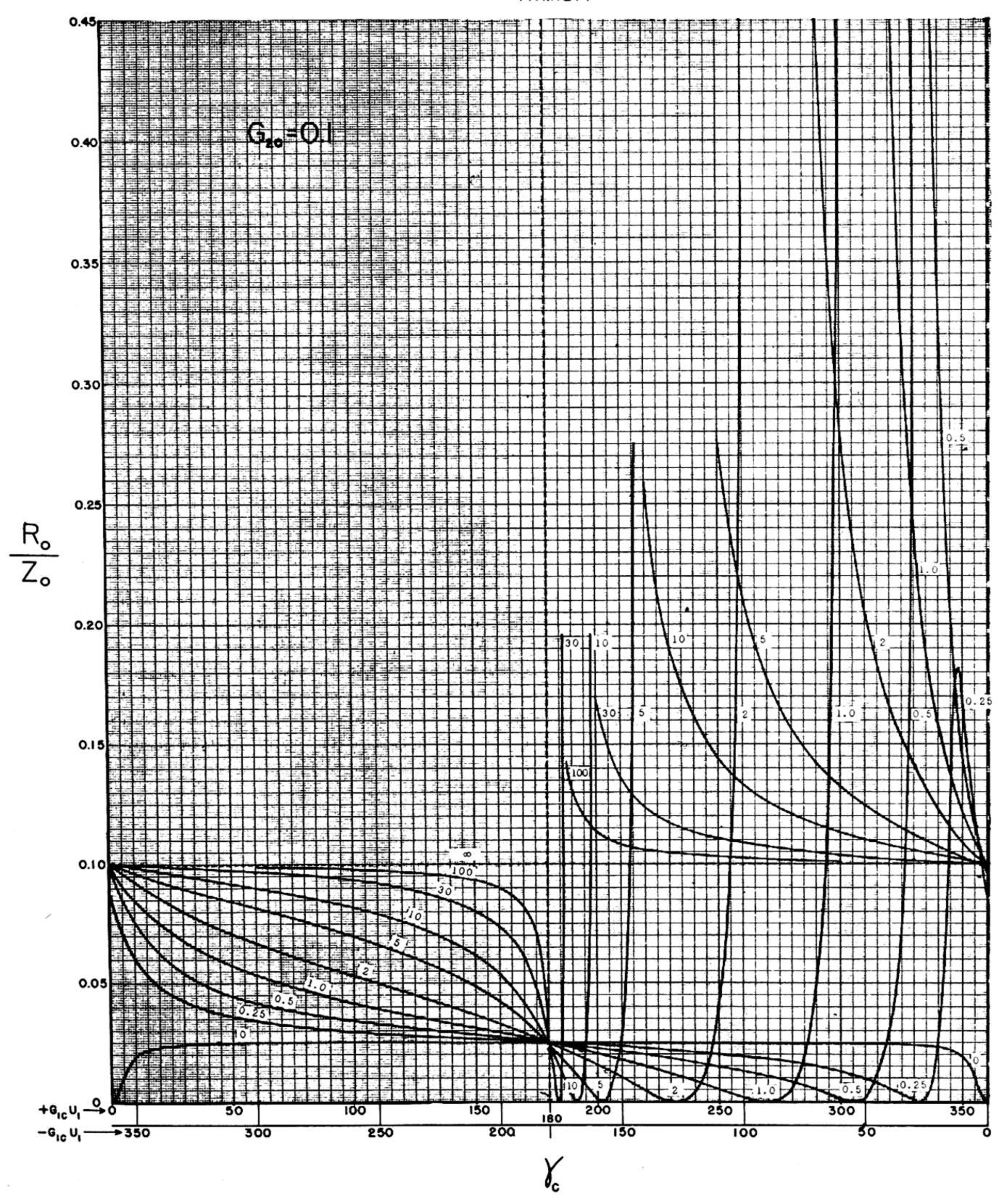


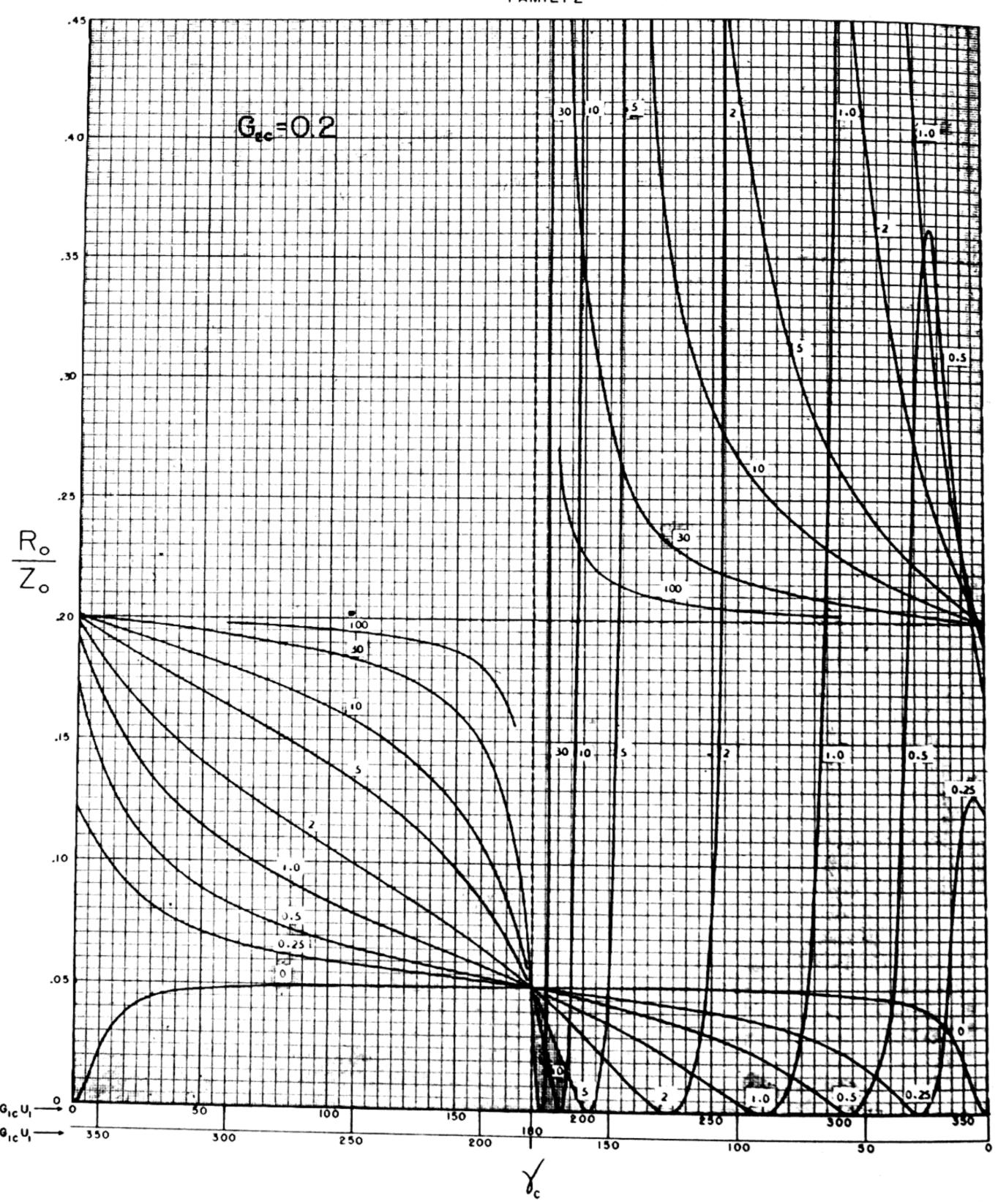


DB. CHART

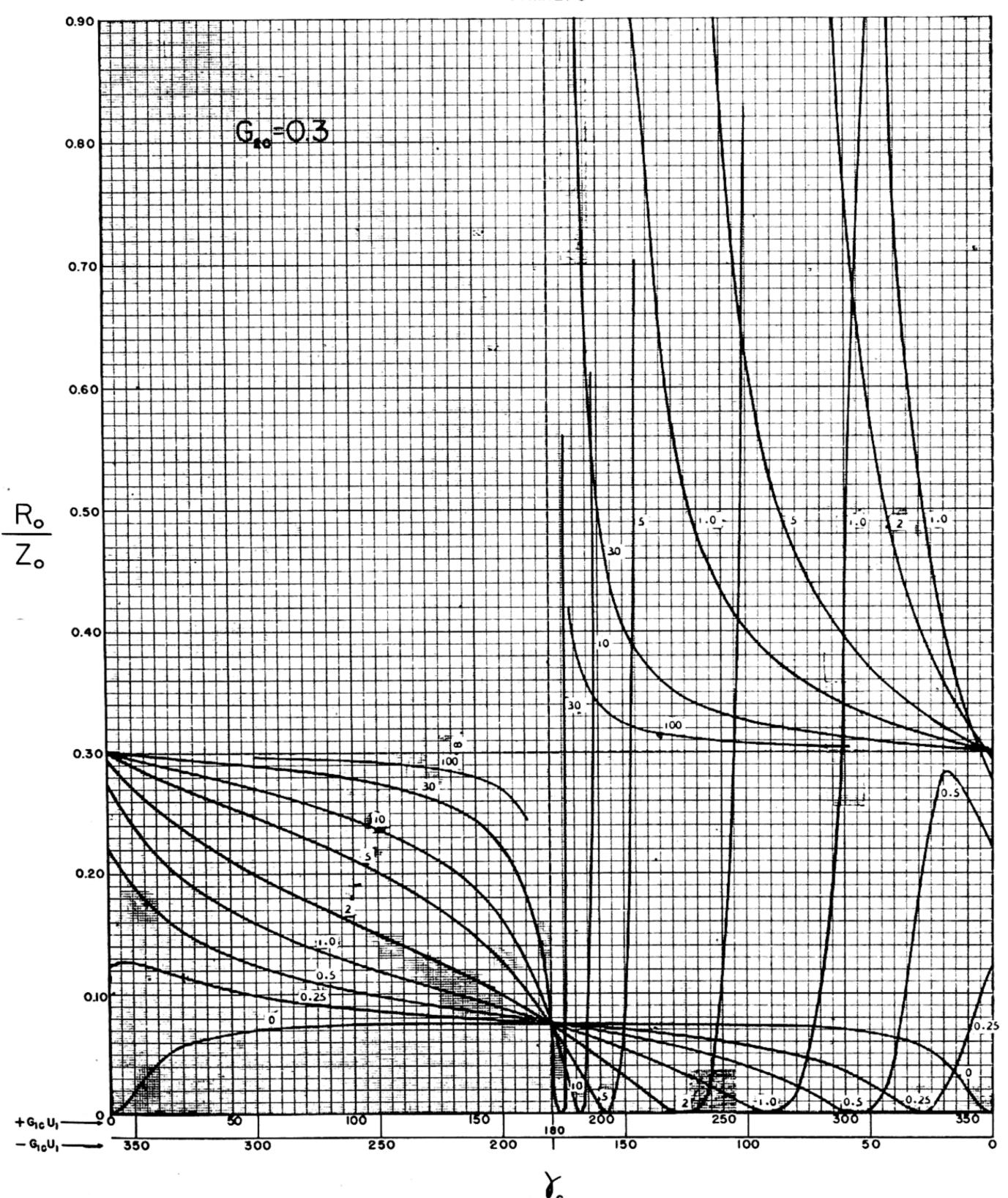
Voltage ratio	Power ratio	-←db→+	Voltage ratio	Power ratio
1. 00	1. 00	0	1. 00	1. 00
0. 944	0.89	0. 5	1.06	1. 12
. 891	. 79	1.0	1. 12	1. 26
. 841	. 71	1. 5	1. 19	1.41
. 79	. 63	2.0	1. 26	1. 59
. 75	. 56	2. 5	1. 33	1.78
. 71	. 50	3. 0	1.41	2.00
. 67	. 45	3. 5	1. 50	2. 24
. 63	. 40	4. 0	1. 59	2. 51
. 60	. 35	4. 5	1. 68	2.82
. 56	. 32	5. 0	1.78	3. 16
. 53	. 28	5. 5	1.88	3. 55
. 50	. 25	6. 0	2.00	3. 98
. 47	. 22	6. 5	2. 11	4. 47
. 45	. 20	7. 0	2. 24	5. 01
. 42	. 18	7. 5	2. 37	5. 62
. 40	. 16	8. 0	2. 51	6. 31
. 38	. 14	8. 5	2. 66	7. 08
. 35	. 13	9. 0	2. 82	7. 94
. 33	. 11	9. 5	2. 99	8. 91
. 32	. 10	10.0	3. 16	10.0
. 30	. 089	10. 5	3. 35	11.2
. 28	. 079	11.0	3. 55	12. 6
. 27	. 071	11.5	3. 76	14. 1
. 25	. 063	12.0	3. 98	15. 9
. 24	. 056	12. 5	4. 22	17. 8
. 22	. 050	.13. 0	4. 47	20. 0
. 21	. 045	13. 5	4. 73	22. 4
. 20	. 040	14. 0	5. 01	25. 1
. 19	. 035	14. 5	5. 31	28. 2
. 18	. 032	15. 0	5. 62	31.6
. 17	. 028	15. 5	5. 96	35. 8
. 16	. 025	16. 0	6. 31	39. 8
. 15	. 022	16. 5	6. 68	44. 7
. 14	. 020	17. 0	7. 08	50. 1
. 13	. 018	17. 5	7. 50	56. 2
. 13	. 016	18. 0	7. 94	63. 1
. 12	. 014	18. 5	8. 41	70. 8
. 11	. 013	19. 0	8. 91	
. 11	. 011	19. 5	9. 44	79. 4
. 10	. 010	20. 0	10. 00	89. 1
		20.0	10.00	100. 0



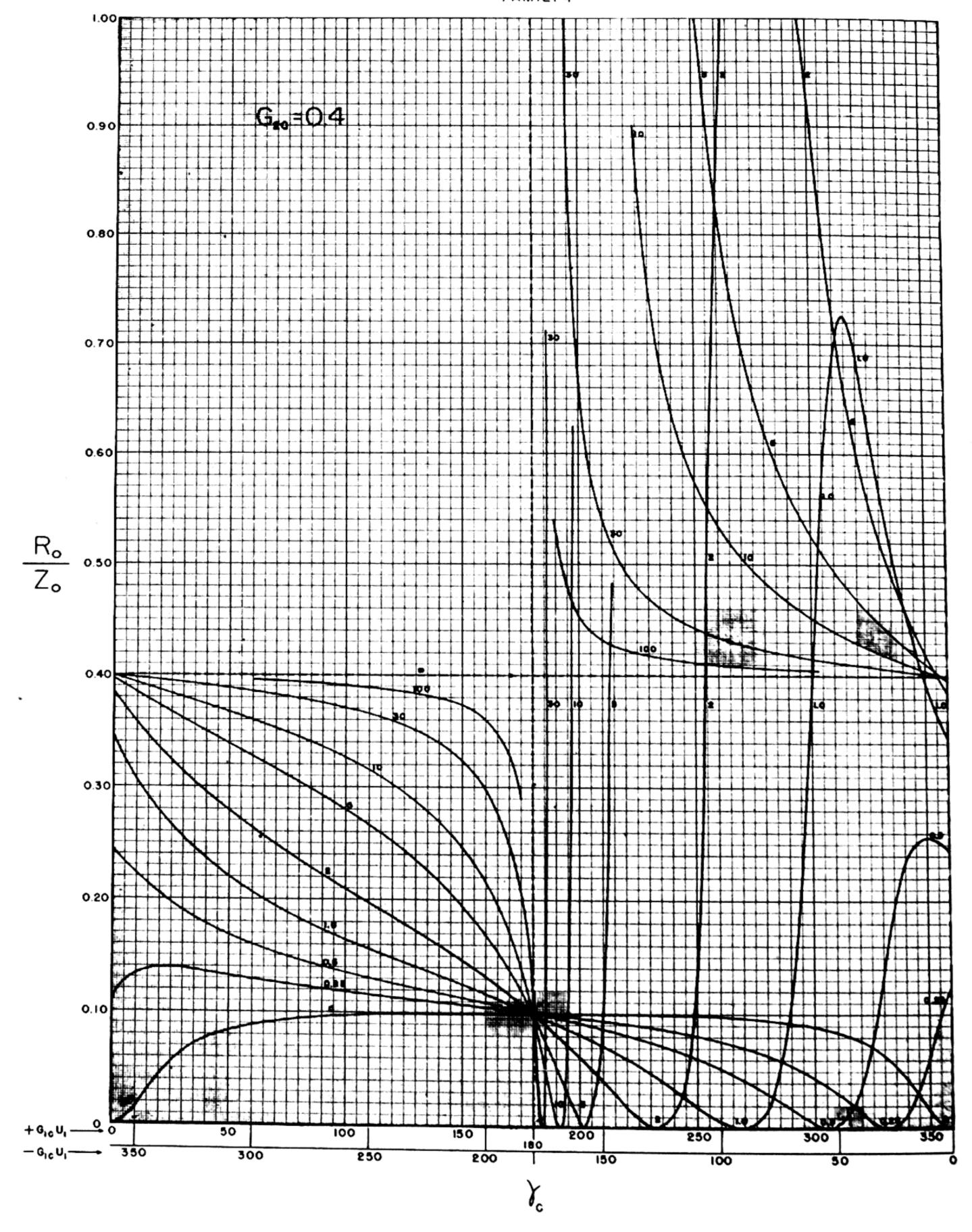




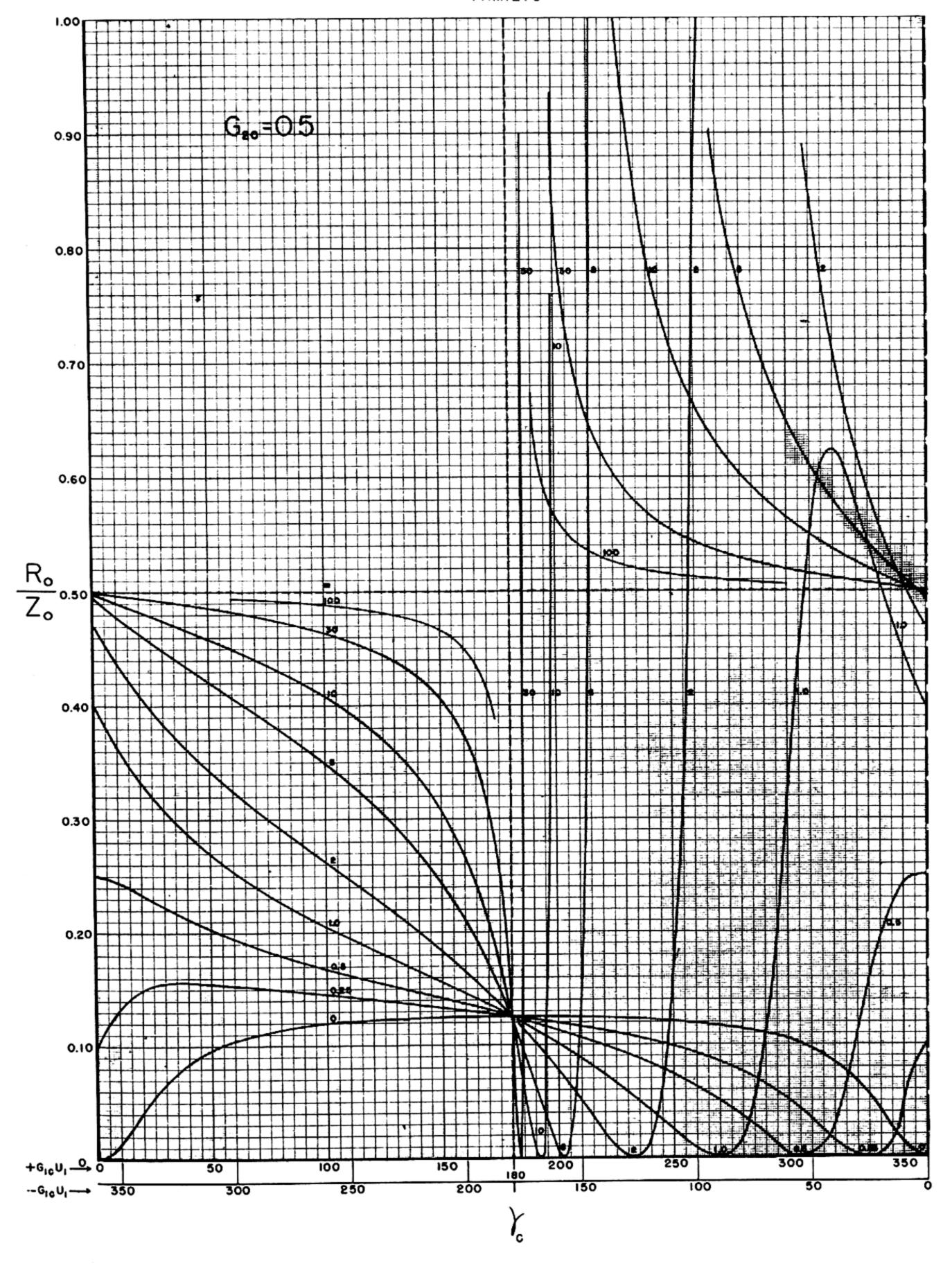


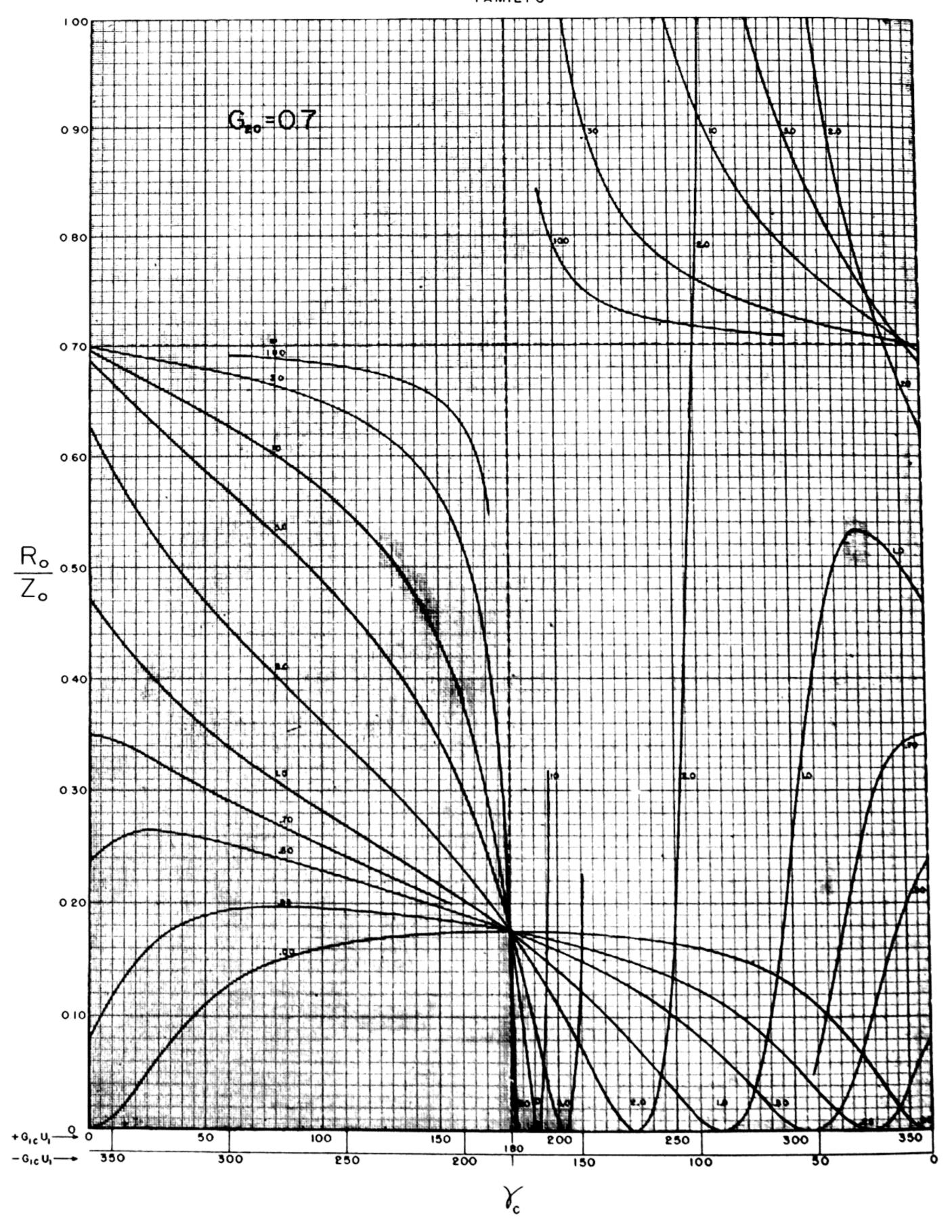




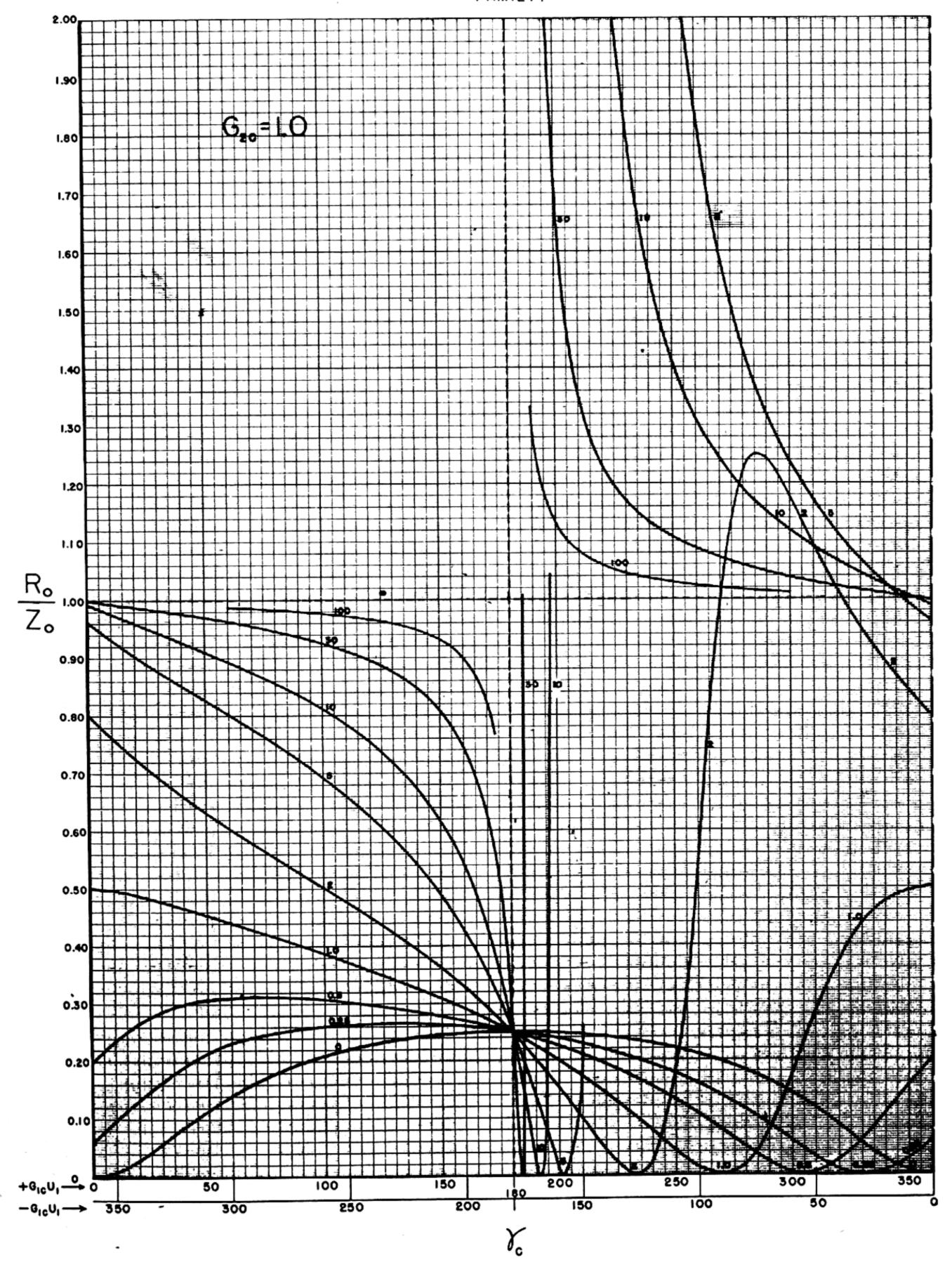


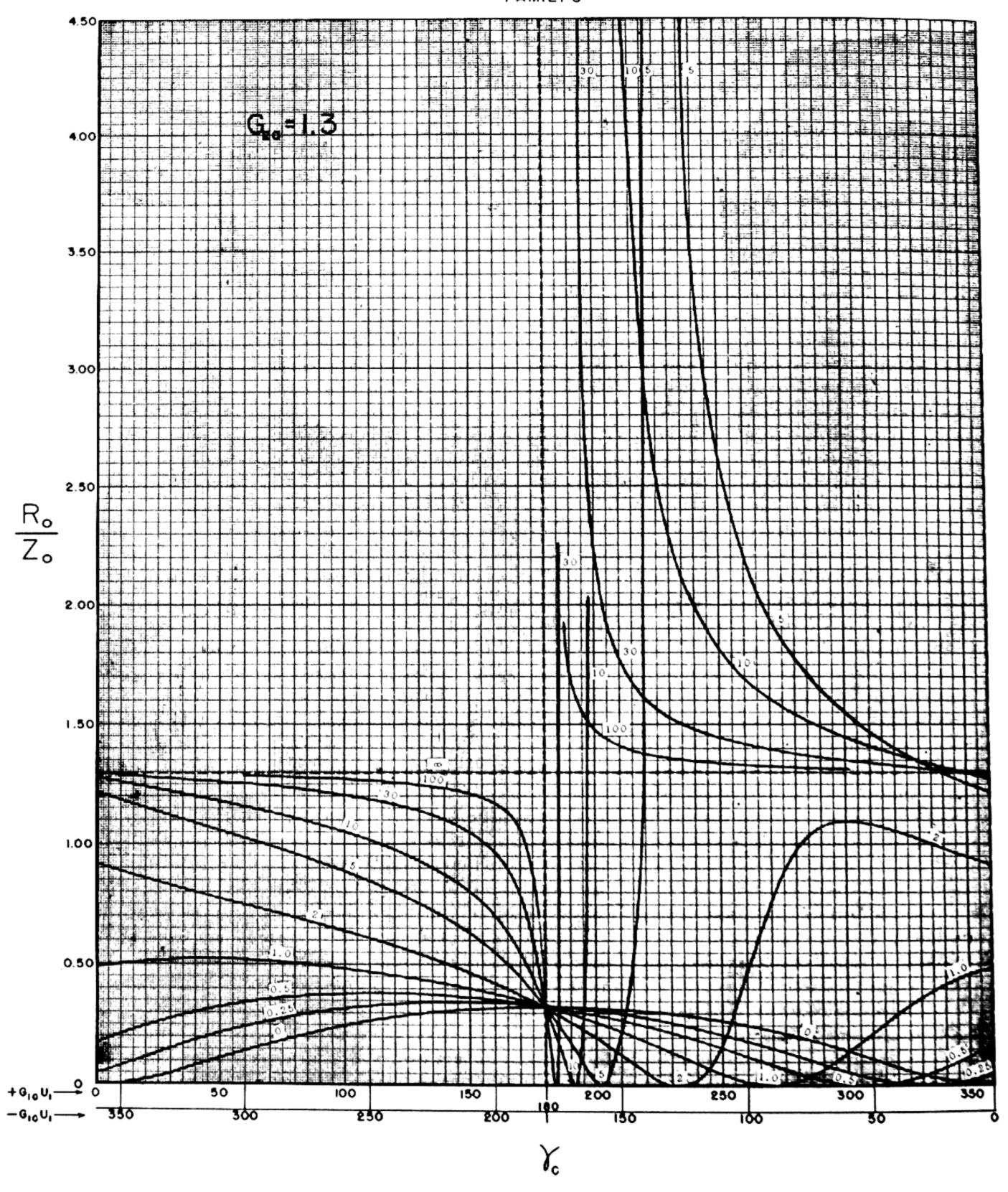


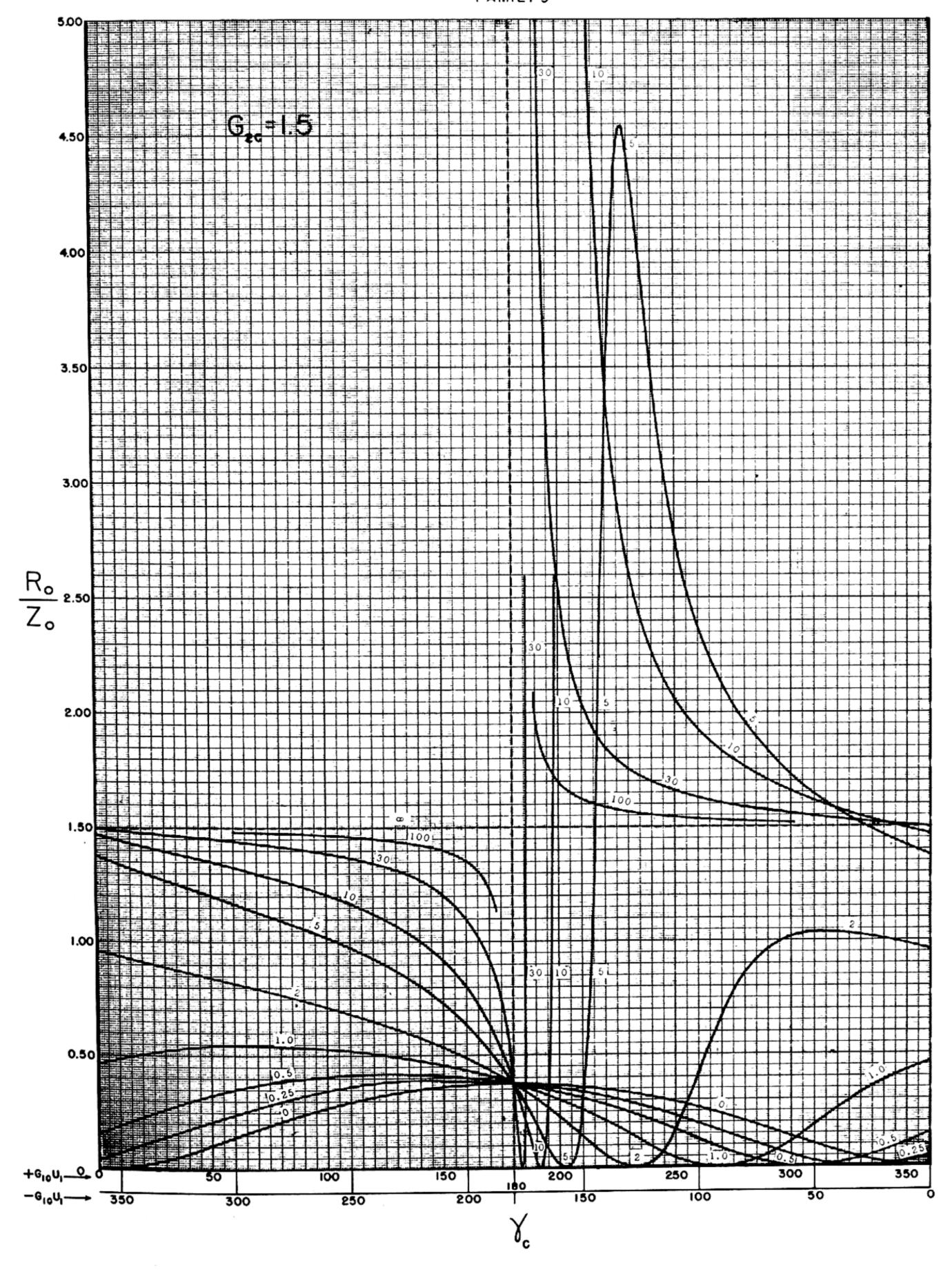




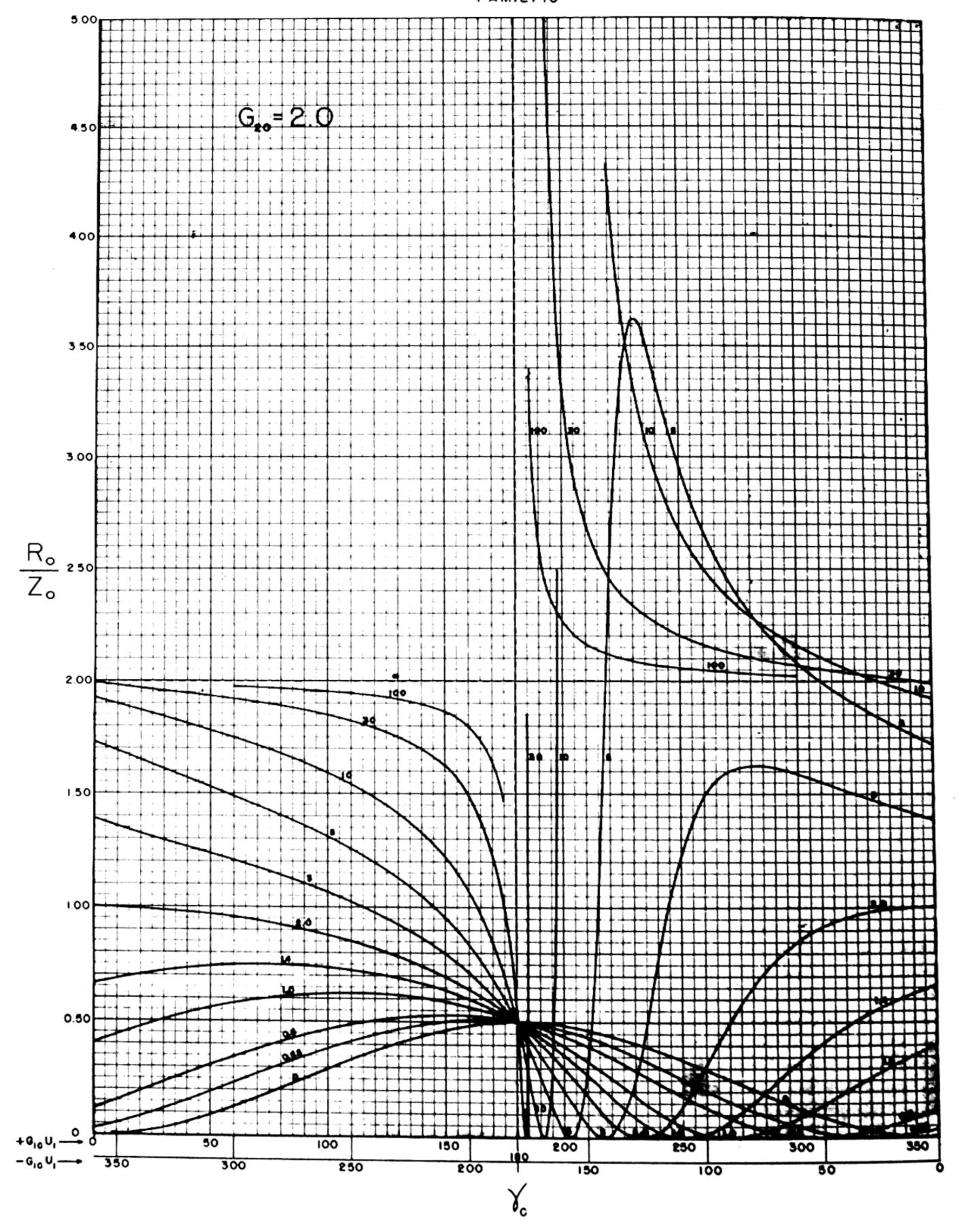




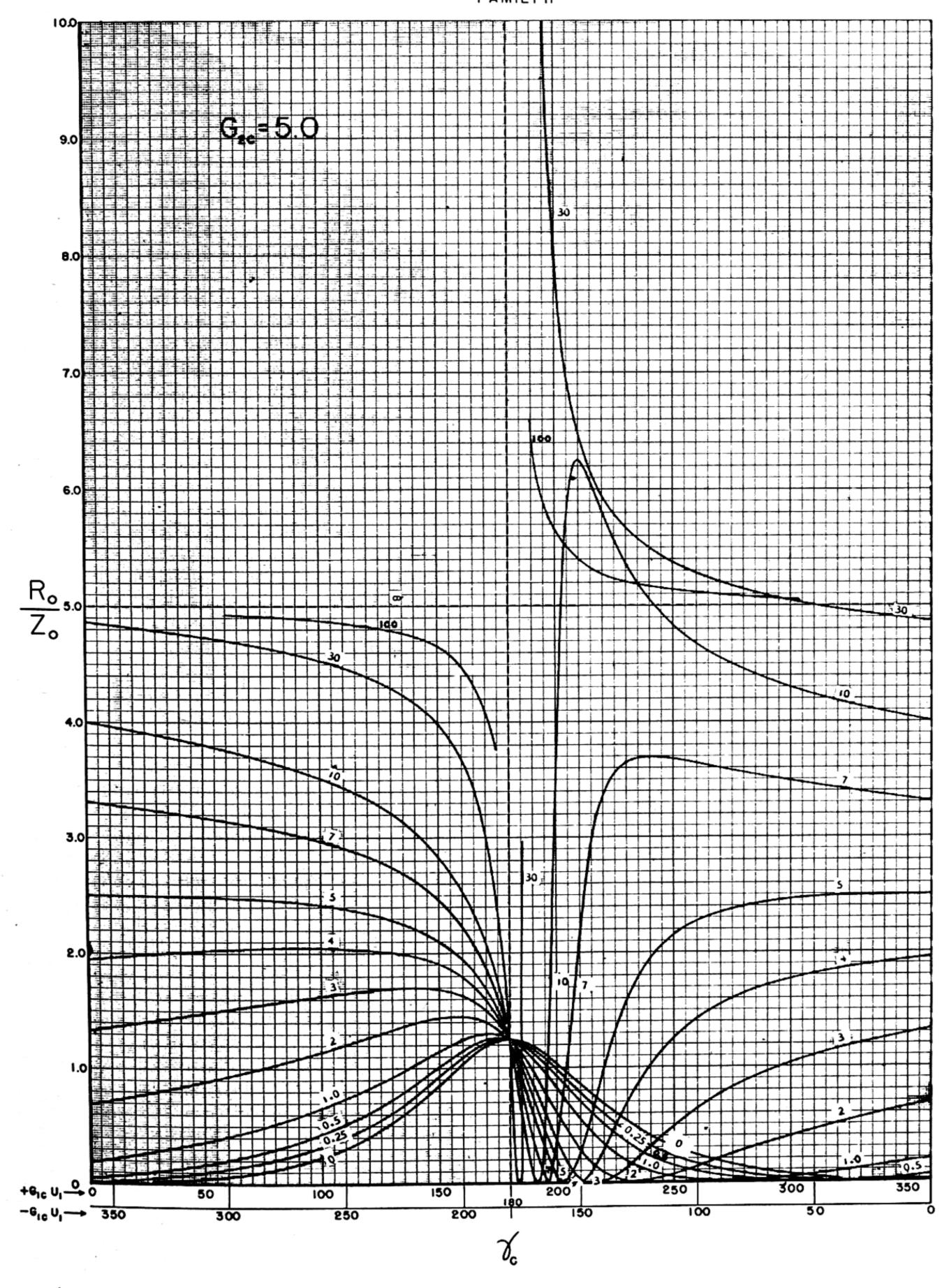




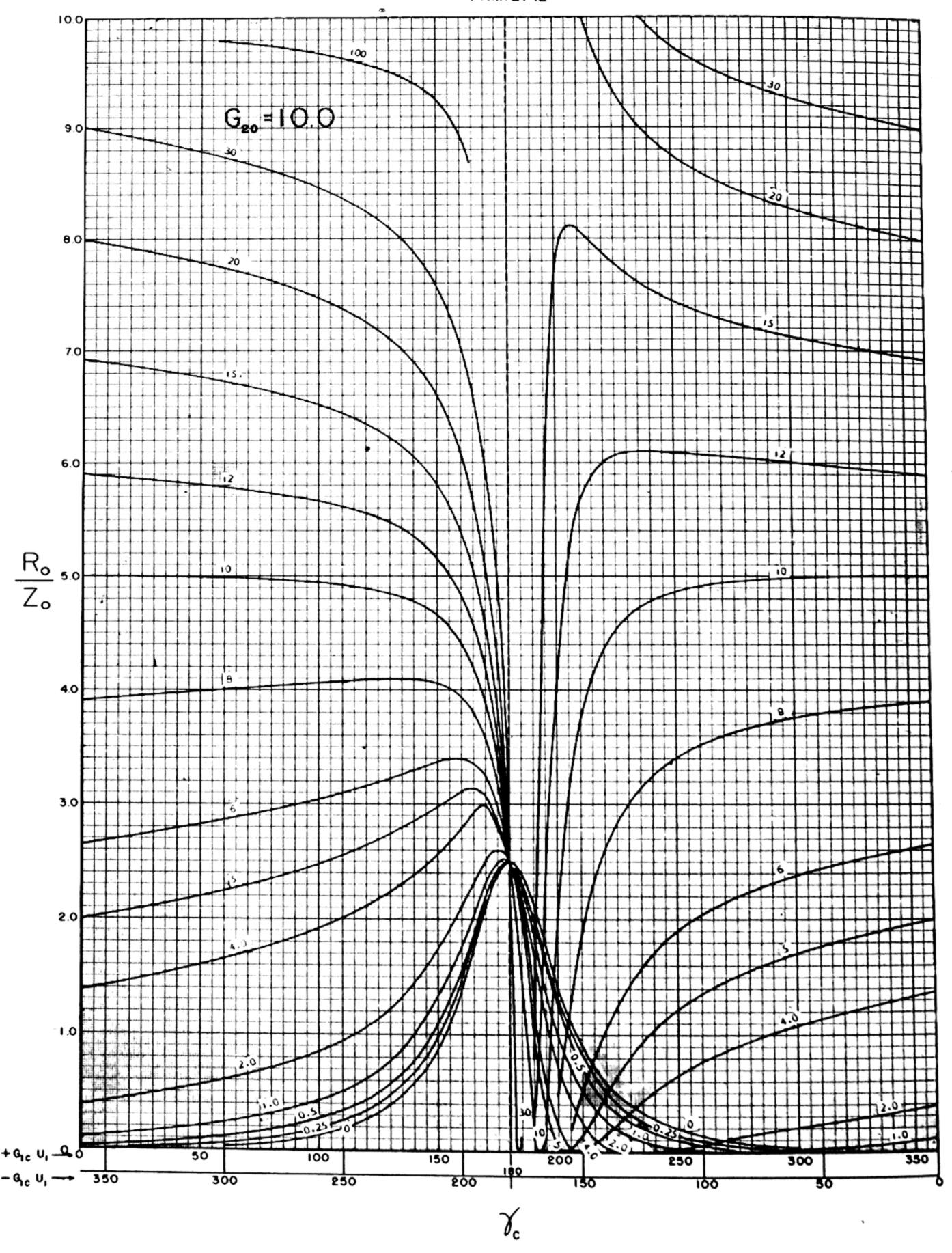


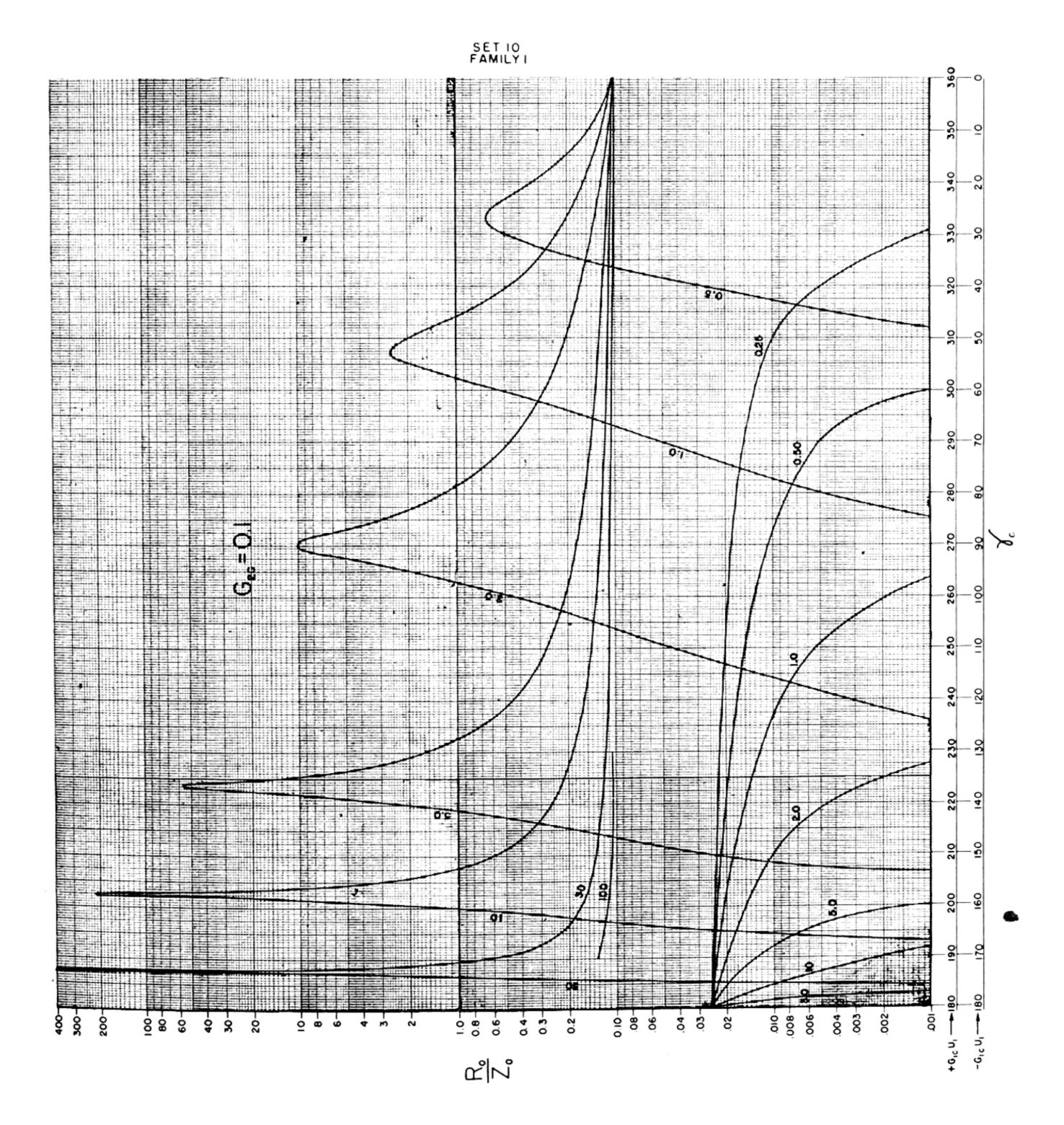


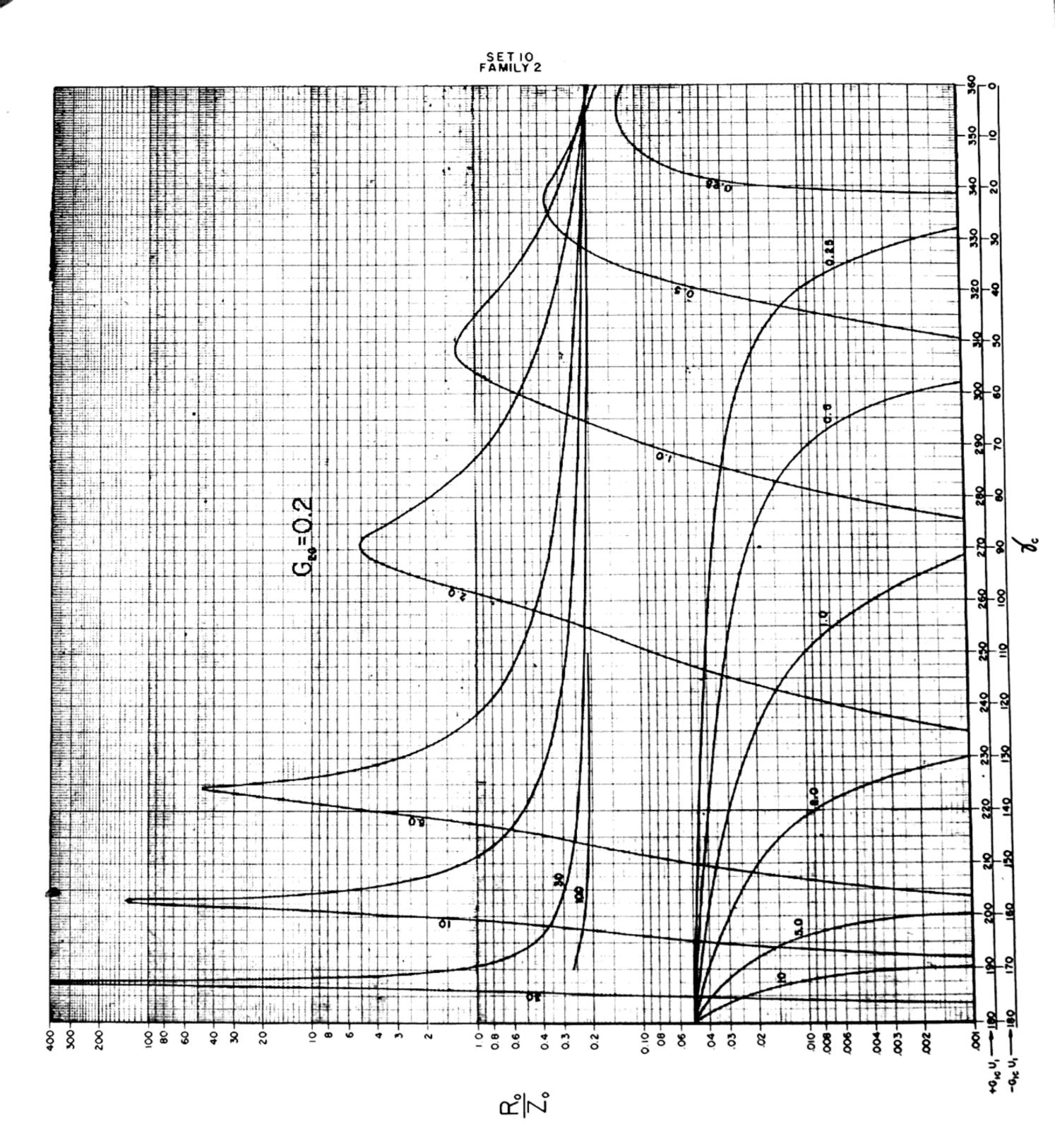
SET 9 FAMILY II

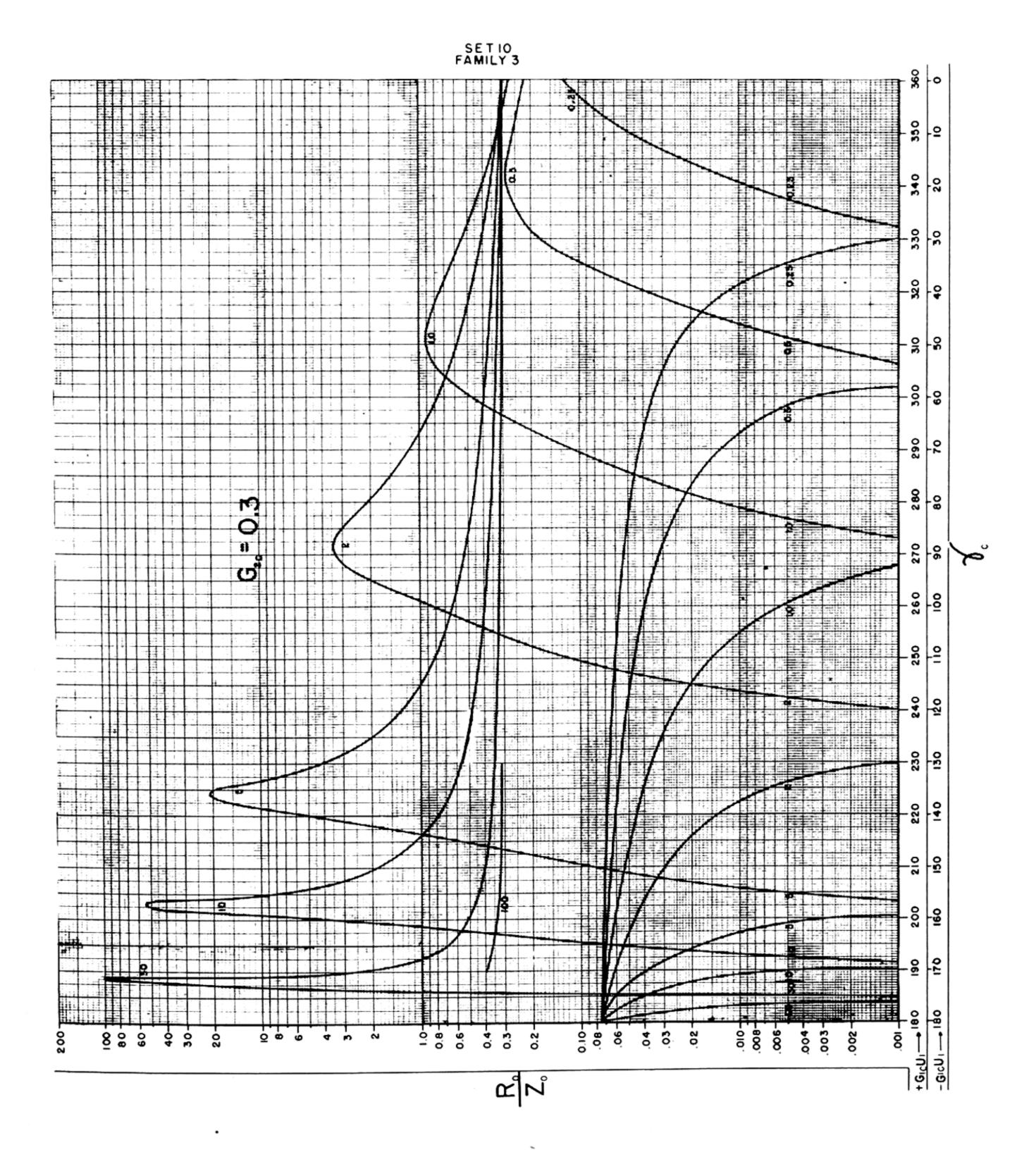


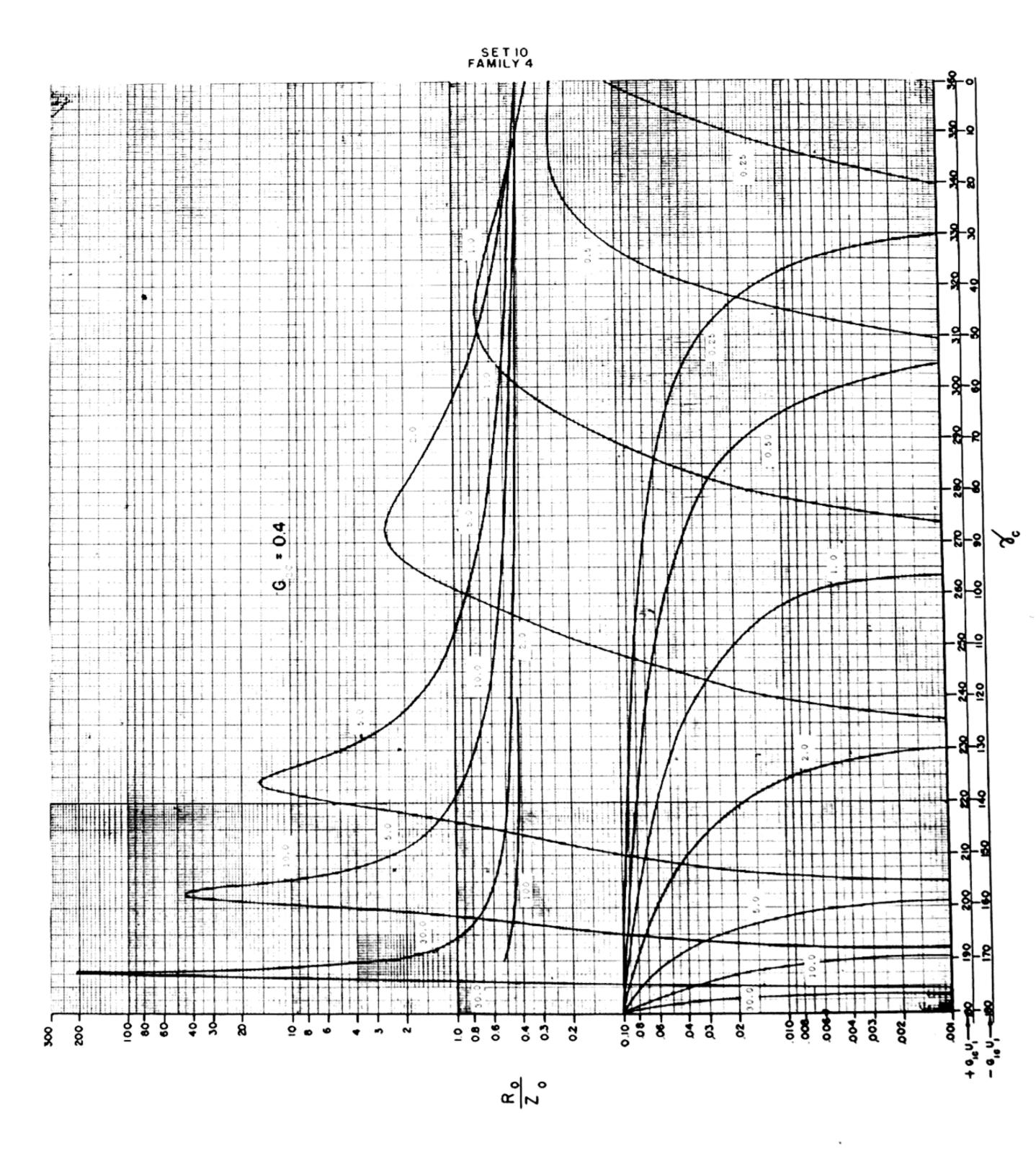


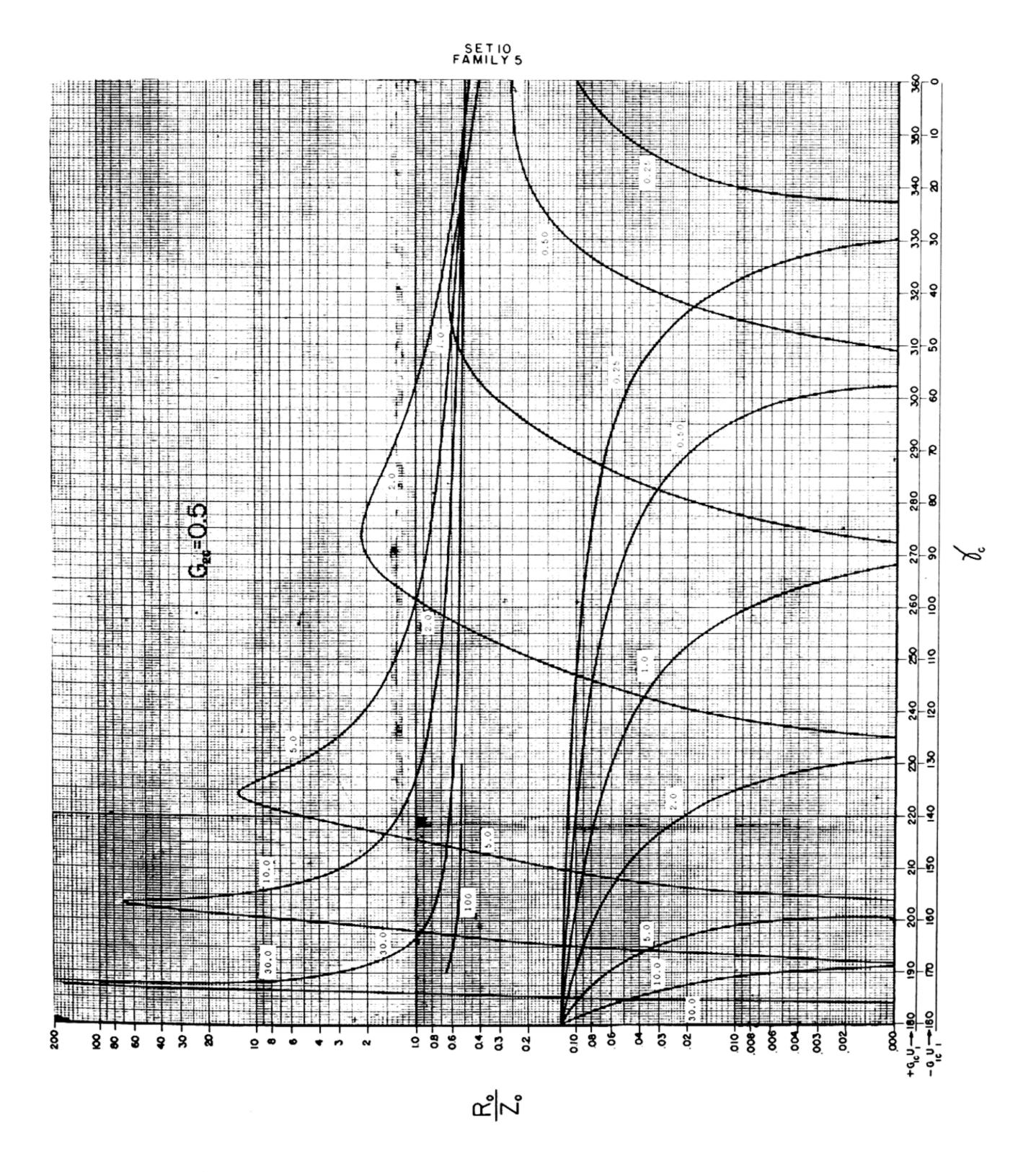


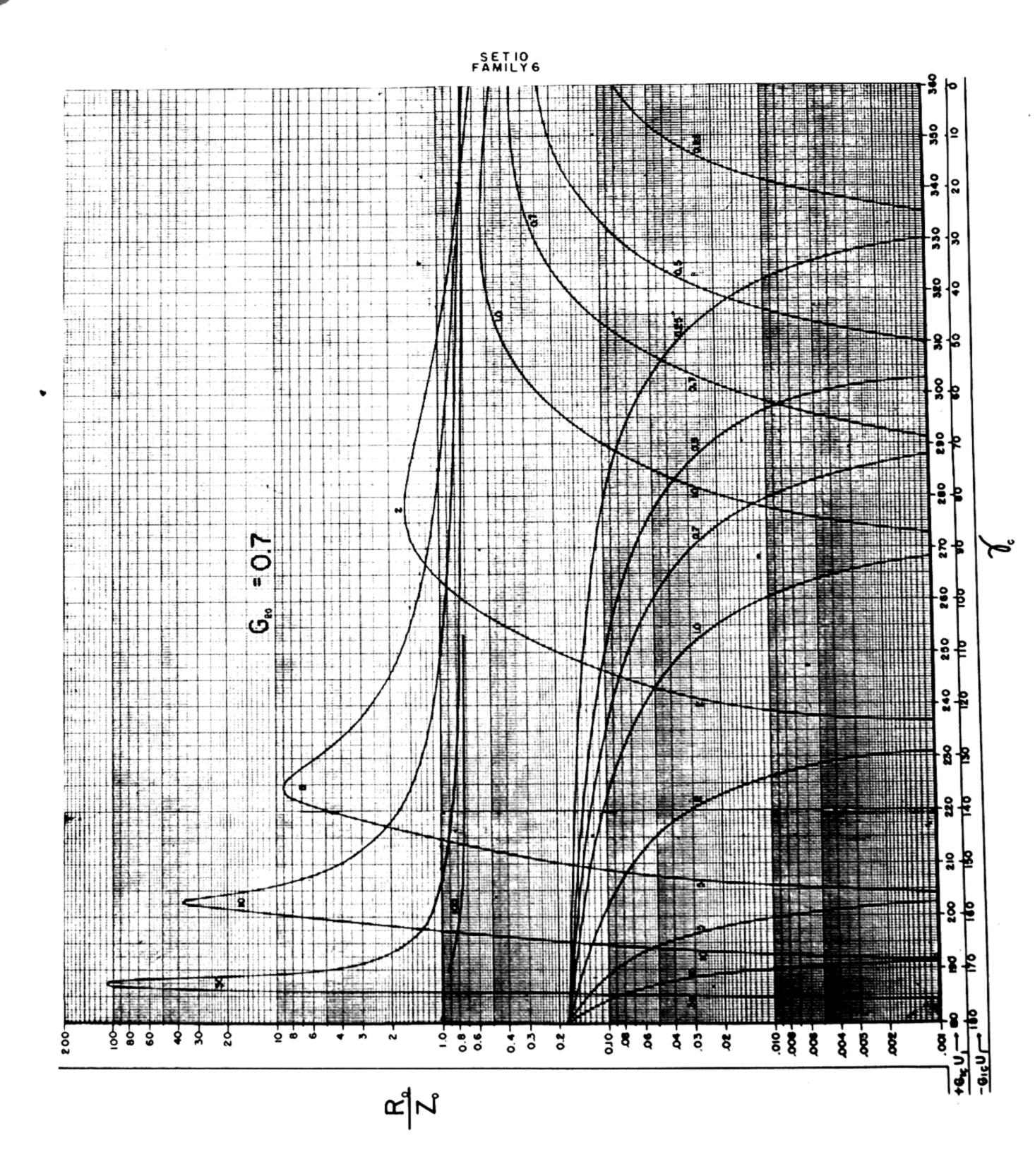


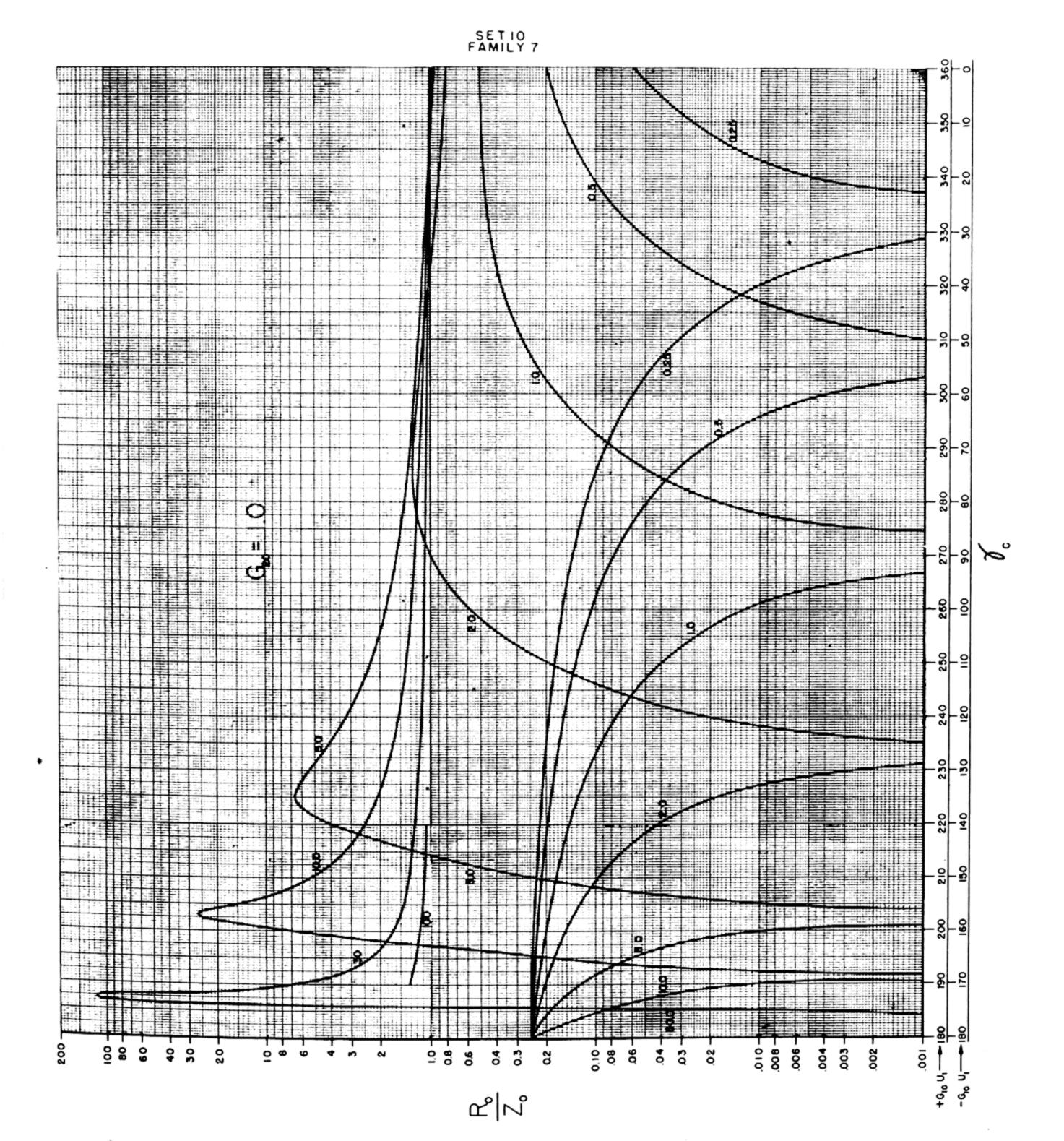


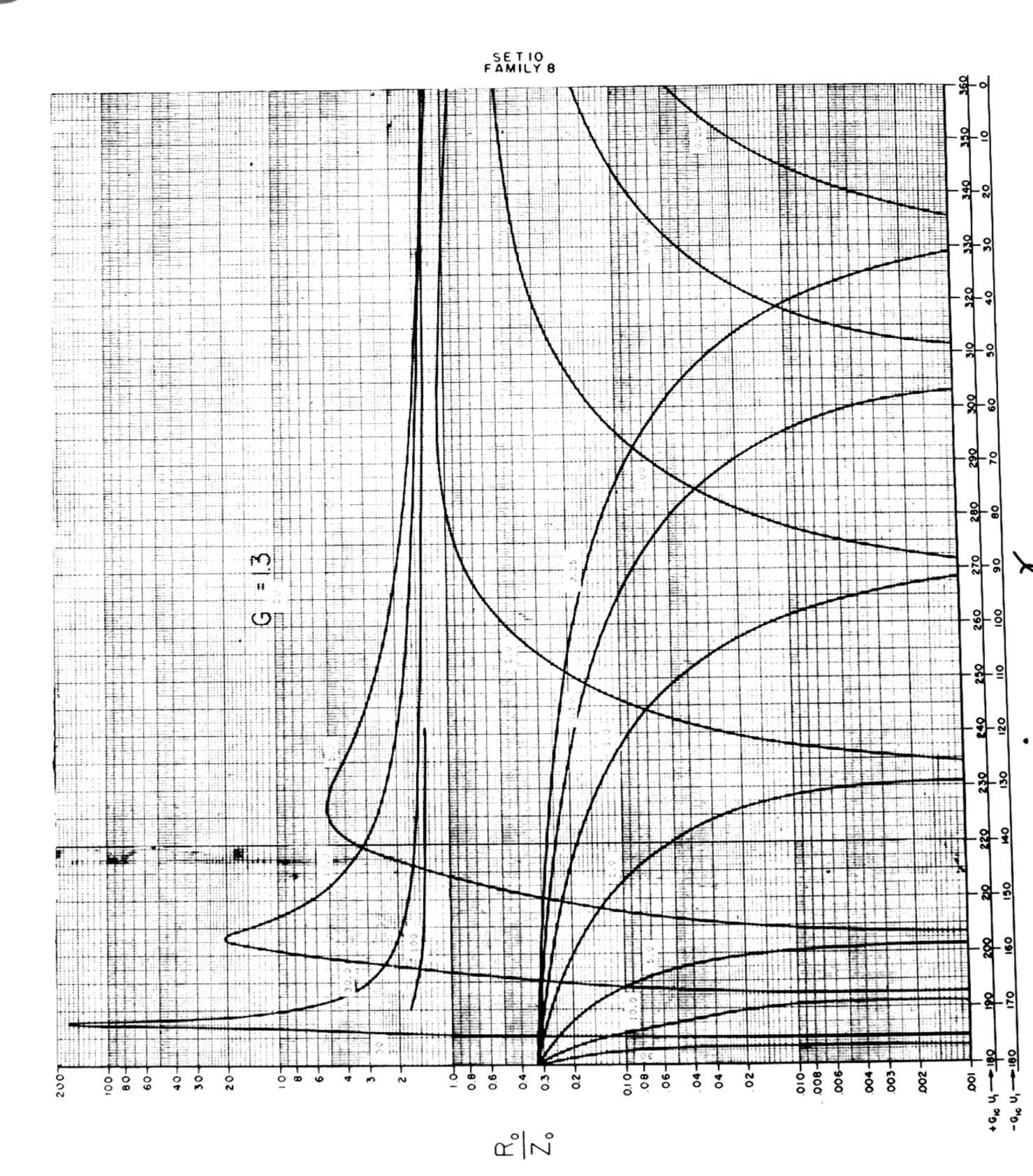


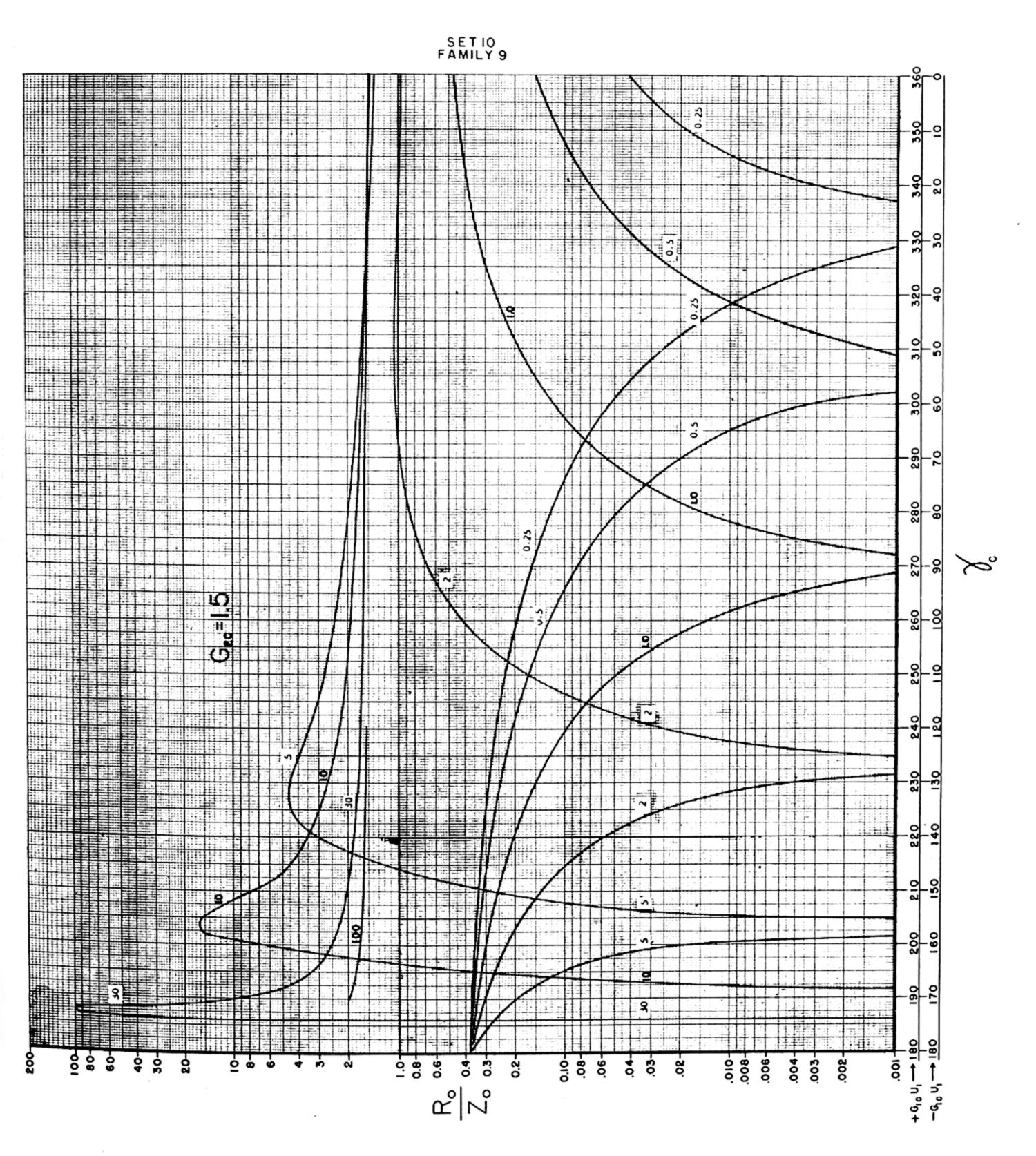


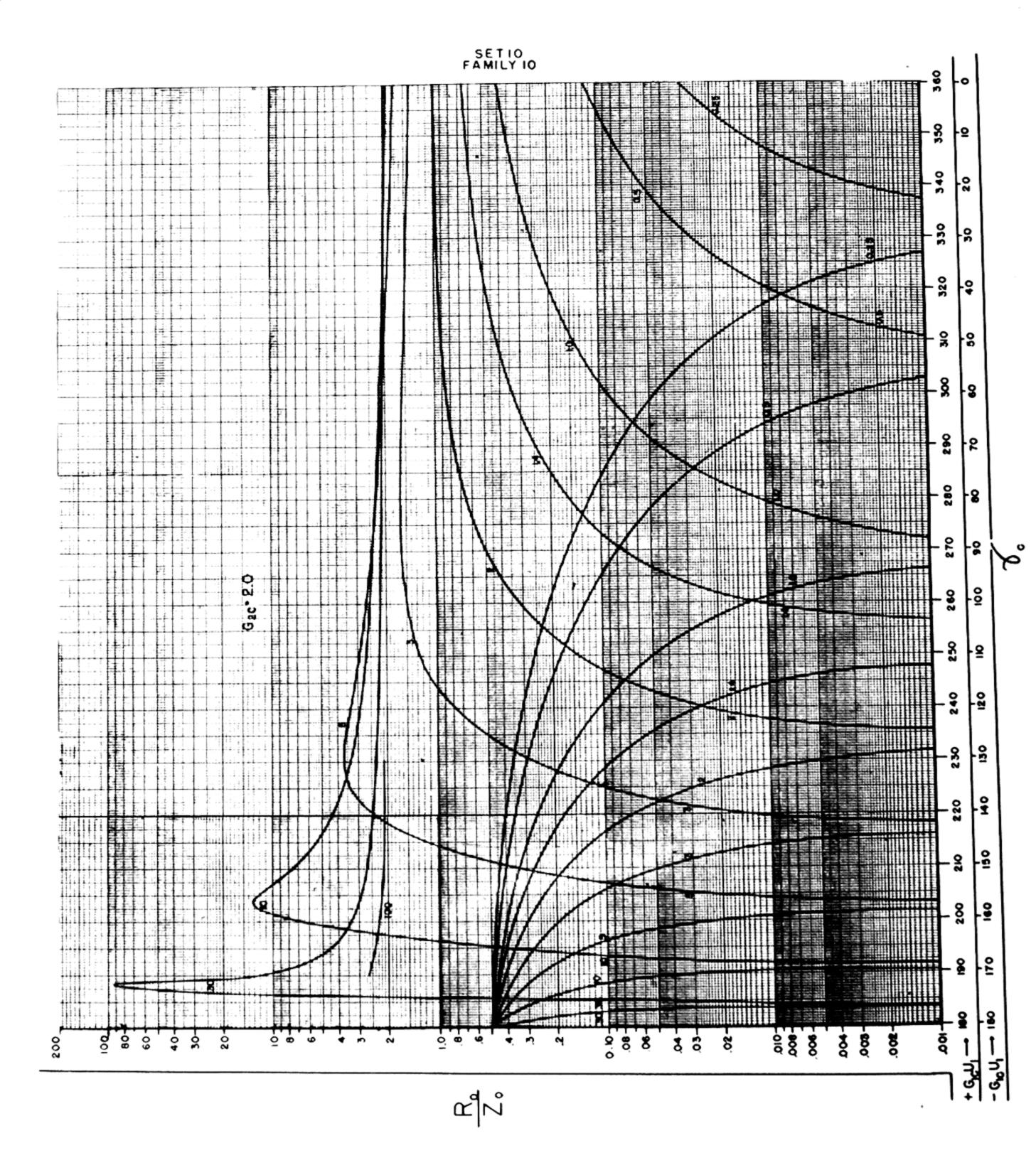


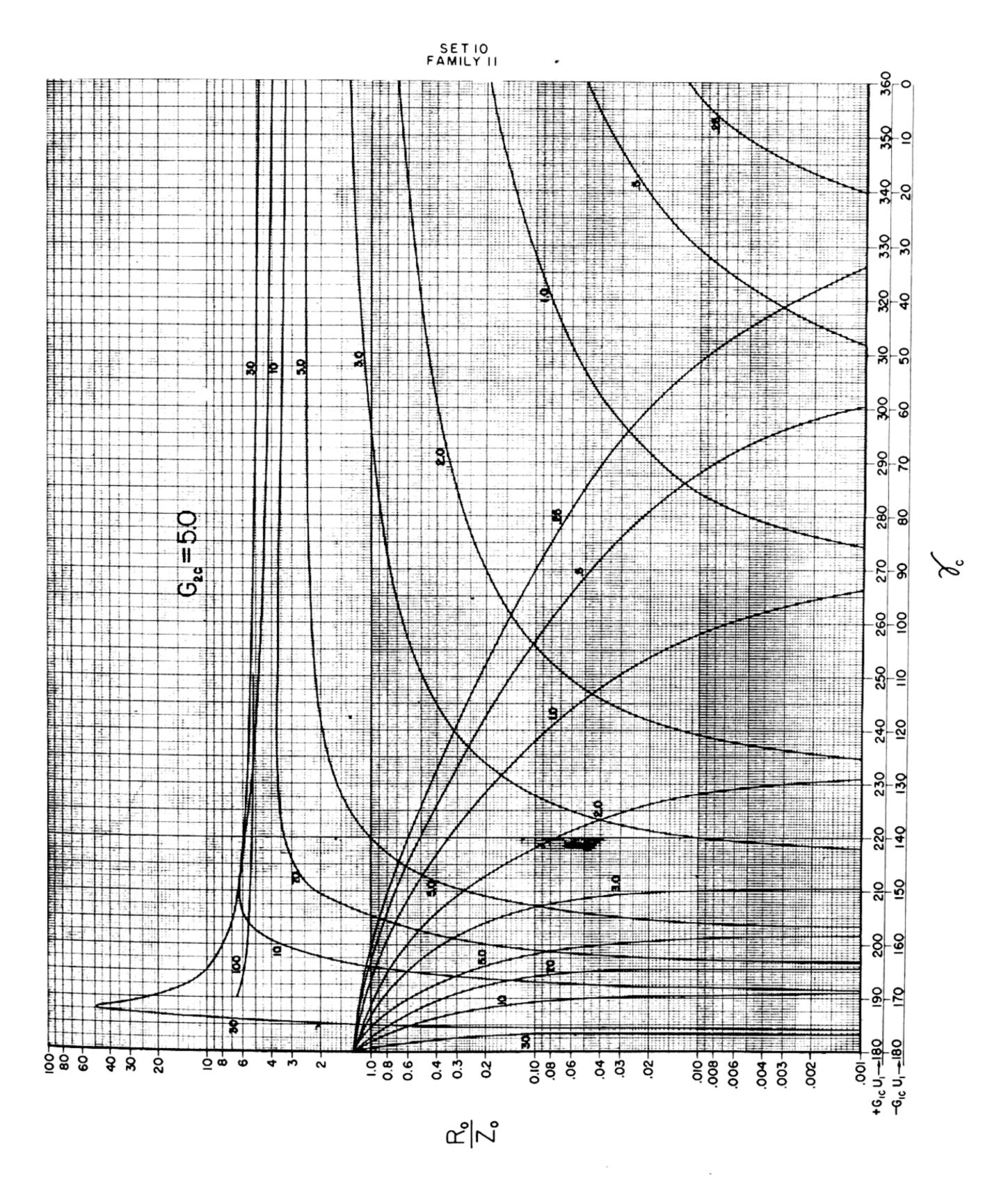


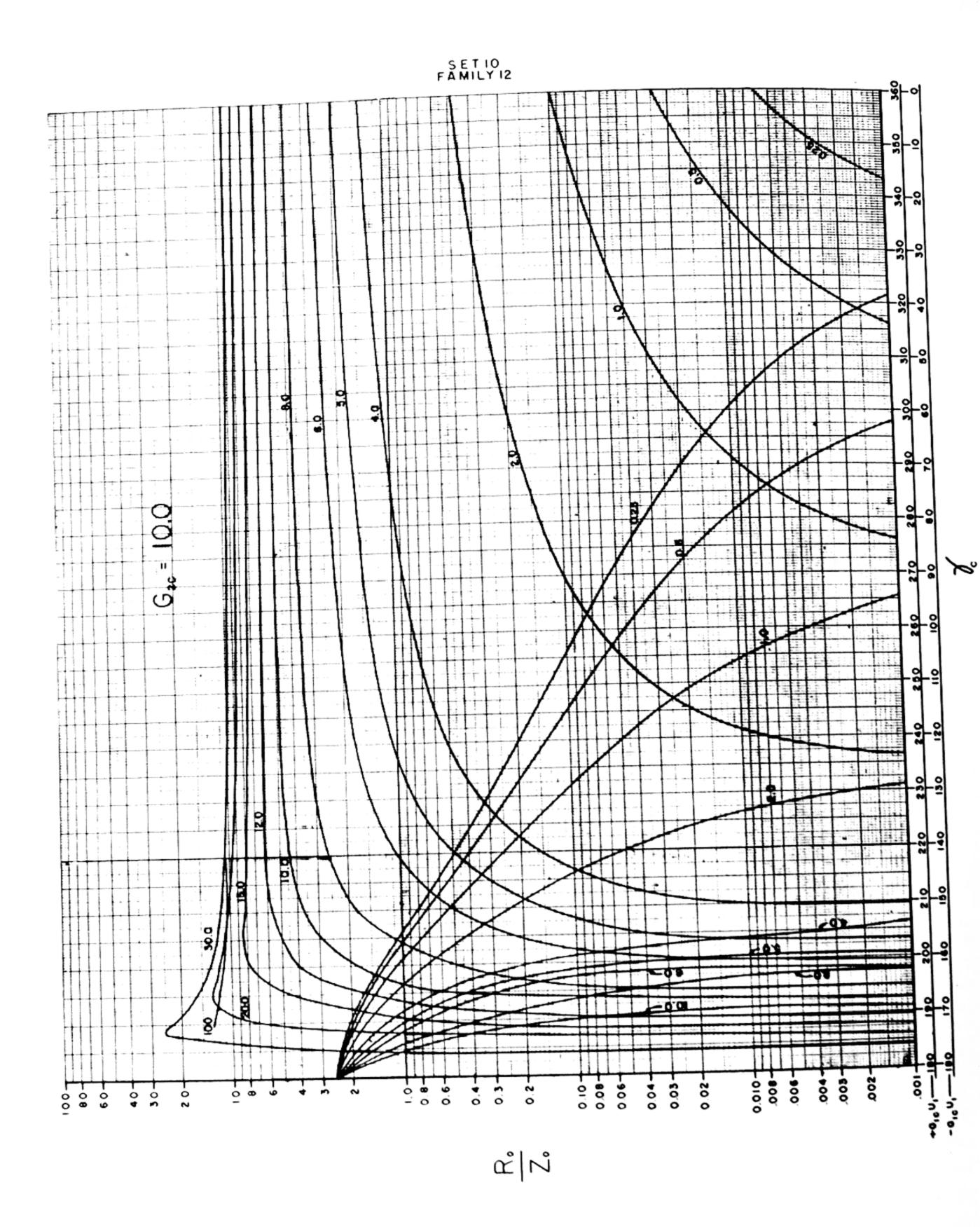




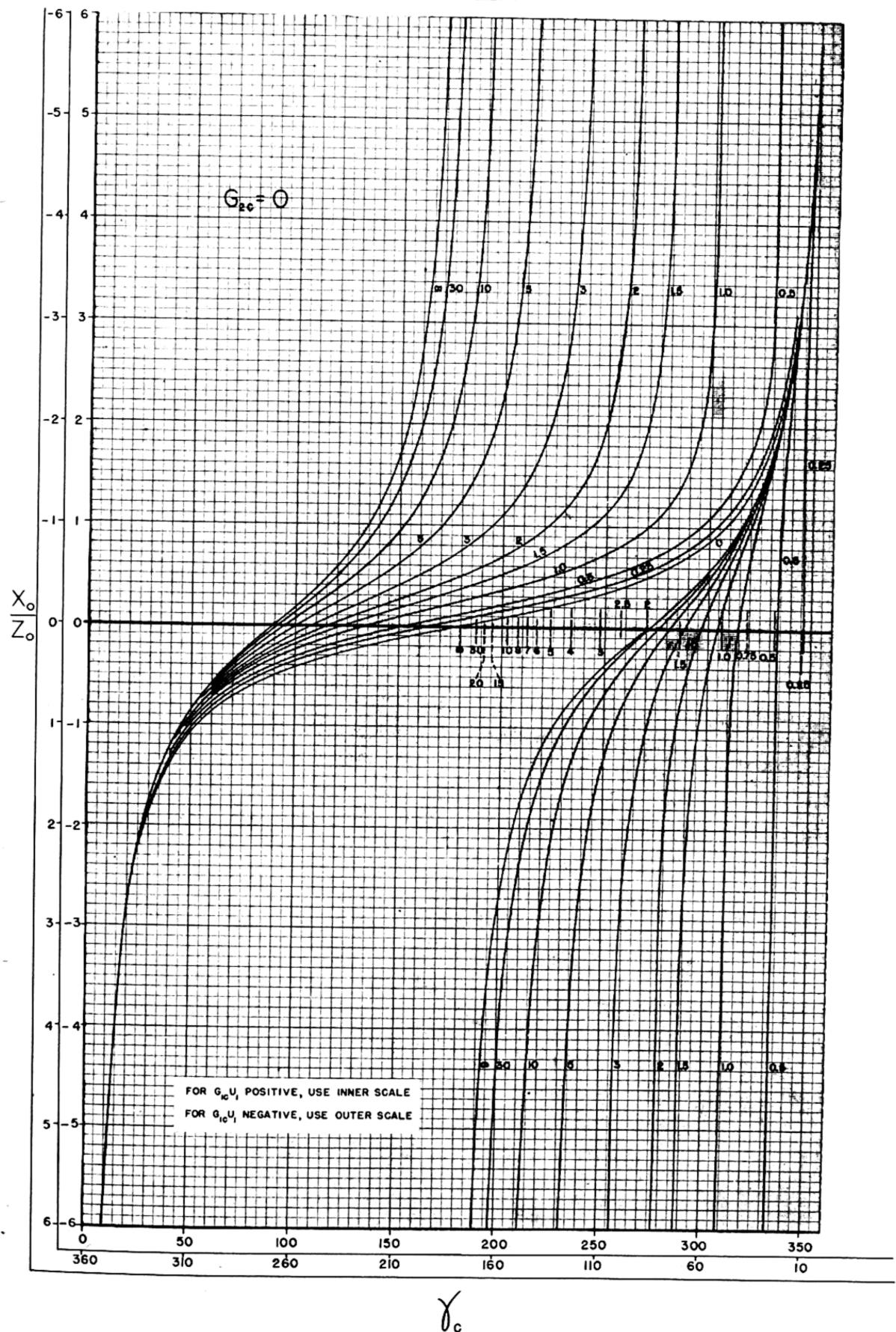




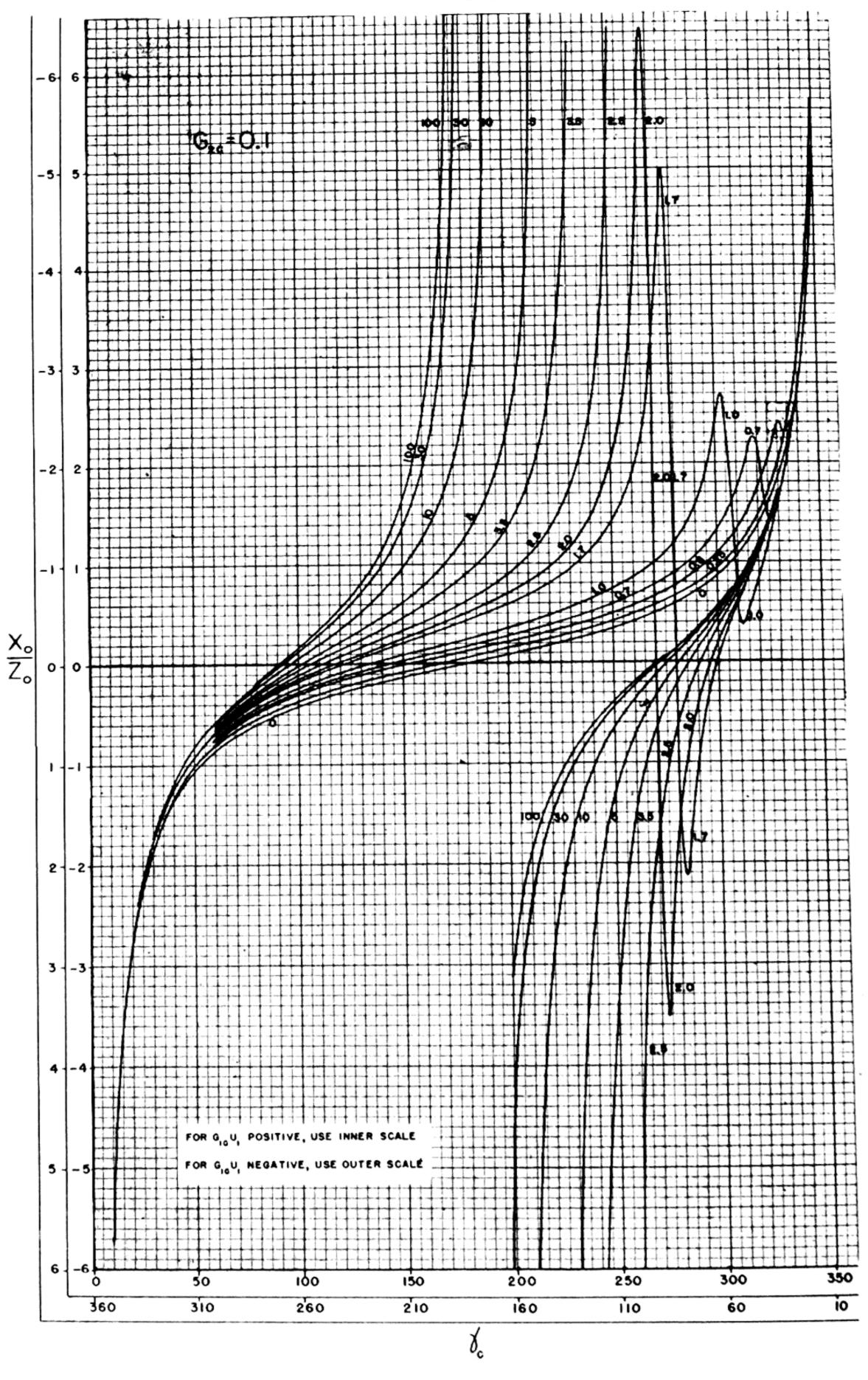


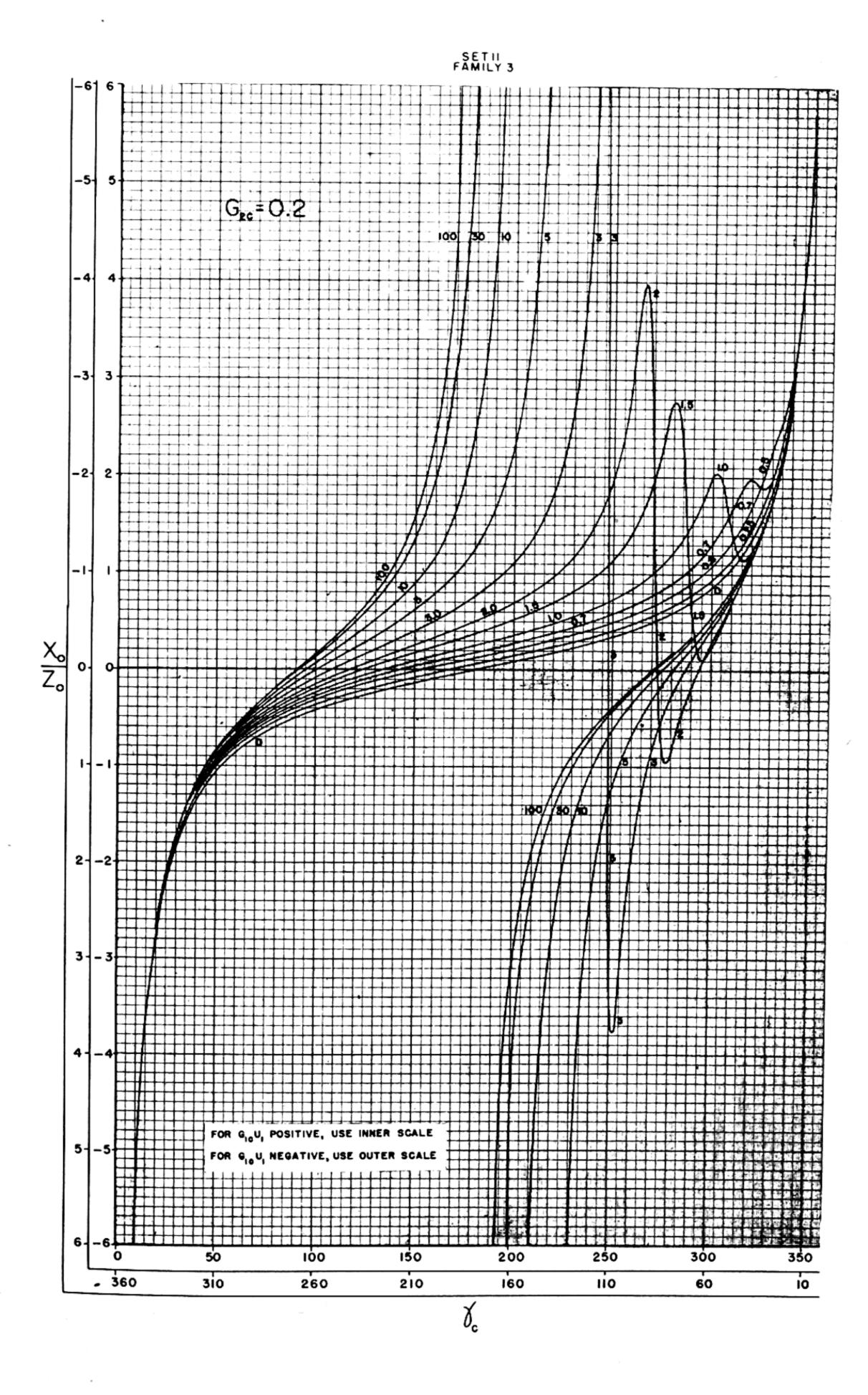




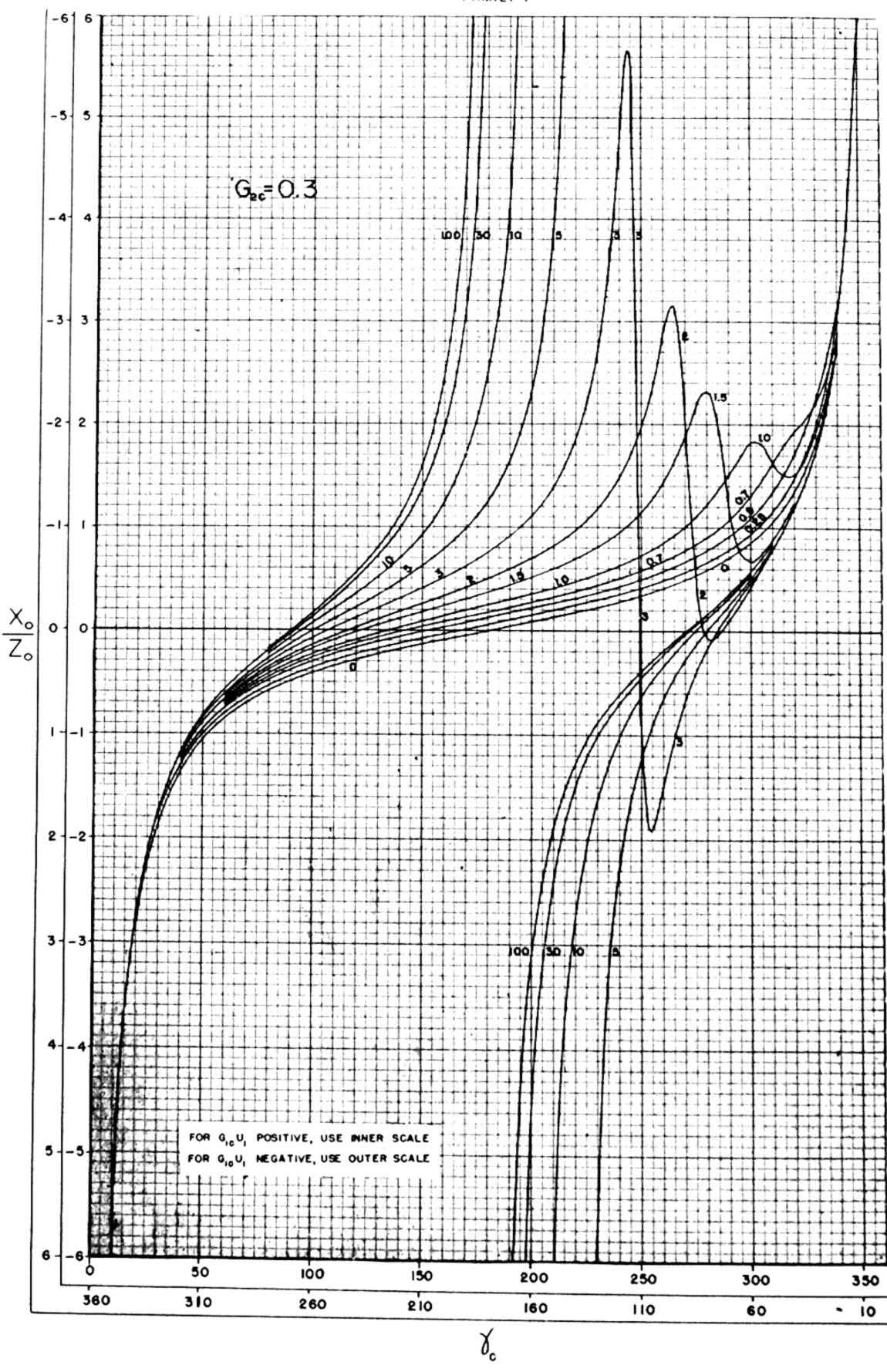


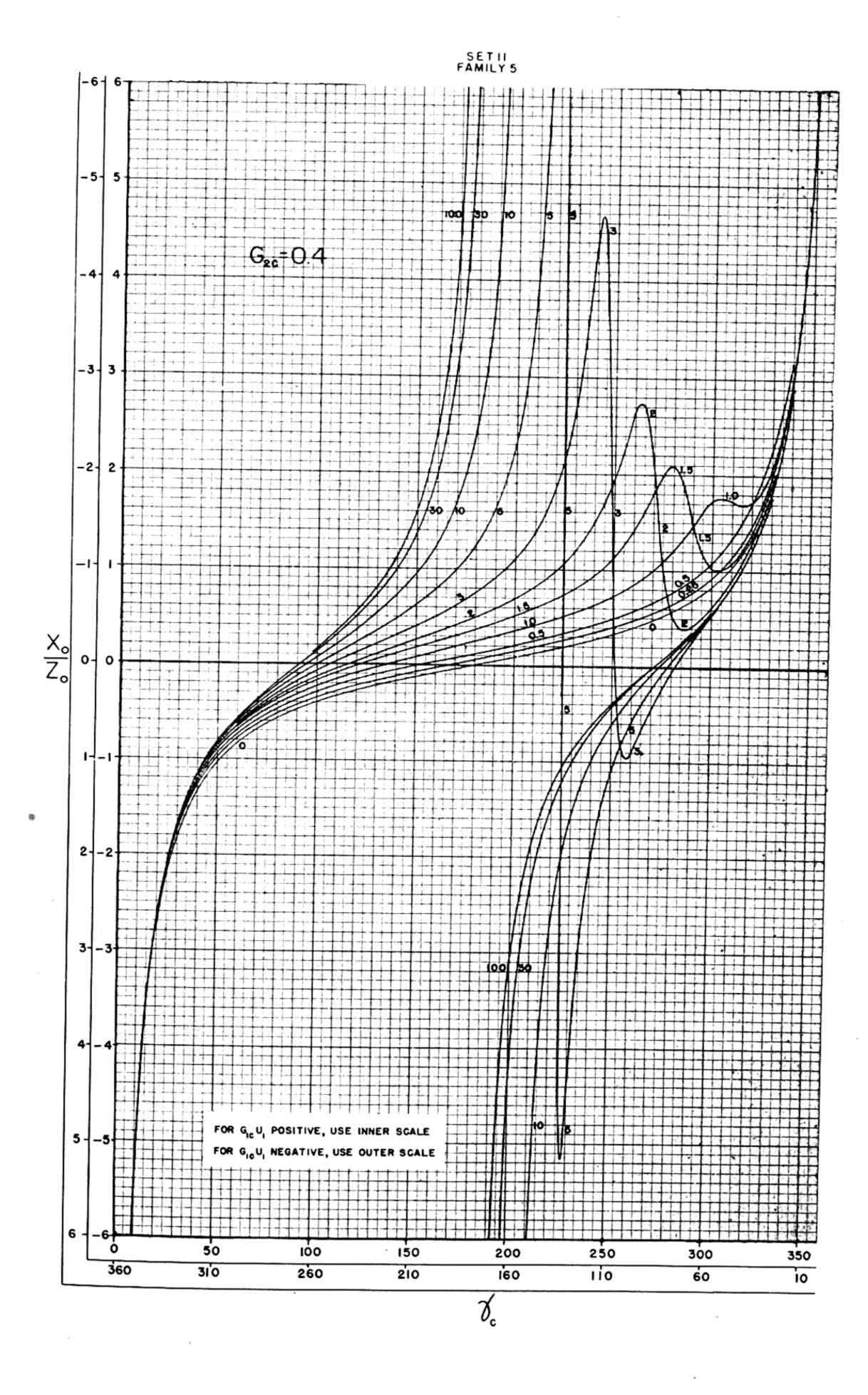




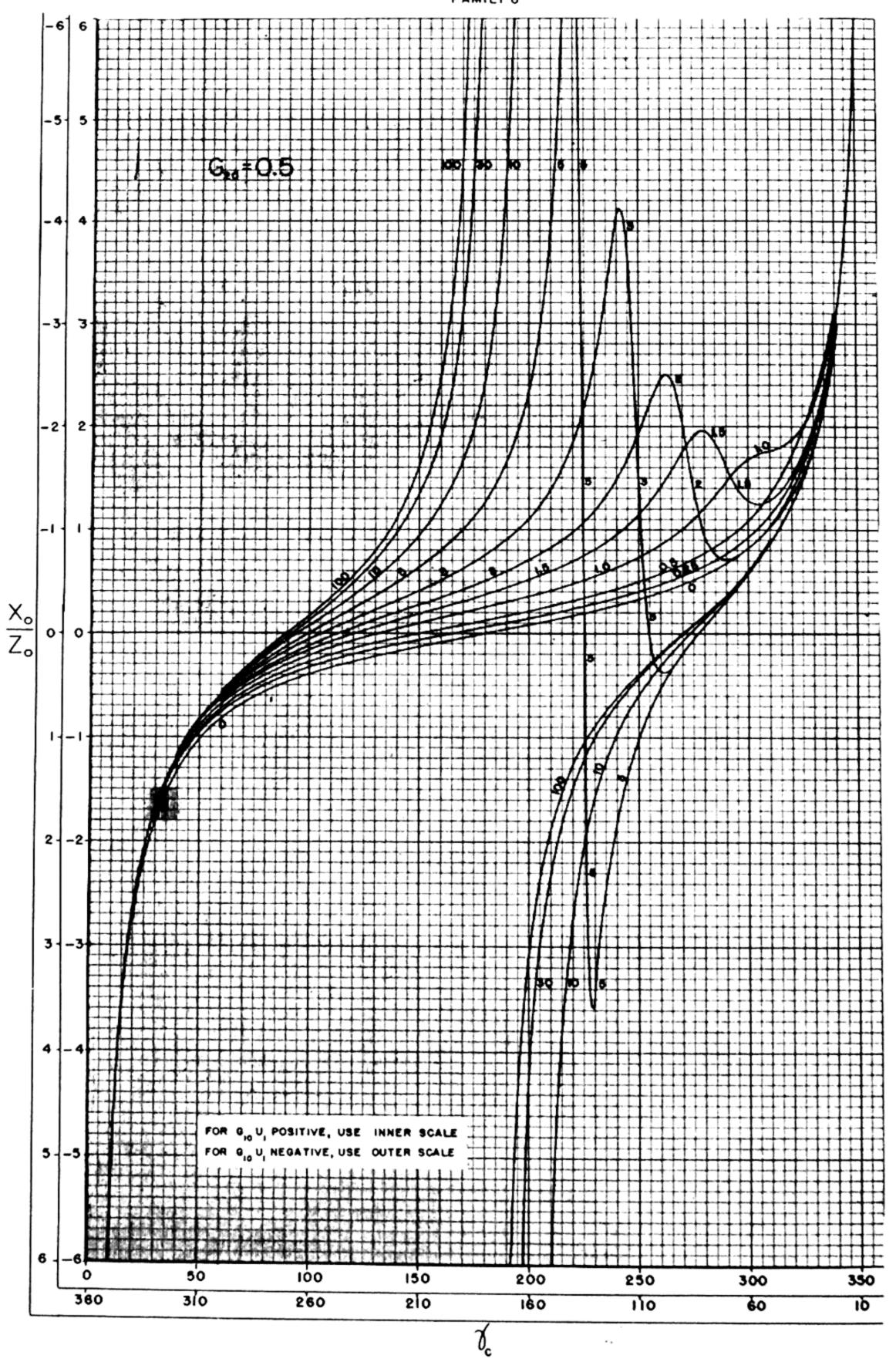


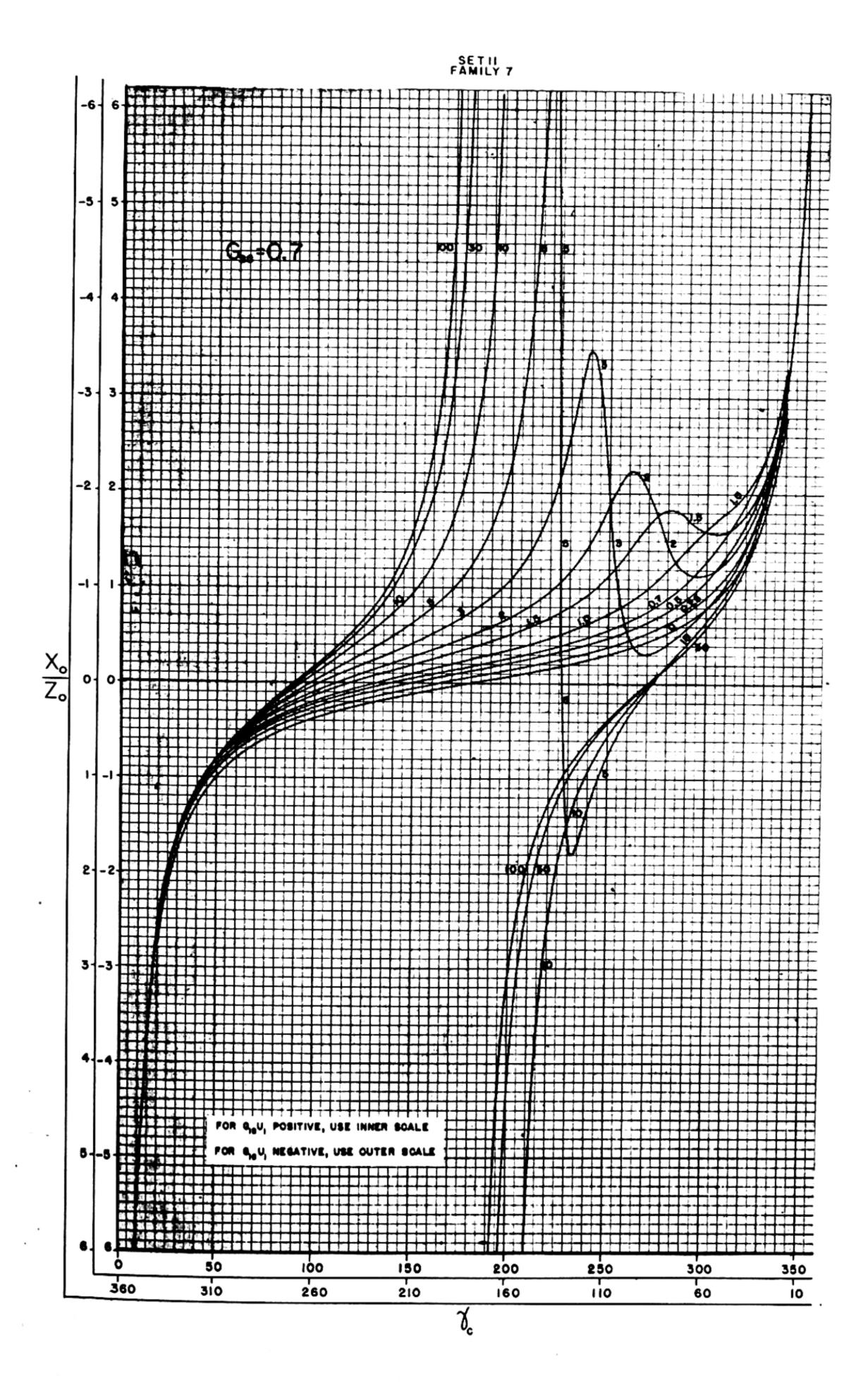


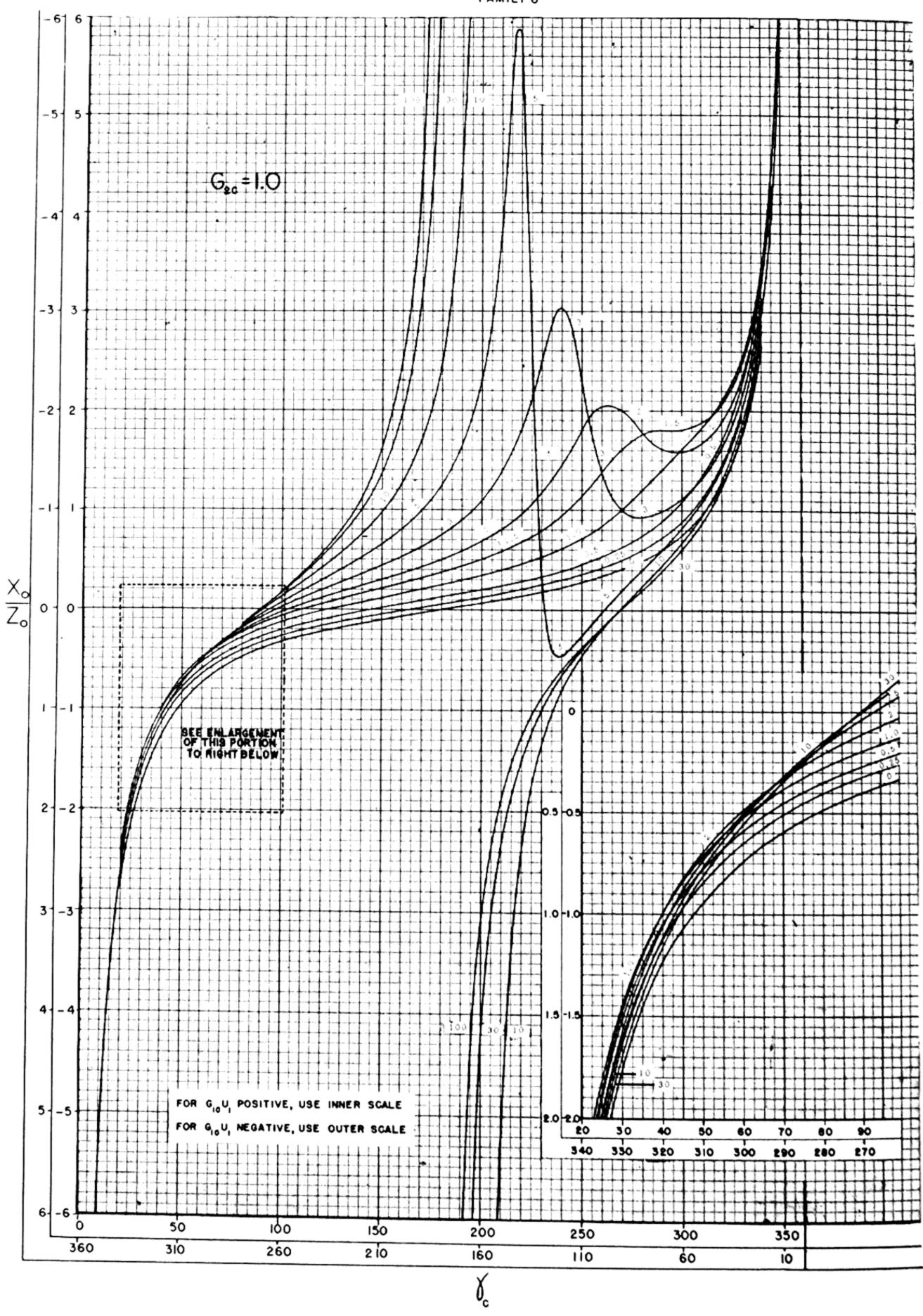


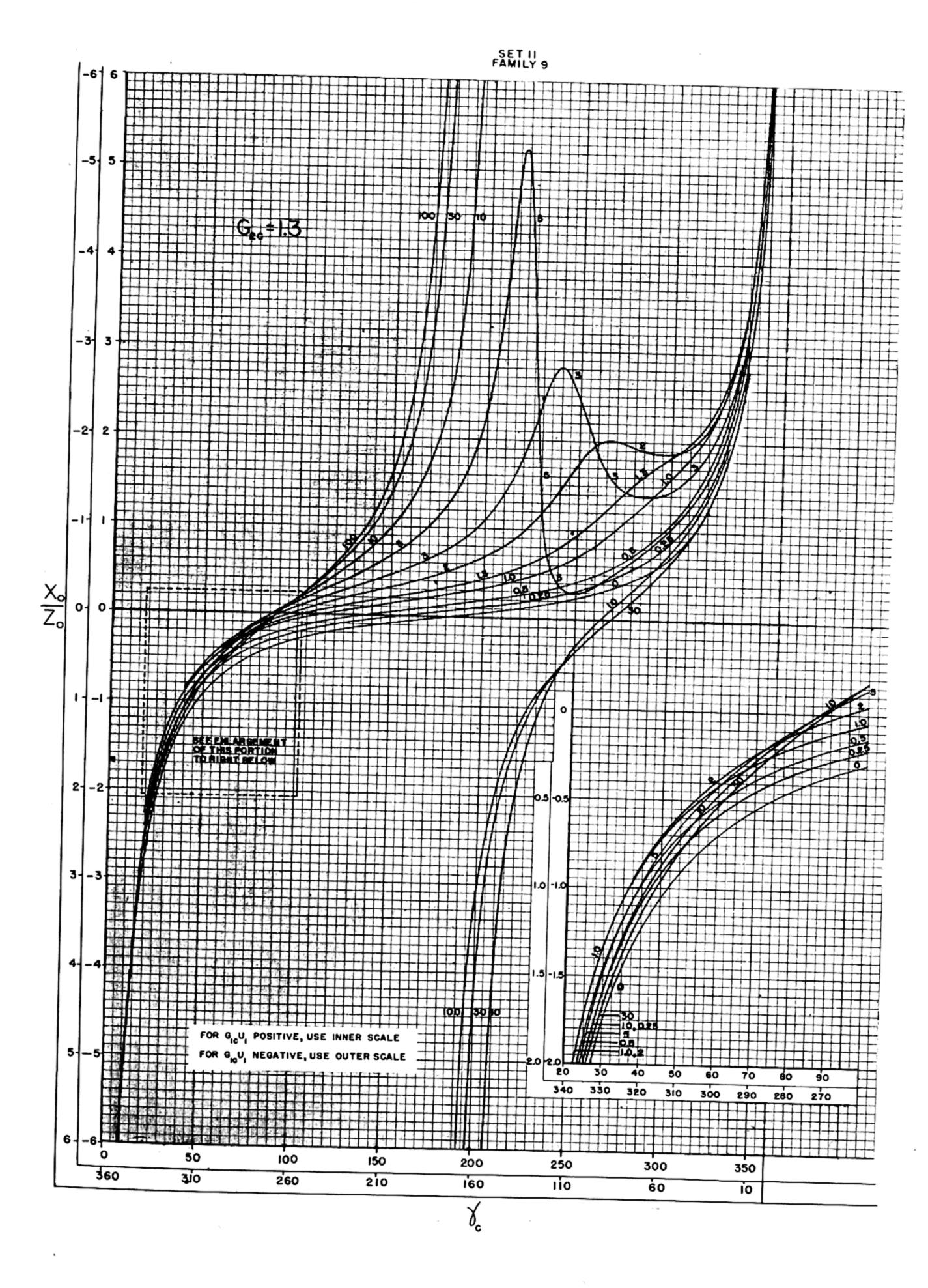


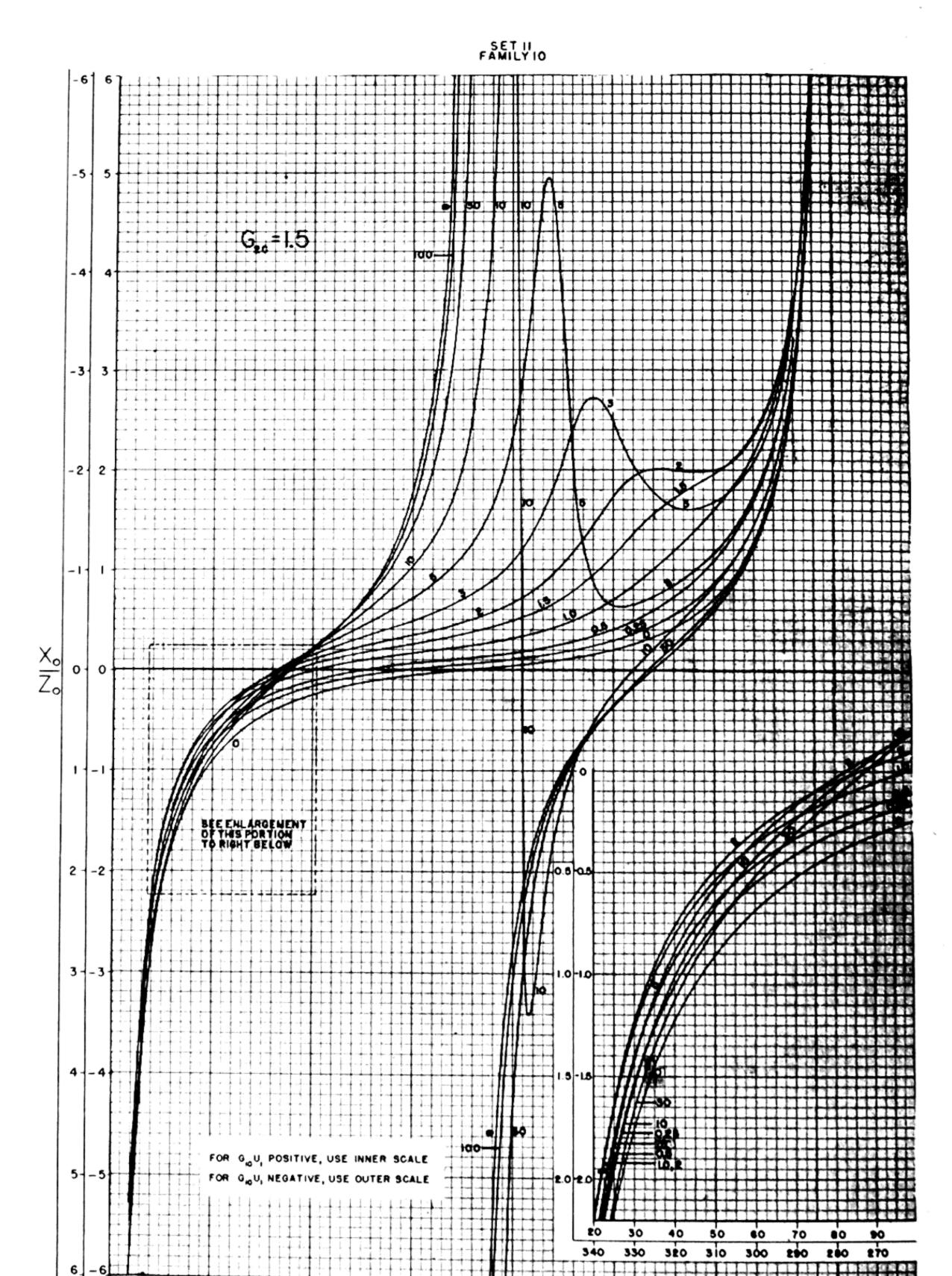


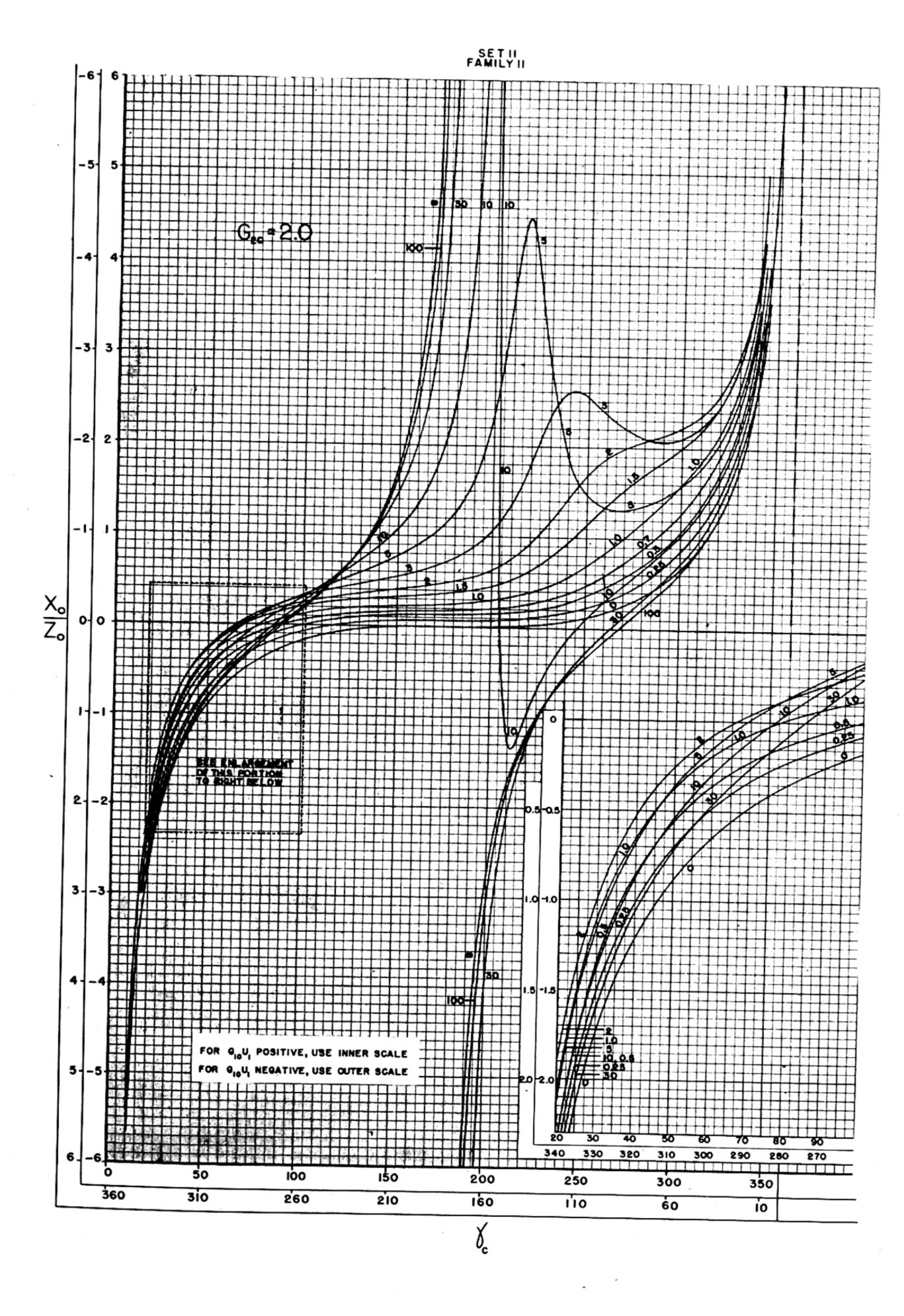




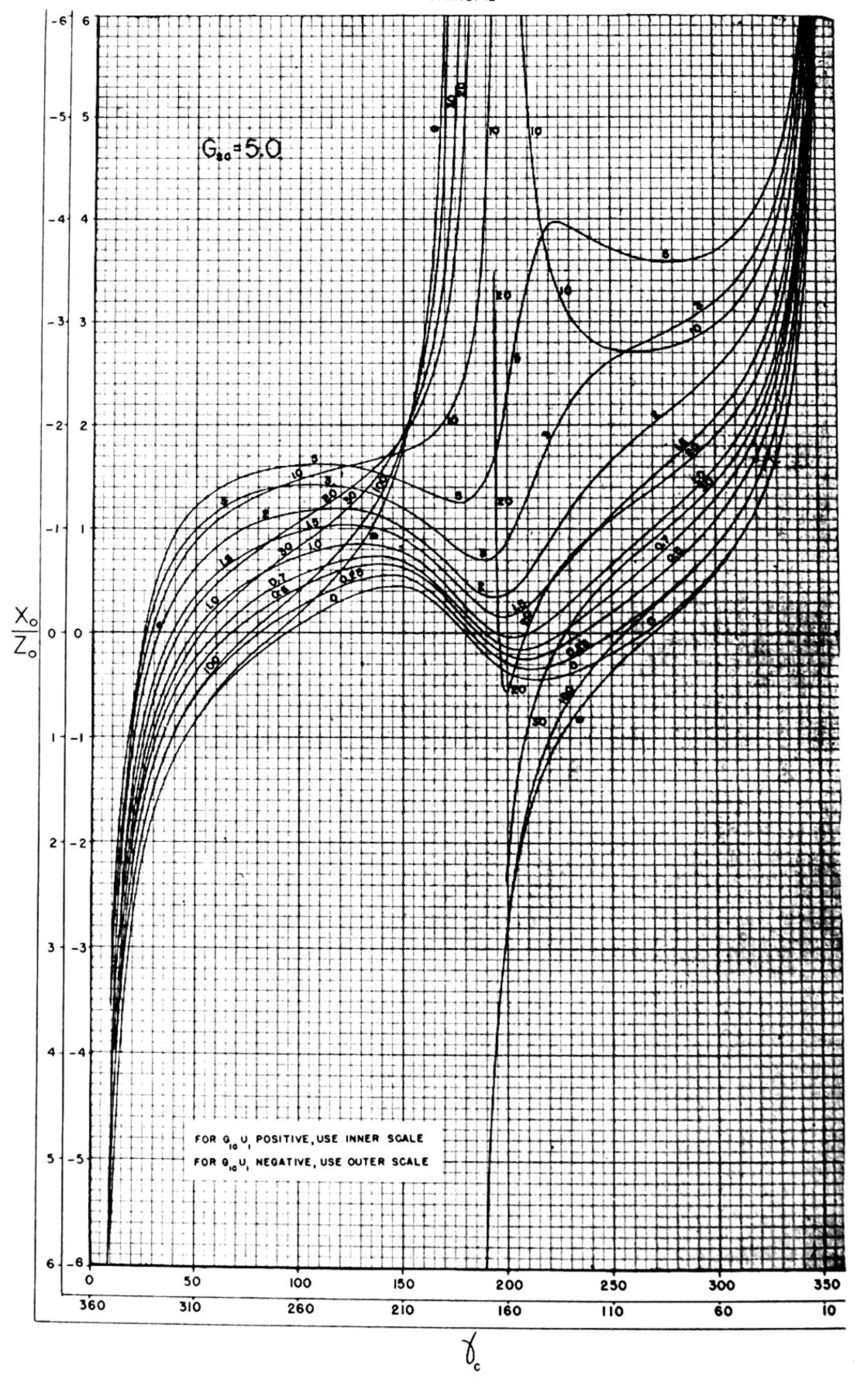




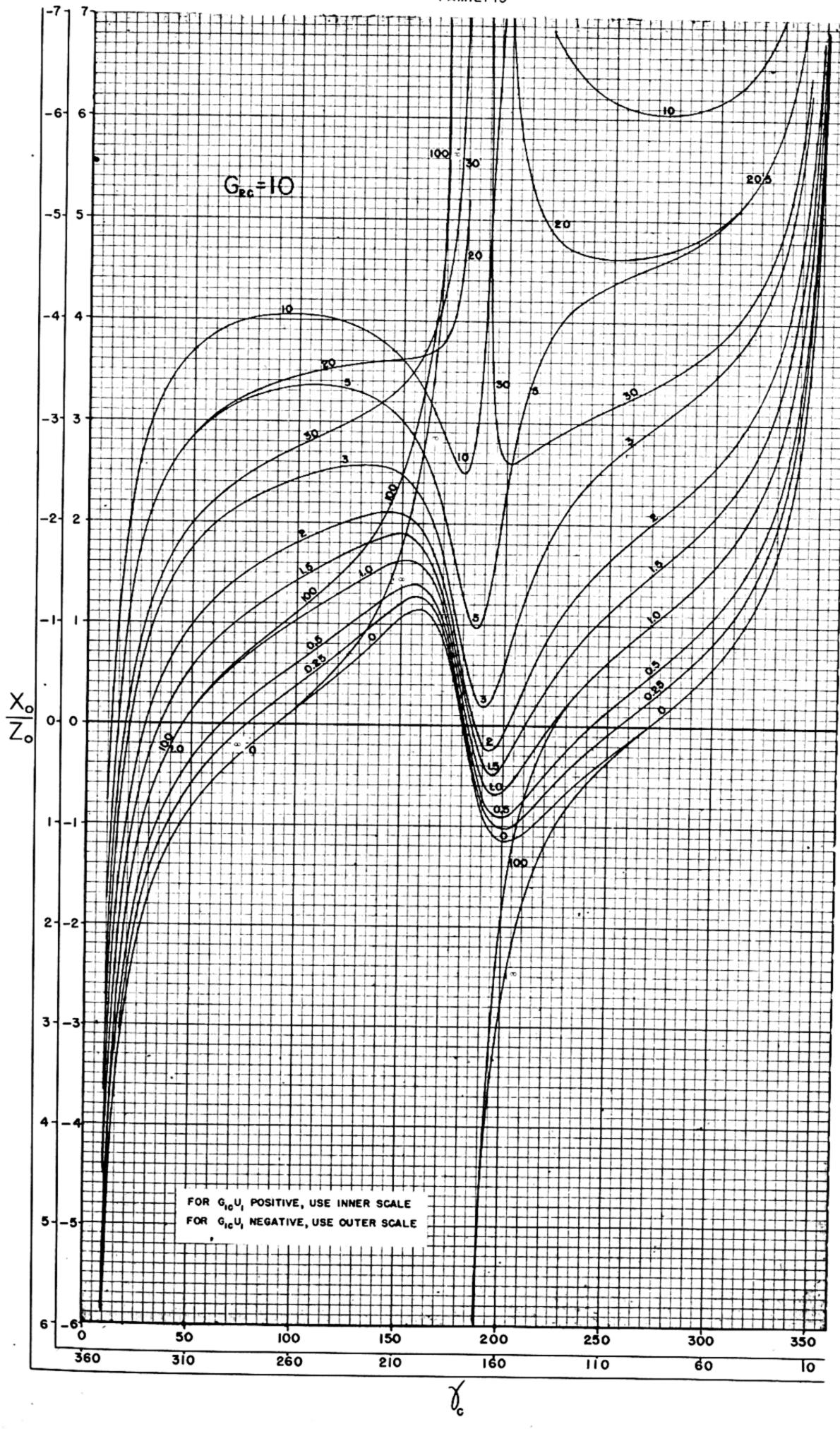


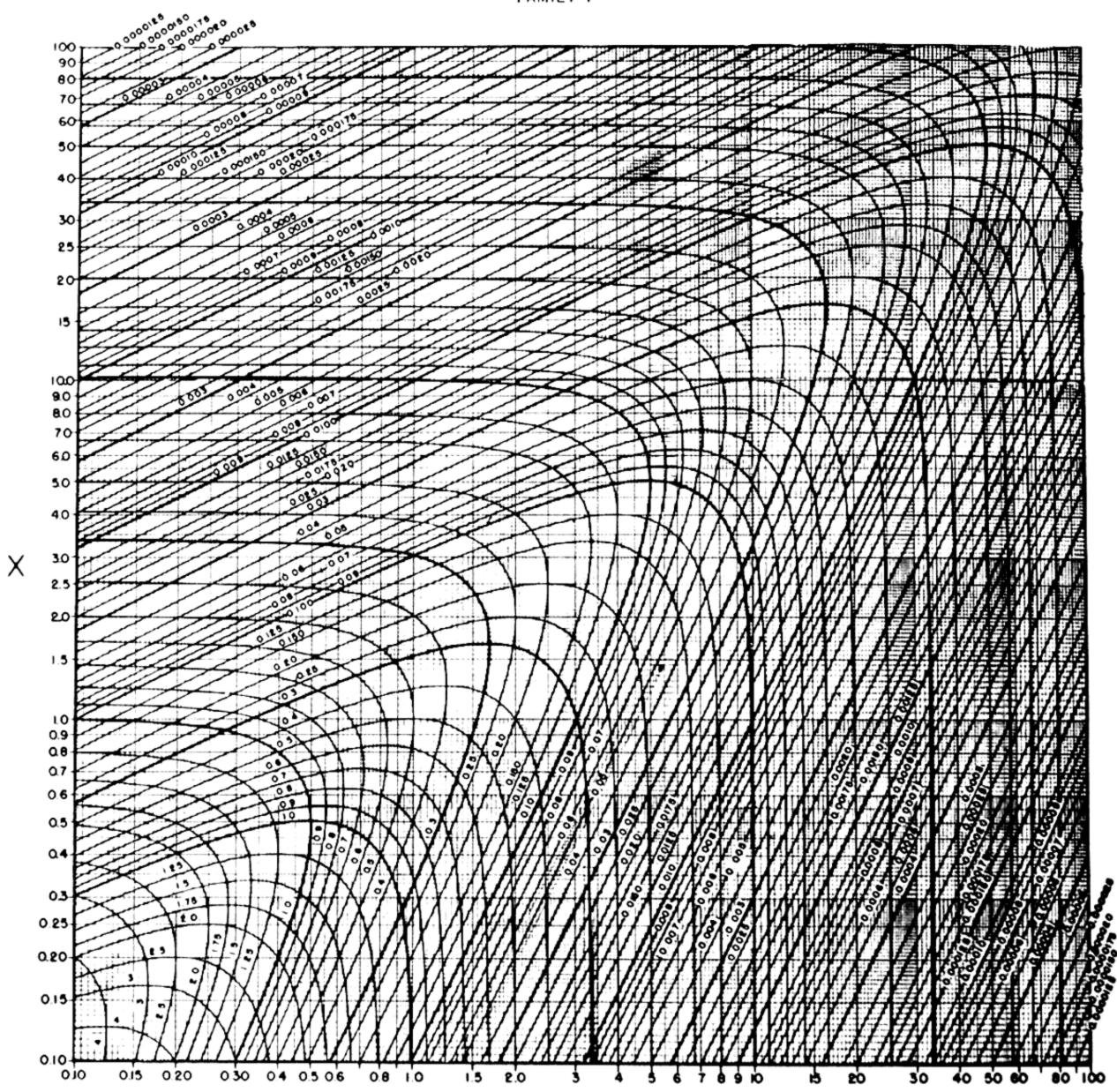








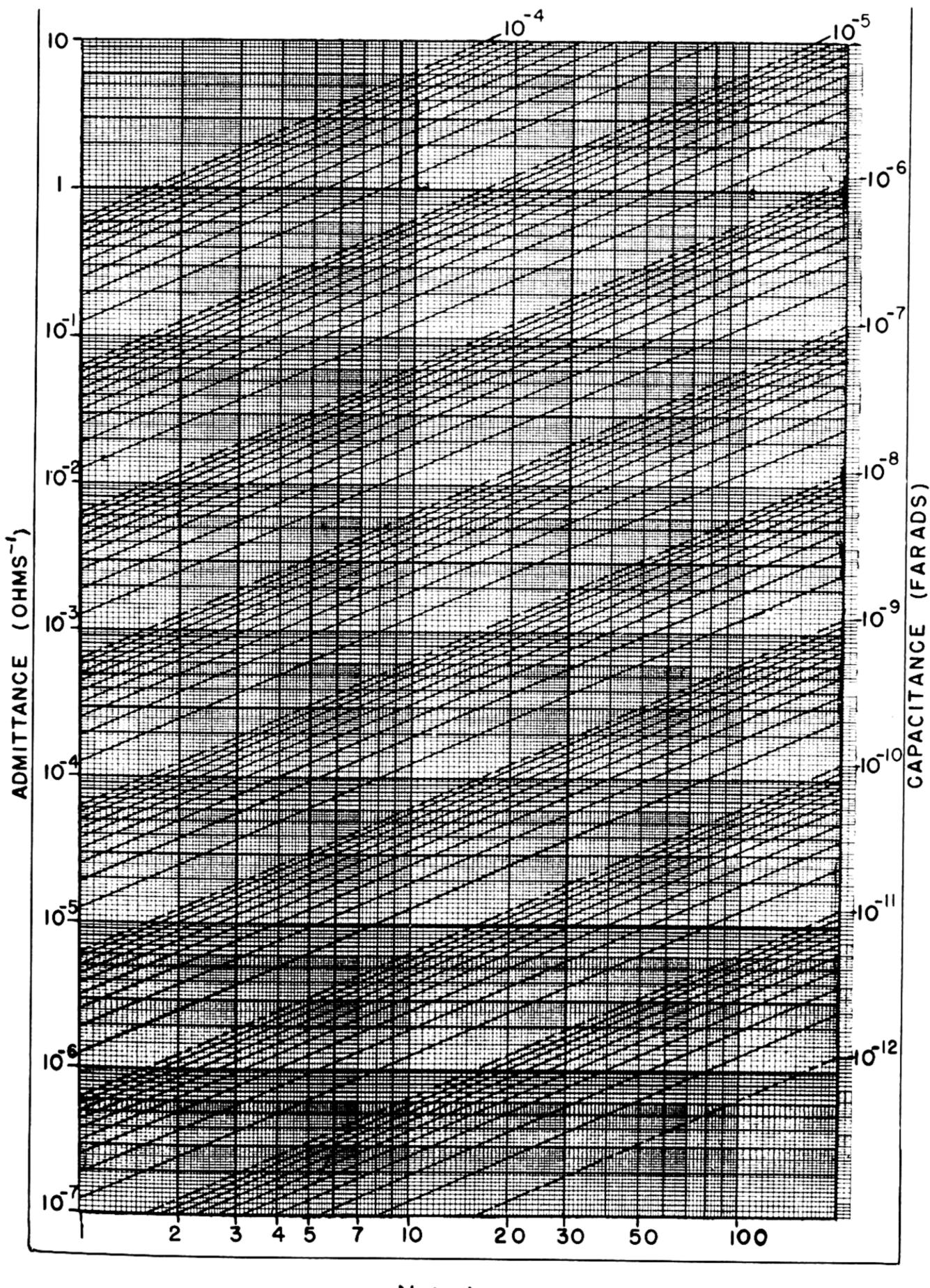




R

100

SET 13 FAMILY 1



N (k.c)

THE JAMMU & KASHMIR UNIVERSITY LIBRARY.

DATE LOANED

Vol Accession N	Vo.		Annual Control
		,	
	The state of the s		
	The state of the s		

SECTION 6

SENSITIVITY AND ACQUSTIC INPUT IMPEDANCE

Sensitivity is of fundamental importance in the design of many crystal systems such as hydrophones and accelerometers. The curves of this section are concerned with its determination for systems composed of any crystal, any backing material combination, and any one of a wide range of electrical impedances. The acoustic input impedance into the projector may also be obtained from the curves of this section. This quantity is useful in evaluating the pressure distribution over the face of a projector in terms of the free field pressure of the incident wave.

As in the previous section, it is convenient first to describe the curves roughly and then to illustrate their use by an example.

The curves are divided into three sets. The first set (consisting of fifteen families, pages 111 to 124) shows the quantity $-Z_M/Z_0$ plotted as a function of γ_c (obtained from Section 1). Z_M is the mechanical impedance into the projector, per crystal. It is the product of the acoustic input impedance into the projector multiplied by the area of a single crystal. (See Table 2, page 11 for the values of the characteristic impedances.) The parameter from curve to curve is the quantity $G_{1c}U_1$ which characterizes the backing material and is defined in Section 3, page 19. The parameter from family to family

is the quantity $\theta = j \frac{\varphi^2}{Z_0} (R_{L1} + j X_{L1})$, where

$$R_{L1}+jX_{L1}=$$
electrical load per crystal $\varphi=\frac{d}{s}l_w$
 $l_w=$ width of crystal in meters. $\frac{d}{s}=$ ratio of the piezoelectric constant to the elastic modulus (See Part II, Section 1) $Z_0=\rho_c V_c l_t l_w$ kg/sec

Ordinarily the load is purely capacitive, and for such loads.

$$\theta = \frac{\varphi^2}{Z_0} \left(\frac{1}{\omega C} \right),$$

where C=capacitive load (the sum of the longitudinally clamped capacity of the crystal, the cable capacity, and the capacity of the

cable termination. With only one exception (which is explained later) all the curves of this set have been plotted for a purely capacitive load, using the above expression for θ .

The first sheet of this set, covering the range $\theta \le 0.1$, differs from the others in several respects:

- 1. Z_M/Z_0 is plotted rather than $-Z_M/Z_0$;
- 2. Over part of the range of Z_M/Z_0 the linear scale is replaced by a logarithmic scale.
- 3. The value of Z_M/Z_0 obtained from this curve $(\theta \le 0.1)$ is not exact and the following correction may be added to it for greater accuracy:

$$\theta \left(\frac{\frac{1}{\cos \gamma_{\epsilon}}}{\overline{G_{1\epsilon}U_{1}} - \sin \gamma_{\epsilon}} \right).$$

This correction term is negligible except for values of the parameters which make the denominator of the expression small. If only the approximate form of the sensitivity curve is desired, the correction may be ignored over the whole range.

When the resistive component of the impedance is not negligible as compared to the reactive component, θ should be calculated from

$$\theta = j \frac{Z_0}{\varphi^2} \left(R_{\mathbf{L}1} + j X_{\mathbf{L}1} \right)$$

and the first family of Set 14 used, providing $|\theta| \le 0.1$. If $|\theta| > 0.1$, $\frac{Z_M}{Z_0}$ should be calculated directly from the formulas given in Part II.

The next set (page 125) consists of a single curve in which the ratio $|P_2/P_+|$ is plotted as a function of $Z_a/\rho_w V_w$ where

 P_2 =pressure at the face of the crystal,

 P_{+} =free field sound pressure in the medium driving the projector,

 Z_a =acoustic input impedance into the crystal system at the crystal face, and

 $\rho_w V_w$ =characteristic impedance of the medium driving the projector.

This curve gives a close approximation when the receiving face is several wave lengths across, and the incident wave is normal to the face. When these conditions are not satisfied, the diffraction pattern can be calculated from the geometrical configuration and the input acoustic impedance. From the diffraction pattern, the pressure at the crystal face follows immediately. For systems such as accelerometers, the pressure or velocity at the crystal face is known when the accelerometer is so small that it does not appreciably disturb the system under measurement. When pressure is known, the third set of curves can be used directly; when velocity is known, the method given in Part II, Section 5 can be used.

The third set of curves, page 126, shows the

quantity $\frac{1}{\delta} \frac{E_0}{P_2}$ as a function of γ_c (obtained from

Section 1) where $G_{1c}U_1$ (defined in Section 3) is the parameter from curve to curve. E_0 is the voltage which would be produced if the longitudinally clamped capacity of the crystal were zero and if no external electrical load were present. This voltage is not realizable physically but is convenient for calculations. P_2 is

the pressure at the crystal face. $\delta = \frac{l_t}{d/s}$, where

 l_t is the distance between the electroded faces of the crystal, and d/s is the quantity defined on page 103. When d/s is in MKS units, and l_t is in meters, E_0/P_2 will be in volts per newton/meter². To change to volts per dyne/cm² divide by 10.

Detailed use of the curves will be illustrated by the following example: 1000 X-cut Rochelle salt crystals in parallel are mounted on a flat steel plate 1 cm thick and 36 cm in diameter. The crystals are 2 cm long, 1.27 cm wide, and 0.64 cm thick. The temperature is assumed to be 5° C. The sensitivity will be determined in volts per dyne/cm² for the open circuit condition, the only electrical load being the longitudinally clamped capacity of the crystals. The curves appear on pages 106 to 110. Ordinarily it is not necessary to plot the quantities shown here. They are plotted for this example to illustrate the general variation to be expected.

This system is one of those which was analyzed to some extent in Section 5 on *Electrical Input Impedance*. The input impedance and the transmitting response appear on pages 52 and 55 of that section.

First to be determined is the acoustic input impedance, Z_a . For this γ_c is determined from Section 1; $G_{1c}U_1$ is determined from Section 3; and the quantities θ , φ , Z_0 and C_0 are determined from the following relations

$$\theta = \frac{\varphi^2}{Z_0} \left(\frac{1}{\omega C_0} \right); \ \varphi = (d/s) l_w;$$

$$Z_0 = \rho_c V_c A_c$$
; $C_0 = \frac{K L_c l_w}{4\pi l_s} (1.1)(10)^{-12}$

Graphs of d/s and K for X-cut Rochelle salt as a function of temperature are given on pages 60 and 61. For this particular example $\varphi = 4.14(10)^{-2}$ coulombs/meter; $C_0 = 0.473(10)^{-10}$ farads; $Z_0 = 4.85 (10)^2$ kg/sec. Using the values of γ_c , θ , and $G_{1c}U_1$ with the first set of curves we obtain the ratio Z_M/Z_0 , where $Z_M = Z_e A_e$ (the product of the acoustic input impedance and the area of the crystal). Z_e then follows directly:

$$Z_a = \frac{Z_M}{Z_0} \cdot \frac{Z_0}{A_c}$$

See page 106 for the curve of Z_a vs. N. Z_a is equal to zero at resonance.

We now obtain the ratio $|(P_2/P_+)|$ of the pressure amplitude at the projector face to the free field pressure amplitude as a function of the frequency N. Since the projector in the present example is several wave lengths in diameter, and all elements are similar, we can use the graph on page 125 in this evaluation. This graph shows the variation of $|P_2/P_+|$ plotted as a function of $Z_a/(\rho_a V_a)$ where $\rho_a V_a$ is the characteristic impedance of the medium

driving the projector. $\left|\frac{P_2}{P_+}\right| = 0$ at the resonant

frequency, but over most of the frequency range, $|P_2/P_+|$ is very closely equal to 2. See the graph on page 107.

If the projector is less than several wavelengths in diameter, the diffraction pattern can be calculated from the input acoustic impedance and the geometrical configuration. The pressure amplitude distribution over the projector face then follows immediately from the diffraction pattern.

It is clear that if the projector can be subdivided into several regions, each region being composed of similar elements, and the diameter of each region being several wave lengths, then the curve of $|P_2/P_+|$ vs. $Z_a/\rho_w V_w$, page 125, can be applied to each of these regions separately.

The third set of curves is used next to obtain $\frac{1}{\delta} \frac{E_0}{P_2}$. In this expression, P_2 is the pressure amplitude at the crystal face, E_0 is the voltage already defined and $\delta = \frac{l_t}{(d/s)}$. For this example, $\delta = 0.195(10)^{-2}$ meter³/coulomb. The quantity E_o/P_2 , obtained by multiplying $\frac{1}{\delta} \cdot \frac{E_0}{P_2}$ by δ , is plotted as a function of frequency on page 108.

The final quantity needed in the evaluation of the sensitivity is the motional reactance X_{ϵ} determined when the force on the crystal face

is zero. $X_{\bullet} = \left(\frac{X_0}{Z_0}\right) \frac{Z_0}{\varphi^2}$, where X_0/Z_0 is obtained

from the X_0/Z_0 curve for $G_{2c}=0$ in Section 5. For this example $Z_0/\varphi^2=0.283(10)^6$ ohms.

The sensitivity is given by:

$$\frac{E_L}{P_+} = \frac{P_2}{P_+} \frac{E_0}{P_2} \frac{X_L}{X_{\epsilon} + X_L}$$

where $X_L = -1/(\omega C)$. C is the capacity of the electrical load as defined on page 103. The units of E_L/P_+ are volts per newton/meter². To change these units to volts per dyne/cm², divide by 10.

A graph of the sensitivity for this example is given on page 110. A decibel scale in which zero db is taken as 1 volt per dyne/cm² is used. Note that the receiving sensitivity has its maximum at 56 kc, and the peak in the

transmitting response (Section 5, page 55) occurs at 56 kc.

The quantity just discussed is usually called the "open circuit" sensitivity. By "open circuit", we mean that the only electrical element in the circuit is the longitudinally clamped capacity of the crystals.

The open circuit sensitivity of ADP and Y-cut Rochelle salt projectors is comparable to that of the X-cut Rochelle salt just discussed. X-cut Rochelle salt, however, has the advantage of a lower input electrical impedance, so that the sensitivity as measured at the terminals of a cable would be higher than the sensitivity of similar projectors of ADP or Y-cut Rochelle salt with the same cable.

The numerical values of E_L/P_+ , calculated from the expression given above as the product of three quantities, become inaccurate near the resonant frequencies since P_2/P_+ is zero and $X_L/(X_c+X_L)$ is infinite at this point. If there is doubt concerning the accuracy of the sensitivity near resonance as obtained from the curves and the expression given above, it may be calculated from

$$\left| \frac{E_L}{P_+} \right| = \frac{2\varphi}{\rho_2 V_2 \omega C} \left| \frac{\tan \frac{\gamma_e}{2} + G_{1e} U_1}{\theta + \left(\frac{1}{\tan \gamma_e} - G_{1e} U_1\right)} \right|$$

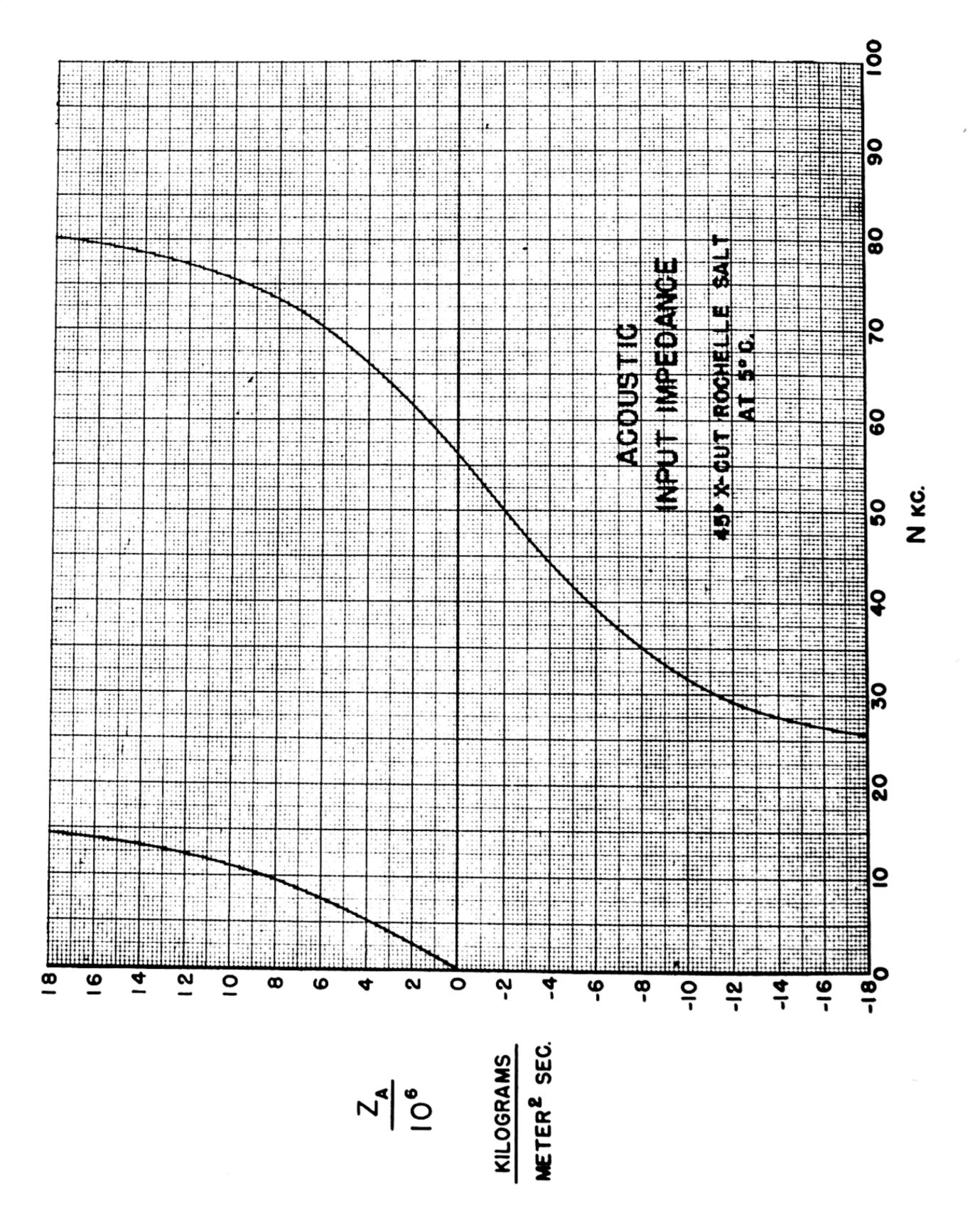
the components of which have no zeros or infinities in the neighborhood of resonance.*

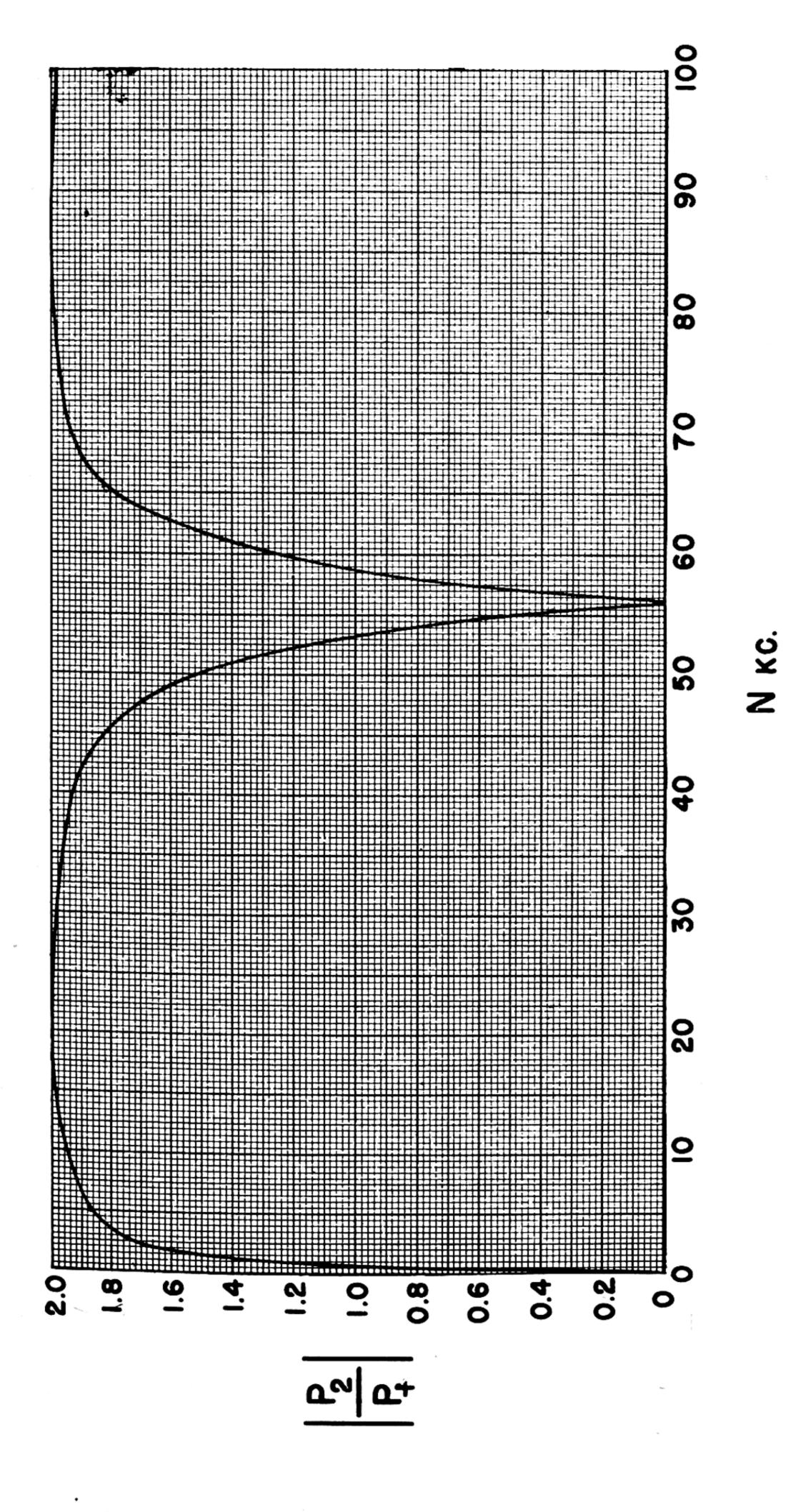
C is the capacity (external load plus longitudinally clamped capacity of the crystal).

The sensitivity as obtained in this section will be lowered by losses in the glue joint, method of mounting, and other effects. For example, if the projector has an efficiency of 60%, the sensitivity will be lowered about 4.5 db. A more complete discussion is given in Section 7, page 127.

*The complete expression for sensitivity has the following form for capacitive loading:

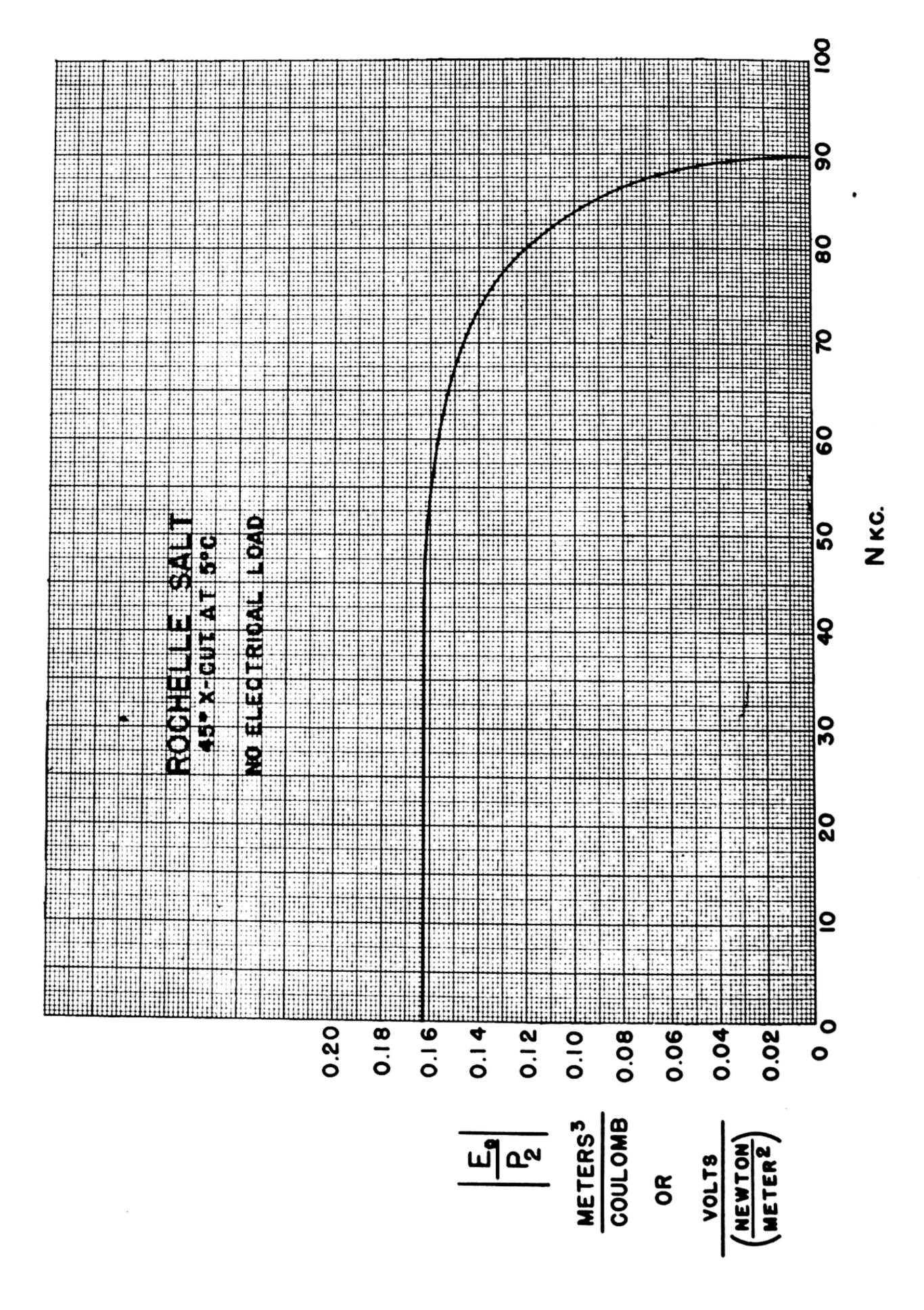
$$\left| \frac{E_L}{P_+} \right| = \frac{2\varphi}{\rho_2 V_2 \omega C} \cdot \left| \frac{\tan \frac{\gamma_c}{2} + G_{1c} U_1}{\theta + \left(\frac{1}{\tan \gamma_c} - G_{1c} U_1\right)} \right| \cdot \left| \frac{\left(\frac{\rho_2 V_2}{Z_a}\right)}{\sqrt{1 + \left(\frac{\rho_2 V_2}{Z_a}\right)^2}} \right|.$$

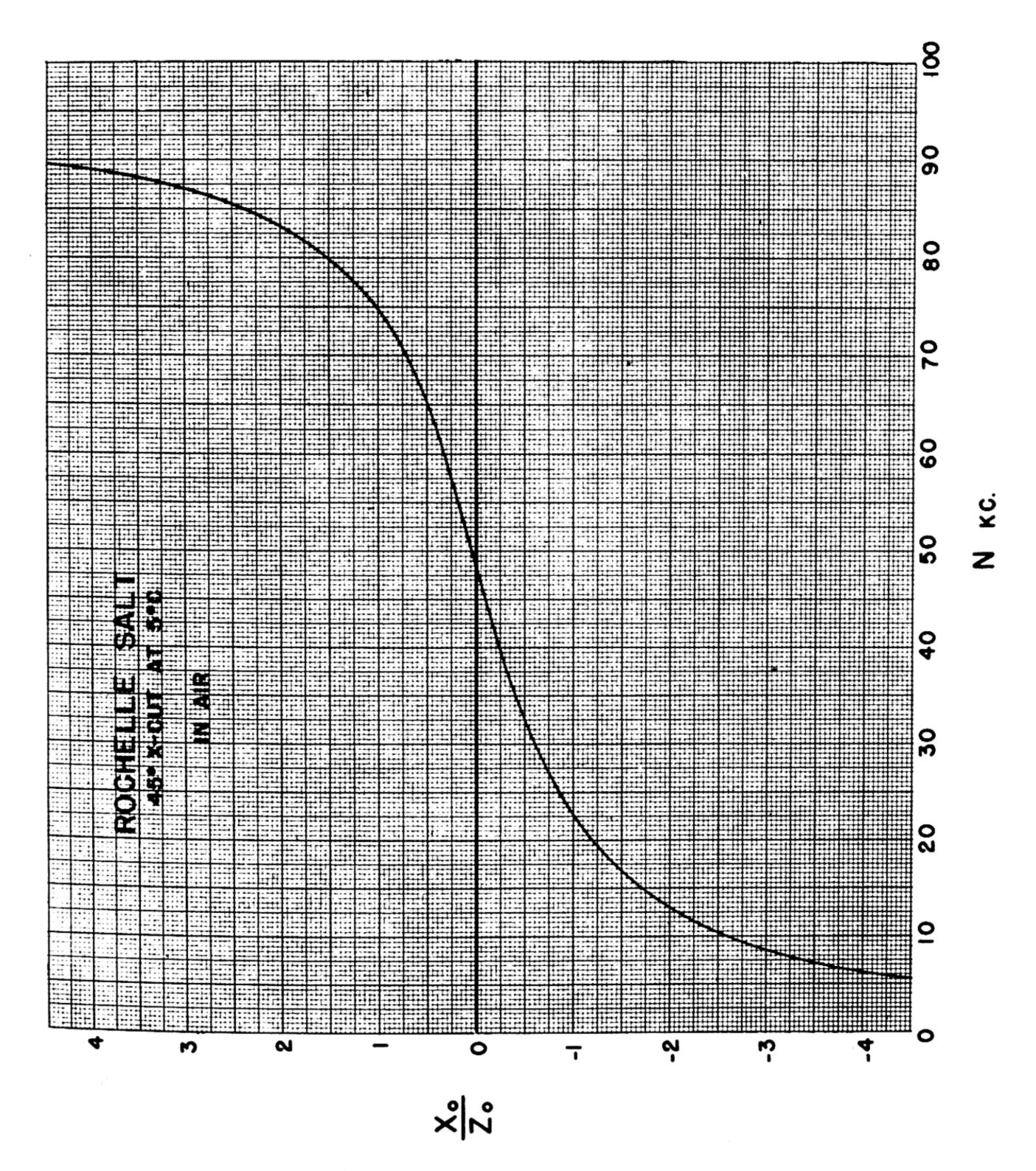


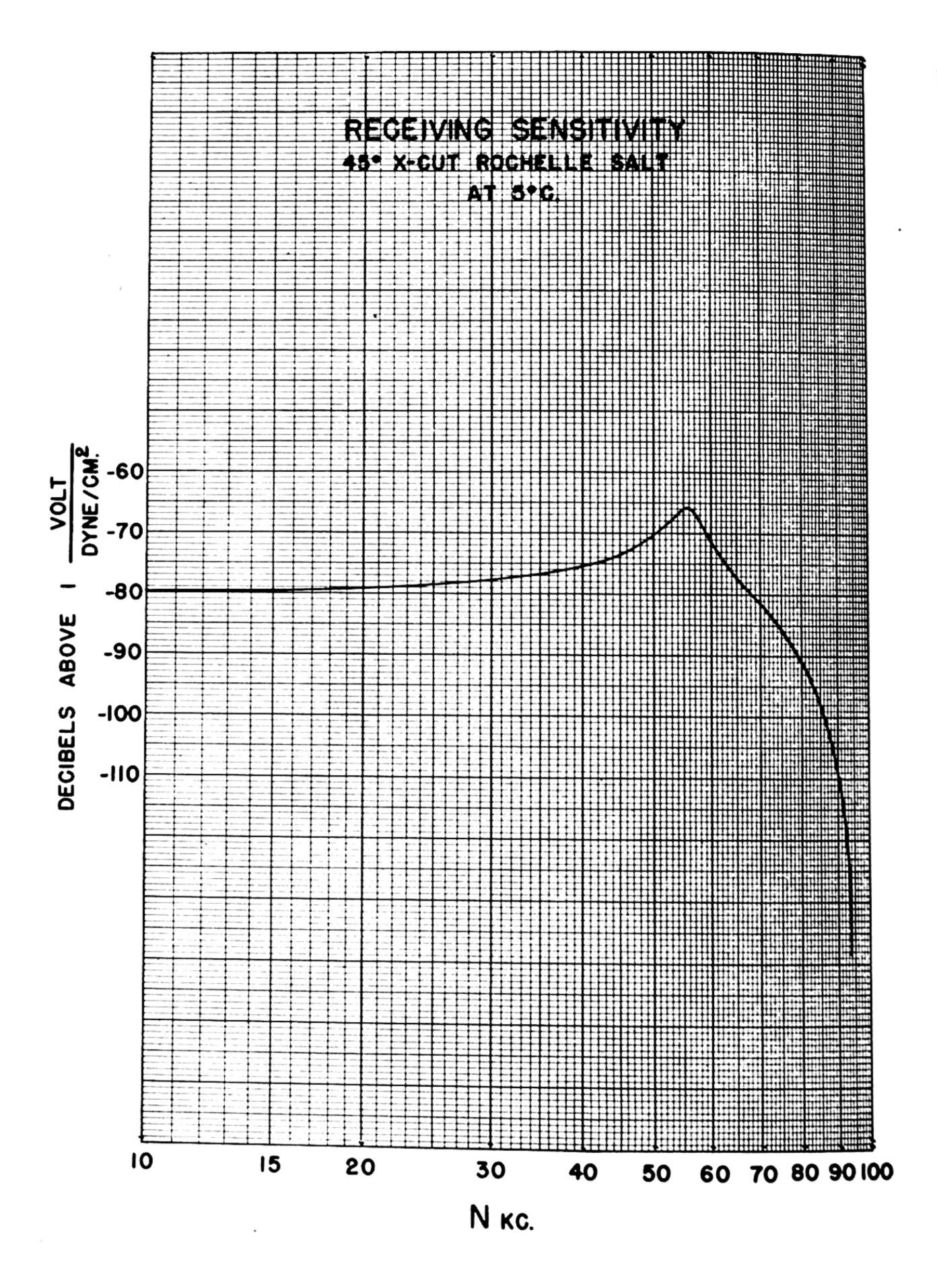


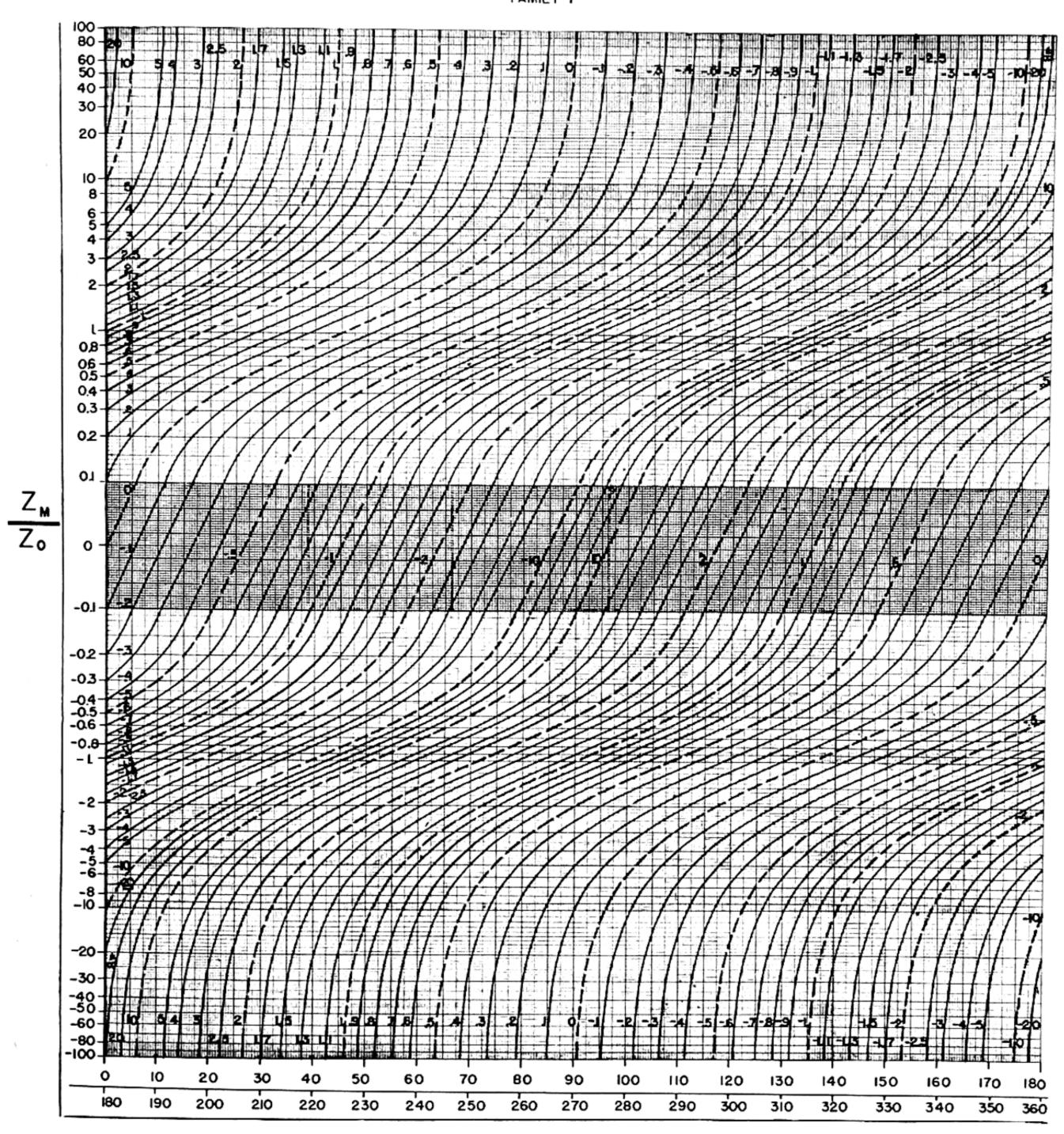
PRESSURE AT PROJECTOR FACE

45° X-CUT ROCHELLE SALT AT 5°C.

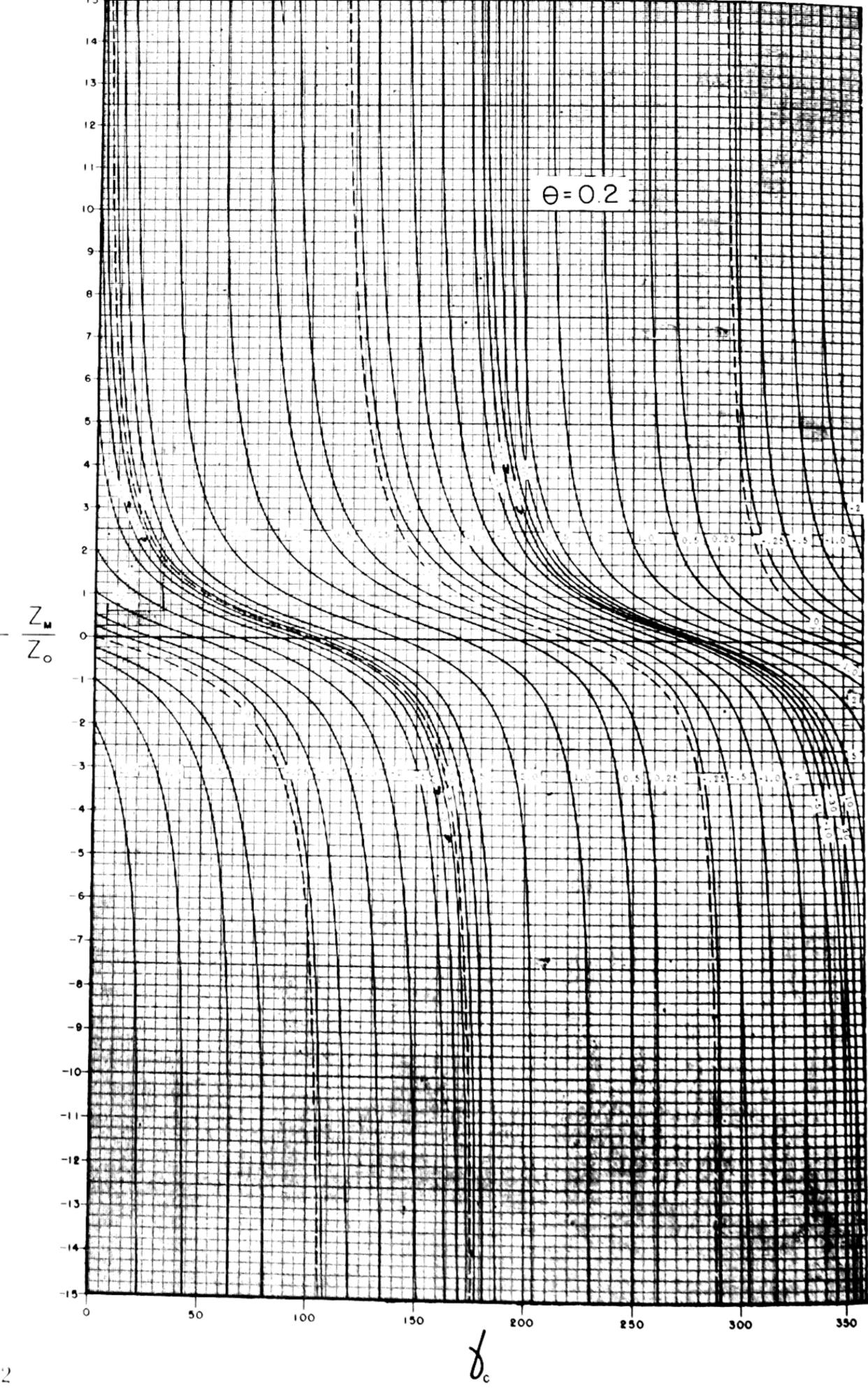


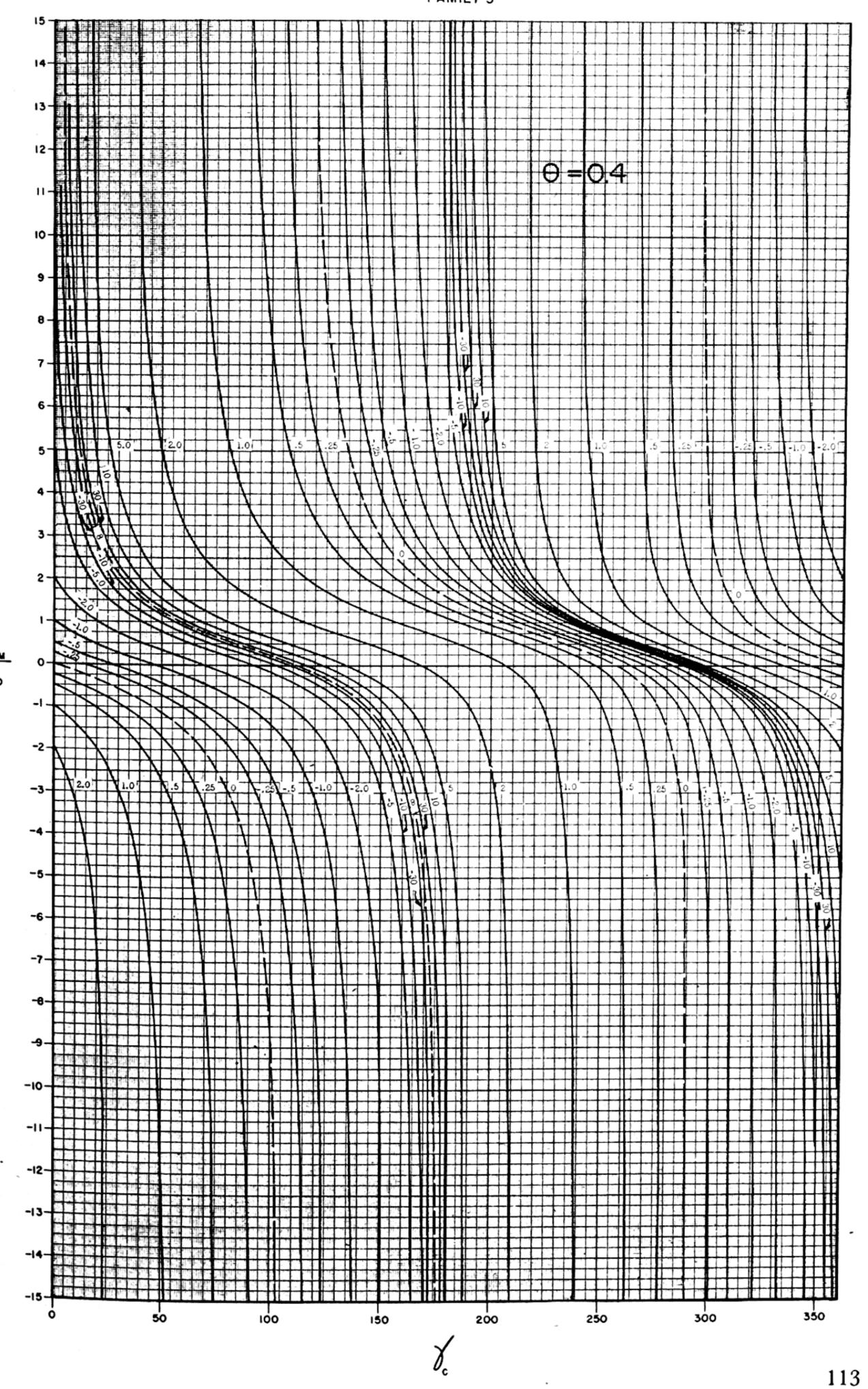


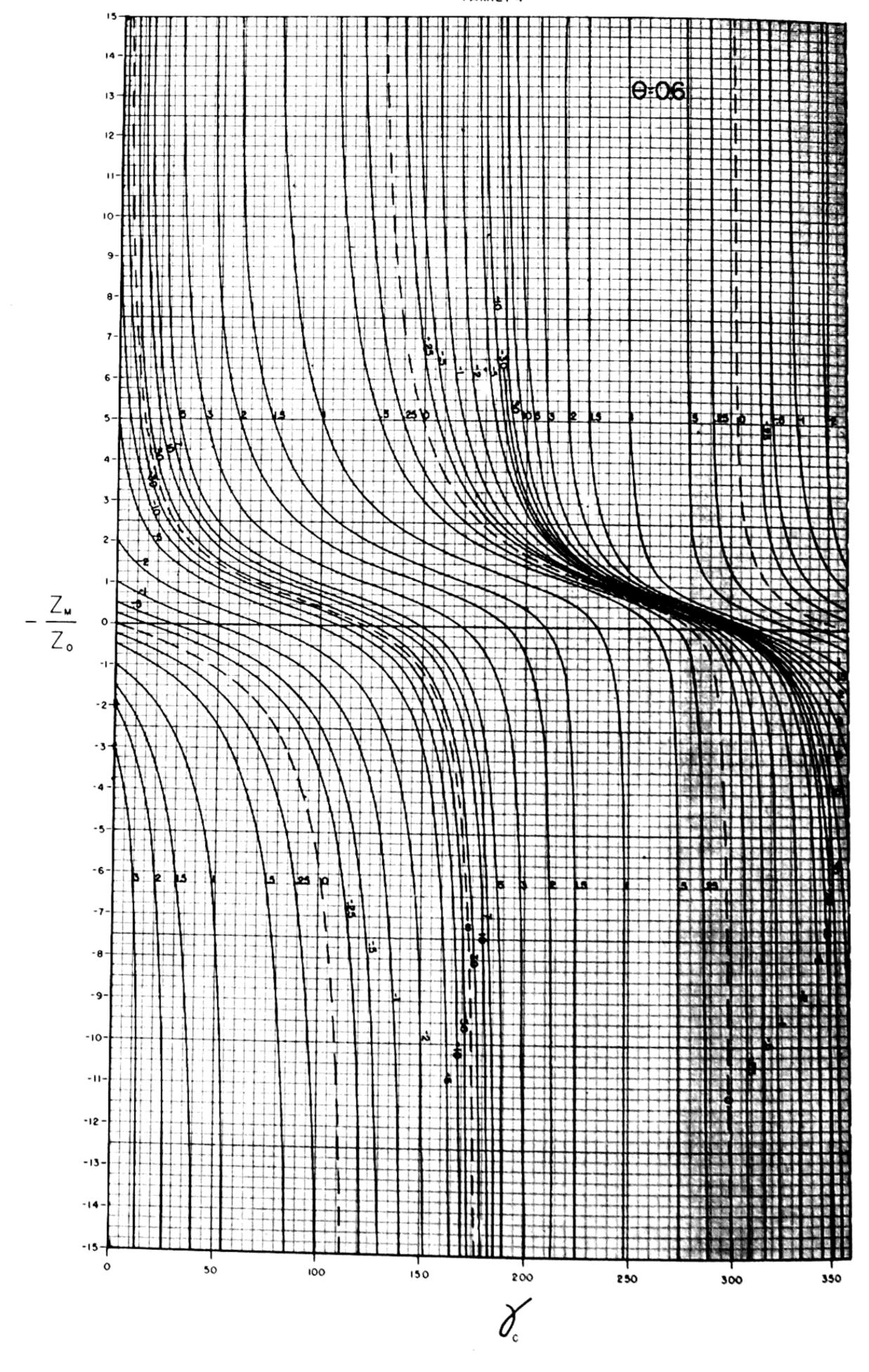




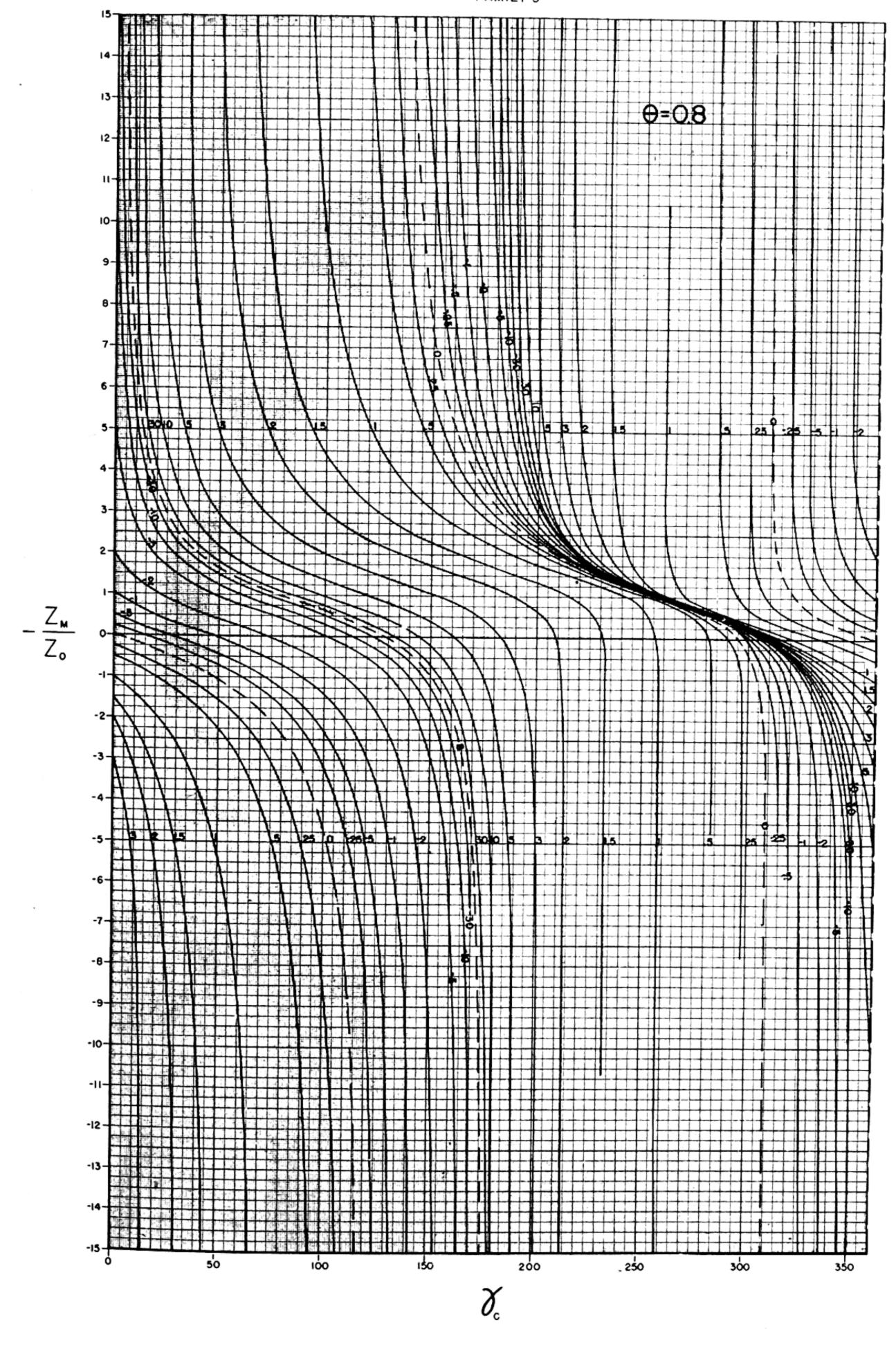
V_C
(PARAMETER = G_{IC}U_I)
Θ ≤ 0.1

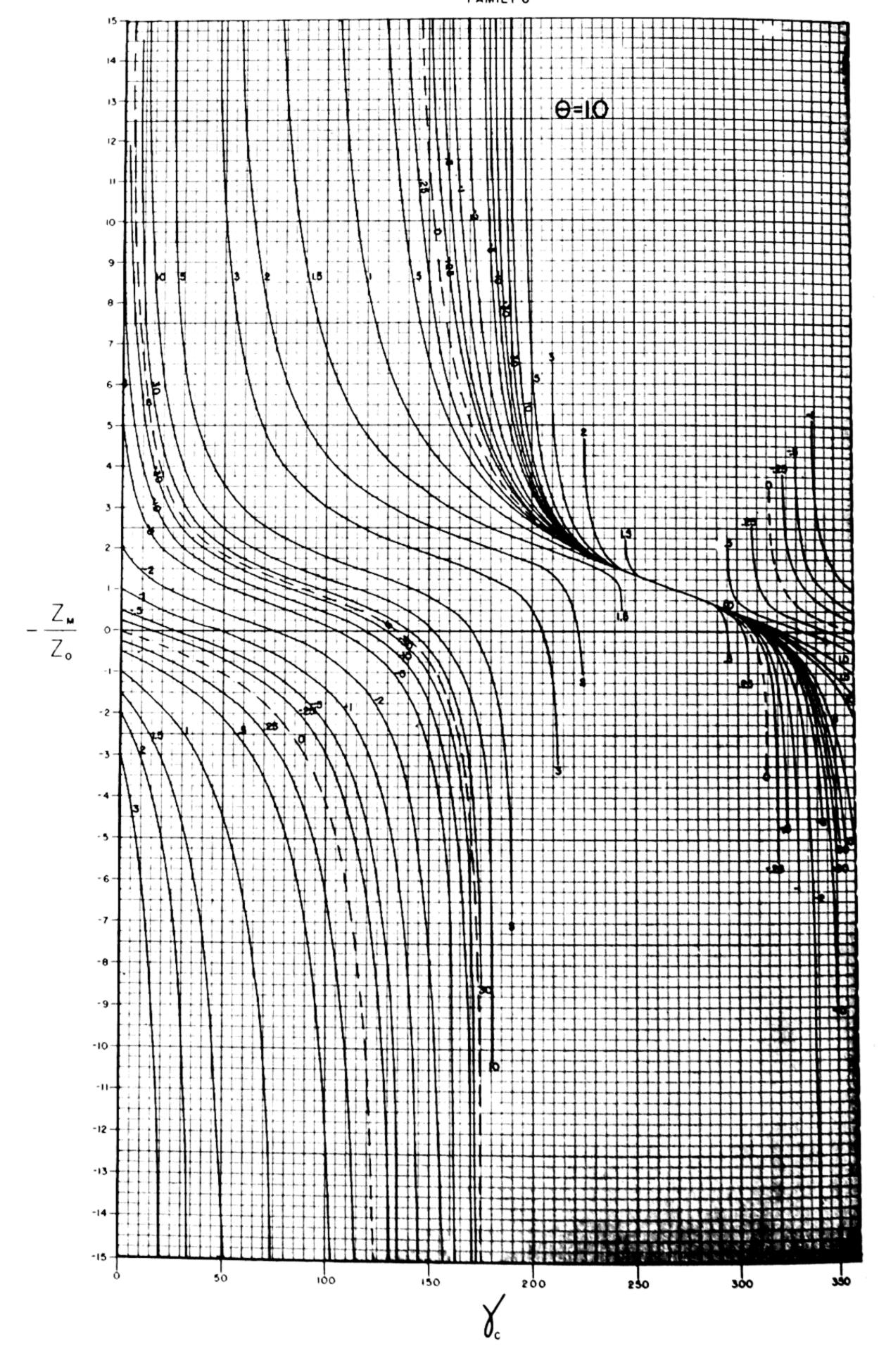


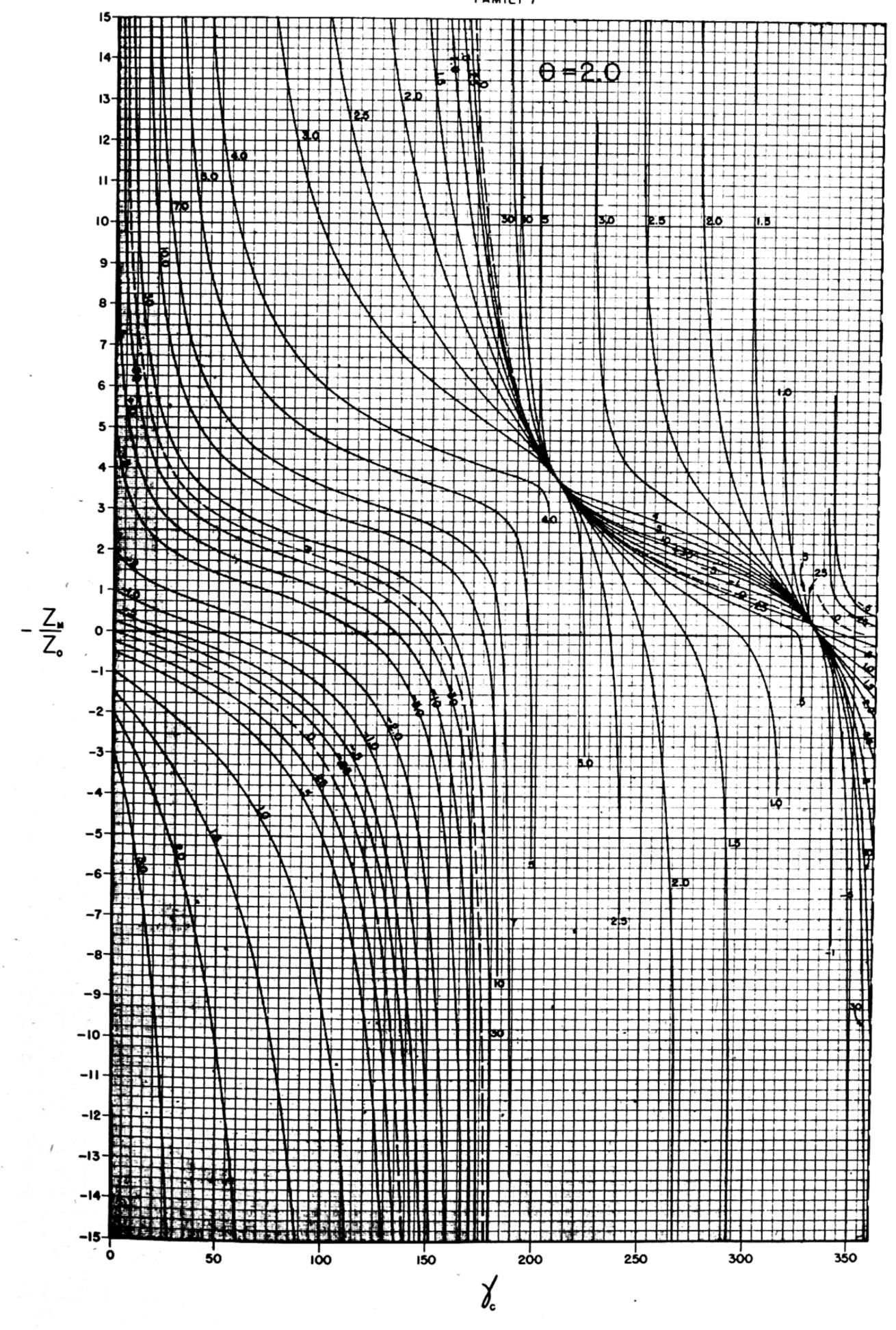




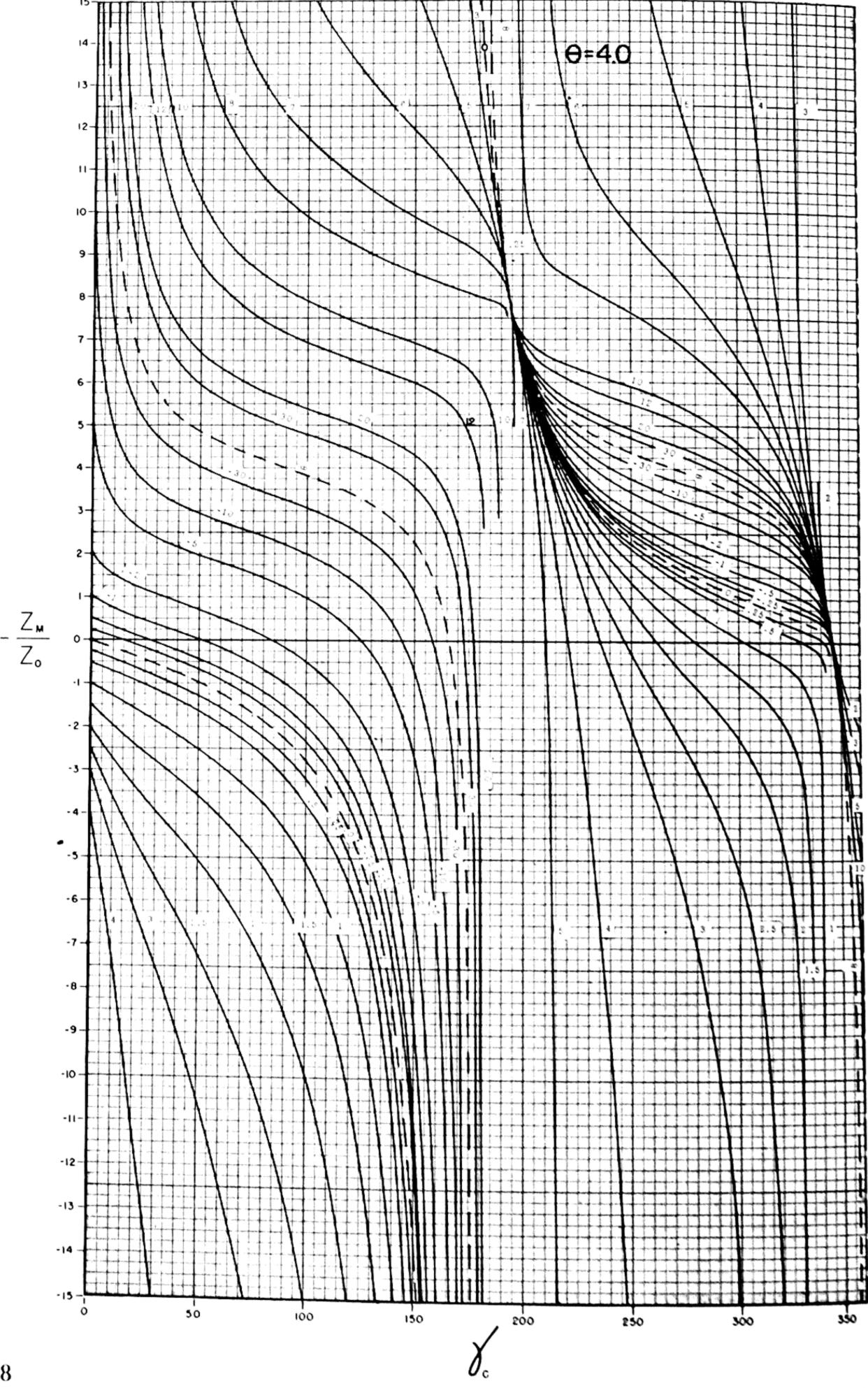




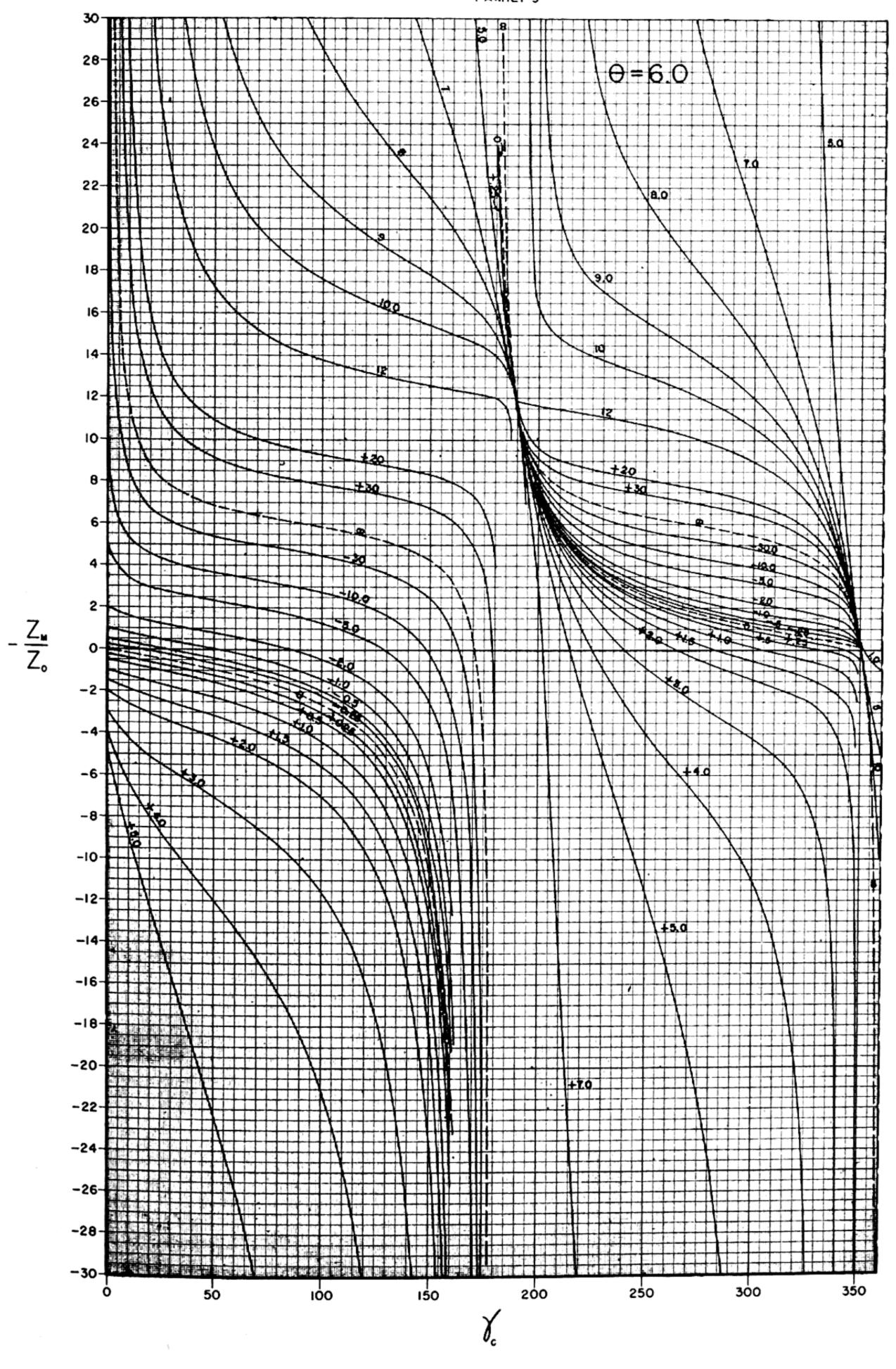


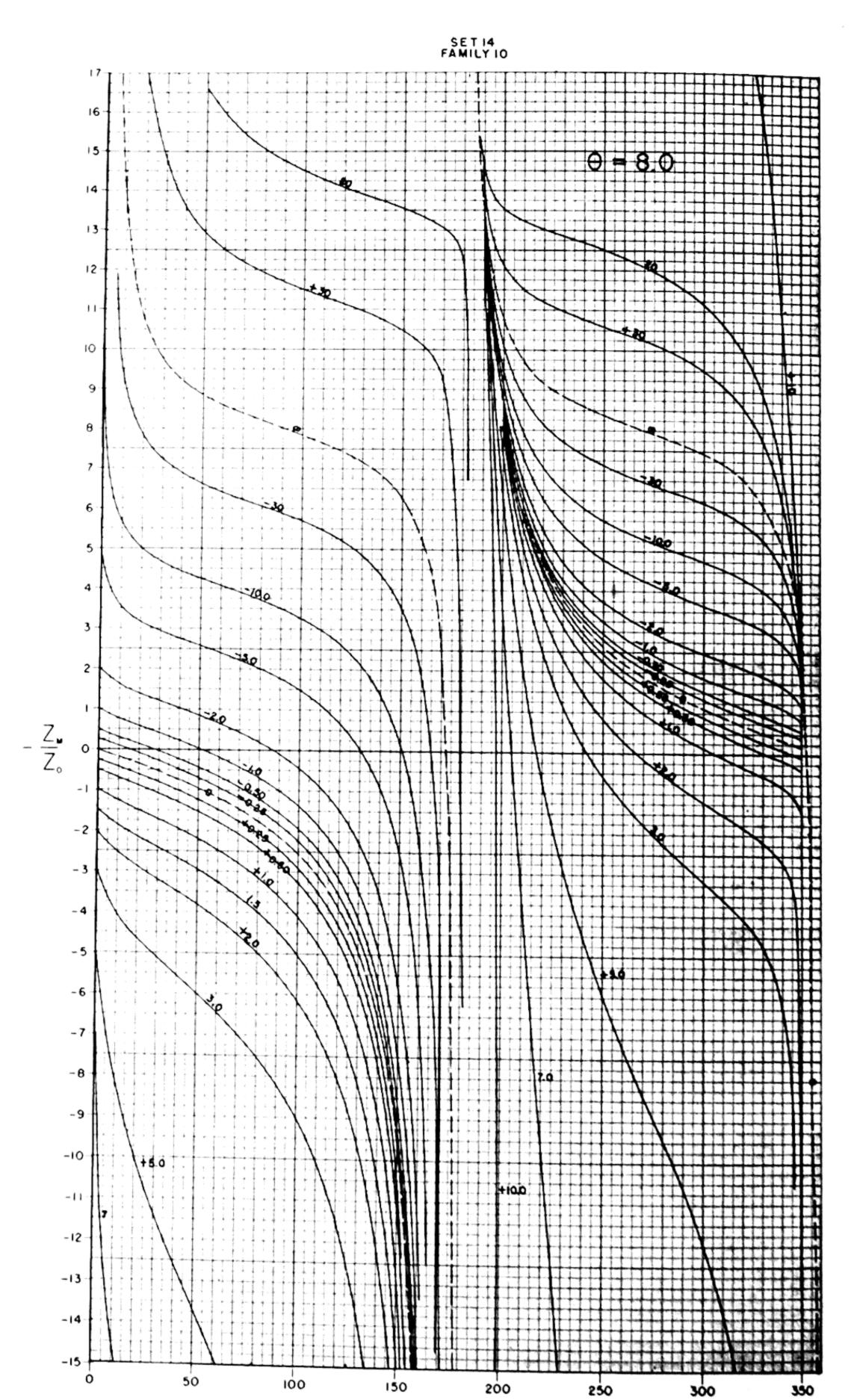




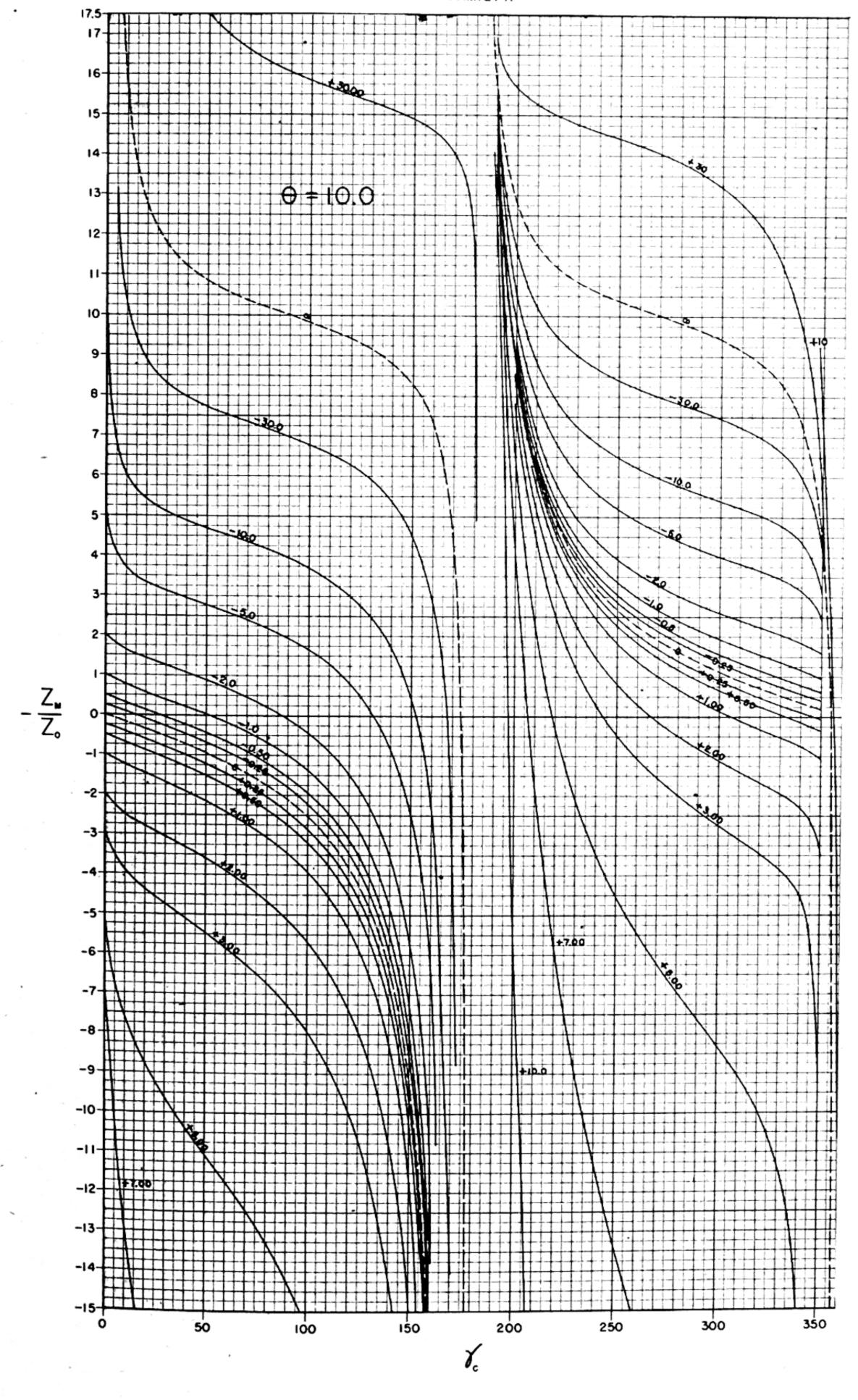


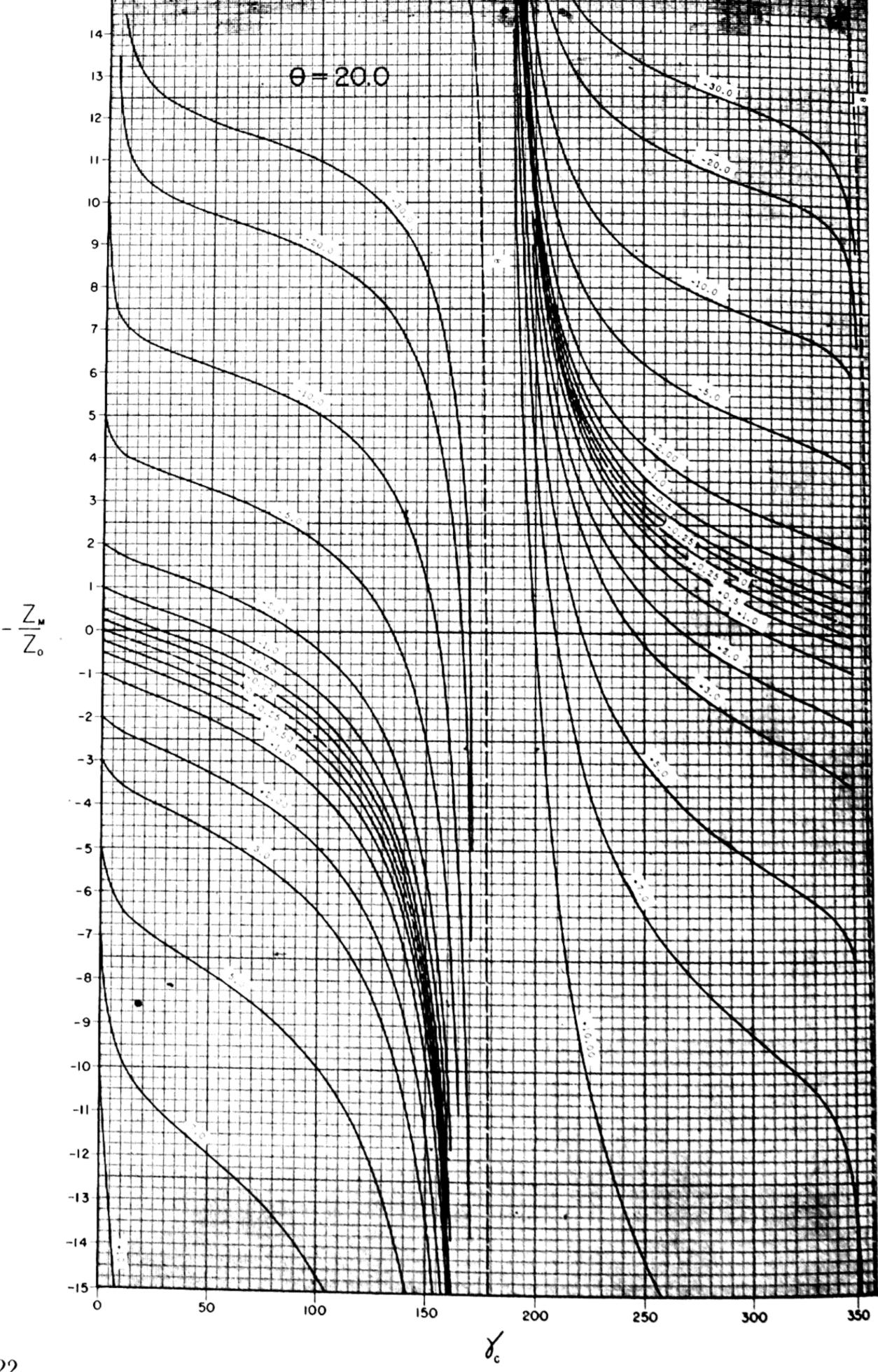




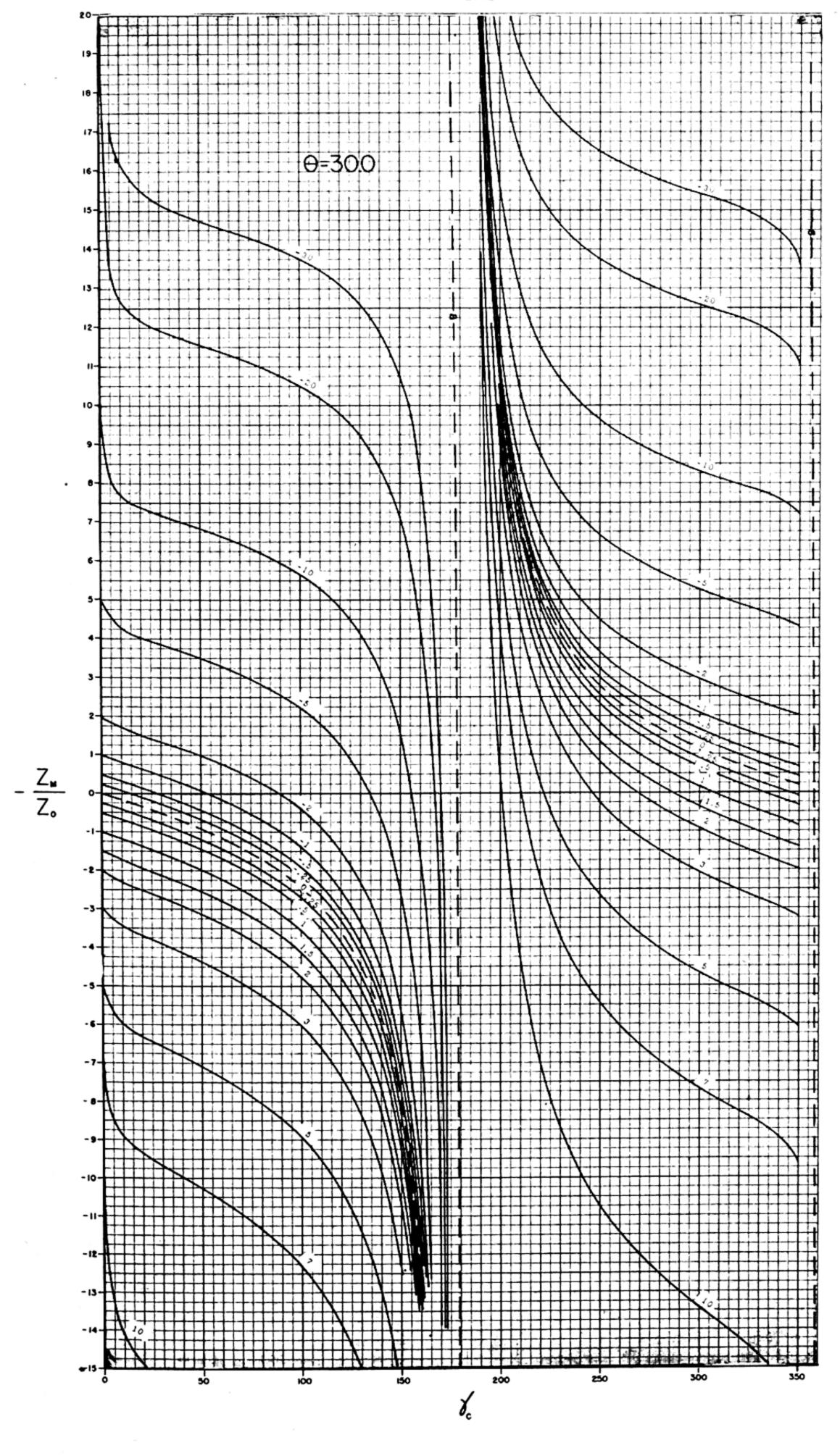


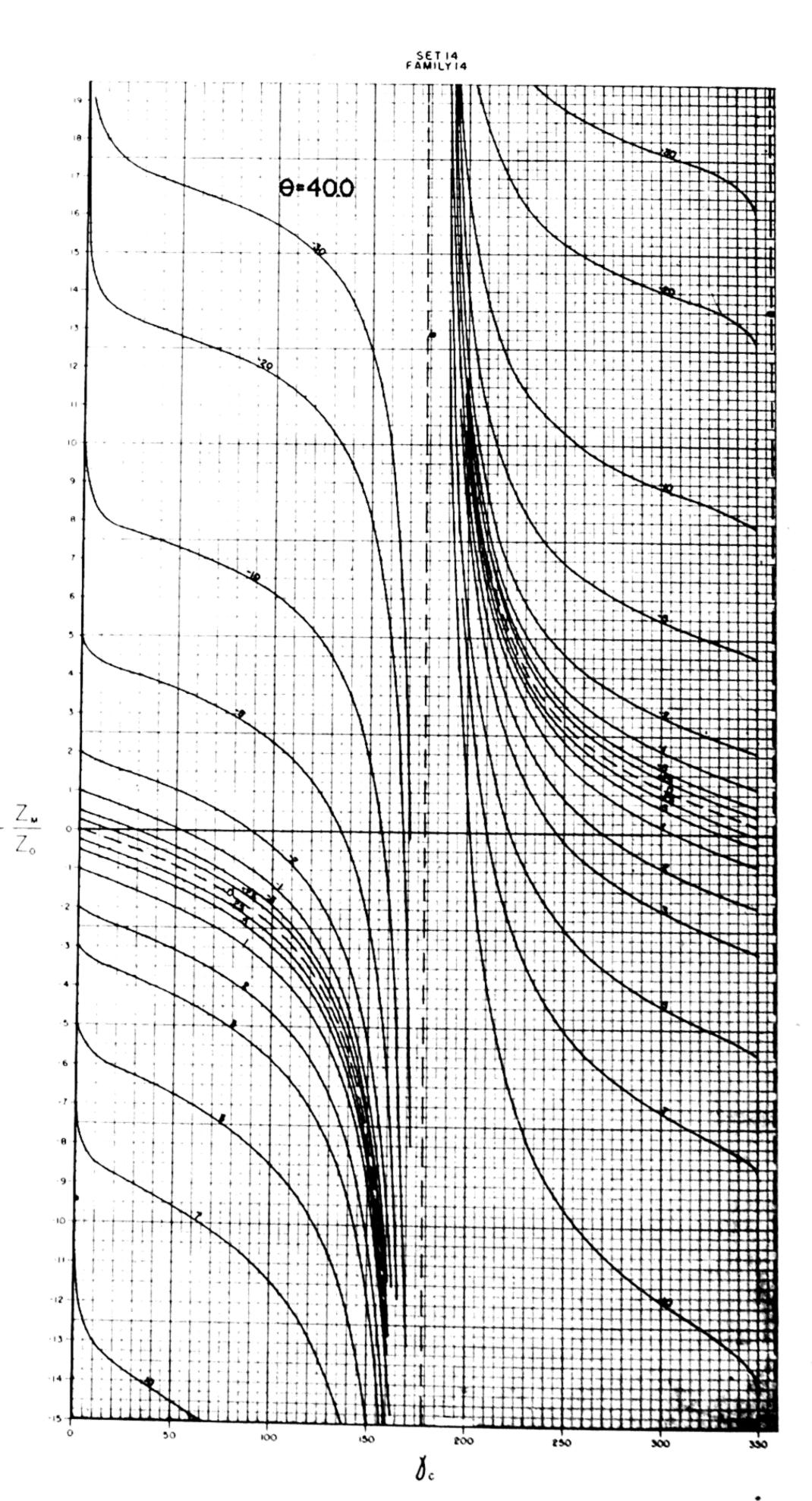




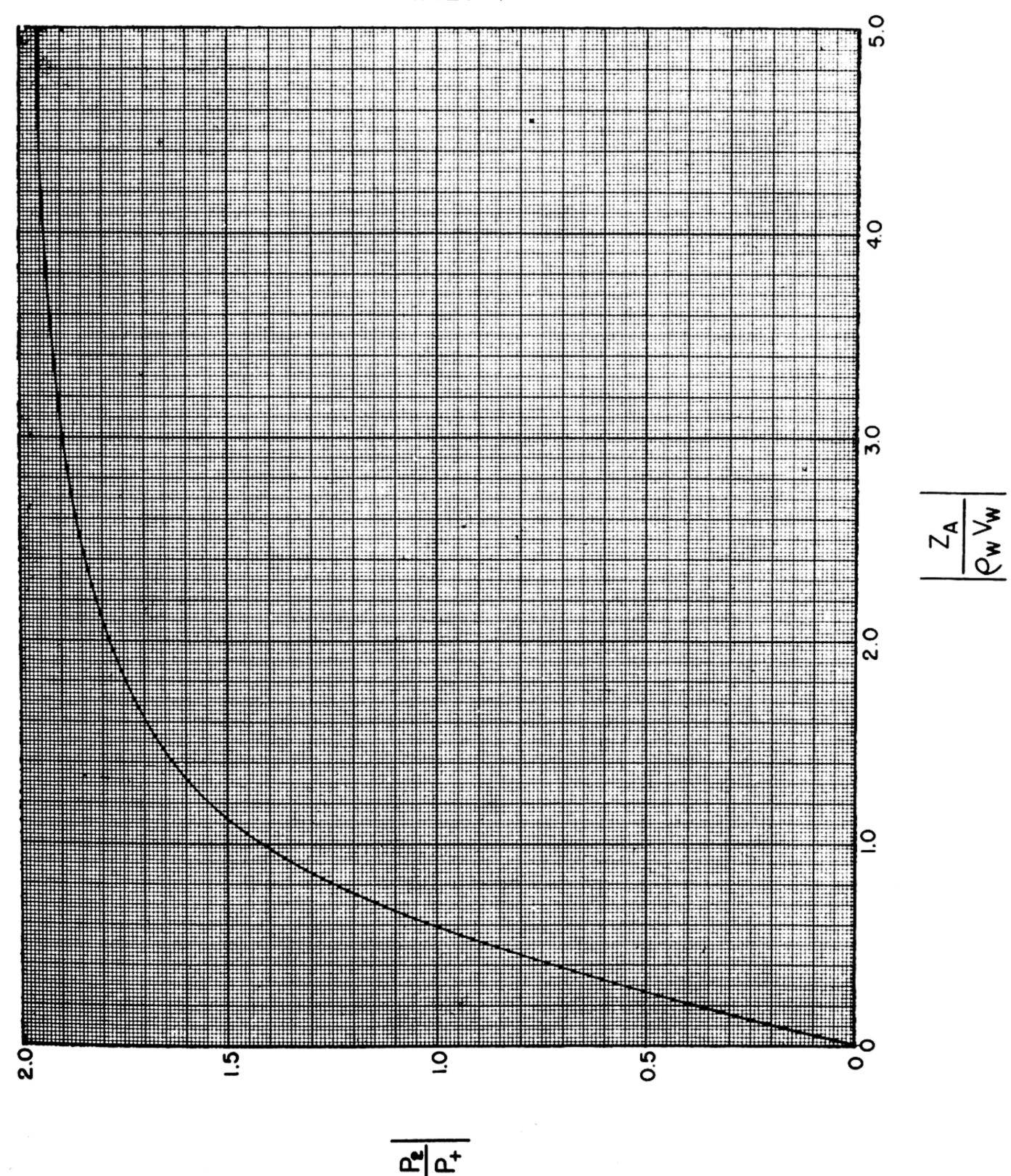


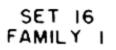


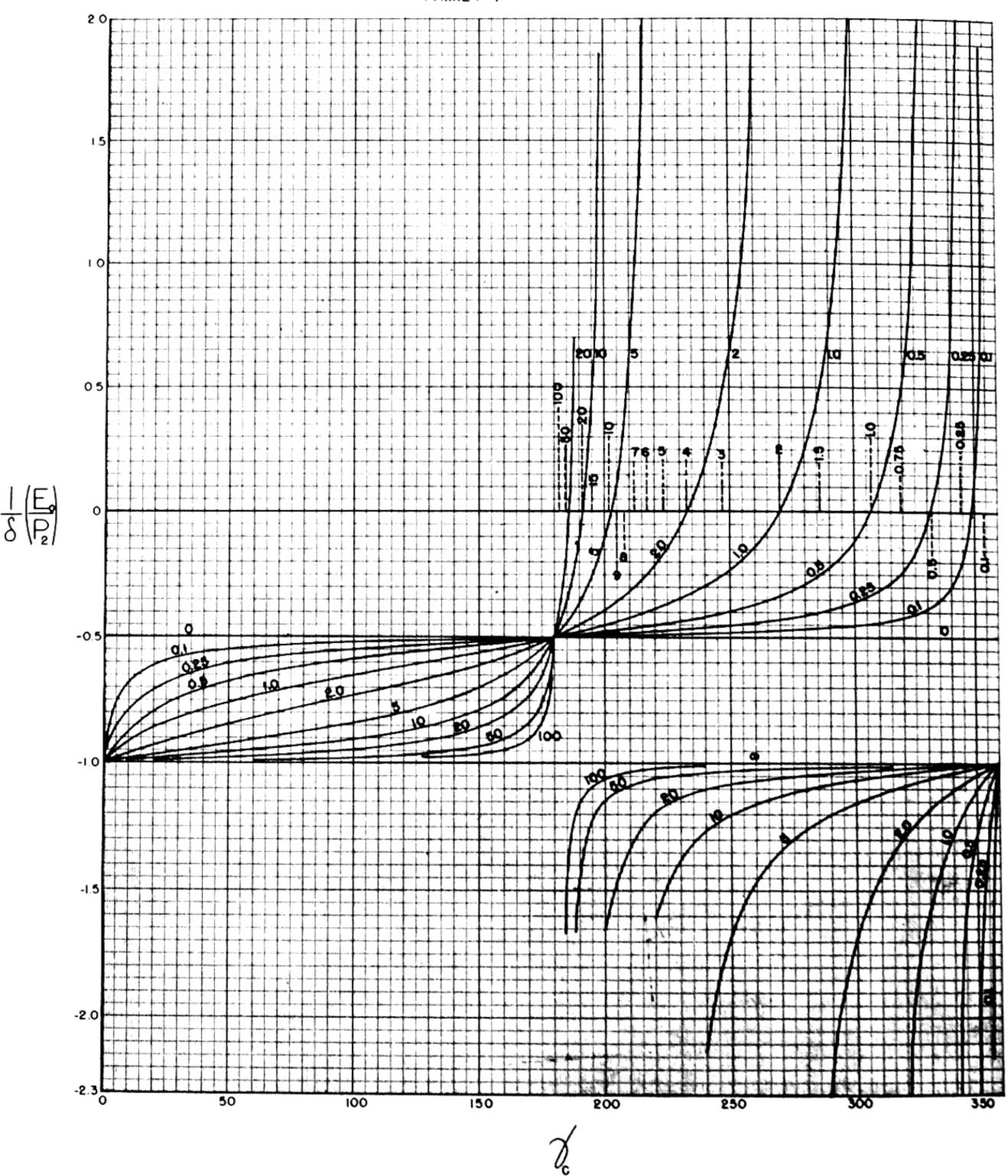




SET 15 FAMILY 1







SECTION 7 EFFICIENCY AND STRESS

In Section 5 on transmitting response, it is assumed that power is dissipated only by radiation into the driven medium and by electrical loss in the vibrating system and coupling circuits. In order to obtain the efficiency, the power input per unit current input must be calculated. The efficiency is obviously the ratio of power output per unit current input (transmitting response) to power input per unit current input unit current input.

Mechanical motion, however, gives rise to losses in the vibrating system in addition to radiation losses. Some dissipation occurs in the crystal and backing material, and a loss is introduced by the holder, but the most serious loss usually occurs in the joints between the crystal and backing material. Although very little quantitative information is available on this subject (and therefore no losses have been incorporated in the calculation of the curves) we do know that the dissipation in the crystal and backing material is usually rather small, and that the loss caused by the holder can be minimized by clamping the vibrating system at a displacement node. Thus, if proper precautions have been taken in the mounting, the glue joint becomes our chief concern. A method will be suggested later in this section for estimating the loss in glue joints whenever data on the characteristics of glue joints are available.

Such losses probably would not have been included in the general curves even if data were available because of the tremendous increase in the amount of calculation and in the number of curves required. Furthermore, the power losses cause a negligible shift in the resonant frequencies and in the positions of the maxima and minima of the response characteristics. The effect on the magnitude of the transmitting response and the receiving sensitivity can be

approximated by subtracting a suitable number of db. from the response characteristics. This assumes that the designer can make an estimate of the efficiency to be expected from a projector, or has available some data on loss characteristics of glue joints. For example, if a projector has an efficiency of 60 percent, 2.2 db. should be subtracted from the transmitting response (expressed in terms of total power) and 4.5 db. from the sensitivity. (A db. chart appears on page 62.)

When the loss in the glue joints under various conditions of stress and frequency is known, the efficiency can be estimated fairly

well as follows:

From the transmitting response (expressed in total power output) and the radiating area of the projector, a value for the intensity at the crystal radiating face is obtained:

$$I = \frac{\text{Total power radiated}}{\text{Radiating area}} (10)^{7}$$

where I is the intensity in ergs/sec per cm² when the total power is expressed in watts and the area in cm². The pressure amplitude at the crystal face is obtained from

$$P_2 = \sqrt{I \rho_w V_w}$$

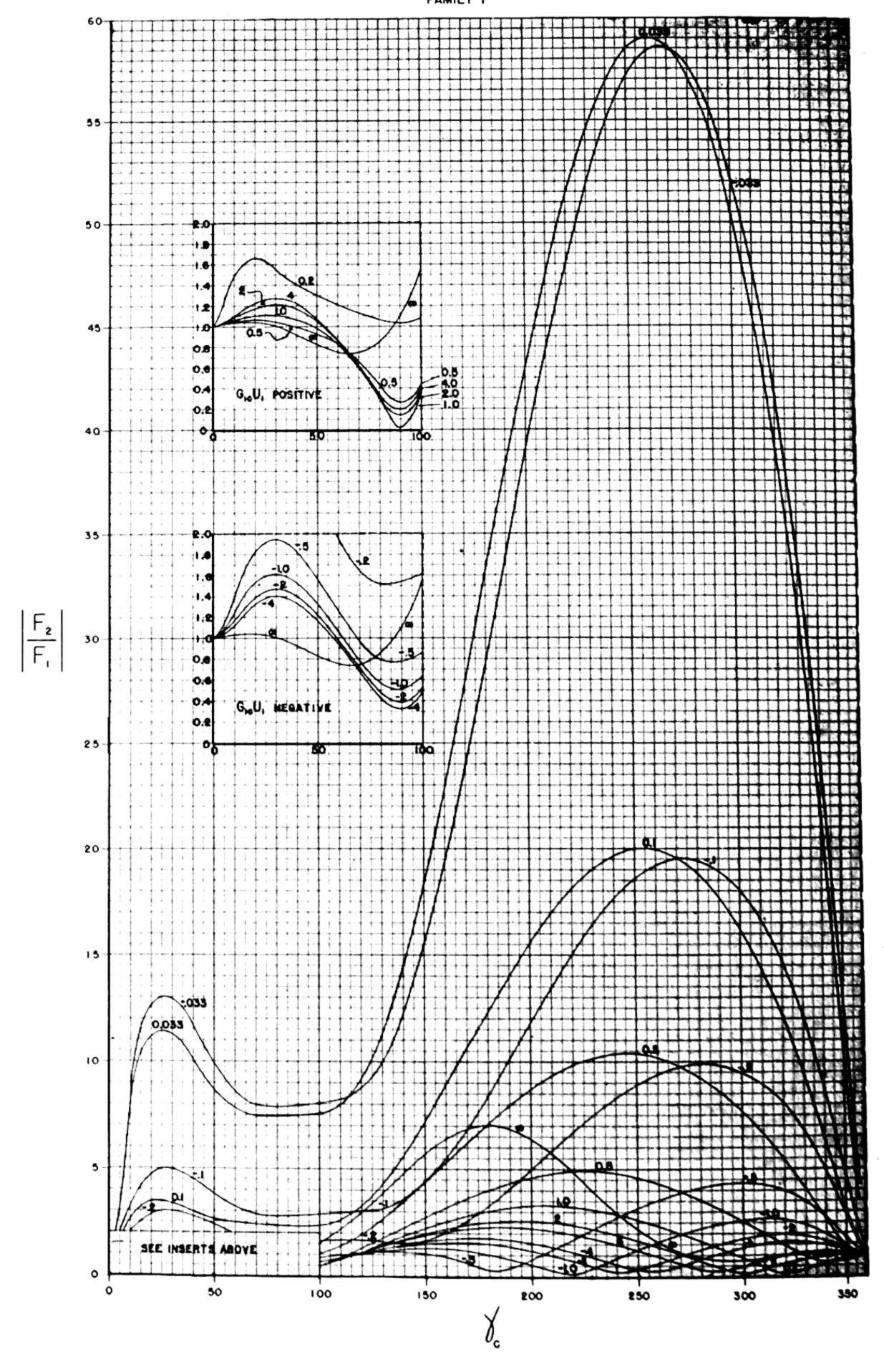
 P_2 is the pressure amplitude (r. m. s.) in dynes/cm² when $\rho_w V_w$ is the characteristic impedance of the driven medium in cgs units, and I is

the intensity calculated above.

Multiplying the pressure amplitude by the area of a single crystal, A_c , yields the force per crystal at the crystal face, F_2 . From $G_{1c}U_1$ (defined in Section 3, page 19), and γ_c (defined in Section 1), F_2/F_1 is evaluated by using the family of curves on page 128 of this section. This family of curves holds only for ADP crystals radiating into water. F_1 , the force at the glue joint is obtained by dividing F_2 by the value of F_2/F_1 . Then, from the data on losses in glue joints as a function of stress and frequency, an estimate of the efficiency can be made:

An estimate of the lowering of the transmitting response and receiving sensitivity, based on this efficiency, can then be made as previously described (Sections 5 and 6).





SECTION 8

ACOUSTIC INPUT IMPEDANCE OF PARTICULAR **BACKING MATERIAL SYSTEMS**

This section presents curves of the acoustic input impedance of a few particular backing material combinations. These curves will facilitate the design of backing systems. The curves (pages 130 to 149) show the impedance per unit area for single and multiple systems of aluminum, brass, lead, and steel. Longitudinal and plate velocities are included.

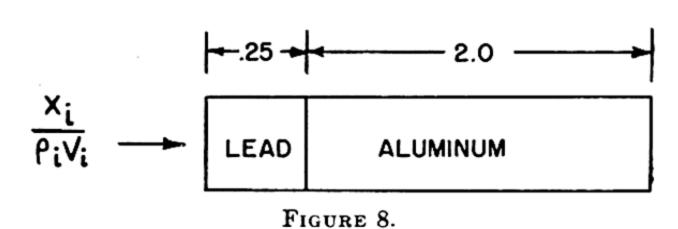
The acoustic impedance (jX_i) is plotted in cgs units along the vertical axis on a combination linear and inverse scale. Frequency from 0 to 100 kc is plotted along the horizontal on a linear scale. The parameter associated with each curve is the length of the backing material. To evaluate the quantity $G_{ie}U_{i}$ from the acoustic impedance as obtained from this section, see Section 3, page 19.

The first set of curves (eight families, pages 130 to 137) cover single materials for lengths

between 0.25 cm to 15 cm.

The second set (three families, pages 138 to 140) covers the lead-aluminum combinations. Labels on the curves give the dimensions of the components in cm. The material given last in the label is the one into which the curve gives the impedance. For example, if the label reads

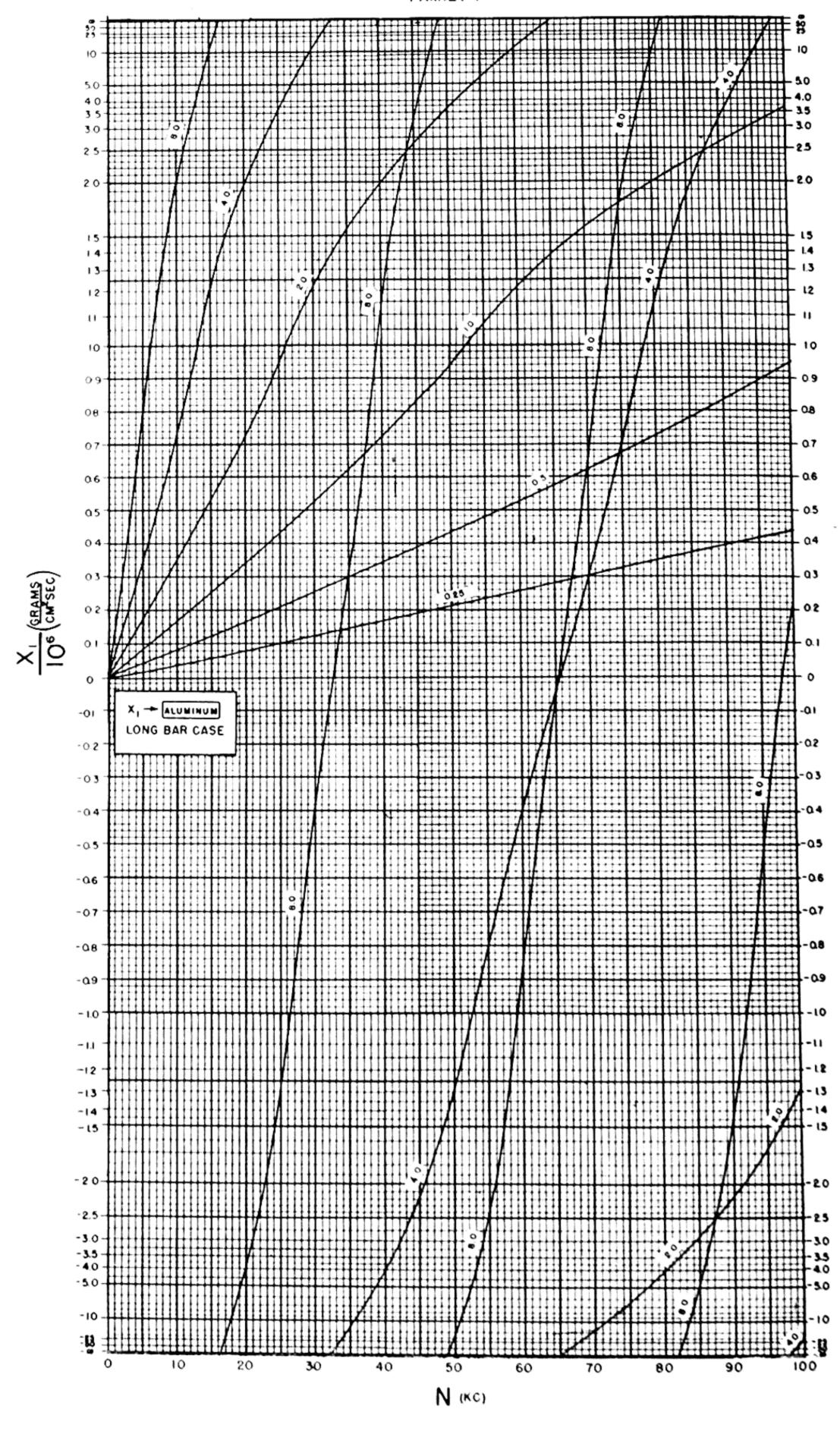
"2.0AL + 0.25LE", the curve gives the acoustic input impedance (per unit area) into the lead end of the system illustrated by Figure 8. For longitudinal velocities the characteristic impedances of lead and aluminum are practically equal, so that separate curves for aluminum plus lead and lead plus aluminum systems are not necessary. For plate velocities, however, the characteristic impedances are different for these materials and separate curves are given.

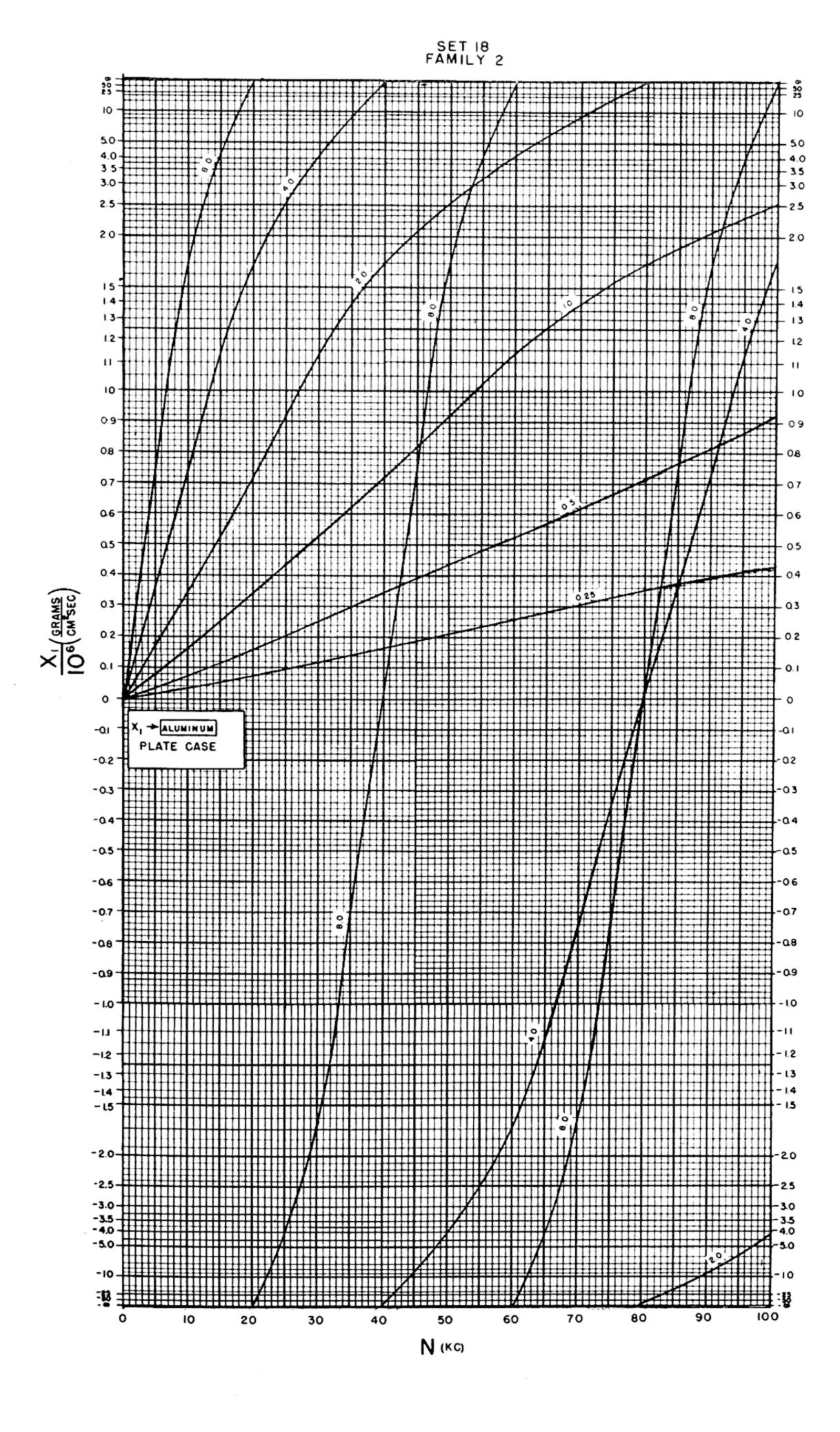


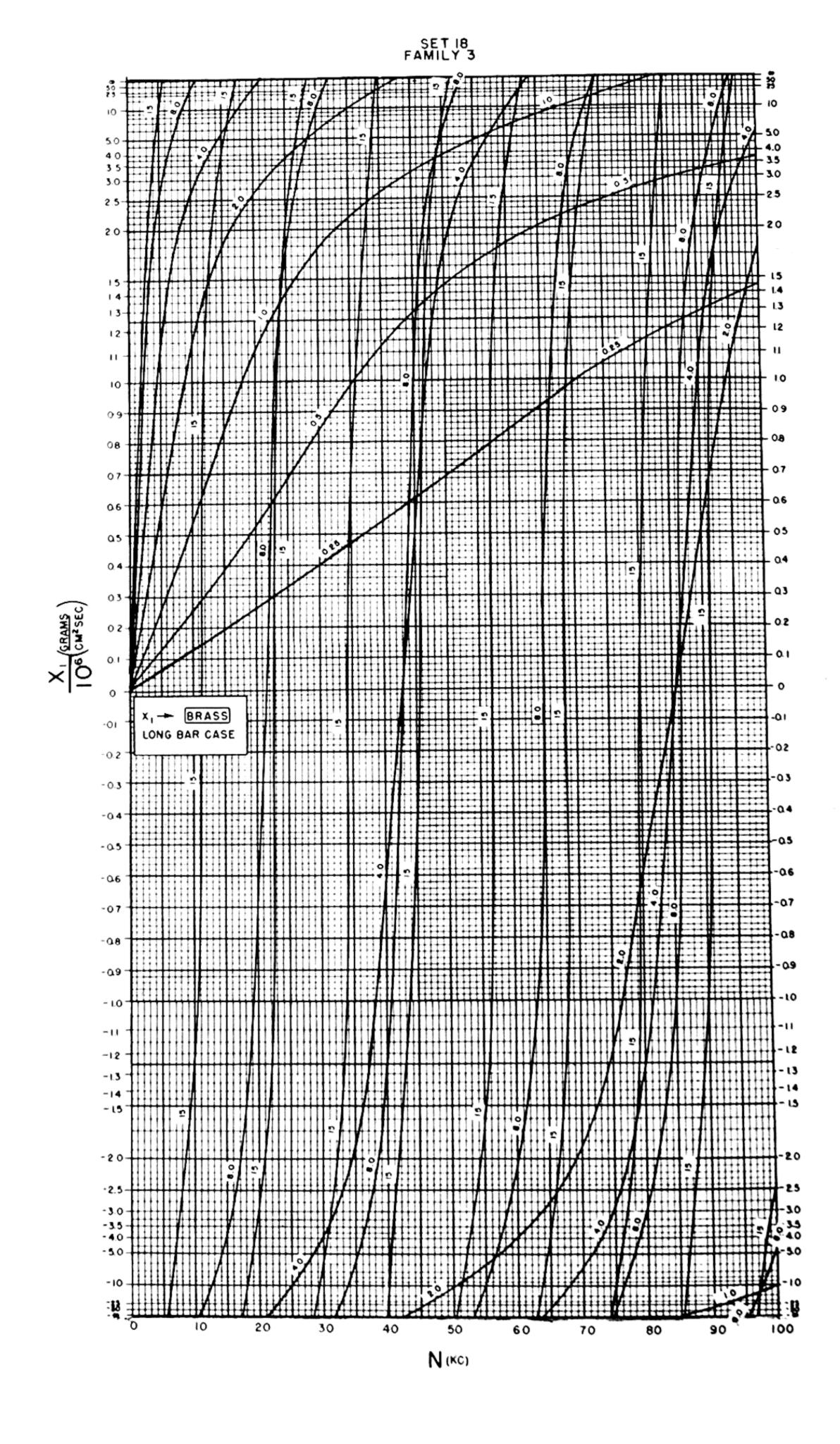
The third set (eight families, pages 141 to 148) covers the aluminum plus steel, steel plus aluminum, and steel plus lead, lead plus steel combinations.

The last family (page 149) shows the impedance of the particular triple system, lead plus aluminum plus lead.

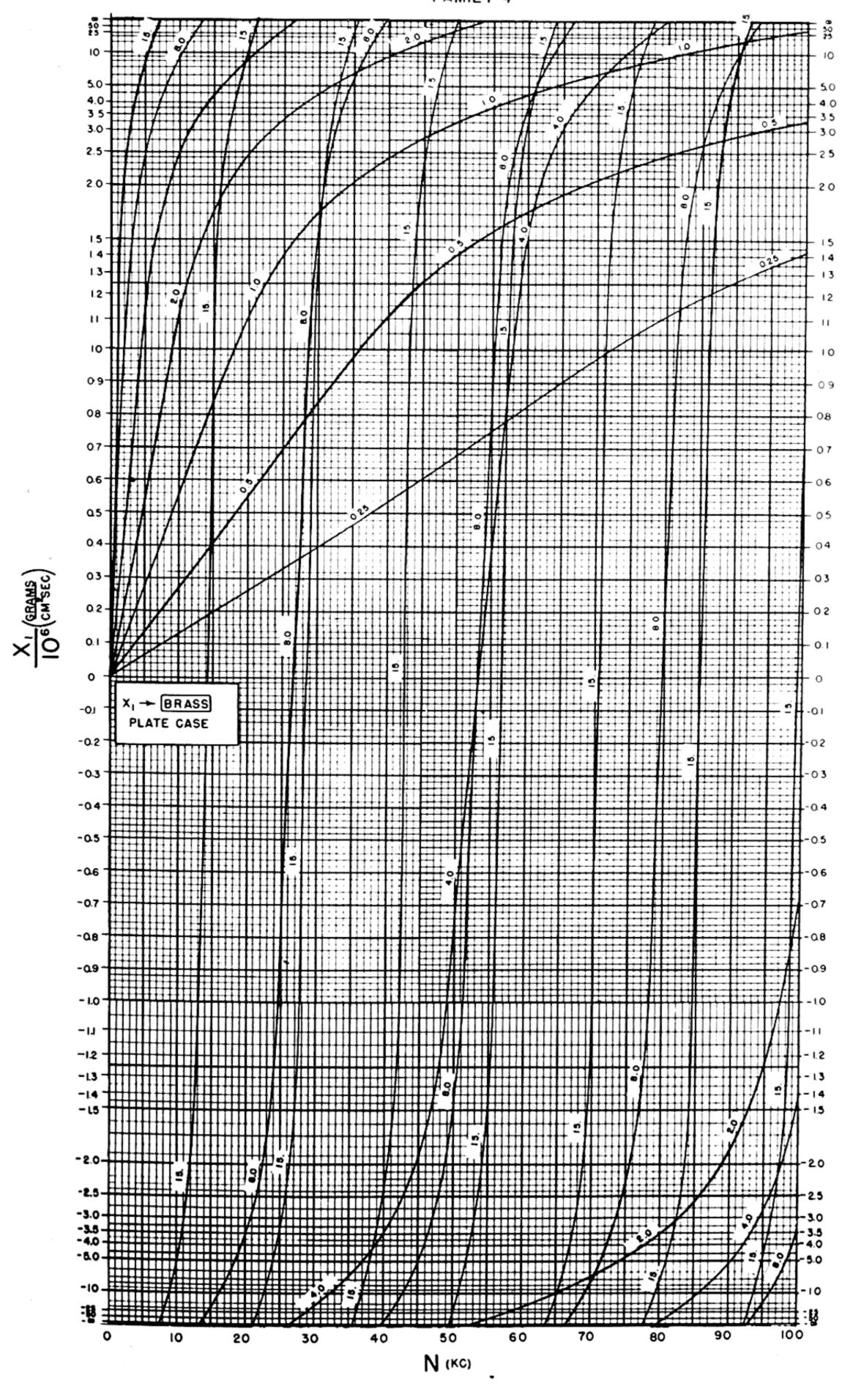




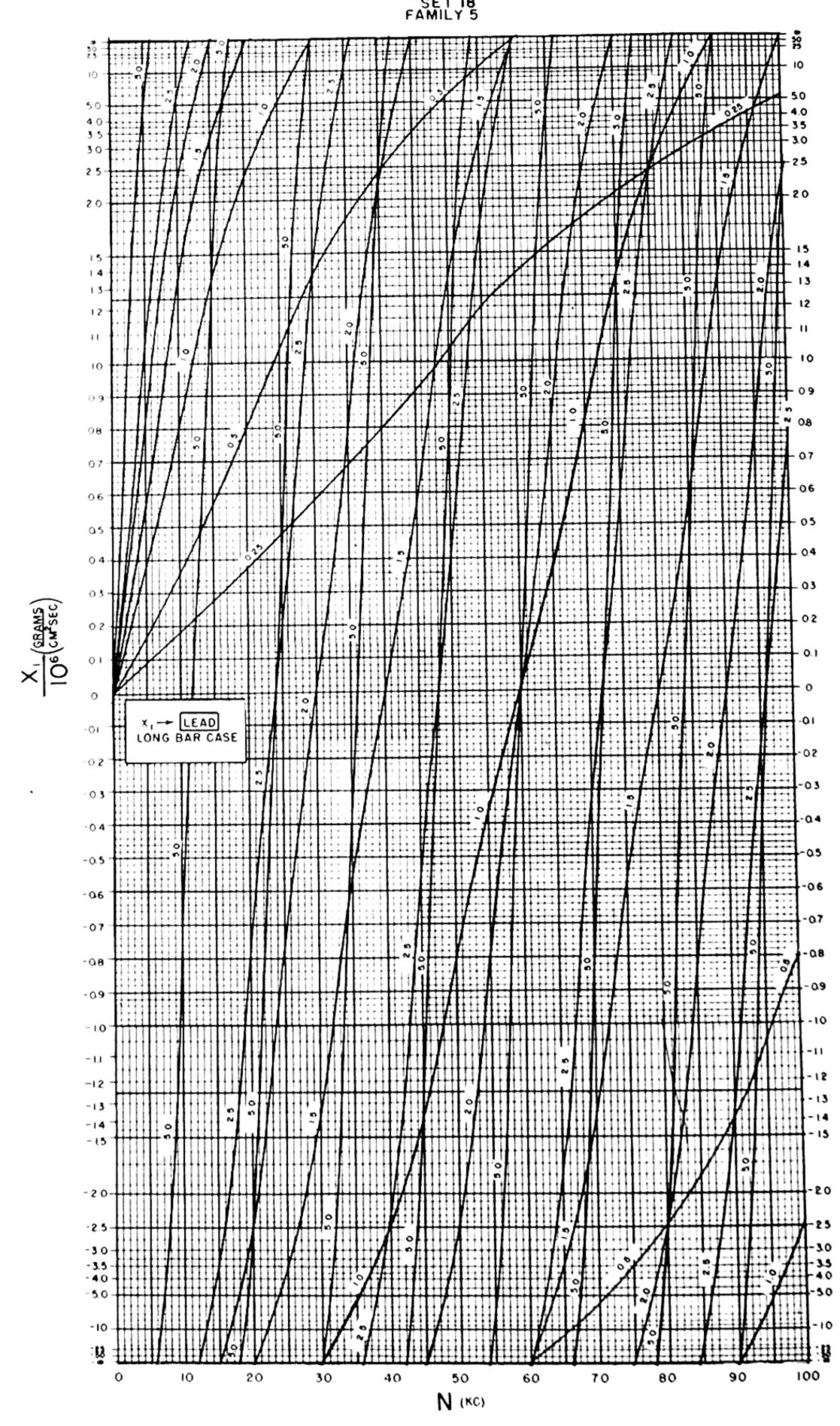




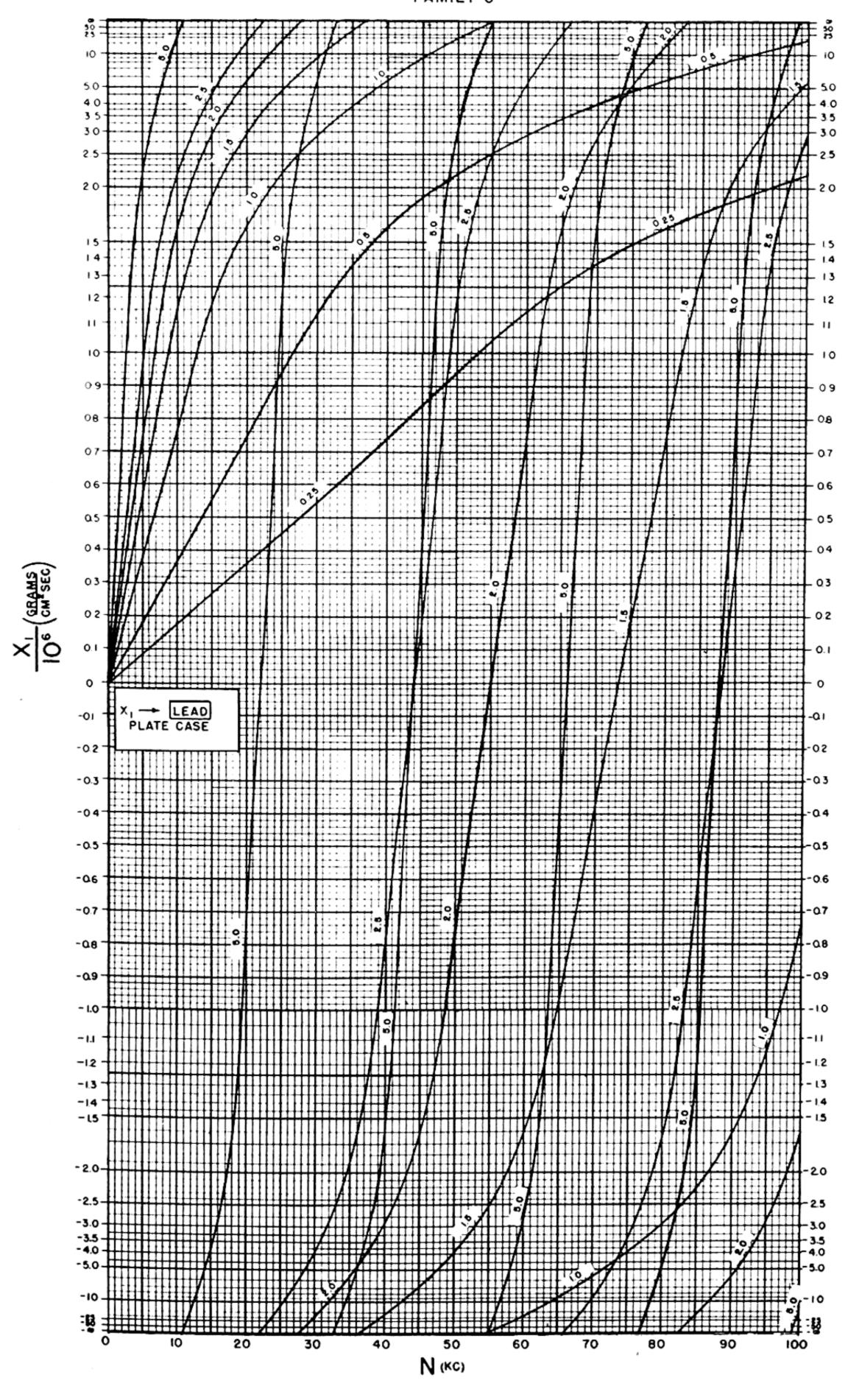




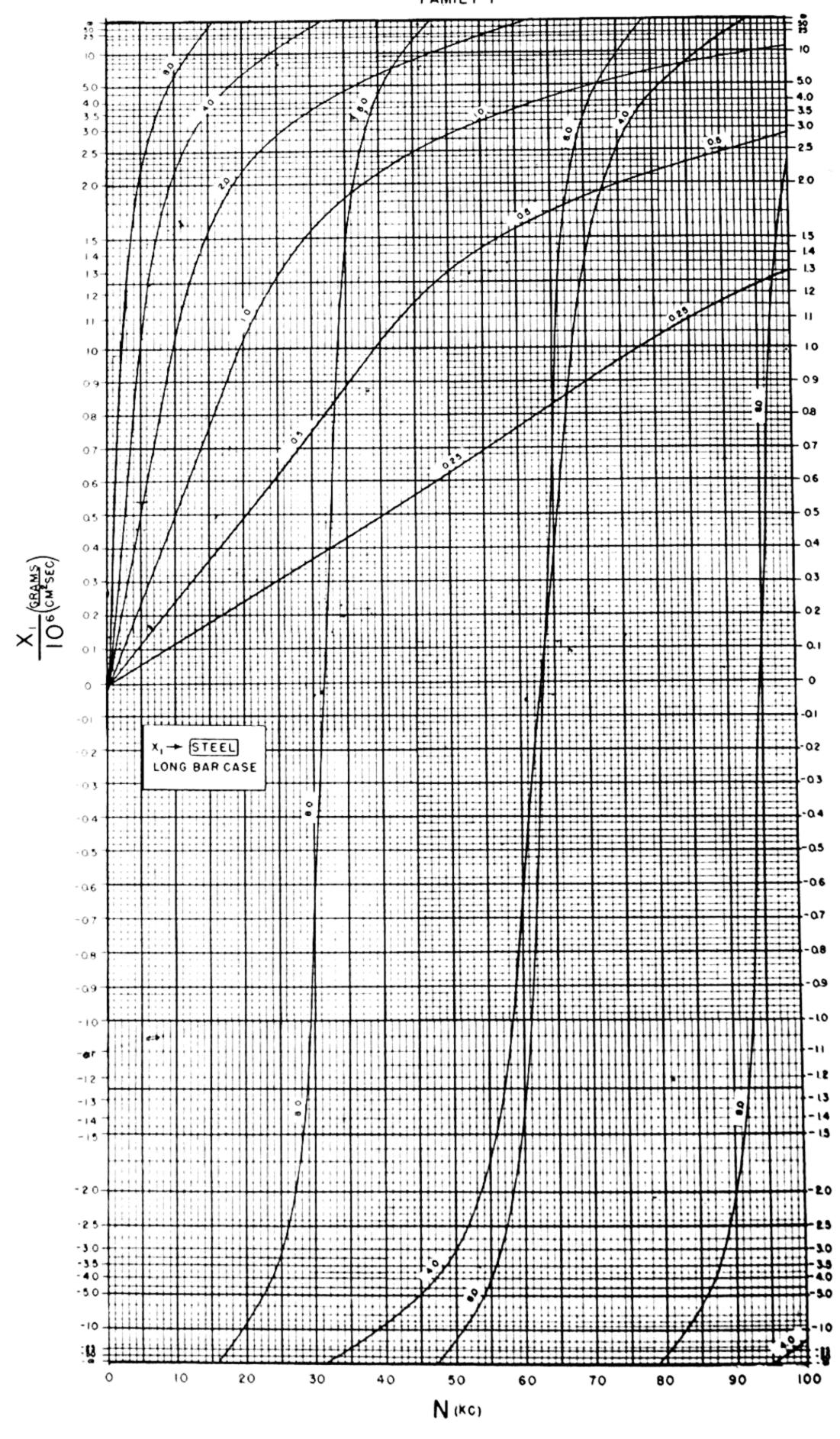


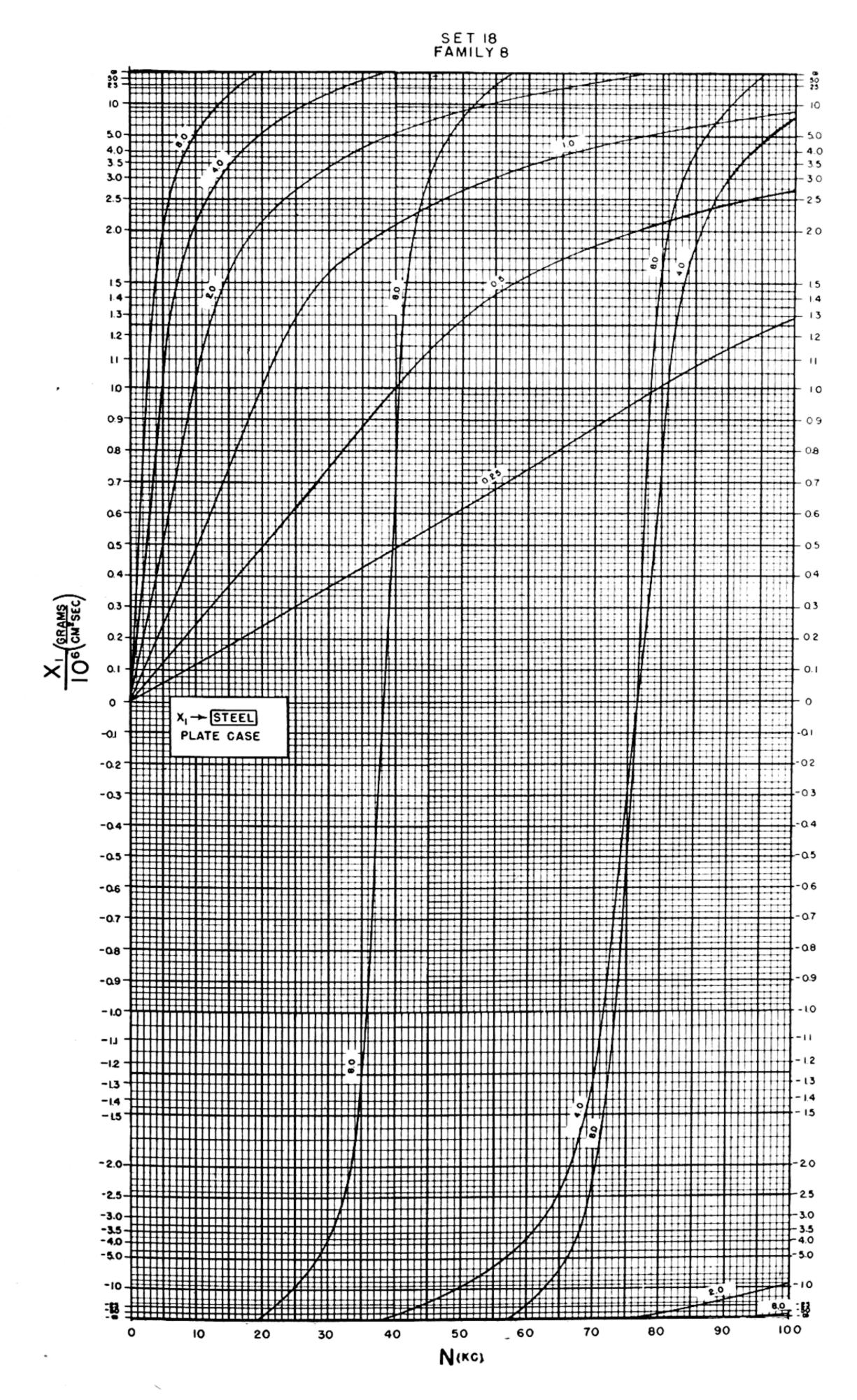


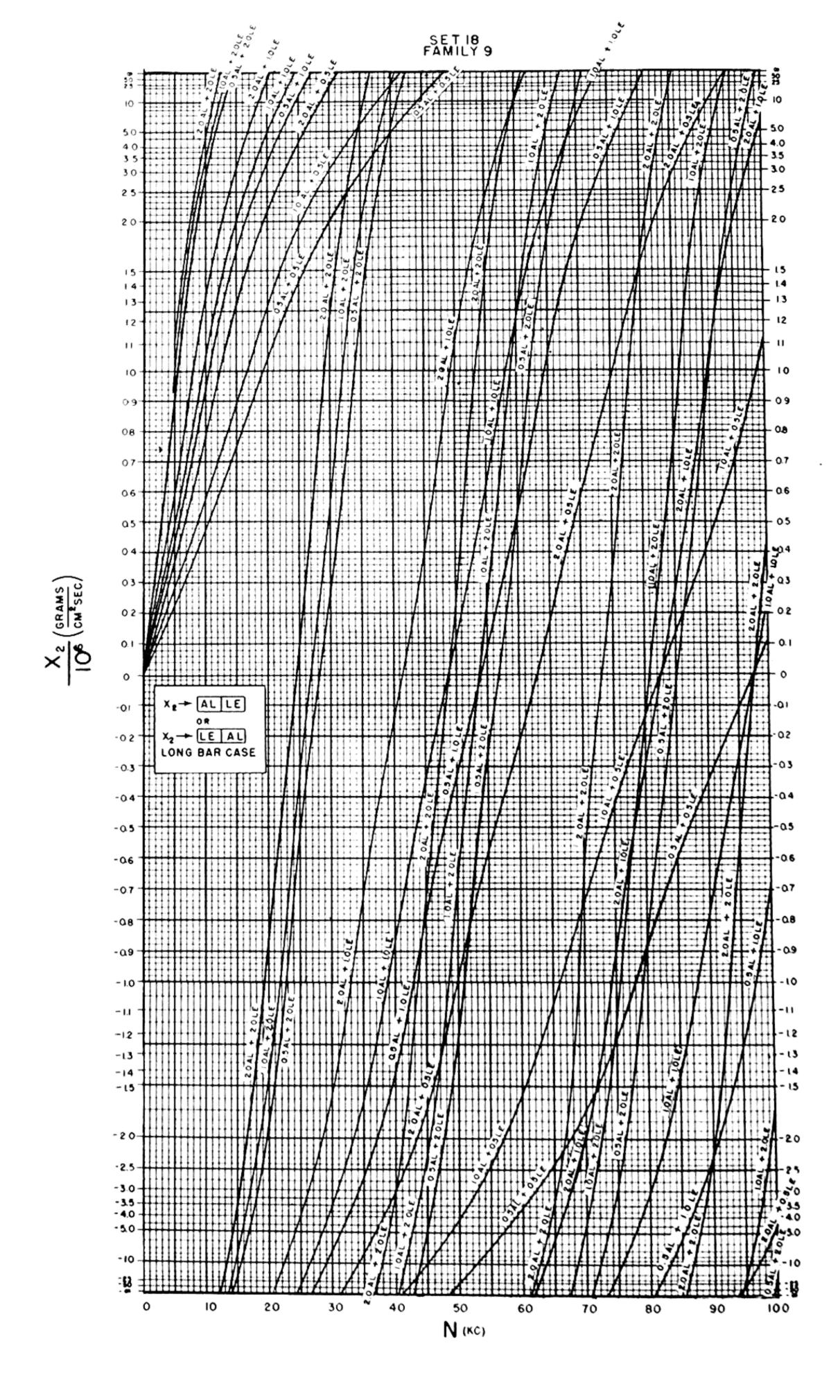


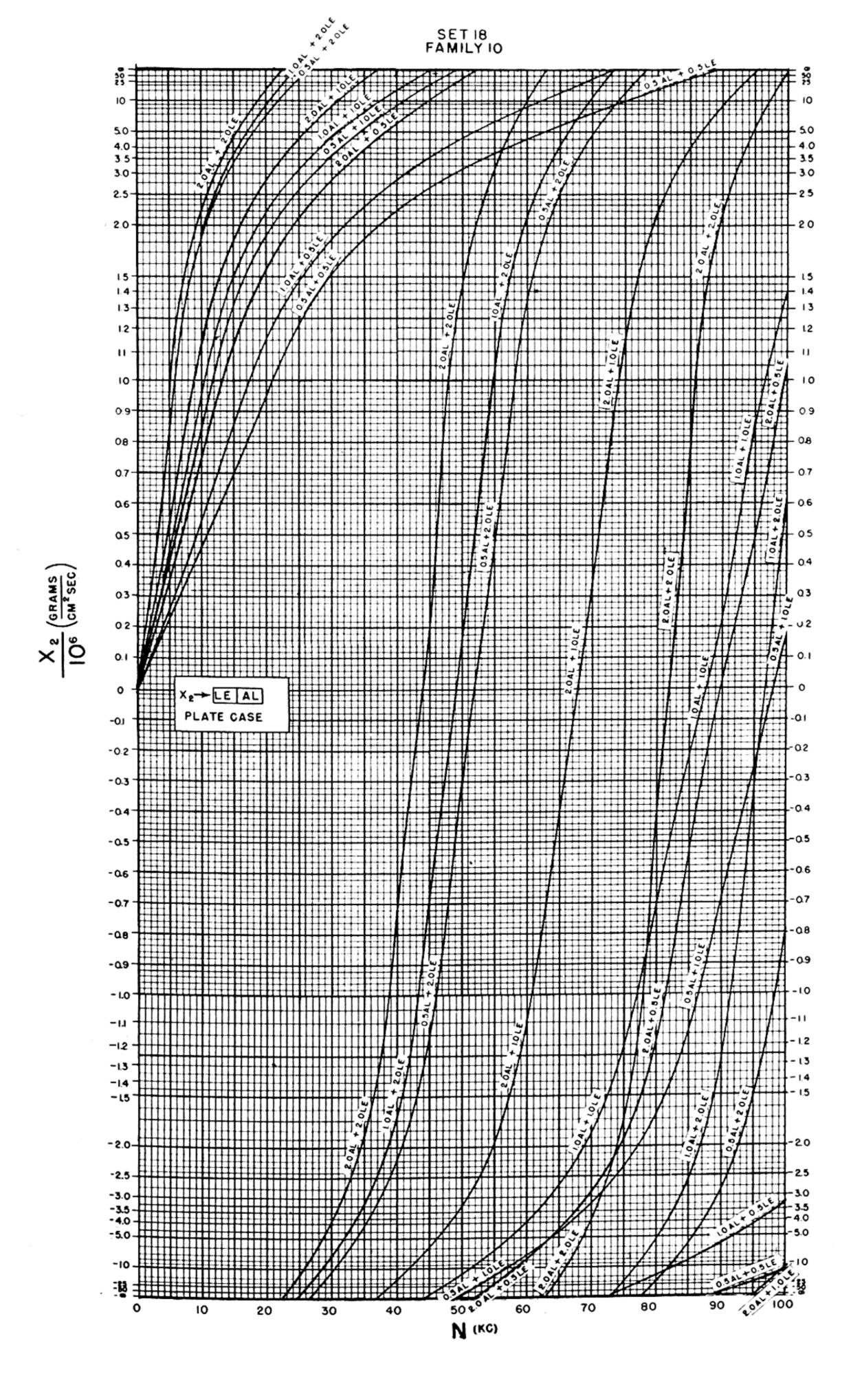


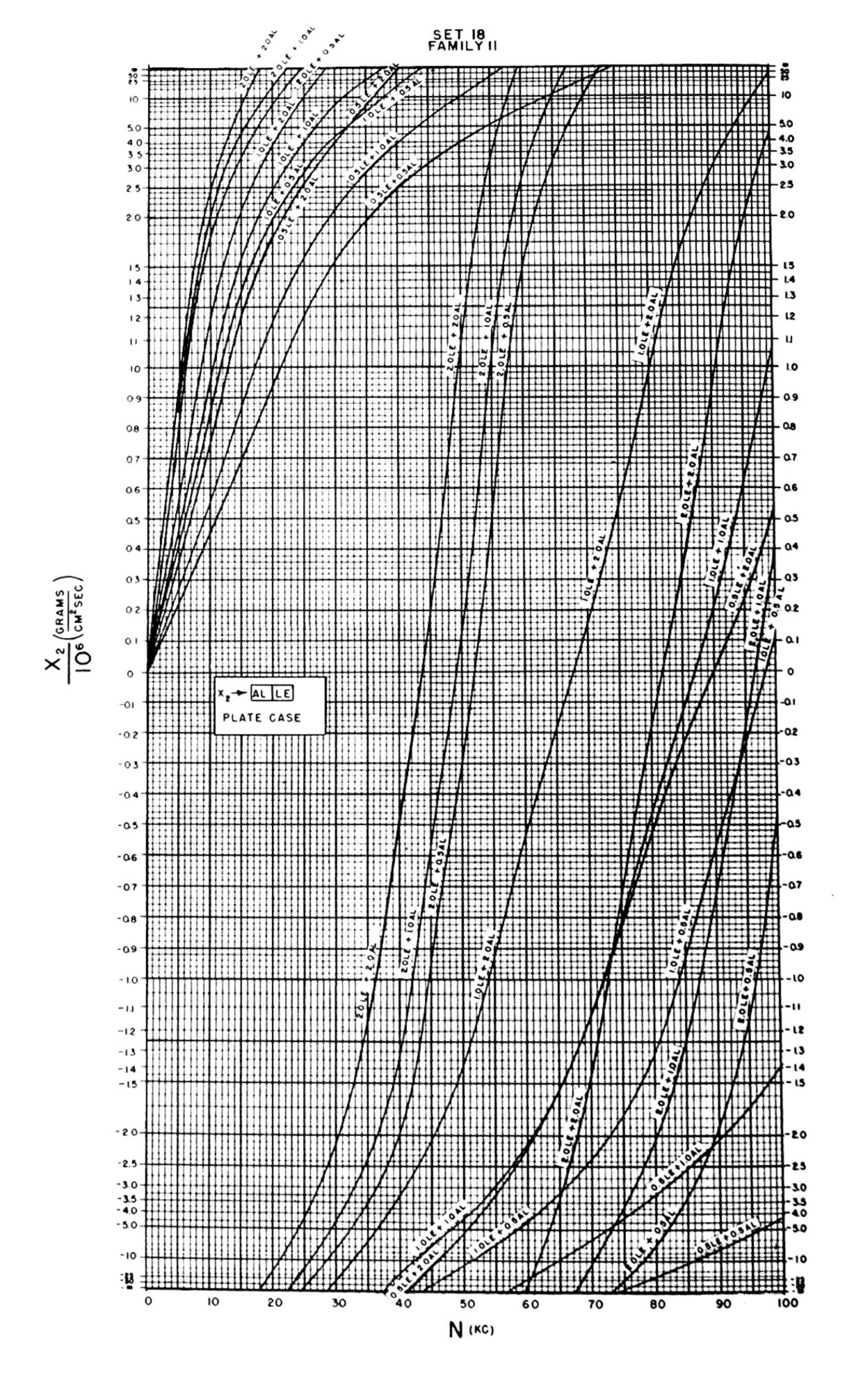


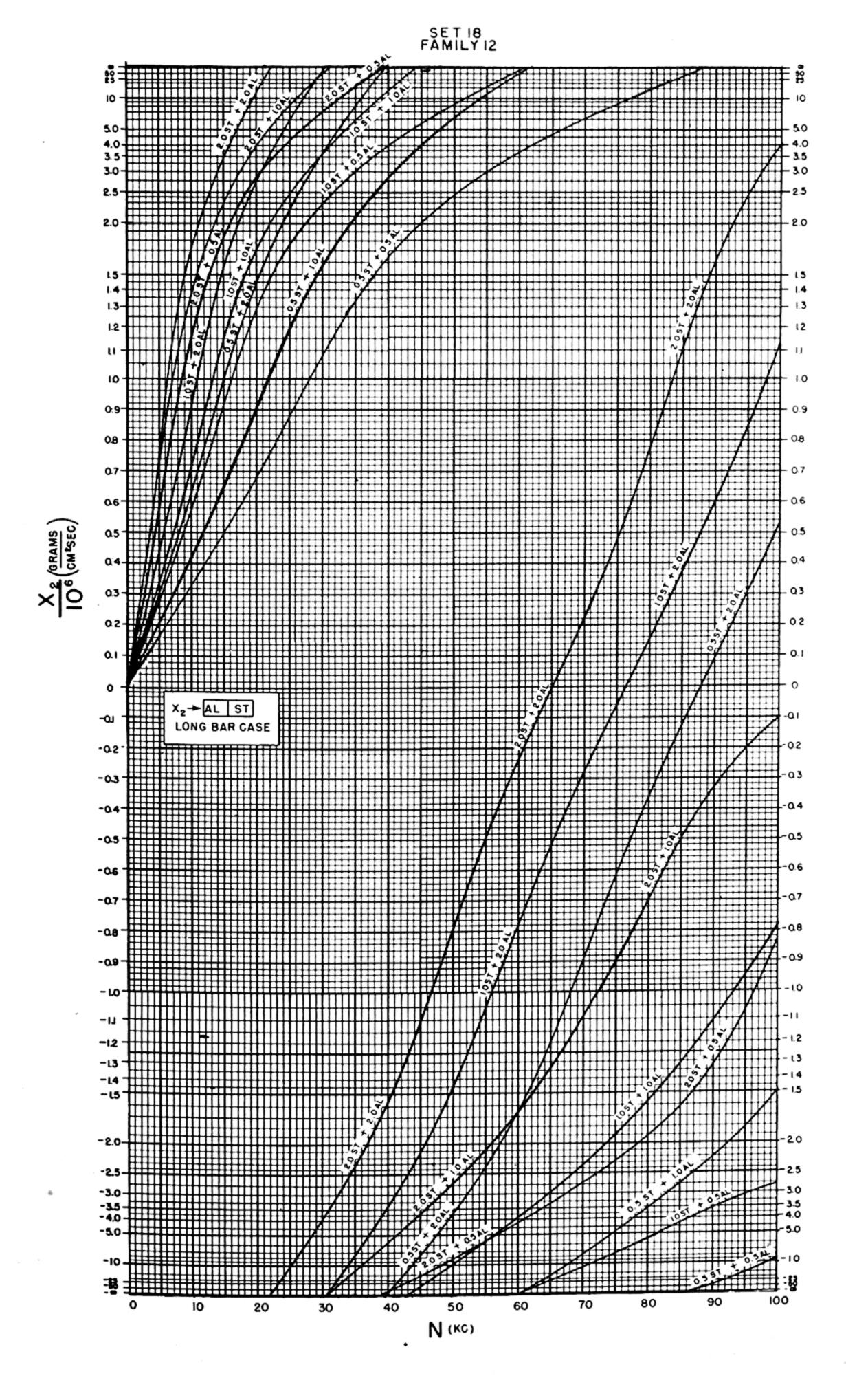


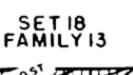


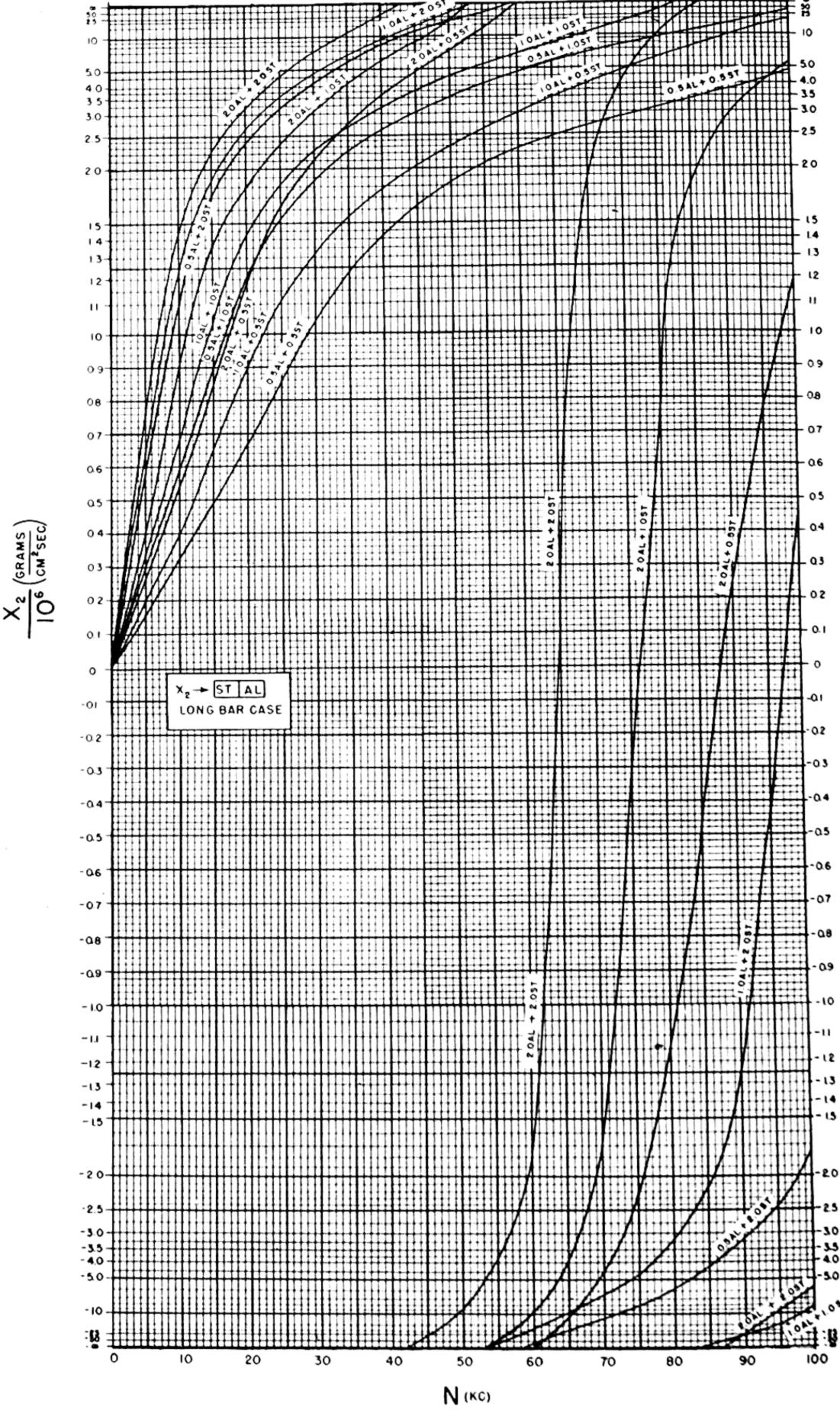


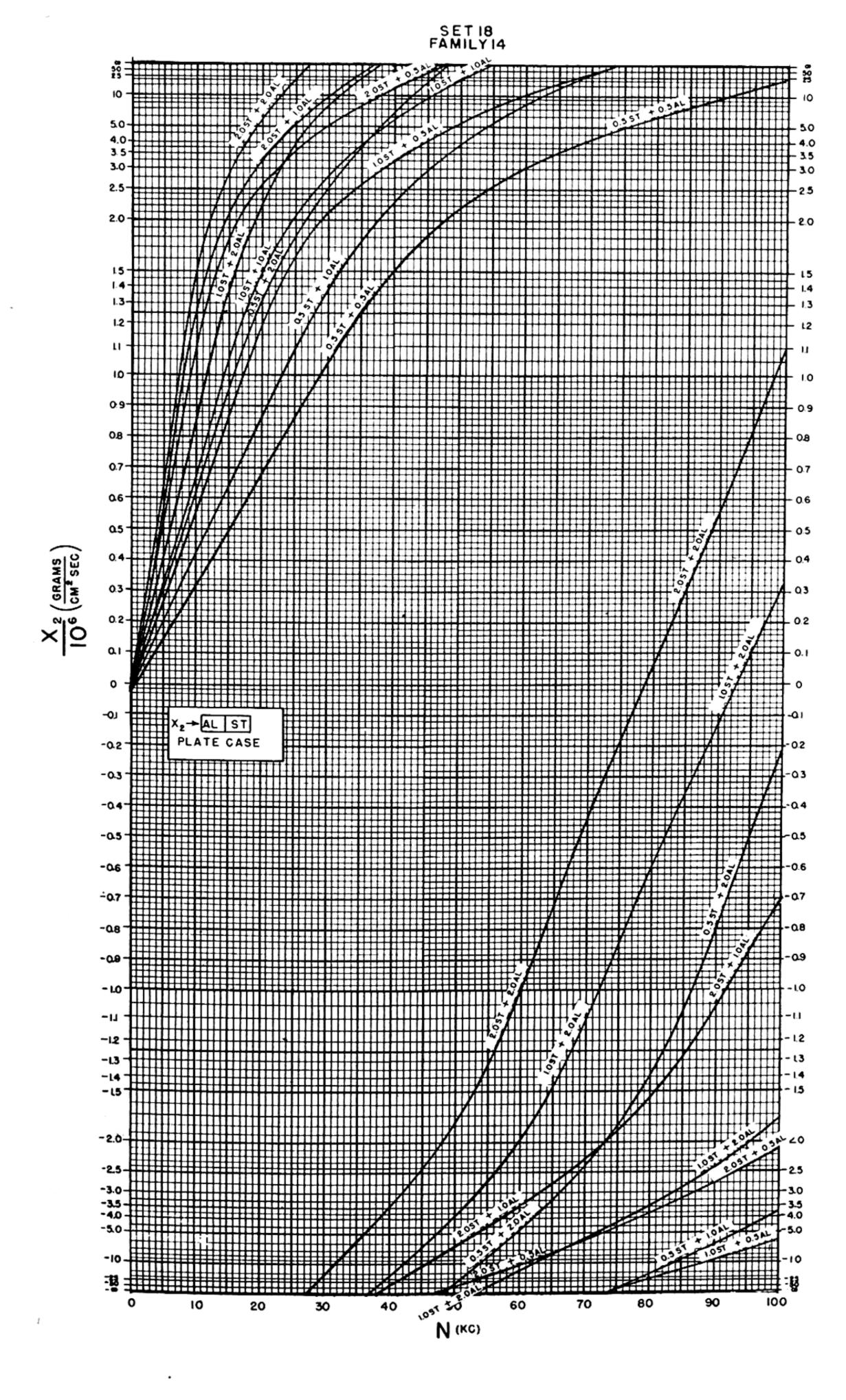


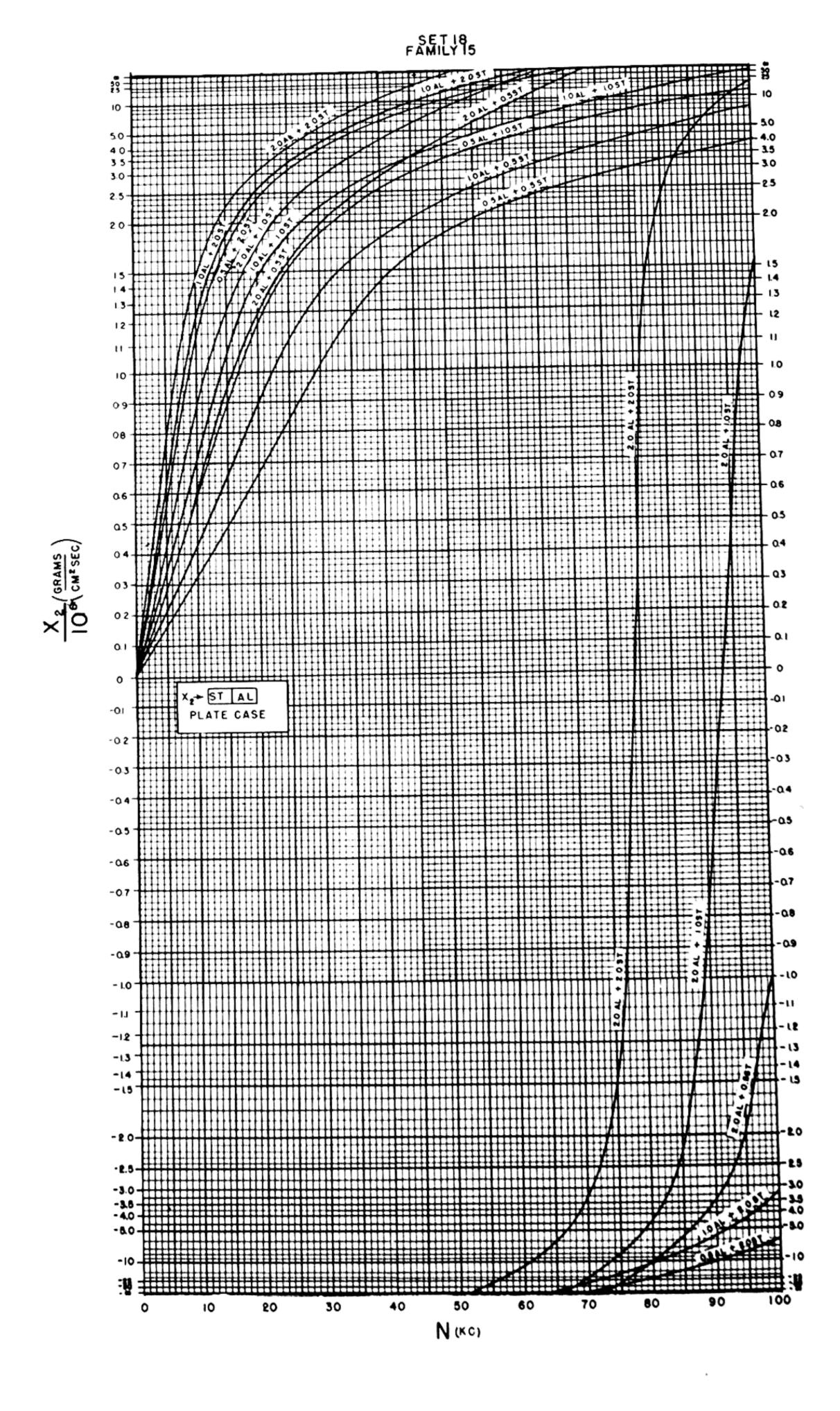




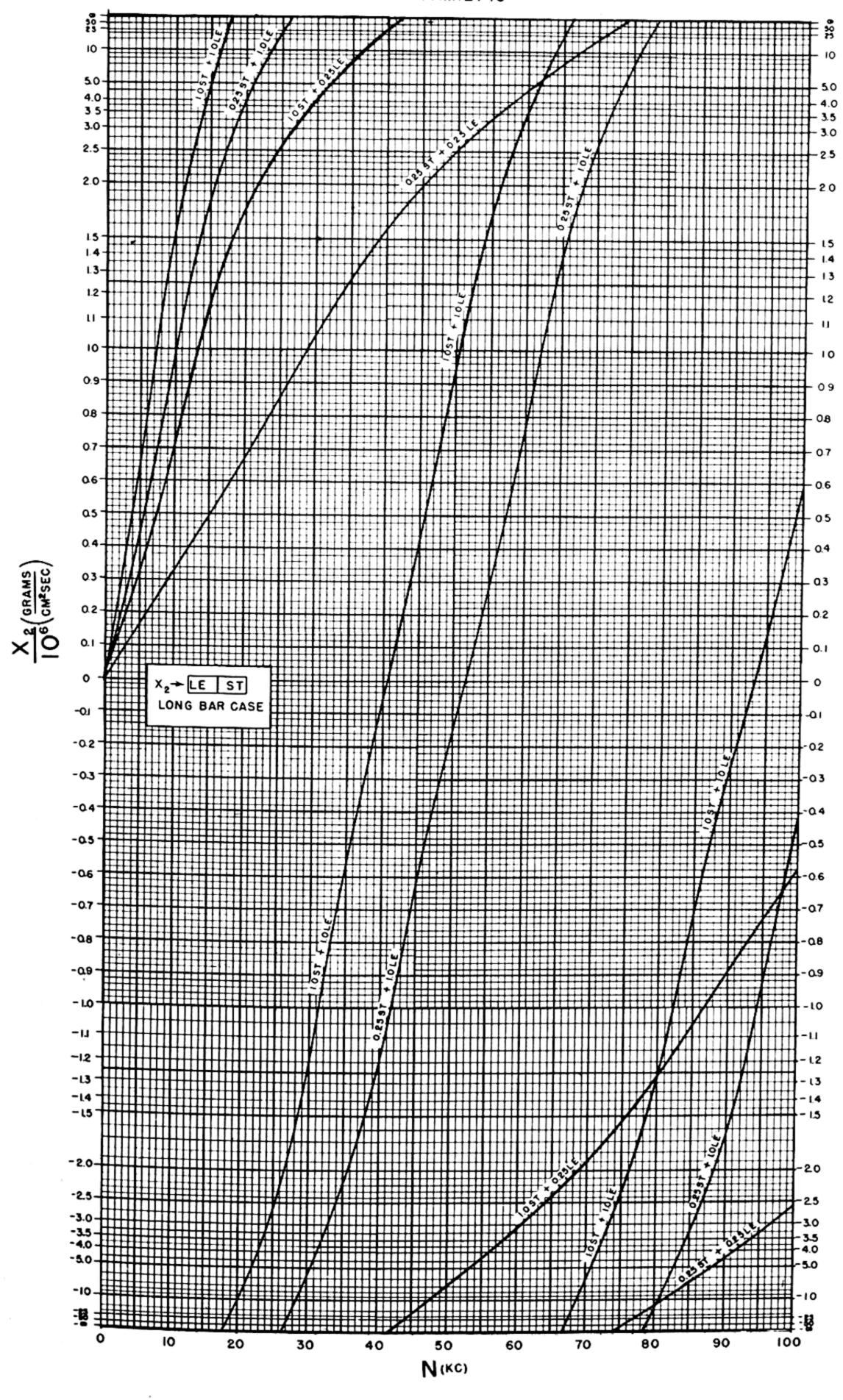


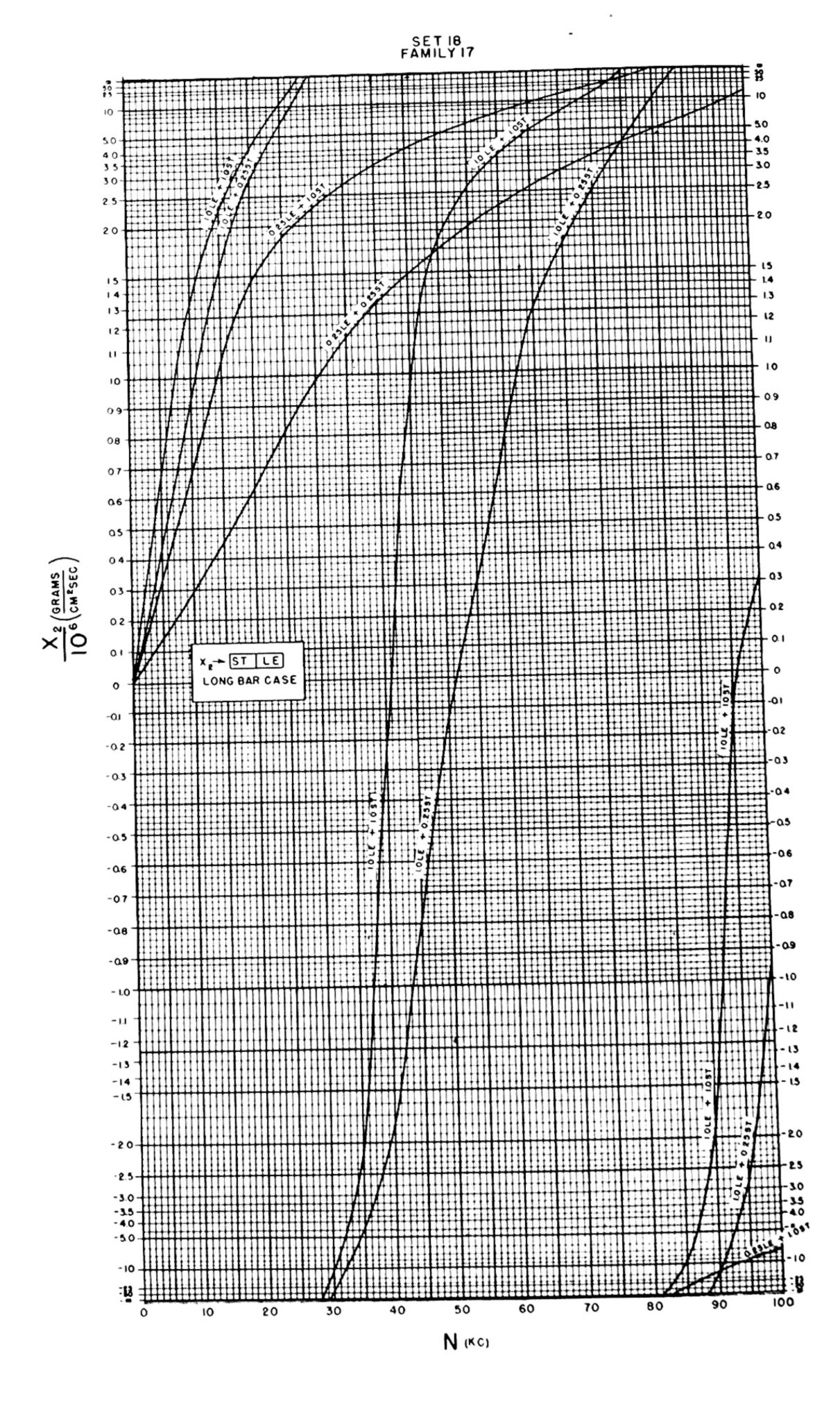


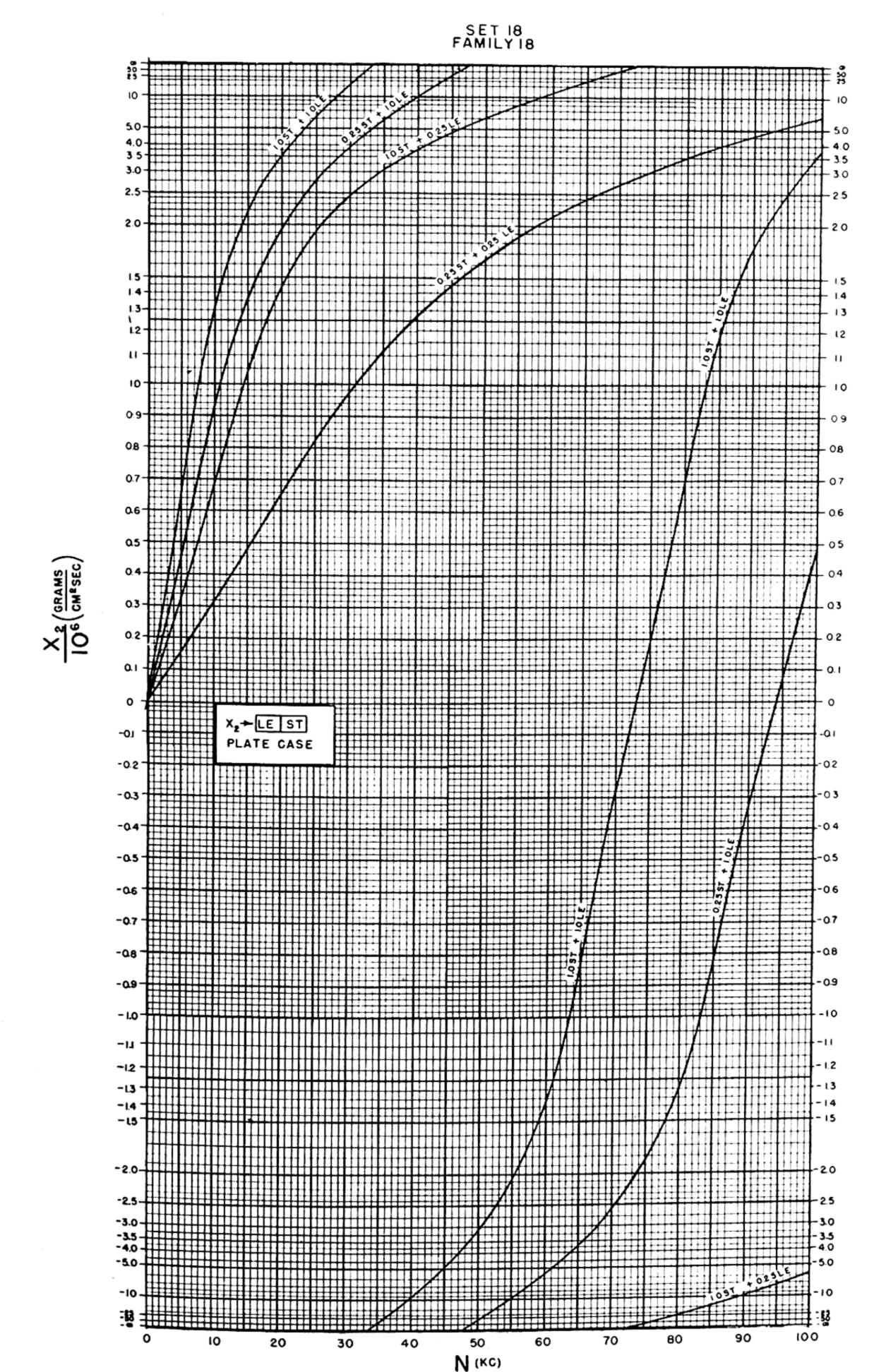




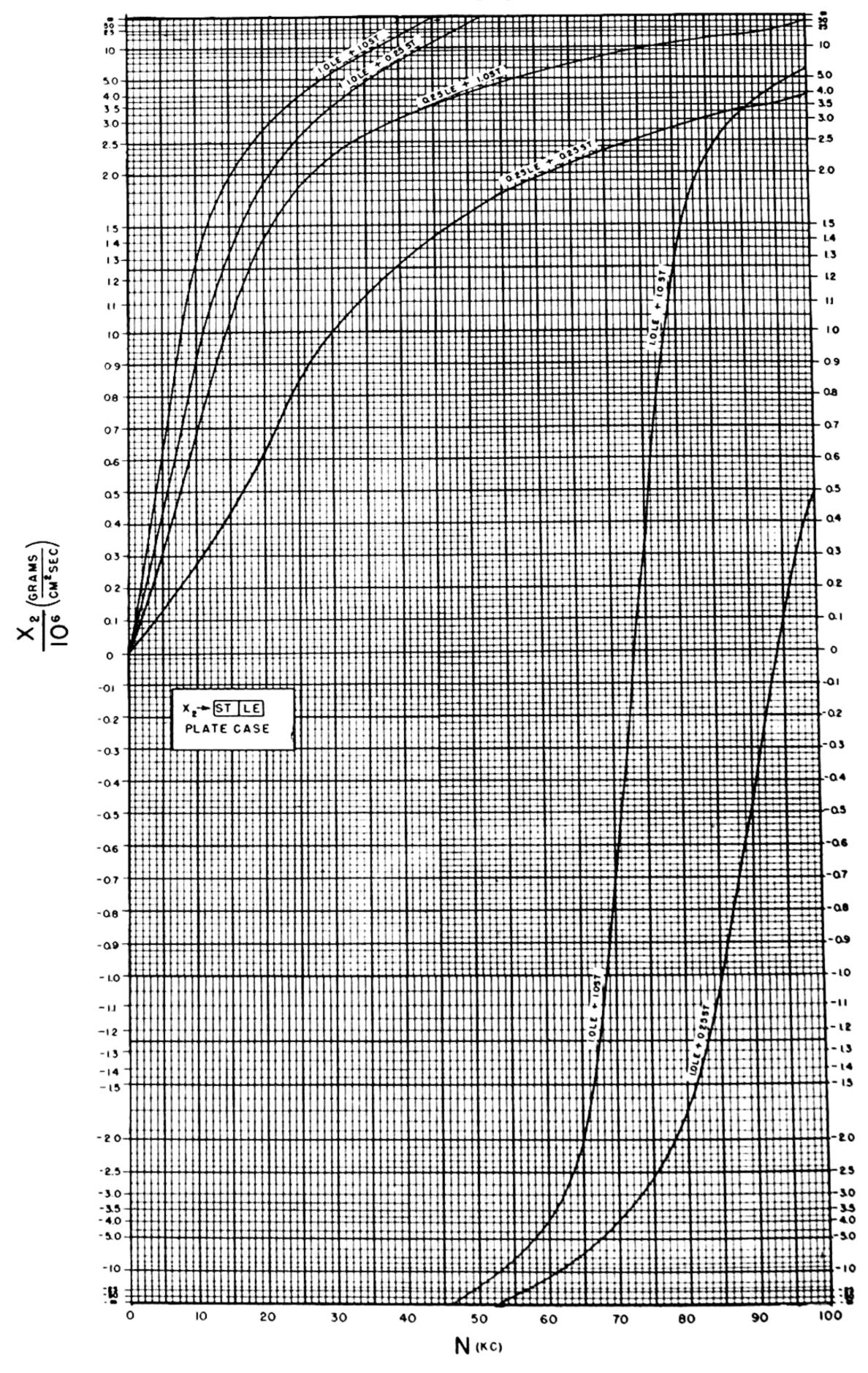




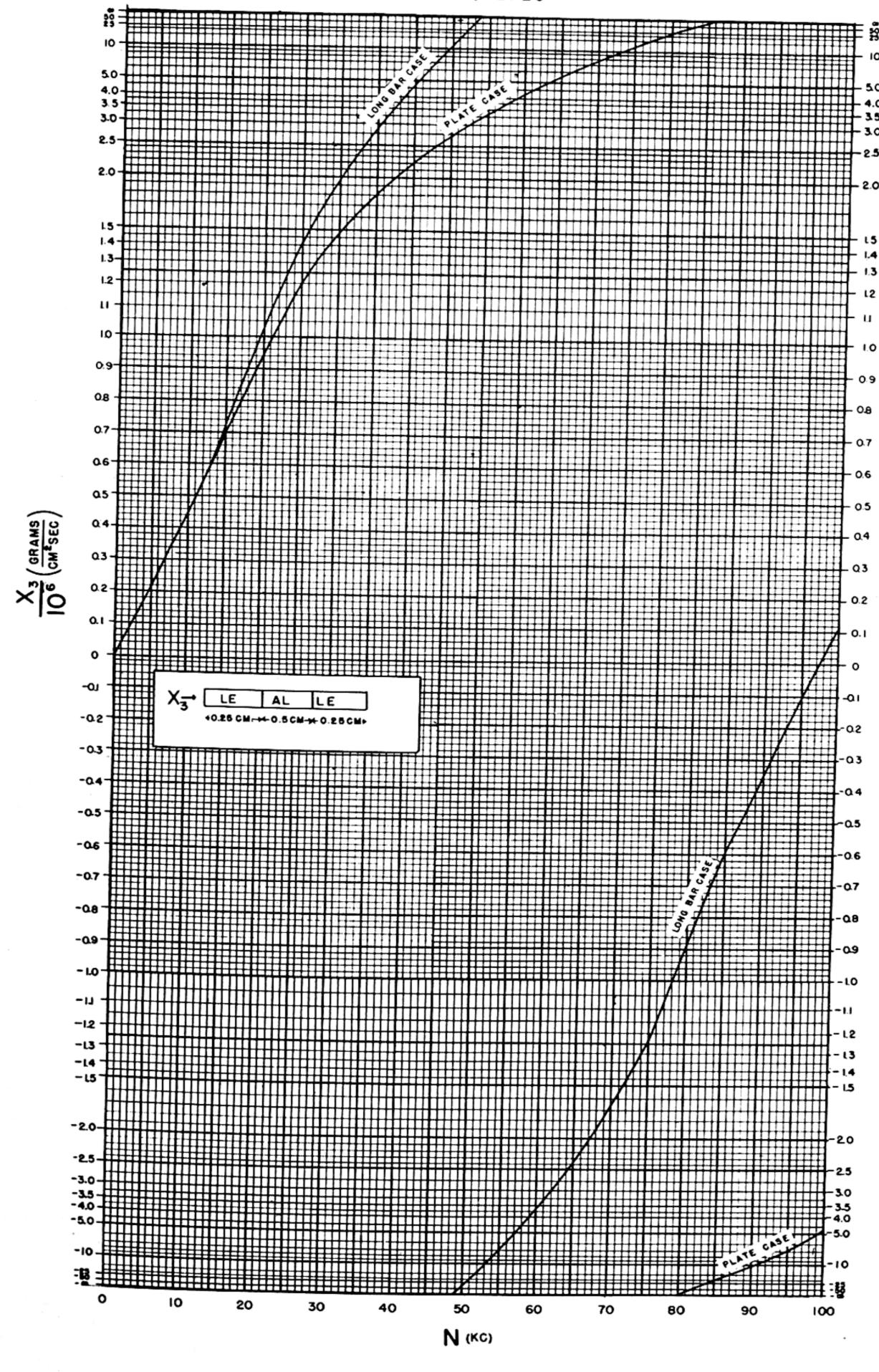












THE JAMMU & KASHMIR UNIVERSITY LIBRARY.

DATE LOANED

	Сору		
Accession No.			
	And the second second		
	9	:	
		• .	
	•		
		•	
		n. com anne	
\$ }			
	1		
:		The state of the s	
		9	

SECTION 1 FUNDAMENTAL EQUATIONS

The one-dimensional theory presented here is based on the fundamental piezoelectric equations. From these equations and the boundary conditions, expressions are derived which relate stress, particle velocity, current, and voltage for a vibrating crystal. Solutions are expressed in terms of the mechanical boundary conditions (particle velocity and force at one end of the crystal) and the electrical conditions (current and voltage).

The equations hold exactly for a crystal whose length is large compared to its width. In practice a ratio of 3 to 1 is satisfactory. For crystals with a smaller ratio, or for crystals with clamped sides, the equations give a good approximation if the elastic constant is considered to be dependent on the ratio of width to wavelength. A discussion of this approximation will be found in Part I, Section 1. The piezoelectric and dielectric constants may also vary somewhat with the dimensions but such variations are neglected in the present discussion.

The last three equations of this section serve as a basis for the theoretical development of the succeeding sections. Symbols represent total amplitude in all equations of this section. The last three equations, however, are equally valid when the symbols represent root-mean-square values, which are used throughout the remaining sections. Terms and symbols used in the development are defined in Appendix A. In this section a bar over the symbol designates a time dependent quantity; the same symbol without a bar designates a time independent quantity.

The fundamental equations governing the motion of a crystal* are:

(a)
$$\frac{\partial^2 \bar{\xi}}{\partial x^2} = \frac{1}{V_e^2} \frac{\partial^2 \bar{\xi}}{\partial t^2}$$
; $V_c = \sqrt{\frac{1}{\rho_c s}}$

(b)
$$\bar{i}_d = \frac{1}{4\pi} \frac{\partial \bar{E}_f}{\partial t} + \frac{\partial \bar{P}}{\partial t}$$
 (1)

(c)
$$-\overline{y} = s\overline{Y} + d\overline{E}_f$$
 or $-y = sY + dE_f$

(d)
$$\overline{P} = d\overline{Y} + K\overline{E}_f$$
 or $P = dY + KE_f$

where the symbols are defined as follows:

 ξ =particle displacement

 E_f =field intensity

P = polarization

 $i_d = \text{current density}$

Y = stress

y = strain

K=susceptibility

d = piezoelectric constant

s = elastic constant

 ρ_c = density of crystal

These expressions are now used to obtain relations between the particle velocity ξ , the force F, the current i, and the voltage E.

Time variation, for sinusoidal vibration, can be separated from the wave equation by letting $\bar{\xi} = \xi e^{j\omega t}$. The differential equation then takes the form:

$$\frac{d^2\xi}{dx^2} + \left(\frac{\omega}{V_c}\right)^2 \xi = 0,$$

Obviously $\dot{\xi}$ satisfies the same equation:

$$\frac{d^2\dot{\xi}}{dx^2} + \left(\frac{\omega}{V_c}\right)^2 \dot{\xi} = 0, \tag{2}$$

the solution of which is:

$$\dot{\xi} = A \cos\left(\frac{\omega}{V_{\epsilon}}\right) x + B \sin\left(\frac{\omega}{V_{\epsilon}}\right) x.$$
 (3)

At x=0, $\dot{\xi}=\dot{\xi}_1$. Therefore, $A=\dot{\xi}_1$.

To evaluate the other constant, B, we express the strain in terms of the displacement:

$$y = \frac{\partial \xi}{\partial x}$$
.

Since

$$\dot{\xi} = j\omega \xi$$

we have:

$$y = \frac{1}{j\omega} \frac{\partial \xi}{\partial x}$$

On differentiating (3) we obtain:

$$\frac{\partial \dot{\xi}}{\partial x} = -\left(\frac{\omega}{V_c}\right) \dot{\xi}_1 \sin\left(\frac{\omega}{V_c}\right) x + B\left(\frac{\omega}{V_c}\right) \cos\left(\frac{\omega}{V_c}\right) x. \tag{4}$$

If we now substitute $Y=F/l_{\ell w}$ and $E_f=E/l_{\ell w}$ into Eq. (1-c), it becomes:

$$-y = s \frac{F}{l l_w} + d \frac{E}{l_\iota}$$

^{*}See Mueller, Properties of Rochelle Salt, Phys. Rev. 57, 829 (1940). See also Appendix C.

Using $-y = -\frac{1}{i\omega} \frac{\partial \dot{\xi}}{\partial x}$ and substituting from (4), the following expression results:

$$\left[\frac{s}{l_{\ell}l_{\omega}}F + \frac{d}{l_{\ell}}E\right] = \frac{1}{j\omega}\left(\frac{\omega}{V_{\ell}}\right)\left[\xi_{1}\sin\left(\frac{\omega}{V_{\ell}}\right)x - B\cos\left(\frac{\omega}{V_{\ell}}\right)x\right]$$
(5)

At x=0, $F=F_1$. Therefore,

$$B = -jV_{\epsilon} \left[\frac{s}{l_{\ell}l_{\omega}} F_{1} + \frac{d}{l_{\ell}} E \right].$$

Substituting this expression for B into (3) we have:

$$\dot{\xi} = \dot{\xi}_1 \cos\left(\frac{\omega}{V_{\epsilon}}\right) x - jV_{\epsilon} \left[\frac{sF_1 + dl_w E}{l_{\ell}l_w}\right] \sin\left(\frac{\omega}{V_{\epsilon}}\right) x.$$

Introducing

$$V_{\epsilon} = \sqrt{1/\rho_{\epsilon}s}$$

gives:

$$\dot{\xi} = \dot{\xi}_1 \cos\left(\frac{\omega}{V_c}\right) x - \frac{j\left[F_1 + \frac{d}{s}l_w E\right]}{l_c l_w(\rho_c/s)^{\frac{1}{2}}} \sin\left(\frac{\omega}{V_c}\right) x. \tag{6}$$

Upon substituting the value of B into Eq. (5) and using $V_e = \sqrt{1/\rho_e s}$ we obtain:

$$\left[F + \frac{dl_w}{s}E\right] = \left[F_1 + \frac{dl_w}{s}E\right] \cos\left(\frac{\omega}{V_c}\right)x - j\dot{\xi}_1 l_w (\rho_c/s)^{\gamma_s} \sin\left(\frac{\omega}{V_c}\right)x. \tag{7}$$

Equations (6) and (7) express the force, F, and particle velocity, $\dot{\xi}$, in terms of the fundamental constants of the system, the boundary conditions, and the voltage. An expression involving the current is still needed. We proceed in the following manner.

The total current \overline{i} is given in terms of the current density \overline{i}_d as

$$\tilde{i} = \int_0^{L_t} \tilde{i}_d l_w dx = l_w \int_0^{L_t} \tilde{i}_d dx, \text{ or } i = l_w \int_0^{L_t} i_d dx.$$
(8)

From (1-b),

$$\bar{i}_d = \frac{1}{4\pi} \frac{\partial \bar{E}_f}{\partial t} + \frac{\partial \bar{P}}{\partial t}$$

Letting

$$\overline{E}_{f} = E_{f}e^{j\omega t},$$

$$\overline{P} = Pe^{j\omega t},$$
and $\overline{i}_{d} = i_{d}e^{j\omega t}$
we get: $i_{d} = j\omega \left[\frac{1}{4\pi}E_{f} + P\right]$.

After replacing Y by $\frac{F}{l J_n}$ and E_f by E/l_t in (1-d) we have

$$P = \frac{d}{l_{i}l_{w}}F + K\frac{E}{l_{i}}$$

Substituting this expression for P in the expression for i_d yields:

$$i_{d}=j\omega\left[\frac{1}{4\pi}\frac{E}{l_{i}}+\frac{d}{l_{i}l_{w}}F+K\frac{E}{l_{i}}\right].$$

Equation (8) now becomes:

$$i=j\omega l_{w}\int_{0}^{L_{t}}\left[\left(\frac{1}{4\pi}+K\right)\frac{E}{l_{t}}+\frac{d}{l_{t}l_{w}}F\right]dx. \tag{9}$$

Solving (7) for F, substituting the resulting expression in (9), and integrating, we obtain:

$$i = j\omega l_{w} \left\{ \left(\frac{1}{4\pi} + K \right) \frac{E}{l_{\iota}} L_{\iota} + \frac{d}{l_{\iota} l_{w}} \left[-\frac{dl_{w}}{s} E L_{\iota} + \frac{V_{\iota}}{\omega} \left(F_{1} + \frac{dl_{w}}{s} E \right) \sin \frac{\omega}{V_{\iota}} L_{\iota} + \frac{1}{s} \left(\frac{V_{\iota}}{s} \right)^{\kappa} \dot{\xi}_{1} \left(\frac{V_{\iota}}{s} \right) \left(\cos \frac{\omega}{V_{\iota}} L_{\iota} - 1 \right) \right] \right\}.$$

$$(10)$$

This expression can be simplified considerably by simple algebraic manipulation. Equation (6), when written for $\xi_2(x=L_c)$, becomes

$$\dot{\xi}_{2} = \dot{\xi}_{1} \cos\left(\frac{\omega}{V_{e}} L_{e}\right) - j \frac{\left[F_{1} + \frac{d}{s} l_{w} E\right]}{l_{e} l_{w}(\rho_{e}/s)^{\frac{1}{16}}} \sin\left(\frac{\omega}{V_{e}}\right) L_{e}.$$

Rewriting, we obtain:

$$\left[F_1 + \frac{d}{s}l_w E\right] \sin\left(\frac{\omega}{V_c} L_c\right) = -jl_d l_w \left(\frac{\rho_c}{s}\right)^{\aleph} \left[\dot{\xi}_1 \cos\left(\frac{\omega}{V_c} L_c\right) - \dot{\xi}_2\right]$$

Substituting this in (10), eliminating ρ_{ϵ} by means of $V_{\epsilon} = \sqrt{\frac{1}{\rho_{\epsilon}s}}$, and rearranging, we get:

$$i = j\omega l_{w} \left[\frac{EL_{c}}{l_{i}} \left(\frac{1}{4\pi} + K - \frac{d^{2}}{s} \right) + j\frac{d}{\omega s} (\dot{\xi}_{2} - \dot{\xi}_{1}) \right]$$

$$= j\frac{\omega El_{w}L_{c}}{4\pi l_{i}} \left(1 + 4\pi K - \frac{4\pi d^{2}}{s} \right) - \frac{dl_{w}}{s} (\dot{\xi}_{2} - \dot{\xi}_{1}).$$

$$C_{o} = \frac{l_{w}L_{c}}{4\pi l_{i}} \left(1 + 4\pi K - 4\pi \frac{d^{2}}{s} \right)$$

If we let

we can write the simplified form:

$$E(j\omega C_o) = i + \frac{dl_w}{s} (\dot{\xi}_2 - \dot{\xi}_1). \tag{11}$$

We now have the three equations (6), (7), and (11) which relate ξ , F, i, and E. These are used as a basis for the remainder of the theory given in Part II. We reprint them here for convenience in reference:

(a)
$$\dot{\xi} = \dot{\xi}_{1} \cos\left(\frac{\omega}{V_{c}}\right) x - j \frac{[F_{1} + \varphi E]}{Z_{0}} \sin\left(\frac{\omega}{V_{c}}\right) x$$
(b)
$$[F + \varphi E] = [F_{1} + \varphi E] \cos\left(\frac{\omega}{V_{c}}\right) x - j \dot{\xi}_{1} Z_{0} \sin\left(\frac{\omega}{V_{c}}\right) x$$
(c)
$$Ej\omega C_{0} = i + \varphi(\dot{\xi}_{2} - \dot{\xi}_{1})$$
(12)

where

$$Ej\omega C_0 = i + \varphi(\dot{\xi}_2 - \dot{\xi}_1)$$

$$V_c = \sqrt{\frac{1}{\rho_c s}}$$

$$\omega = 2\pi f$$

$$C_0 = \frac{l_w L_c}{4\pi l_i} \left(1 + 4\pi K - \frac{4\pi d^2}{s}\right)$$

$$\varphi = \frac{dl_w}{s}$$

$$Z_0 = l_i l_w \left(\frac{\rho_c}{s}\right)^{\frac{1}{2}} = l_i l_w \rho_c V_c$$

 C_0 is called the longitudinally clamped capacity throughout Part I. It is the capacity of the crystal when $\dot{\xi}_1 = \dot{\xi}_2 = 0$.

Equations (12) are sufficient for a complete determination of the crystal system. It should be noted that the three equations are unchanged when root-mean-square values are substituted for amplitudes. Root-mean-square values are to be understood in all equations in the remaining sections.

SECTION 2 ELECTRICAL INPUT IMPEDANCE

A general expression for the electrical input impedance of a crystal, terminated at each end in any acoustic impedance, is derived here from equations (12) in the preceding section. The expression is then simplified for the case of a crystal terminated in a purely resistive load (representing radiation) on one end, and a purely reactive load (representing the effect of the backing material) on the other end.

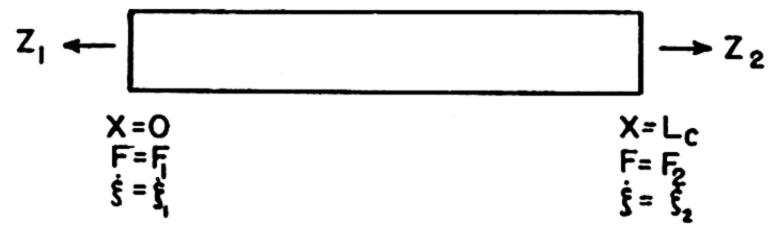


FIGURE 9.

In the following discussion, Z's with single numerical subscripts $(Z_1, Z_2, --)$ represent mechanical impedance; i. e., the ratio of force to velocity. Z's with the subscript a and a numerical subscript $(Z_{a1}, Z_{a2}, ---)$ represent acoustic impedance; i. e., the ratio of pressure to velocity. Definitions and conventions will be found in Appendix A.

At $x=L_{\epsilon}$, equations (12) become:

(a)
$$\dot{\xi}_{2} = \dot{\xi}_{1} \cos\left(\frac{\omega}{V_{c}}\right) L_{c} - j \frac{[F_{1} + \varphi E]}{Z_{0}} \sin\left(\frac{\omega}{V_{c}}\right) L_{c}$$

(b) $[F_{2} + \varphi E] = [F_{1} + \varphi E] \cos\left(\frac{\omega}{V_{c}}\right) L_{c} - j \dot{\xi}_{1} Z_{0} \sin\left(\frac{\omega}{V_{c}}\right) L_{c}$
(c) $j \omega C_{0} E = i + \varphi(\dot{\xi}_{2} - \dot{\xi}_{1})$ (13)

If we terminate the crystal in mechanical impedances Z_1 and Z_2 as shown in Fig. 9, then $F_1 = -Z_1 \dot{\xi}_1$ and $F_2 = Z_2 \dot{\xi}_2$. (Note the sign convention, page 170, in Appendix A.)

Substituting these relations in (13) and collecting terms:

(a)
$$\xi_{1} \left[\cos \frac{\omega L_{c}}{V_{c}} + j \frac{Z_{1}}{Z_{0}} \sin \frac{\omega L_{c}}{V_{c}} \right] - \xi_{2} = \frac{j\varphi E}{Z_{0}} \sin \frac{\omega L_{c}}{V_{c}}$$
(b)
$$\xi_{1} \left[Z_{1} \cos \frac{\omega L_{c}}{V_{c}} + j Z_{0} \sin \frac{\omega L_{c}}{V_{c}} \right] + Z_{2} \xi_{2} = -\varphi E \left(1 - \cos \frac{\omega L_{c}}{V_{c}} \right)$$
(c)
$$\varphi(\xi_{2} - \xi_{1}) + i = j\omega C_{c} E.$$
(14)

Letting

$$a_{11} = \cos \frac{\omega L}{V_e} + j \frac{Z_1}{Z_0} \sin \frac{\omega L_e}{V_e}$$

$$a_{12} = -1$$

$$a_{21} = Z_1 \cos \frac{\omega L_e}{V_e} + j Z_0 \sin \frac{\omega L_e}{V_e}$$

$$a_{22} = Z_2$$

$$b_1 = \frac{j}{Z_0} \sin \frac{\omega L_e}{V_e}$$

$$b_2 = \left(1 - \cos \frac{\omega L_e}{V_e}\right)$$

expressions (14) become:

(a)
$$\dot{\xi}_1 a_{11} + \dot{\xi}_2 a_{12} = b_1 \varphi E$$

(b) $\dot{\xi}_1 a_{21} + \dot{\xi}_2 a_{22} = -b_2 \varphi E$
(c) $\varphi(\dot{\xi}_2 - \dot{\xi}_1) + i = j\omega C_0 E$ (15)

Solving (a) and (b) for ξ_1 and ξ_2 ,

$$\dot{\xi}_{1} = \frac{\begin{vmatrix} b_{1}\varphi E & a_{12} \\ -b_{2}\varphi E & a_{22} \end{vmatrix}}{\begin{vmatrix} a_{11} & a_{12} \\ a_{21} & a_{22} \end{vmatrix}} = E\varphi\beta_{1} \quad \text{where } \beta_{1} = \frac{\begin{vmatrix} b_{1} & a_{12} \\ -b_{2} & a_{22} \end{vmatrix}}{\begin{vmatrix} a_{11} & a_{12} \\ a_{21} & a_{22} \end{vmatrix}}$$

$$\dot{\xi}_{2} = \frac{\begin{vmatrix} a_{11} & b_{1}\varphi E \\ a_{21} & -b_{2}\varphi E \end{vmatrix}}{\begin{vmatrix} a_{11} & a_{12} \\ a_{21} & a_{22} \end{vmatrix}} = E\varphi\beta_{2} \quad \text{where } \beta_{2} = \frac{\begin{vmatrix} a_{11} & b_{1} \\ a_{21} & -b_{2} \end{vmatrix}}{\begin{vmatrix} a_{11} & a_{12} \\ a_{21} & a_{22} \end{vmatrix}}$$

$$(16)$$

and substituting into (c) yields:

$$i=j\omega C_0E-\varphi^2E(\beta_2-\beta_1)$$

or

$$i = E[j\omega C_0 - \varphi^2(\beta_2 - \beta_1)].$$

Then the electrical input impedance Z_{ϵ} becomes:

$$Z_{\bullet} = \frac{E}{i} = \frac{1}{j\omega C_0 + \varphi^2(\beta_1 - \beta_2)}.$$
 (17)

This expression can be represented by either of the equivalent electrical circuits shown in Fig 10 (a) and 10 (b).

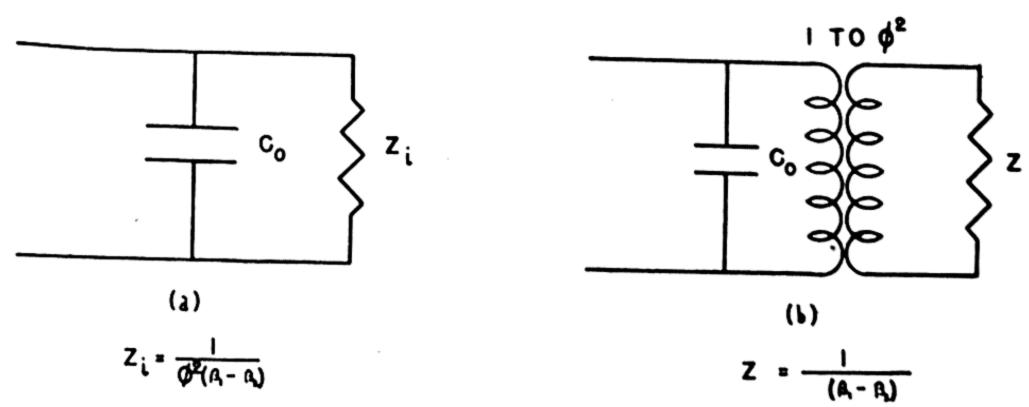


FIGURE 10.

We must now find an explicit form for the quantity $\frac{1}{\beta_1 - \beta_2}$.

Upon substituting for β_1 and β_2 their values in terms of the Z's and after some algebraic manipulation, we obtain:

$$\frac{1}{\beta_1 - \beta_2} = Z_0 \frac{\left[\left(\frac{Z_1}{Z_0} + \frac{Z_2}{Z_0} \right) \cos \gamma_\epsilon + j \sin \gamma_\epsilon \left(\frac{Z_1}{Z_0} \cdot \frac{Z_2}{Z_0} + 1 \right) \right]}{-2(1 - \cos \gamma_\epsilon) + j \sin \gamma_\epsilon \left(\frac{Z_1}{Z_0} + \frac{Z_2}{Z_0} \right)}$$
(18)

where
$$\gamma_c = \frac{\omega L_c}{V_c}$$
.

If the load on one end of the crystal is purely reactive (backing material) and that on the other end is purely resistive (radiation), we can write:

$$\frac{Z_1}{Z_0} = jG_{1\epsilon}U_1$$

$$\frac{Z_2}{Z_0} = G_{2c}$$

where $G_{1c}U_1$ is then the impedance (per unit area) presented to the crystal by the backing material divided by the characteristic impedance of the crystal, and G_{2c} is the characteristic impedance of the medium into which the crystal is radiating divided by the characteristic impedance of the crystal.

Now, letting

$$R_0 + jX_0 = \frac{1}{\beta_1 - \beta_2}$$

and making use of (18), we find:

(a)
$$\frac{R_0}{Z_0} = G_{2c} \frac{[(G_{1c}U_1 \sin \gamma_c) + (1 - \cos \gamma_c)]^2}{\sin^2 \gamma_c + [(G_{1c}U_1 \sin \gamma_c) + 2(1 - \cos \gamma_c)]^2}$$

(b)
$$\frac{X_0}{Z_0} = \frac{G_{2e}^2(G_{1e}U_1\sin\gamma_e - \cos\gamma_e)\sin\gamma_e - (G_{1e}U_1\cos\gamma_e + \sin\gamma_e)[(G_{1e}U_1\sin\gamma_e) + 2(1 - \cos\gamma_e)]}{G_{2e}^2\sin^2\gamma_e + [(G_{1e}U_1\sin\gamma_e) + 2(1 - \cos\gamma_e)]^2}.$$
 (19)

In terms of these two quantities we can write an expression for the motional electrical impedance Z_i defined in Fig. 10-a:

$$Z_1 = \frac{Z_0}{\varphi^2} \left(\frac{R_0}{Z_0} + j \frac{X_0}{Z_0} \right)$$

 Z_i is combined with the impedance of the purely electrical part of the system (C_o , coupling circuits, etc.) to give the total electrical input impedance.

Curves which may be used to evaluate R_0/Z_0 and X_0/Z_0 for any particular projector are given in Part I, Section 5. A discussion of the electrical input impedance is also given in that section.

THE JAMMU & KASHMIR UNIVERSITY LIBRARY.

VolCopyAccession No.					
	The state of the s				
		e			

SECTION 3 ACOUSTIC INPUT IMPEDANCE

Acoustic input impedance is of importance in the calculation of the sensitivity of such equipment as projectors and accelerometers as well as in the determination of the interaction between the crystal system and the system under measurement. In this section we obtain an expression for the acoustic input impedance into one end of the crystal for any reactive termination on the other end, and for various electrical loading conditions.

We begin with the fundamental equations (12) on page 153 and let $x=L_c$.

 $\frac{\omega L_c}{V_c}$, the equations are:

(a)
$$\xi_{2} = \xi_{1} \cos \gamma_{e} - j \frac{[F_{1} + \varphi E]}{Z_{0}} \sin \gamma_{e}$$

(b) $[F_{2} + \varphi E] = [F_{1} + \varphi E] \cos \gamma_{e} - j \xi_{1} \sin \gamma_{e}$
(c) $j \omega C_{0} E = i + \varphi (\xi_{2} - \xi_{1})$. (20)

Now, let the electrical terminating impedance R_i+jX_i be designated by jZ_i . This form is used for convenience in combining with the $j\omega C_0E$ term of (20-c), also because the termination is usually largely reactive in the cases of interest. Then, from the definition of jZ_i

$$Z_i = X_i - jR_i$$

Since $i = -\frac{E}{iZ}$ *, (20-c) becomes:

$$j\left[\omega C_0-\frac{1}{Z_t}\right]E=\varphi(\dot{\xi}_2-\dot{\xi}_1);$$

solving for E,

$$E = \frac{\varphi(\xi_2 - \dot{\xi}_1)}{j \left[\omega C_0 - \frac{1}{Z_t}\right]}.$$
 (21)

If the termination is a pure condenser, $\frac{1}{Z_1} = -\omega C_0$, and

$$E = \frac{\varphi(\dot{\xi}_2 - \dot{\xi}_1)}{j\omega(C_0 + C)}.$$

With equation (21) for the voltage E in terms of the electrical load and the particle velocities, we can proceed with the derivation by substituting this expression into (20-a) and (20-b). We note, also, that since one end of the crystal is terminated in a mechanical impedance Z_1 (backing material), we have $F_1 = -Z_1 \xi_1^*$.

Equations (20-a) and (20-b) then become:

(a)
$$\dot{\xi}_{2} = \dot{\xi}_{1} \cos \gamma_{c} - j \frac{\left[-Z_{1}\dot{\xi}_{1} + \frac{\varphi^{2}(\dot{\xi}_{2} - \dot{\xi}_{1})}{j(\omega C_{o} - 1/Z_{i})} \right]}{Z_{0}} \sin \gamma_{c}$$

(b) $\left[F_{2} + \frac{\varphi^{2}(\dot{\xi}_{2} - \dot{\xi}_{1})}{j(\omega C_{o} - \frac{1}{Z_{i}})} \right] = \left[-Z_{1}\dot{\xi}_{1} + \frac{\varphi^{2}(\xi_{2} - \dot{\xi}_{1})}{j(\omega C_{o} - \frac{1}{Z_{i}})} \right] \cos \gamma_{c} - j\dot{\xi}_{1}Z_{o} \sin \gamma_{c}.$

(22)

^{*}See Appendix A, page 170.

Solving (22-a) for ξ_1 , we find:

$$\dot{\xi}_{1} = \dot{\xi}_{2} \frac{1 + \frac{\varphi^{2}}{(\omega C_{0} - 1/Z_{t})} \frac{\sin \gamma_{\epsilon}}{Z_{0}}}{\cos \gamma_{\epsilon} + \left[jZ_{1} + \frac{\varphi^{2}}{(\omega C_{0} - 1/Z_{t})} \right] \frac{\sin \gamma_{\epsilon}}{Z_{0}}}$$
(23)

Equation (22-b) may be rearranged to give:

$$F_2 + \xi_2 \left[\frac{\varphi^2 (1 - \cos \gamma_c)}{j(\omega C_0 - 1/Z_i)} \right] = \xi_1 \left[\frac{\varphi^2 (1 - \cos \gamma_c)}{j(\omega C_0 - 1/Z_i)} - Z_1 \cos \gamma_c - jZ_0 \sin \gamma_c \right]$$
(24)

Substituting expression (23) for $\dot{\xi}_1$ into (24) and simplifying, we obtain the following form:

$$-\frac{F_2}{\xi_2 Z_0} = \frac{\frac{\varphi^2}{(\omega C_0 - 1/Z_1)Z_0} [2j(1 - \cos \gamma_\epsilon) + (Z_1/Z_0) \sin \gamma_\epsilon] + (Z_1/Z_0) \cos \gamma_\epsilon + j \sin \gamma_\epsilon}{\cos \gamma_\epsilon + \frac{\varphi^2}{(\omega C_0 - 1/Z_1)Z_0} \sin \gamma_\epsilon + j(Z_1/Z_0) \sin \gamma_\epsilon}$$
(25)

Letting

$$\theta = \frac{\varphi^2}{(\omega C_0 - 1/Z_i)Z}$$

and remembering that $Z_1/Z_0=jG_{1c}U_1$ expression (25) becomes:

$$-\frac{F_2}{\xi_2 Z_0} = j \frac{\theta[2(1-\cos\gamma_\epsilon) + G_{1\epsilon}U_1\sin\gamma_\epsilon] + G_{1\epsilon}U_1\cos\gamma_\epsilon + \sin\gamma_\epsilon}{\cos\gamma_\epsilon - G_{1\epsilon}U_1\sin\gamma_\epsilon + \theta\sin\gamma_\epsilon}.$$
 (26)

Now, $-\frac{F_2}{\xi_2}$ is the mechanical input impedance Z_M . See Fig. 11.

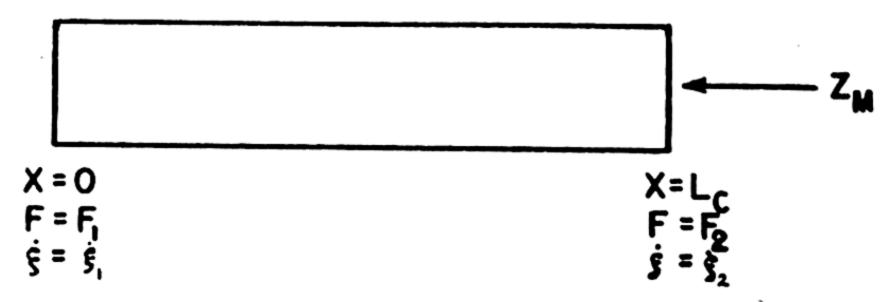


FIGURE 11.

Writing (26) in terms of tan γ_c , we obtain:

$$\frac{Z_M}{Z_o} = j \frac{\theta[2 \tan (\gamma_c/2) + G_{1c}U_1] + [1 + G_{1c}U_{1c}/\tan \gamma_c]}{\theta + [(1/\tan \gamma_c) - G_{1c}U_1]}.$$
(27)

Curves of Z_M/Z_0 are given in Section 6, Part I. The first family of curves shows the variation of Z_M/Z_0 for $|\theta| \le 0.1$. The remaining curves of the set are plotted for real values of θ between +0.1 and +40.0. This is the case of essentially capacitative loading; i.e., $\frac{1}{Z_1} = -\omega C$, so that $\theta = \frac{\varphi^2}{(\omega C_0 - 1/Z_1)Z_0}$ becomes $\theta = \frac{\varphi^2}{\omega(C_0 + C)Z_0}$.

The acoustic input impedance Z_a is given by:

$$Z_a = \frac{Z_M}{Z_o} \rho_c V_c$$
, since $\frac{Z_M}{Z_o} = \frac{Z_a A_c}{\rho_c V_c A_c} = \frac{Z_a}{\rho_c V_c}$.

 $A_{\epsilon}=l_{\omega}l_{\epsilon}$ is the area of the end of the crystal.

The acoustic input impedance is used in calculating sensitivity (explained in Section 6 of Part I) or in determining the effect of the measuring device on the system under measurement.

THE JAMMU & KASHMIR UNIVERSITY LIBRARY.

Vol Accession N	(in	OOK No.	

SECTION 4 RESONANT FREQUENCY

Since it is often necessary to obtain quickly estimates of the resonant frequencies of a given crystal system, a method for their determination which does not involve plotting a reactance curve is very convenient. This section presents such a method for an undamped system.

The effect of damping (from radiation or other causes) on resonant frequency is very small in many systems; consequently we can approximate the resonant frequencies very closely by calculations which ignore the damping. For systems in which damping causes a large shift in resonant frequencies, a reactance curve should be plotted and the resonant frequencies determined from its zeros.

The electrical resonant frequencies are taken to be the frequencies at which the reactive component of the motional impedance goes to zero. Frequencies at which the reactive component has a minimum not zero are designated as secondary resonances. For example see Sections 2, 4 and 5 of Part I. Secondary resonances are described in Section 5, Part I.

When there is no damping,

 $Z_1/Z_0 = jG_{1e}U_1$

and

 $Z_2/Z_0 = jG_{2c}U_2;$

that is, the loads are purely reactive.

It should be noted that the general curves of Part I apply to systems with a reactive load on one end and a resistive load on the other end. When damping is ignored in such a system the resistive load on the radiating face of the crystal is taken equal to zero. It is desirable, however, to have resonant frequency curves for systems which have a reactive load on each end.

Formulas giving the resonant frequencies for undamped systems will be derived by considering the zeros of the function

$$\frac{1}{\beta_1 - \beta_2} \tag{28}$$

where β_1 and β_2 are defined on page 156 of Part II. The condition for resonance then reduces to

$$j[G_{1c}U_1 + G_{2c}U_2] \cos \gamma_c + j \sin \gamma_c [-G_{1c}U_1G_{2c}U_2 + 1] = 0.$$
 (29)

when the substitutions $Z_1/Z_o=jG_{1e}U_1$ and $Z_2/Z_o=jG_{2e}U_2$ are made.

Equation (29) can be rearranged into

$$\tan \gamma_{c} = -\frac{G_{1c}U_{1} + G_{2c}U_{2}}{1 - G_{1c}U_{1}G_{2c}U_{2}}.$$
(30)

If we let

$$\tan \alpha_1 = G_{1e}U_1$$

and

$$\tan \alpha_2 = G_{2c}U_2$$

equation (30) becomes:

$$\tan \gamma_{c} = -\tan (\alpha_{1} + \alpha_{2}),$$

or

$$\gamma_c + \alpha_1 + \alpha_2 = n\pi$$
 $n = 1, 2, 3 - - -$ (31)

and n = 1 gives the condition for first resonance, n = 2 the condition for second resonance, etc.

For the particular case of a single backing material on each end

$$\alpha_{1} = \tan^{-1} G_{1\epsilon} U_{1} = \tan^{-1} \left[\frac{\rho_{m1} V_{m1}}{\rho_{\epsilon} V_{\epsilon}} \tan \frac{\omega l_{m1}}{V_{m1}} \right],$$

$$\alpha_{2} = \tan^{-1} G_{2\epsilon} U_{2} = \tan^{-1} \left[\frac{\rho_{m2} V_{m2}}{\rho_{\epsilon} V_{\epsilon}} \tan \frac{\omega l_{m2}}{V_{m2}} \right].$$
(32)

When the crystal has a reactive load on only one end and there is no damping, equation (31) reduces to

$$\gamma_c + \alpha_1 = n\pi \tag{33}$$

Curves and a complete discussion of resonant frequency are given in Section 2, Part I.

SECTION 5 SENSITIVITY

Formulas for the calculation of sensitivity are presented in this section with the method of derivation indicated, but no mathematical details are given. The formulas express sensitivity in terms of either voltage output per unit pressure applied, or voltage output per unit velocity applied. It is obvious that sensitivity is important in the design of devices to be used for measuring pressure or velocity, such as projectors used as hydrophones and accelerometers.

When the crystal device disturbs the system to be measured (i. e., when the system being measured does not act like a pure force generator or a pure velocity generator to the measuring instrument), the pressure or velocity presented to the crystal system can be obtained by determining the interaction between the systems. A necessary quantity in this evaluation is the acoustic input impedance into the crystal system.

Steps in the calculation of sensitivity are as follows:

- 1. A voltage E_0 is calculated from the known pressure or velocity at the crystal face. This voltage E_0 is not a measurable quantity but is the voltage which would be measured at the electrodes of the crystals under no external load and no longitudinally clamped capacity.
- 2. The electrical input impedance Z_{ϵ} is calculated for the proper termination on the driven face of the crystal. When pressure is used as the working variable the proper termination is zero acoustic impedance, $G_{2\epsilon}=0$; when velocity is used as the working variable the proper termination is infinite acoustic impedance, $G_{2\epsilon}=\infty$.
- 3. The voltage across the given electrical load (the sensitivity) is calculated by placing a generator in series with the electrical input impedance and the given load. The E. M. F. of the generator is the E_0 obtained in Step 1 and the electrical input impedance is the Z_0 calculated in Step 2.

If the interaction mentioned in the first paragraph is not negligible, the pressure or velocity at the crystal face is determined from a knowledge of the acoustic input impedance into the crystal system. See Section 3, Part II and Section 6, Part I. For plane projectors several wave lengths in diameter, the pressure at the interface in terms of the free field sound pressure is given approximately by

$$\left| \frac{P_2}{P_+} \right| = \frac{2Z_a/\rho_2 V_2}{\sqrt{1 + (Z_a/\rho_2 V_2)^2}} \tag{34}$$

where Z_a is the acoustic input impedance, $\rho_2 V_2$ is the characteristic impedance of the medium driving the projector, P_2 is the pressure at the face, and P_+ is the free field sound pressure. This formula follows directly from the definition of the acoustic impedance. The force per crystal, F_2 , is then the pressure, P_2 , times the cross-sectional area of the crystal, $l_1 l_w$: $F_2 = P_2 l_1 l_w$

The velocity at the crystal face in terms of the free field pressure is given approximately by

$$\left| \frac{\dot{\xi}_2}{P_+} \right| = \left(\frac{2}{\rho_2 V_2} \right) \frac{(\rho_2 V_2 / Z_a)}{\sqrt{1 + (\rho_2 V_2 / Z_a)^2}} \tag{35}$$

where the symbols are the same as those defined for equation (34).

The voltage E_o can be obtained from the fundamental relations (12), Part II, Section 1, by letting $x=L_c$, i=0, and $C_o=0$. When this is done the following relations for the voltage E_o result:

$$-\varphi \frac{E_0}{F_2} = \frac{\tan \frac{\gamma_c}{2} + G_{1c}U_1}{2 \tan \frac{\gamma_c}{2} + G_{1c}U_1} \quad \text{or} \quad \frac{1}{\delta} \frac{E}{P_2} = -\frac{\tan \frac{\gamma_c}{2} + G_{1c}U_1}{2 \tan \frac{\gamma_c}{2} + G_{1c}U_1}$$
(36)

or
$$\frac{E_0}{\overline{F_2}} = -\left(\frac{1}{\varphi}\right) \frac{\tan\frac{\gamma_c}{2} + G_{1c}U_1}{2\tan\frac{\gamma_c}{2} + G_{1c}U_1}$$
 where
$$\delta = \frac{l_c}{d/e},$$

$$\frac{\varphi}{Z_0} \frac{E_0}{\xi_2} = j(\tan \frac{\gamma_c}{2} + G_{1c}U_1)$$
or
$$\frac{E_0}{\xi_2} = j \frac{Z_0}{\varphi} (\tan \frac{\gamma_c}{2} + G_{1c}U_1)$$
(37)

Expression (36) gives E_0 in terms of the force, F_2 , and (37) gives E_0 in terms of the velocity, ξ_2 . Expression (36) is plotted in Section 6, Part I.

The input electrical impedance for the crystal terminated in zero impedance $(G_{2e}=0)$ can be obtained by multiplying the X_0/Z_0 obtained from the curves on page 87, Section 5, Part I by Z_0/φ^2 ; i.e., $Z_* = j \frac{Z_0}{z^2} \frac{X_0}{Z}$.

The electrical impedance for infinite terminating impedance ($G_{2c} = \infty$) can be obtained from

$$Z_{\bullet} = j \frac{Z_0}{\varphi^2} \left(\frac{G_{1c} U_1 - \cot \gamma_c}{Z_c} \right). \tag{38}$$

The zero termination should be used in conjunction with expression (36) and the infinite termination with (37).

The expression for the voltage across a given electrical load (see Fig. 12 for illustration) is:



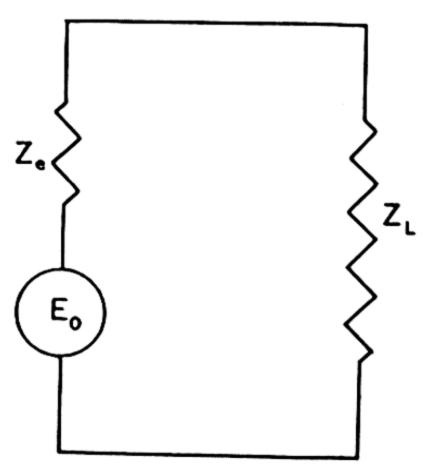


FIGURE 12.

If (39) is combined with (36) and (37), we obtain the two following convenient forms for sensitivity in terms of force and velocity:

$$\frac{E_L}{F_2} = \left(\frac{Z_L}{Z_e + Z_L}\right) \left(-\frac{1}{\varphi}\right) \left(\frac{\tan\frac{\gamma_e}{2} + G_{1e}U_1}{2\tan\frac{\gamma_e}{2} + G_{1e}U_1}\right) \tag{40}$$

$$\frac{E_{L}}{\xi_{2}} = \left(\frac{Z_{L}}{Z_{\iota} + Z_{L}}\right) \left(j \frac{Z_{0}}{\varphi}\right) \left(\tan \frac{\gamma_{c}}{2} + G_{1c}U_{1}\right)$$
(41)

A discussion of sensitivity characteristics is given in Section 6, of Part I.

SECTION 6 STRESS

In this section an expression is developed for obtaining the stress distribution in the crystal, a quantity which is useful in evaluating the losses in the glue joints which fasten the crystal to the remainder of the system. The particle velocity, useful in determining the position of mounting, can be obtained in a similar fashion.

The fundamental equation determining the stress is equation (12-b) of Section 1, Part II, repeated here for convenience:

$$(F+\varphi E) = (F_1 + \varphi E) \cos \frac{\omega}{V_c} x - j \xi_1 Z_0 \sin \frac{\omega}{V_c} x. \tag{42}$$

Now

$$\dot{\xi}_1 = \varphi E \beta_1 \\
\dot{\xi}_2 = \varphi E \beta_2$$

 β_1 and β_2 are defined on page 156. From (16)

$$E = \frac{\dot{\xi}_1}{\varphi \beta_1} = -\frac{F_1}{Z_1 \varphi \beta_1}.$$

On substituting into expression (42) we obtain:

$$\left(F - \frac{F_1}{Z_1 \beta_1}\right) = \left(F_1 - \frac{F_1}{Z_1 \beta_1}\right) \cos \frac{\omega}{V_c} x + jF_1 \left(\frac{Z_0}{Z_1}\right) \sin \frac{\omega}{V_c} x. \tag{43}$$

Let
$$\mu + j\nu = \frac{1}{\beta_1 Z_1}$$
; $\gamma_c = \frac{\omega L_c}{V_c}$

then (43) becomes, after rearranging:

$$\frac{F}{F_1} = (\mu + j\nu) + (1 - \mu - j\nu) \cos\left(\gamma_c \frac{x}{L_c}\right) + j\frac{Z_0}{Z_1} \sin\left(\gamma_c \frac{x}{L_c}\right). \tag{44}$$

For a crystal with a reactive load on one end and resistive load on the other, $Z_0/Z_1 = -j/(G_{1c}U_1)$ from definition of $G_{1c}U_1$. When this is substituted into (44) the absolute value of F/F_1 is given by:

$$\left|\frac{F}{F_1}\right| = \left[\left[\mu\left(1 - \cos\gamma_c \frac{x}{L_c}\right) + \cos\gamma_c \frac{x}{L_c} + \frac{1}{G_{1c}U_1}\sin\gamma_c \frac{x}{L_c}\right]^2 + \left[\nu\left(1 - \cos\gamma_c \frac{x}{L_c}\right)\right]^2\right]^{\frac{1}{2}}$$
(45)

Explicit formulas [for μ and ν can readily be obtained. After some algebraic manipulation the following forms result:

(a)
$$\mu = -\frac{1}{G_{1c}U_{1}} \frac{(1 - \cos \gamma_{c}) + (G_{2c})^{2} \sin \gamma_{c} \cos \gamma_{c}}{(1 - \cos \gamma_{c})^{2} + (G_{2c})^{2} \sin^{2}\gamma_{c}} + \frac{\cos \gamma_{c}(1 - \cos \gamma_{c}) - (G_{2c})^{2} \sin^{2}\gamma_{c}}{(1 - \cos \gamma_{c})^{2} + (G_{2c})^{2} \sin^{2}\gamma_{c}}$$
(b)
$$\nu = \frac{G_{2c}}{G_{1c}U_{1}} \frac{\cos \gamma_{c}(1 - \cos \gamma_{c}) - \sin \gamma_{c}}{(1 - \cos \gamma_{c})^{2} + (G_{2c})^{2} \sin^{2}\gamma_{c}} + \frac{G_{2c} \sin \gamma_{c}}{(1 - \cos \gamma_{c})^{2} + (G_{2c})^{2} \sin^{2}\gamma_{c}}$$
(46)

When $x=L_c$, expression (45) gives the ratio of the force at the driven end, F_2 , to the force at the glue joint, F_1 . This ratio is plotted in Section 7, Part I for various values of $G_{1c}U_1$ and for the particular value of G_{2c} corresponding to the ratio of the characteristic impedances of water and ADP crystals.

THE JAMMU & KASHMIR UNIVERSITY LIBRARY.

VolAccession	C	_	
		,	
	17 - 1 de marie		
- 10 miles	120 /20		

APPENDIX A SYMBOLS, DEFINITIONS, CONVENTIONS

A table of symbols and their definitions is given on the following pages. The various conventions used are also included in this Appendix.

SYMBOLS AND DEFINITIONS

A subscript c refers to the crystals; subscripts 1 and 2 refer to the left and right ends of the crystal respectively.

ROMAN	SYMBOLS	ROMAN	SYMBOLS
SYMBOL	DEFINITION	SYMBOL	
\boldsymbol{A}	Area	P	DEFINITION
C_{0}	Longitudinally clamped capacity	$\stackrel{1}{P_1}$	Pressure
,	of crystal	$\stackrel{r}{P_2}$	Pressure at end 1 of crystal
C_{oT}	Longitudinally clamped capacity	$\stackrel{\scriptstyle \scriptstyle P_+}{P_+}$	Pressure at end 2 of crystal
	of crystal combination	R+jX	Free field sound pressure Reciprocal of $G+jB$
d	Piezoelectric constant	J21	
E	Voltage	R_{0}	ex. $R_{TM} + jB_{TM} = 1/(G_{TM} + jB_{TM})$ R_0/φ^2 is the resistive component of
E_f	Field strength	V	the motional impedance.
F	Force	$R_{\mathfrak{c}}+jX_{\mathfrak{c}}$	Motional impedance per crystal
$egin{array}{c} F_1 \ F_2 \end{array}$	Force at left end of crystal	8	Elastic constant (reciprocal of
I'2	Force at right end of crystal		Young's Modulus for a long
G_{1c}	$\rho_I V_I A_I$		bar)
-10	$\frac{\rho_t V_t}{\rho_c V_c} \frac{A_t}{A_c}$	V	Sound velocity
$(G_{1c}U_1)$	Input impedance present 1 1	V_c	Sound velocity in crystal
•	Input impedance presented by the backing material to the	$V_{\mathfrak{c}}$	Sound velocity in ith backing
,	crystal (per unit area of crystal),		material
	divided by the characteristic	V_{w}	Sound velocity in driven medium
	impedance of the crystal	X_{o}	X_0/φ^2 is the reactive component of
G_i+jB_i	Motional admittance non annual		the motional impedance (per
$G_{TM}+jB_{TM}$	Total motional admittance of crys-	77	crystal)
<i>a</i>	tal combination	X_t	Acoustic reactance
$G_{rc}+jB_{rc}$	Admittance of cable (coupling	Y	Stress
	network) plus admittance of	Z_0	Strain
	longitudinally clamped capacity		$l_{\it t}l_{\it w} ho_{\it c}V_{\it c}$
a i in	or crystal combination	Z_{M}	Mechanical impedance, the ratio
$G_T + jB_T$	Total admittance	7	of force to velocity
G_{2c}		Z_{Mi}	Mechanical impedance of the ith material
~26	$\frac{\rho_2 V_2}{\rho_c V_c} \frac{A_2}{A_c}$	Z_a	Acoustic impedance, the mechan-
i		24	ical impedance per unit area or
i i _e	Current		ratio of pressure to velocity,
K	Current density	Z_{ai}	Acoustic impedance of the ith
L	Dielectric susceptibility Length	~a:	material
L_{ϵ}	Length of crystal	Z_{\bullet} .	Electrical impedance
L_t	Length of the att 1	Z_i	Motional impedance per crystal
l.,	Length of the ith backing material Width of crystal		(contribution of the mechanical
l_t	Distance between the		motion of the crystal to the
	Distance between electroded faces		electrical impedance)
P	(thickness of crystal) Polarization	$\jmath Z_\iota$	Electrical terminating impedance
	- ~14112# (10I)	Z_{T}	Total electrical input impedance

SYMBOLS AND DEFINITIONS

GREEK SYMBOLS

GREEK SYMBOLS

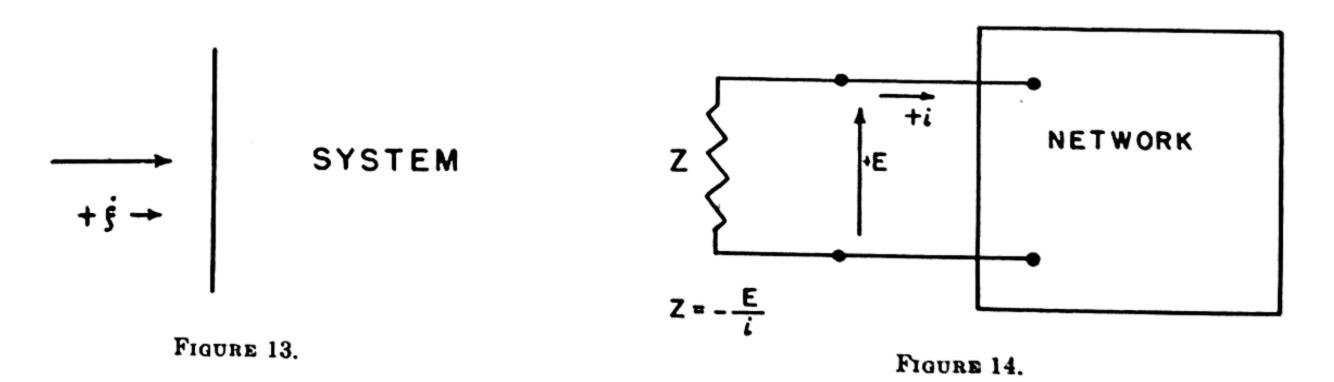
			2 0 2 0
SYMBOL	DEFINITION	SYMBOL	DEFINITION
α_1	$\alpha_1 = \tan^{-1}G_{1c}U_1$		l,
α_2	$\alpha_2 = \tan^{-1}G_{2e}U_2$	δ	$(\overline{d/s})$
~	ωL	$\boldsymbol{ heta}$	$arphi^2/\omega C_0 Z_0$
,	\overline{V}	arphi	$(d/s)l_w$
γ.	$\frac{\omega L_c}{V_c}$ refers to crystal	ρ	Density; ρ_c density of crystal; ρ_w density of driven medium
~ .	$\frac{\omega L_i}{\omega}$ refers to ith backing meterial	ξ	Particle displacement
γ,	$\frac{\omega L_i}{V_i}$ refers to ith backing material. γ_m is sometimes used in referring	ξı	Particle velocity at end 1 of crystal
	to the backing material of single backing material systems.	ξ2	Particle velocity at end 2 of crystal

The following conventions have been used throughout the report.

(1) Time variation is indicated by the positive exponential; i.e., $e^{+j\omega t}$. The acoustic impedance of short lengths of material is then a positive reactance.

(2) In evaluating the input mechanical impedance into a system, the positive direction of the velocity is taken in the direction of the normal directed into the system. See Fig. 13. This convention determines the signs of the impedances terminating the crystal when the positive direction of the particle velocity is taken in the direction of the positive x-axis. The ratio of force to velocity at the left end is negative, and the ratio of force to velocity at the right end is positive.

(3) The convention for electrical terminations is illustrated by Figure 14.



APPENDIX B Units and tables of constants

In this section the various fundamental constants are tabulated for convenience. Two systems of units are used, namely the unrationalized MKS and cgs systems. This will cause no confusion since the units of each quantity and the system used are explicitly stated in all tables and in any place where a new quantity is introduced.

The MKS system is almost always used in calculations leading up to the final result. The final result is in some cases expressed in cgs units since it is realized that the magnitudes of quantities expressed in MKS units may appear unfamiliar. A conversion table for transforming from the MKS to the cgs system or vice versa is included in this appendix.

PHYSICAL CONSTANTS OF VARIOUS MATERIALS

Material	Density	Longitudinal bar velocity	Bulk (plate) velocity	Characteristic impedance (bar velocity)	Characteristic impedance (plate velocity)
Aluminum. Brass. Copper. Lead. Nickel. Steel. Glass. Magnesium.	2. 65 8. 5 8. 93 11. 4 8. 9 7. 8 2. 5–5. 9 1. 74	cm/sec. 5. 25(10) ⁵ 3. 42 3. 58 1. 25 4. 76 5. 05 4.5-5. 5	cm/sec. 6. 4(10) ⁵ 4. 25 4. 6 2. 4 5. 6 6. 1 4. 9-5. 8	g/(cm² sec.) 1. 39(10) ⁶ 2. 90 3. 20 1. 42 4. 23 3. 93 1. 12-3. 2 0. 85	g/(cm² sec.) 1. 70(10) ⁶ 3. 61 4. 11 2. 73 4. 98 4. 98 4. 76 1. 2-3. 4
Water (fresh)Alcohol (ethyl)	1. 00 1. 00 0. 79 13. 6 0. 70	1. 43(10) ⁵ 1. 51 1. 44 1. 46 0. 75		1. 43(10) ⁵ 1. 55 1. 14 19. 8 0. 53	
Air.	1. 29(10)-3	0.331(10)		43	

HYSICAL CONSTANTS OF VARIOUS CRYSTALS

Plated crystal	Density p	Longitudinal bar	Bulk (plate) velocity	Characteristic impedance ρV (bar, velocity)	Dielectric constant, K	Piezoelectric in- teraction con- stant, d/s
	g/cm³	cm/sec. (10)-5	cm/sec. (10)-5	$\frac{g}{cm^2sec}(10)^{-5}$	Basis K(air)=1	sq. meler
ADP (NH,H2PO,) 45° Z-	1.80	3. 28	4.92	5. 90	14. 0	0. 493
Rochalla salt 150 V						
trocucine sail 40 I -cut	1. 77	2.47		4.37	10.0	0.307
Rochelle salt 45° X-cut	1.77	See graph		See graph	See graph	See graph
		Page 10.		page 40.	page 61.	page 60.
Quartz X-cut	2.65	5. 44	5.72	14.4	4.5	0.176
Tourmoline 7						0.170
	2. 98–3. 2		7. 54		5 - 6	0. 333

CONVERSION OF PRACTICAL (GIORGI) UNITS

ELECTROSTATIC, ELECTROMAGNETIC OR GAUSSIAN UNITS

Practical	_	Electrostatic	Electromagnetic	Gaussian
1 meter	11	100 centimeters	100 centimeters	100 centimeters
1 kilogram	11	1,000 grams	1,000 grams	1,000 grams
1 second	11	1 second	1 second	1 second
1 newton	11	(10) ⁵ dynes	(10) ⁶ dynes	(10) ⁵ dynes
1 joule	11	(10) ⁷ ergs	(10) ⁷ ergs	(10) ⁷ ergs
1 coulomb	11	3(10)9 esu of charge	0.1 emu of cherge	3(10) Gaussian units of charge
l ampere	11	3(10)° esu of current	0.1 emu of current	3(10) Gaussian units of current
1 volt	11	$\%(10)^{-2}$ esu of potential	(10) ⁸ emu of potential	1/2(10)-2 Gaussian units of po- tential
1 farad	11	0.9(10)12 esu of capacitance	(10)-9 emu of capacitance	0.9(10)12 Gaussian units of capacitance
1 ohm		1.1(10) ⁻¹² esu of resistance	· (10)° emu of resistance	1.1(10) ⁻¹² Gaussian units of resistance
1 henry	II	1.1(10)-12 esu of inductance	(10)° emu of inductance	(10)° Gaussian units of inductance

DB. CHART

Voltage ratio	Power ratio	d. b	Voltage ratio	Power
1. 00	1. 00	0. 0	1. 00	1. 00
0. 94	0. 89	0. 5	1.06	1. 12
0.89	0. 79	1.0	1. 12	1. 26
0.84	0.71	1.5	1. 19	1. 41
0.79	0. 63	2.0	1. 26	1. 59
0.75	0. 56	2. 5	1. 33	1. 78
0.71	0. 50	3. 0	1.41	2.00
0.67	0.45	3. 5	1. 50	2. 24
0. 63	0.40	4. 0	1. 59	2. 51
0.60	0. 35	4. 5	1. 68	2. 82
0. 56	0. 32	5. 0	1. 78	3. 16
0. 53	0. 28	5. 5	1. 88	3. 55
0. 50	0. 25	6. 0	2.00	3. 98
0. 47	0. 22	6. 5	2. 11	4.47
0.45	0. 20	7. 0	2. 24	5. 01
0.42	0. 18	7. 5	2. 37	5. 62
0.40	0. 16	8. 0	2. 51	6. 31
0.38	0. 14	8. 5	2. 66	7. 08
0. 35	0. 13	9. 0	2. 82	7. 94
0. 33	0. 11	9. 5	2. 99	8. 91
0. 32	0. 10	10.0	3. 16	10.0
0. 30	0. 089	10. 5	3. 35	11. 2
0. 28	0.079	11.0	3. 55	12. 6
0. 27	0.071	11. 5	3. 76	14. 1
0. 25	0.063	12. 0	3. 98	15. 9
0. 24	0. 056	12. 5	4. 22	17. 8
0. 22	0. 050	13. 0	4. 47	20.0
0. 21	0.045	13. 5	4. 73	22.4
0. 20	0.040	14.0	5. 01	25. 1
0. 19	0. 035	14. 5	5. 31	28. 2
0. 18	0.032	15. 0	5. 62	31.6
0. 17	0.028	15. 5	5. 96	35. 8
0. 16	0.025	16. 0	6. 31	39. 8
0. 15	0.022	16. 5	6. 68	44.7
0. 14	0. 020	17. 0	7. 08	50. 1
0. 13	0. 018	17. 5	7. 50	56. 2
0. 13	0. 016	18. 0	7. 94	63. 1
0. 12	0. 014	18. 5	8.41	70. 8
0. 11	0. 013	19. 0	8. 91	79. 4
0. 11	0. 011	19. 5	9.44	89. 1
 0. 10	0. 010	20. 0	10. 00	100. 0

APPENDIX C

LONGITUDINAL AND THICKNESS MODES

In this appendix equations applicable to the calculation of the properties of two types of crystal vibration are derived from the general equations of piezoelectricity. The first type of vibration considered, is designated by the term "longitudinal"; the second, by the term "thickness". The equations for the former type are those used as a basis for the theoretical development given in Part II, Sections 1 to 6. They are stated explicitly on page 151. Equations for the latter or thickness type are similar in form. These have been used to investigate the characteristics of this vibrational state. The results of the analysis are summarized in Appendix D. Also, the reinterpretation of symbols essential for applying the theoretical results of Part II, and the design curves of Part I, to crystals in thickness vibration is presented there.

We proceed with the derivations of the fundamental equations for the two types of vibration. It is desirable to have a shorthand notation to simplify the presentation which follows. Accordingly, the following terminology is employed.

The components of stress are designated by the letter T with subscripts; i.e., $T_1 \cdots T_6$, and

*A. E. H. Love—A Treatise on the Mathematical Theory of Elasticity. Dover, 1944.

$$T_1 = X_2$$
 $T_2 = Y_2$ $T_3 = Z_3$ $T_4 = Y_4$ $T_5 = Z_2$ $T_6 = X_4$

where X_1, \dots, X_n are the symbols used in many texts on elasticity.* The components of strain are likewise designated by S with subscripts; i.e., S_1, \dots, S_n , and

$$S_{1} = \frac{\partial u_{1}}{\partial x_{1}} \qquad S_{2} = \frac{\partial u_{2}}{\partial x_{2}} \qquad S_{3} = \frac{\partial u_{3}}{\partial x_{3}}$$

$$S_{4} = \frac{\partial u_{3}}{\partial x_{2}} + \frac{\partial u_{2}}{\partial x_{3}} \qquad S_{5} = \frac{\partial u_{1}}{\partial x_{3}} + \frac{\partial u_{3}}{\partial x_{1}}$$

$$S_{6} = \frac{\partial u_{2}}{\partial x_{1}} + \frac{\partial u_{1}}{\partial x_{2}}$$

where u_1 , u_2 and u_3 are the components of displacement along the axes of a mutually orthogonal coordinate system. The components of electric field, E, and the polarization, P, are designated by E_i and P_i , (j = 1, 2, 3).

If, then, we choose the stress and field as independent variables, the piezoelectric equations are:

$$S_{1} = S_{11}^{E}T_{1} + S_{12}^{E}T_{2} + S_{13}^{E}T_{3} + S_{14}^{E}T_{4} + S_{15}^{E}T_{5} + S_{16}^{E}T_{6} + d_{11}E_{1} + d_{21}E_{2} + d_{31}E_{3}$$

$$S_{2} = S_{12}^{E}T_{1} + S_{22}^{E}T_{2} + S_{23}^{E}T_{3} + S_{24}^{E}T_{4} + S_{23}^{E}T_{5} + S_{26}^{E}T_{6} + d_{12}E_{1} + d_{22}E_{2} + d_{32}E_{3}$$

$$S_{3} = S_{13}^{E}T_{1} + S_{23}^{E}T_{2} + S_{33}^{E}T_{3} + S_{34}^{E}T_{4} + S_{35}^{E}T_{5} + S_{36}^{E}T_{6} + d_{13}E_{1} + d_{23}E_{2} + d_{32}E_{3}$$

$$S_{4} = S_{14}^{E}T_{1} + S_{24}^{E}T_{2} + S_{34}^{E}T_{3} + S_{44}^{E}T_{4} + S_{43}^{E}T_{5} + S_{46}^{E}T_{6} + d_{14}E_{1} + d_{24}E_{2} + d_{34}E_{3}$$

$$S_{5} = S_{15}^{E}T_{1} + S_{25}^{E}T_{2} + S_{35}^{E}T_{3} + S_{45}^{E}T_{4} + S_{35}^{E}T_{5} + S_{56}^{E}T_{6} + d_{15}E_{1} + d_{25}E_{2} + d_{25}E_{3}$$

$$S_{6} = S_{16}^{E}T_{1} + S_{25}^{E}T_{2} + S_{36}^{E}T_{3} + S_{46}^{E}T_{4} + S_{56}^{E}T_{5} + S_{56}^{E}T_{6} + d_{15}E_{1} + d_{25}E_{2} + d_{25}E_{3}$$

$$P_{1} = d_{11}T_{1} + d_{12}T_{2} + d_{13}T_{3} + d_{14}T_{4} + d_{15}T_{5} + d_{16}T_{6} + k_{15}^{T}E_{1} + k_{12}^{T}E_{2} + k_{15}^{T}E_{3}$$

$$P_{2} = d_{21}T_{1} + d_{22}T_{2} + d_{23}T_{3} + d_{24}T_{4} + d_{25}T_{5} + d_{26}T_{6} + k_{15}^{T}E_{1} + k_{25}^{T}E_{2} + k_{35}^{T}E_{3}$$

$$P_{3} = d_{31}T_{1} + d_{32}T_{2} + d_{33}T_{3} + d_{34}T_{4} + d_{35}T_{5} + d_{36}T_{6} + k_{15}^{T}E_{1} + k_{25}^{T}E_{2} + k_{35}^{T}E_{3}$$

or compactly,

$$S = s^{E}T + d_{i}E$$

$$P = dT + k^{T}E.$$

In these equations certain coefficients may be identically zero. This is determined by the crystal class and the orientation of the crystal with respect to the reference coordinate system. The orientation of the coordinates is chosen in a way convenient for discussing the vibrational state of the cut crystal.

The general equations are now particularized in order to discuss the longitudinal type of vibration. The following properties will be taken as characteristic of this vibrational state:

- (a) The crystal shape is that of a parallelepiped.
- (b) All stress components but one are small enough to be neglected. When the crystal is oriented with the long axis of the system along the x₁ coordinate T₂ = T₃ = T₄ = T₃ = T₆ = 0, T₁ ≠ 0. For many crystal systems this condition implies that one dimension, called the length, is much greater than the other two—width and thickness.
- (c) During vibration plane sections of the parallelepiped perpendicular to the x_1 axis remain plane sections.
- (d) The piezoelectric coupling is such that a field perpendicular to the x_1 axis causes a strain in the direction of that axis.

When the above conditions are imposed on the general equations (1) the particularized form is:

$$S_{1} = s_{11}^{B}T_{1} + d_{21}E_{2} + d_{31}E_{3}$$

$$S_{2} = s_{12}^{B}T_{1} + d_{22}E_{2} + d_{32}E_{3}$$

$$S_{3} = s_{13}^{B}T_{1} + d_{23}E_{2} + d_{33}E_{3}$$

$$S_{4} = s_{14}^{B}T_{1} + d_{24}E_{2} + d_{34}E_{3}$$

$$S_{5} = s_{15}^{B}T_{1} + d_{25}E_{2} + d_{35}E_{3}$$

$$E_{6} = s_{16}^{B}T_{1} + d_{26}E_{2} + d_{36}E_{3}$$

$$P_{1} = d_{11}T_{1} + k_{12}^{T}E_{2} + k_{13}^{T}E_{3}$$

$$P_{2} = d_{21}T_{1} + k_{22}^{T}E_{2} + k_{23}^{T}E_{3}$$

$$P_{3} = d_{31}T_{1} + k_{23}^{T}E_{2} + k_{33}^{T}E_{3}$$

To these equations must be added a dynamical equation. This can be derived in the following manner. Consider a portion of the crystal between two parallel planes perpendicular to the x_1 direction, which is parallel to the long axis of the crystal system and a distance Δx_1 apart. This is illustrated in Figure 15.

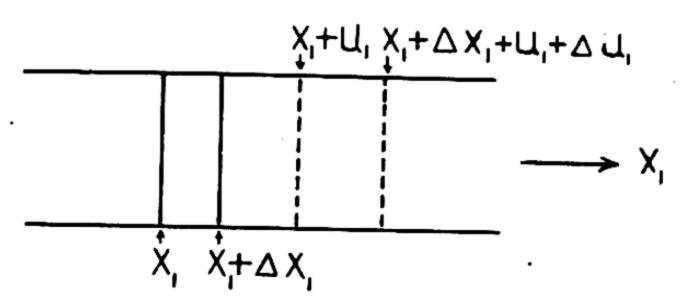


FIGURE 15.

Since this plane section remains a plane section under vibration, Newton's law yields:

$$[(T_1)_{x_1+\Delta x_1} - (T_1)_{x_1}]A = \rho \Delta x_1 A \frac{\partial^2 u_1}{\partial t^2}$$
 (3)

which leads to

$$\frac{\partial T_1}{\partial x_1} = \frac{\partial^2 u_1}{\partial t^2}. (4)$$

A current relation is necessary to the investigation. It may be obtained by noting that the current density at the electroded face of a crystal is given in terms of the time rate of change of the normal component of the electric displacemen D, or symbolically:

$$4\pi i_d = \frac{\partial D_n}{\partial t}.$$

When the crystal system is oriented with the long axis parallel to x_1 , D_n is either D_2 or D_3 . Since

$$i_d = \frac{1}{4\pi} \frac{\partial D_i}{\partial t}$$
 $j = 2 \text{ or } 3$

and

$$D_i = E_i + 4\pi P_i$$

therefore,

$$i_d = \frac{1}{4\pi} \frac{\partial E_i}{\partial t} + \frac{\partial P_i}{\partial t}.$$
 (5)

Equations (2), (4) and (5) constitute the basic equations requisite for the discussion of the longitudinal type of vibration.

Equation (4) may be written in terms of the displacement and the electric field by substituting for T_1 from the first of equations (2) and noticing that $S_1 = \frac{\partial u_1}{\partial x_1}$; i.e.,

$$\frac{\partial^2 u_1}{\partial x_1^2} - d_{21} \frac{\partial E_2}{\partial x_1} - d_{31} \frac{\partial E_3}{\partial x_1} = s_{11}^E \rho \frac{\partial^2 u_1}{\partial t^2}$$

If but one of the piezoelectric coefficients (d_{21}, d_{31}) is large, for convenience of discussion say d_{21} , this equation becomes:

$$\frac{\partial^2 u_1}{\partial x_1^2} - d_{21} \frac{\partial E_2}{\partial x_1} = s_{11}^E \rho \frac{\partial^2 u_1}{\partial t^2}$$

However, if the crystal is electroded on the faces parallel to the x_1 x_3 plane

$$\frac{\partial E_2}{\partial x_1} = 0,$$

and the above equation further reduces to

$$\frac{\partial^2 u_1}{\partial x_1^2} = s_{11}^B \rho \, \frac{\partial^2 u_1}{\partial t^2}. \tag{6}$$

The equations used as the basis of the theory of Part II are obtained from the relations under discussion by making suitable changes in notation and convention.

We collect the first and eighth of equations (2) with d_{31} equal to zero, equation (5) and equation (6) below:

$$S_{1} = s_{11}^{E} T_{1} + d_{21} E_{2}$$

$$P_{2} = d_{21} T_{1} + k_{22}^{T} E_{2}$$

$$i_{d} = \frac{1}{4\pi} \frac{\partial E_{2}}{\partial t} + \frac{\partial P_{2}}{\partial t}$$

$$\frac{\partial^{2} u_{1}}{\partial x_{1}^{2}} = s_{11}^{E} \rho \frac{\partial^{2} u_{1}}{\partial t^{2}}$$

$$(7)$$

Extensional stress has been defined as positive for the derivation of these equations. However, if we consider compressional stress positive, and make the notational changes as indicated in the table, the equations (7) take the form:

(a)
$$\frac{\partial^2 \bar{\xi}}{\partial x^2} = \frac{1}{V^2} \frac{\partial^2 \bar{\xi}}{\partial t^2}$$

(b)
$$\bar{i}_d = \frac{1}{4\pi} \frac{\partial \bar{E}_f}{\partial t} + \frac{\partial \bar{P}}{\partial t}$$
 (8)

(c)
$$-\overline{y} = s\overline{Y} + d\overline{E}_f$$

$$(d) \qquad \overline{P} = d\overline{Y} + K\overline{E}_f$$

These equations are identical to those on page 151.

TABLE OF CORRESPONDING NOTATION

$ar{y}$	←	S_1
$\frac{\overline{y}}{\overline{Y}}$ $\overline{\overline{E}}$ \overline{i}_d		T_1
\overline{E} ,		E_2
\overline{P}		P_2
ξ		u_1
\overline{i}_d		i_d
-d		d_{21}
8		s_{11}^B
K		k_{22}^T
\boldsymbol{x}		x ₁
V_{ϵ}		$\sqrt{1/\rho s}_{11}^B$

The value of d is the negative of the value of dn

In considering the thickness type of vibration, it is advantageous to choose the strain and electric field as the independent variables in the piezo-electric relations. Consequently, the relations for this case can be stated concisely as:

$$T = c^{E}S - e_{t}E$$

$$P = eS + k^{S}E$$
(9)

where the constants c_{ij}^{E} , e_{ij} , and k_{ij}^{S} are functions of the s_{ij}^{E} d_{ij} and k_{ij}^{T} of equations (1), page 176.

The following properties will be taken as defining this type of vibration:

- (a) The crystal form is that of a plate whose thickness is small compared to the other dimensions.
- (b) All strain components but one are small enough to be neglected. When the crystal is

oriented in the coordinate system with the large faces parallel to the x_2x_3 plane $S_2 = S_3 \cdots = S_6 = 0$, $S_1 \neq 0$.

- (c) During vibration plane sections of the plate parallel to the large faces, that is, parallel to the x_2x_3 plane, remain plane sections.
- (d) The piezoelectric coupling is such that a field in the direction of the normal to the x_2x_3 plane gives rise to a stress in the direction of the normal. The remaining two components of the field are small enough to be neglected.

When subjected to these conditions, the general equations (9) become:

$$T_{1} = c_{11}^{B}S_{1} - e_{11}E_{1}$$

$$T_{2} = c_{12}^{B}S_{1} - e_{12}E_{1}$$

$$T_{3} = c_{13}^{B}S_{1} - e_{13}E_{1}$$

$$T_{4} = c_{14}^{B}S_{1} - e_{14}E_{1}$$

$$T_{5} = c_{15}^{B}S_{1} - e_{15}E_{1}$$

$$T_{6} = c_{16}^{B}S_{1} - e_{16}E$$

$$P_{1} = e_{11}S_{1} + k_{11}^{S}E_{1}$$

$$P_{2} = e_{21}S_{1} + k_{13}^{S}E_{1}$$

$$P_{3} = e_{31}S_{1} + k_{13}^{S}E_{1}$$

To this set of equations must be added a dynamical equation. The derivation is the same as that for the preceding case. Consider a plane section parallel to the large faces with thickness Δx_1 . This plane section would, in accordance with the choice of axes previously employed, be parallel to the x_2x_3 plane of the coordinate system. Then

$$(T_1)_{x_1+\Delta x_1} - (T_1)_{x_1} = \rho \Delta x_1 \frac{\partial^2 u_1}{\partial t^2}$$

or

$$\frac{\partial T_1}{\partial x_1} = \rho \, \frac{\partial^2 u_1}{\partial t^2}. \tag{11}$$

Similarly, the current density relation has the form:

$$i_d = \frac{1}{4\pi} \frac{\partial E_1}{\partial t} + \frac{\partial P_1}{\partial t}.$$
 (12)

Equations (8), (11) and (12) are the basic equations requisite for the analysis of the thickness type of vibration.

The stress component, T_1 , can be eliminated from equation (11) by substituting from the first of equations (10). This leads to:

$$c_{11}^{E} \frac{\partial S_{1}}{\partial x_{1}} - e_{11} \frac{\partial E_{1}}{\partial x_{1}} = \rho \frac{\partial^{2} u_{1}}{\partial t^{2}}$$

Since $S_1 = \frac{\partial u_1}{\partial x_1}$, this may be written

$$c_{11}^{E} \frac{\partial^{2} u_{1}}{\partial x_{1}} - e_{11} \frac{\partial E_{1}}{\partial x_{1}} = \rho \frac{\partial^{2} u_{1}}{\partial t^{2}}. \tag{13}$$

The term involving the field component, E_1 , can be expressed in terms of the displacement component, u_1 . Due to the absence of free charge in the interior of the crystal, the divergence of the electric displacement is zero, i.e., $\nabla \cdot D = 0$ or

$$\frac{\partial D_1}{\partial x_1} + \frac{\partial D_2}{\partial x_2} + \frac{\partial D_3}{\partial x_3} = 0. \tag{14}$$

However, $D_1 = E_1 + 4\pi P_1$, $D_2 = E_2 + 4\pi P_2$ and $D_3 = E_3 + 4\pi P_3$. Observing that E_2 and E_3 are to be neglected, and that P_2 and P_3 are related to S_1 and E_1 by the last two equations of (10), it follows that:

$$\frac{\partial D_2}{\partial x_2} = 4\pi \left[e_{21} \frac{\partial S_1}{\partial x_2} + k_{12}^S \frac{\partial E_1}{\partial x_2} \right] = 0$$

and

$$\frac{\partial D_3}{\partial x_3} = 4\pi \left[e_{31} \frac{\partial S_1}{\partial x_3} + k_{13}^S \frac{\partial E_1}{\partial x_3} \right] = 0.$$

Equation (14) then yields:

$$\frac{\partial (E_1 + 4\pi P_1)}{\partial x_1} = 0.$$

Therefore,

$$E_1 + 4\pi P_1 = C$$
 or $P_1 = \frac{C - E_1}{4\pi}$

where C is a constant to be determined. When we substitute this expression for P_1 into the seventh equation of (10), namely, $P_1 = e_{11}S_1 + k_{11}^s E_1$,

and differentiate the resultant expression with respect to X_1 we obtain, upon noting that $S_1 = \frac{\partial u_1}{\partial x_1}$:

$$\frac{\partial E_1}{\partial x_1} = -\frac{4\pi e_{11}}{1+4\pi k_{11}^S} \frac{\partial^2 u_{1}}{\partial x_1^2}.$$

Substituting this expression into (13) yields:

$$\left[1 + \frac{4\pi e_{11}^2}{c_{11}^E(1 + 4\pi k_{11}^S)}\right] \frac{\partial^2 u_1}{\partial x_1^2} = \rho/c_{11}^E \frac{\partial^2 u_1}{\partial t^2}. (15)$$

Compiling the equations basic to the discussion of this type of vibration, we have the first and seventh of equations (10), equation (12) and equation (14), or explicitly:

(a)
$$T_1 = c_{11}^E S_1 - e_{11} E_1$$

(b)
$$P_1 = e_{11}S_1 + k_{11}^s E_1$$

(c)
$$i_d = \frac{1}{4\pi} \frac{\partial E_1}{\partial t} + \frac{\partial P_1}{\partial t}$$
 (16)

(d)
$$\left[1 + \frac{4\pi e_{11}^2}{c_{11}^R (1 + 4\pi k_{11}^S)}\right] \frac{\partial^2 u_1}{\partial x_1^2} = \rho/c_{11}^R \frac{\partial^2 u_1}{\partial t^2}$$

Solving 16(a) and 16(b) for S_1 and P_1 in terms of T_1 and E_1 we have:

$$S_1 = \frac{1}{c_{11}^B} T_1 + \frac{e_{11}}{c_{11}^B} E_1$$

$$P_1 = \frac{e_{11}}{c_{11}^R} T_1 + \left(\frac{e_{11}^2}{c_{11}^R} + k_{11}^S\right) E_1.$$

When the definition of stress components is changed so that compressional stress is considered positive and introducing symbols defined as follows:

$$s = \frac{1}{c_{11}^{R}} \qquad d = \frac{e_{11}}{c_{11}^{R}} \qquad K = \left(\frac{e_{11}^{2}}{c_{11}^{R}} + k_{11}^{S}\right)$$

$$\overline{Y} = -T_{1}$$

the equations (15) become:

$$-S_{1} = s\overline{Y} + dE_{1}$$

$$P_{1} = d\overline{Y} + KE_{1}$$

$$i_{d} = \frac{1}{4\pi} \frac{\partial E_{1}}{\partial t} + \frac{\partial P_{1}}{\partial t}$$
(17)

$$\left[1+\frac{4\pi d^2}{s(1+4\pi K-4\pi d^2/s)}\right]\frac{\partial^2 u_1}{\partial x_1^2}=\rho s\frac{\partial^2 u_1}{\partial t^2}$$

Upon introducing the changes in notation given in the table below, equations (17) assume the final form:

$$-\bar{y} = s\bar{Y} + d\bar{E}_{f}$$

$$\bar{P} = d\bar{Y} + K\bar{E}_{f}$$

$$\bar{i}_{d} = \frac{1}{4\pi} \frac{\partial \bar{E}_{f}}{\partial t} + \frac{\partial \bar{P}}{\partial t}$$

$$\frac{\partial^{2}\bar{\xi}}{\partial x^{2}} = \frac{1}{V_{f}^{2}} \frac{\partial^{2}\bar{\xi}}{\partial t^{2}}$$

The symbol K is defined by:

$$K^2 = \frac{4\pi d^2}{s(1 + 4\pi K - 4\pi d^2/s)}$$

TABLE OF CORRESPONDING NOTATION

ī,		S_1
$\frac{\bar{y}}{E}$, \bar{P}	` '	
E,		E_1
P		P_1
ξ		u_1
į,		i_d
\boldsymbol{x}		x1
V_{\bullet}		$\sqrt{\frac{1+K^2}{\rho s}}$

Note: The use of the symbols S, d, K does not imply that the values s, d, K appearing in equations (17) are equal to any of the s_{ij}^E , d_{ij} , k_{ij}^T appearing in equations (2). These symbols are employed so that the similarity of the corresponding equations for the two types of vibration will be immediately recognizable.

APPENDIX D

FUNDAMENTAL EQUATIONS FOR THICKNESS VIBRATION

This appendix contains the results of a detailed analysis of crystals in thickness vibration. The basis for the analysis was the set of equations (17) of Appendix C. These were derived by imposing the conditions defining a thickness vibration on the general equations of piezoelectricity. The conditions which characterize a thickness vibration are presented on page 178.

The crystal imbedded in an orthogonal coordinate system is shown in Figure 16. The large faces are perpendicular to the x_1 axis.

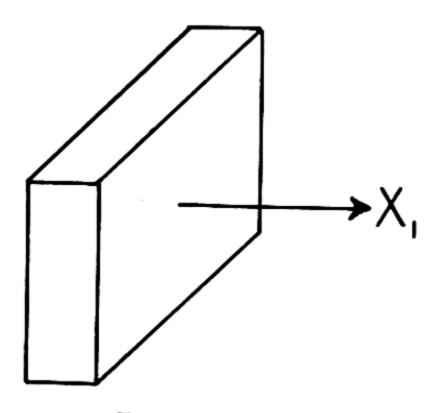


FIGURE 16.

We proceed with the summarization of the results of the analysis. The basic equations for the

thickness vibration as derived in Appendix C are:

$$-\bar{y} = s\bar{Y} + d\bar{E}_{f}$$

$$\bar{P} = d\bar{Y} + K\bar{E}_{f}$$

$$i_{d} = \frac{1}{4\pi} \frac{\partial \bar{E}_{f}}{\partial t} + \frac{\partial \bar{P}}{\partial t}$$

$$\frac{\partial^{2}\bar{\xi}}{\partial x^{2}} = \frac{1}{V_{c}^{2}} \frac{\partial^{2}\bar{\xi}}{\partial t^{2}}$$
(18)

where s, d and K are related to the fundamental constants of the crystal as follows:

$$s = \frac{1}{c_{11}^{E}}, \qquad d = -\frac{e_{11}}{c_{11}^{E}}, \qquad K = \left(\frac{e_{11}^{2}}{c_{11}^{E}} + k_{11}^{S}\right).$$

(See Appendix C equations (9).)

These equations (18) are identical in form with the basic equations (8) for the longitudinal state of vibration. However, due to the difference in the orientation of the electric field in the two cases, the theory based on these two sets of relations is not identical.

The following four equations summarize the results of the analysis of the thickness type of vibration:

(a)
$$\dot{\xi}(1+\Delta) = \dot{\xi}_1 \left[(1+\Delta) \cos \frac{\omega x}{V_{\epsilon}} - K^2 \frac{V_{\epsilon}}{\omega L_{\epsilon}} \left(1 + \cos \frac{\omega L_{\epsilon}}{V_{\epsilon}} \right) \sin \frac{\omega x}{V_{\epsilon}} \right] - j \frac{[F_1 + \varphi E]}{Z_0} \sin \frac{\omega x}{V_{\epsilon}}$$

(b)
$$\left[F(1+\Delta) + \varphi E\left(1 + K^2\left(1 - \cos\frac{\omega x}{V_{\epsilon}}\right)\right)\right]$$

$$= \left[F_1(1+\Delta) + \varphi E\right] \cos\frac{\omega x}{V_{\epsilon}} - K^2 F_1\left(\frac{V_{\epsilon}}{\omega L_{\epsilon}}\sin\frac{\omega L_{\epsilon}}{V_{\epsilon}}\right)\left(1 - \cos\frac{\omega x}{V_{\epsilon}}\right)$$

$$-j\dot{\xi}_1 Z_0(1+K^2)\left[\sin\frac{\omega x}{V_{\epsilon}}(1+\Delta) - K^2\frac{V_{\epsilon}}{\omega L_{\epsilon}}\left(1 - \cos\frac{\omega L_{\epsilon}}{V_{\epsilon}}\right)\left(1 - \cos\frac{\omega x}{V_{\epsilon}}\right)\right]$$
(19)

(c)
$$E(j\omega C_0) = i + \varphi(\dot{\xi}_2 - \dot{\xi}_1)$$

(d)
$$E_{I}(1 + \Delta) = \frac{E}{L_{e}} \left[1 + K^{2} \left(1 - \cos \frac{\omega x}{V_{e}} \right) \right] + \frac{F_{1}}{L_{e}} \frac{K^{2}}{\varphi} \left[\frac{V_{e}}{\omega L_{e}} \sin \frac{\omega L_{e}}{V_{e}} - \cos \frac{\omega x}{V_{e}} \right] + j \dot{\xi}_{1} \frac{Z_{0}}{L_{e}} \frac{K^{2}}{\varphi} \left[\frac{V_{e}}{\omega L_{e}} \left(\cos \frac{\omega L_{e}}{V_{e}} - 1 \right) \left(1 + K^{2} \left(1 - \cos \frac{\omega x}{V_{e}} \right) \right) + \sin \frac{\omega x}{V_{e}} (1 + \Delta) \right]$$

where

$$V_{\epsilon} = \sqrt{\frac{1+K^2}{\rho s}} \qquad C_0 = \frac{A}{4\pi L_{\epsilon}} (1 + 4\pi K - 4\pi d^2/s)$$

$$\varphi = \frac{d}{s} \left(\frac{A}{L_{\epsilon}}\right) \qquad K^2 = \frac{4\pi d^2}{s(1 + 4\pi K - 4\pi d^2/s)}$$

$$Z_0 = A\left(\frac{\rho}{s(1+K^2)}\right)^{\frac{1}{2}} \qquad \Delta = K^2\left(1 - \frac{V_{\epsilon}}{\omega L_{\epsilon}}\sin\frac{\omega L_{\epsilon}}{V_{\epsilon}}\right),$$

A is the area of the large faces of the crystal and L_{ϵ} is the thickness of the crystal. The remaining symbols are defined in Appendix A. The time dependence of the various quantities has been eliminated from these equations (unbarred symbols).

The equations (19) should be compared with equations (1), Part II. The corresponding equation for the electric field is not given on page 151 of Part II. It is $E_f = \frac{E}{L}$.

We find, upon examination of the two sets of equations, that the only terms which are not the

same in the corresponding equations are those multiplied by K^2 . For most crystal cuts in use, with the exception of X-cut Rochelle Salt $K^2 \leq 0.1$. Consequently, the terms involving K^2 may be neglected in many investigations of the properties of crystal systems. To this approximation, the fundamental equations are identical to those for the longitudinal type. Therefore, when no greater accuracy is required the design curves of Part I can be used for the discussion of the various characteristics of crystal systems in this type of vibration. The only changes necessary are the redefining of the parameters φ , Z_0 and C_0 viz.:

$$\varphi = \frac{d}{s} \left(\frac{A}{L_c} \right) \qquad Z_0 = A(\rho/s)^{\frac{1}{2}} \qquad C_0 = \frac{A}{4\pi L_c} \left(1 + 4\pi K - 4\pi d^2/s \right)$$

For convenient reference, we tabulate the fundamental equations for the thickness vibration where terms involving K^2 have been neglected.

(a)
$$\dot{\xi} = \dot{\xi}_1 \cos \frac{\omega x}{V_c} - j \frac{[F_1 + \varphi E]}{Z_0} \sin \frac{\omega x}{V_c}$$

(b)
$$[F + \varphi E] = [F_1 + \varphi E] \cos \frac{\omega x}{V_{\epsilon}} - j \dot{\xi}_1 Z_0 \sin \frac{\omega x}{V_{\epsilon}}$$

(c)
$$E(j\omega C_0) = i + \varphi(\dot{\xi}_2 - \dot{\xi}_1)$$

(d)
$$E_{t} = E/L_{\epsilon}$$

where

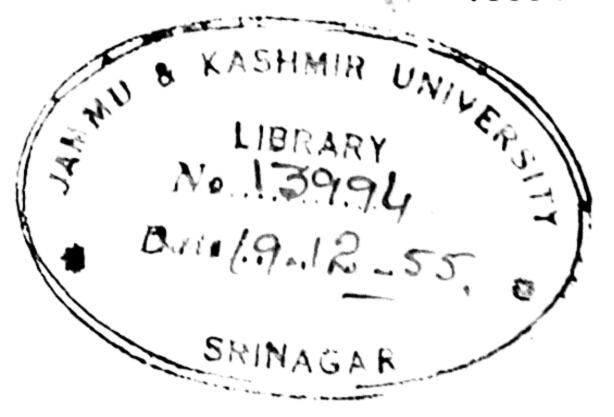
$$V = \sqrt{\frac{1}{\rho s}} \qquad C_0 = \frac{A}{4\pi L_c} (1 + 4\pi K - 4\pi d^2/s)$$

$$\varphi = \frac{d}{s} \frac{A}{L_c} \qquad Z_0 = A \left(\frac{\rho}{s}\right)^{\frac{1}{2}}.$$

A is the area of the large faces of the crystal.

L, is the thickness of the crystal.





THE JAMMU & KASHMIR UNIVERSITY LIBRARY.

DATE LOANED

Vol	_Сору
Accession No.	

THE JAMMU & KASHMIR UNIVERSITY LIBRARY.

DATE LOAND

Class No	Book No
	Сору

Charge of one of one of one of one of one of the for each will be date.

While in their poster of the date.

The for each will be held to one of the book. The book of the book.